Regulation of the organokines FGF21 and chemerin by diet –

Metabolic and molecular effects in liver and adipose tissue of obese human subjects

---

Nicole Seebeck

Univ.-Diss.

zur Erlangung des akademischen Grades
"doctor rerum naturalium"
(Dr. rer. nat.)
in der Wissenschaftsdisziplin
"Physiologie und Pathophysiologie"

eingereicht an der
Mathematisch-Naturwissenschaftlichen Fakultät
Institut für Ernährungswissenschaften
der Universität Potsdam
und
Deutsches Institut für Ernährungsforschung Potsdam-Rehbrücke (DIfE)

Ort und Tag der Disputation: Potsdam, 27. Mai 2020

Contents

I.   Index of Tables

Appendix

II.   Index of Figures

III. Abbreviations

ACC1	Acetyl-CoA carboxylase
ACOX1	Acyl-CoA oxidase 1
ACTA2	Alpha-smooth muscle actin 2
Adipo-IR	Adipose tissue insulin resistance
ADIPOQ	Adiponectin
ALT	Alanine transaminase
AST	Aspartate transaminase
AT	Adipose tissue
ATF4	Activating transcription factor 4
ATGL	Adipose triglyceride lipase
ANOVA	Analysis of variance
ATF4	Activating transcription factor 4
BiP	Binding immunoglobulin protein (also known as GRP78)
BCAA	Branched-chain amino acids
BMI	Body mass index
BSA	Bovine serum albumin
CCRL2	C-C chemokine receptor-like 2
CD	Cluster of differentiation
cDNA	Complementary DNA
CHOP	C/EBP homologous protein (also known as DDIT3)
ChREBP	Carbohydrate regulatory element-binding protein
CID	Clinical investigation day
CMKLR1	Chemokine-like receptor 1
COL	Collagen
CRP	C-reactive protein
CVD	Cardiovascular disease
DEXA	Dual-energy X-ray absorptiometry
DMEM	Dulbecco's modified eagle medium
DMSO	Dimethyl sulfoxide
DPP4	Dipeptidyl-peptidase 4
DPR	Dietary protein restriction
ECL	Electrochemiluminescent
EDTA	Ethylenediaminetetraacetic acid
eIF2α	Eukaryotic translation initiation factor 2 alpha
ELISA	Enzyme linked immunosorbent assay
EMR1	EGF-like module receptor 1
EN%	Percentage of energy intake
ER	Endoplasmic reticulum
ERK1/2	Extracellular signal-regulated kinase 1/2

F	Female
FASN	Fatty acid synthase
FBS	Fetal bovine serum
FFA	Free fatty acids
FGF21	Fibroblast growth factor 21
FGFR	FGF receptor
γ-GT	Gamma-Glutamyl Transferase
GPR1	G protein-coupled receptor 1
GWAS	Genome-wide association study
HbA1c	Glycated hemoglobin
HDL	High-density lipoprotein cholesterol
HES6	Hes Family BHLH Transcription Factor 6
HF	High-saturated-fat diet
HNF4α	Hepatocyte Nuclear Factor 4 alpha
hMSC	Human mesenchymal stromal cells
HOMA-IR	Homeostasis model assessment for insulin resistance
HP	High-protein diet
HPRT	Hypoxanthine-guanine phosphoribosyltransferase
HRT	Horseradish peroxidase
HSL	Hormone sensitive lipase
IFNγ	Interferon gamma
IHL	Intrahepatic lipids
IL	Interleukin
INSM1	Insulinoma-associated protein 1
IRE1α	Inositol-requiring enzyme 1 alpha
IRS1	Insulin receptor substrate 1
LDL	Low-density lipoprotein cholesterol
LP	Low-protein diet
LPL	Lipoprotein lipase
M	Male
MAPK	Mitogen-activated protein kinase
MCP1	Monocyte chemoattractant protein 1
MMP9	Metalloproteinase 9
MRI$_{spect}$	Proton magnetic resonance spectroscopy
NAFLD	Non-alcoholic fatty liver disease
NASH	Non-alcoholic steatohepatitis
NEFA	Non-esterified fatty acid
NFκB	Nuclear factor kappa-light-chain-enhancer of activated B cells
NLRP3	NLR family pyrin domain containing 3
PBMC	Peripheral blood mononuclear cells
PBS	Phosphate buffered saline

PGC1α	Peroxisome proliferator-activated receptor gamma, coactivator 1 alpha
PPAR	Peroxisome proliferator activated receptor
qRT-PCR	Quantitative real-time polymerase chain reaction
RBC	Red blood cells
RBP4	Retinol-binding protein 4
RIN	RNA integrity number
RNAi	RNA interference
RPLP0	Ribosomal protein lateral stalk subunit P0
SAF	Steatosis-activity-fibrosis
SAT	Subcutaneous adipose tissue
SCD1	Stearoyl-CoA desaturase 1
SEM	Standard error of the mean
SNP	Single nucleotide polymorphism
siRNA	Small interfering RNA
SREBP1c	Sterol regulatory element-binding protein 1c
T2DM	Type 2 diabetes mellitus
TAG	Triacylglycerides
TIG2	Termed tazarotene-induced gene 2
TIMP1	Tissue inhibitor of metalloproteinase 1
TNFα	Tumor necrosis factor alpha
TGFβ	Transforming growth factor beta
VAT	Visceral adipose tissue
VLDL	Very-low density lipoprotein
WAT	White adipose tissue
WHO	World Health Organization
WHR	Waist-to-hip-ratio
XBP1	X-box binding protein 1
XBP1s	Spliced X-box binding protein 1

1. Introduction

1.1 Liver and adipose tissue in metabolic diseases

The World Health Organization (WHO) describes obesity as a complex condition that represents an escalating global epidemic. Obesity poses a major risk for a number of severe, diet-related noncommunicable diseases, including diabetes mellitus type 2 (T2DM), cardiovascular disease (CVD), hypertension, stroke, musculoskeletal disorders, and certain forms of cancer (WHO, Fact Sheet on Obesity and Overweight, 2018). Apart from its health implications, overweight and obesity are often perceived as a psychological burden and reduce overall quality of life. In parallel with excess weight gain and physical inactivity, the number of patients living with diabetes has increased worldwide (WHO, Global Report on Diabetes, 2016). T2DM is characterized by tissues, including muscle, fat and liver, becoming less responsive or even resistant to insulin leading to uncontrolled blood glucose levels (Saltiel and Kahn, 2001).

Adiposity and T2DM increase the risk to develop non-alcoholic fatty liver disease (NAFLD) (Lade et al., 2014). NAFLD refers to an excess accumulation of lipid droplets in the liver unrelated to alcohol abuse (Chalasani et al., 2012). A fatty liver is diagnosed when the relative triacylgliceride (TAG) content in the liver exceeds 5.6% (Szczepaniak et al., 2005). In parallel with other metabolic disorders, the prevalence of NAFLD is on the rise and represents a growing global health issue (Younossi et al., 2018). NAFLD covers a spectrum of liver conditions characterized by the accumulation of TAG in the liver (hepatic steatosis), which at an initial stage does not affect liver function and is considered benign. By various mechanisms not yet fully understood, the disease may progress to non-alcoholic steatohepatitis (NASH), the presence of inflamed liver tissue and hepatocellular damage, which predisposes for serious liver-related complications (e.g. fibrosis, cirrhosis, hepatocellular carcinoma) and extrahepatic diseases such as CVD and T2DM (Chalasani et al., 2012; Haas et al., 2016). For example, overweight but metabolically healthy individuals with fatty liver more often develop impaired glucose metabolism (Heianza et al., 2014).

Emerging evidence point towards an important role of the complex crosstalk between metabolically active organs aiming to maintain or restore metabolic homeostasis through exchanging humoral messengers (Staiger et al., 2017). In particular, signaling between liver and adipose tissue has raised great interest (Kim, 2016; Moschen et al., 2012; Ye et al., 2017).

Besides its function in storing lipids and providing free fatty acids (FFA) for TAG synthesis, adipose tissue secretes a variety of endocrine signaling factors, such as cytokines and adipokines (Fasshauer and Bluher, 2015). In response to chronic overnutrition, adipose tissue

may fail to adapt and becomes dysfunctional which is characterized by insulin resistance, inflammation, altered adipokine release and ectopic fat accumulation (Bluher, 2013; Kloting and Bluher, 2014). Donnelly et al. estimated that about 60% of hepatic fatty acids originate from adipose tissue (Donnelly et al., 2005; Fabbrini et al., 2008). Furthermore, adipose tissue insulin resistance is commonly associated with NAFLD and disease severity (Bril et al., 2014; Seppala-Lindroos et al., 2002). The inability of insulin to suppress lipolysis causes an increased supply of FFA, which are under healthy conditions only transiently stored or re-secreted as very-low density lipoprotein (VLDL) but are accumulating when supplied in excess amounts (Bugianesi et al., 2005).

In the obese state, adipose tissue also becomes the source of inflammatory cytokines that are released into the circulation. A low-grade systemic inflammation due to adipocyte hypertrophy and macrophage infiltration is one of the major contributing factors to chronic diseases such as NASH, CVD, and T2DM (Gregor and Hotamisligil, 2011). Especially abdominal obesity turned out to be a strong independent predictor of death (Pischon et al., 2008).

1.1.1 Organokines mediate inter-tissue crosstalk

It is well established that metabolic organs communicate with each other regarding the regulation of energy homeostasis and whole-body metabolism (Oh et al., 2016). The term *organokines* summarizes factors that are predominantly produced and secreted by the respective tissue and act through autocrine, paracrine or endocrine signaling thus mediating inter-tissue crosstalk (Choi, 2016). These factors are mostly low-molecular weight proteins and mainly include cytokines, hormones and growth factors (Stefan and Haring, 2013). Despite some inconsistencies in the terminology, cytokines are generally considered to be immunomodulatory agents, while other bioactive molecules are mostly categorized according to their major (but not exclusive) place of synthesis and secretion, including adipokines (adipose tissue), hepatokines (liver) or myokines (skeletal muscle) (Oh et al., 2016; Stefan and Haring, 2013).

Adipokines signal adipose tissue functional status to peripheral and central target tissues, such as brain, liver, muscle, pancreas, and the immune system in order to induce metabolic adaptations (Fasshauer and Bluher, 2015; Stephens, 2012). Release of adipokines, such as leptin, adiponectin and chemerin, is altered in obesity which is thought to play a pivotal role in the onset of metabolic disease (Bluher, 2013). Marked differences in adaptive capacity and adipokine expression have been found between the visceral (VAT) and subcutaneous adipose tissue (SAT) depot (Wang et al., 2005). While SAT is less metabolically active, excess VAT has been shown to secrete several inflammatory factors and detrimental adipokines and is

associated with metabolic dysfunction, dyslipidemia and uncontrolled blood glucose levels (Ibrahim, 2010; Oh et al., 2016).

Similar to adipocytes, hepatocytes secrete inflammatory markers into the circulation in states of energy excess (Stefan and Haring, 2013). There is emerging evidence indicating that NAFLD alters the secretion of hepatokines from the liver (Meex and Watt, 2017). Several hepatokines have been linked to the induction of metabolic dysfunction (Meex and Watt, 2017). However, other proteins released from the liver, including fibroblast growth factor 21 (FGF21), are associated with beneficial effects on energy metabolism and metabolic parameters in blood (BonDurant and Potthoff, 2018).
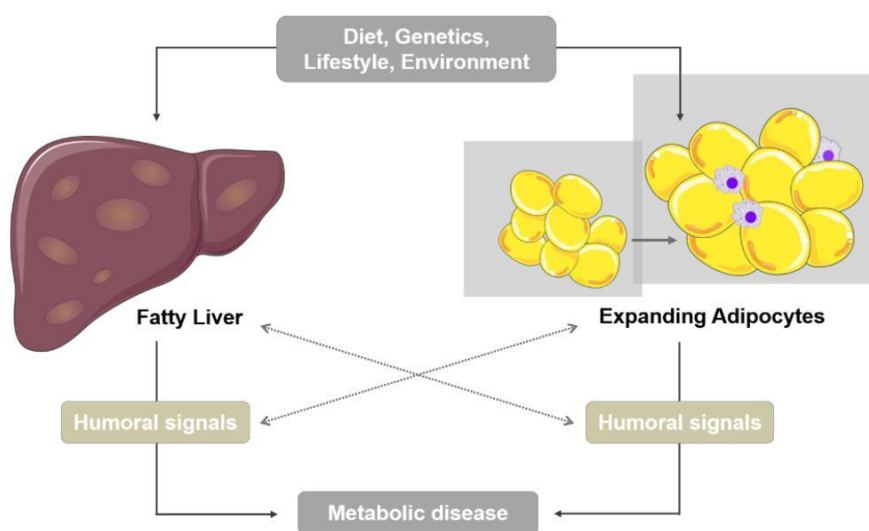
Figure 1 | Adipose tissue-liver crosstalk in metabolic disease. Chronic energy excess results in an expansion of adipose tissue and ectopic fat deposition such as an accumulation of lipids in the liver. Hypertrophic and hypoxic adipocytes become insulin resistant and release a variety of signaling molecules while apoptotic adipocytes attract resident macrophages that further amplify the inflammatory response. In parallel, stressed hepatocytes communicate with extrahepatic tissues aiming to restore metabolic homeostasis. These processes are thought to strongly affect the pathogenesis of metabolic diseases related to an increased release of inflammatory signals into the circulation. Figure modified from (Stefan and Haring, 2013), produced with graphics from servier medical art (servier.com), licensed under creative commons.

Chemerin and FGF21 represent emerging endocrine factors that have been implicated in the regulation of metabolic homeostasis as well as the onset of metabolic disease, including obesity, T2DM, and NAFLD. Recently, in a cross-sectional cohort of more than 1000 subjects, Ebert and coworkers identified chemerin and FGF21 as potential biomarkers for facets of the metabolic syndrome (Ebert et al., 2018). The nutrient-dependent regulation of these two factors in blood, adipose tissue, and liver of obese subjects is the major focus of this thesis.

1.2   The hepatokine FGF21

In humans, the FGF21 gene is located on chromosome 19 and encodes a protein of 208 amino acids. In 2000, FGF21 was first identified and characterized on the cDNA level (Nishimura et

al., 2000). Interest in FGF21 emerged when the human recombinant came up as a hit in an *in vitro* glucose uptake assay in murine 3T3-L1 adipocytes (Kharitonenkov et al., 2005). Since then FGF21 has been intensively studied, mainly in mice, as a potential therapeutic for obesity and T2DM. However, different strains of mice show variable effects on body weight and glucose/lipid metabolism (Gimeno and Moller, 2014). Similarly, FGF21 knock-out mice grow and develop normally and are fertile (Badman et al., 2009; Hotta et al., 2009). Data in humans are still fragmentary and its physiological role remains complex and under debate (Lewis et al., 2019).

In mice and humans, 22 genes of the FGF superfamily exist which may be functionally grouped into three subfamilies (Oulion et al., 2012). (1) intracellular FGFs lacking a signal peptide (FGF11 – FGF14), (2) autocrine/paracrine acting FGFs with high heparin-binding capacities, and (3) circulating FGFs with low heparin-binding capacities (FGF19 and FGF21) (Goetz et al., 2007). FGF21, together with FGF19 and FGF23, belongs to the metabolically active FGFs which are devoid of proliferative activity (Kharitonenkov et al., 2005). FGF21 is produced and released into the circulation predominantly by the liver but has also been found to be expressed, to a lower extent, in pancreas, testes, gastrointestinal tract, brain, skeletal muscle, and brown and white adipose tissue (WAT) (Petryszak et al., 2016). In humans, expression in extrahepatic tissues is neglectable under basal conditions but extensively inducible in response to certain physiological stimuli or pathological conditions (Petryszak et al., 2016; Staiger et al., 2017). At the target site, FGF21 binds to and activates FGF receptor tyrosine kinases (FGFR) with seven isoforms existing in mammals (1b, 1, 2b, 2c, 3b, 3c, 4) (Lee et al., 2018). Signal transduction involves phosphorylation of extracellular signal-regulated kinases (ERKs) and is dependent on the FGFR cofactor β-Klotho (KLB) (Ogawa et al., 2007). While FGFR1 and FGFR2 are rather ubiquitously expressed, the restricted KLB expression determines the tissue specificity of FGF21 (Ito et al., 2000; Yang et al., 2012).

1.2.1 Role as a metabolic regulator

In a large cross-sectional study with more than 800 subjects, serum FGF21 was shown to correlate with age, body mass index (BMI), fat mass, waist/hip circumference, as well as insulin and glucose metabolism (Kralisch et al., 2013). In diabetic or obese animal models, pharmacological application of FGF21 reduces body weight and prevents diet-induced obesity by increasing energy expenditure (BonDurant and Potthoff, 2018; Lundasen et al., 2007; Markan and Potthoff, 2016). Furthermore, infusions of FGF21 are effective in lowering blood glucose levels, improving lipid profiles, and increasing insulin sensitivity (Holland et al., 2013; Li et al., 2018; Lin et al., 2013). In contrast, circulating FGF21 levels are greatly increased in several obesity-associated disorders, including diabetes, the metabolic syndrome, and NAFLD.

In mice, hepatic *Fgf21* expression is induced during fasting or ketosis in a Pparα dependent manner (Badman et al., 2007; Inagaki et al., 2007; Lundasen et al., 2007). Results from Badman and colleagues indicate that FGF21 is essential for preventing the accumulation of hepatic TAG and the development of fatty liver during ketogenic diet (Badman et al., 2009). Thus, it was proposed that FGF21 plays a role in the adaptation to ketosis (Domouzoglou and Maratos-Flier, 2011). However, subsequent studies in humans could not confirm the FGF21 response to fasting as observed in mice (Staiger et al., 2017). FFA seem not to increase but rather decrease circulating FGF21 in humans (Dushay et al., 2010; Matikainen et al., 2012; Schmid et al., 2015). Treatment with PPARα or PPARγ agonists only modestly increase FGF21 expression. Furthermore, FGF21 blood concentrations only react to prolonged fasting of at least 7 days despite changes in tissue gene expression (Dushay et al., 2010; Fazeli et al., 2015; Galman et al., 2008). The fact that a rise in ketone bodies precedes the induction of FGF21 indicates that FGF21 is not driving starvation-mediated ketogenesis. Furthermore, markers of tissue breakdown were found to be predictive for serum FGF21 concentrations (Fazeli et al., 2015). Thus, the role of FGF21 during starvation in humans is still under debate. FGF21 was proposed to regulate the utilization of energy from tissue break-down during the late adaptive response to starvation (Fazeli et al., 2015). The discrepancy between mice and humans might be explained by the overall higher metabolism of mice (Staiger et al., 2017).

A variety of liver-stress circumstances potently increase FGF21 production such as, fasting, endoplasmic reticulum (ER) stress, liver injury, fatty or inflamed liver, and liver cancer (Dasarathy et al., 2011; Domingo et al., 2010; Maida et al., 2016; Yang et al., 2013). Furthermore, FGF21 serum concentrations are associated with liver transaminases (Kralisch et al., 2013). A large body of evidence indicates that FGF21 is produced and released into the circulation when the function of the liver is compromised in any way to act on extrahepatic tissues, particularly adipose tissue, to restore and maintain metabolic homeostasis (Kim and Lee, 2015; Luo and McKeehan, 2013).

In adipose tissue, FGF21 regulates genes involved in glucose uptake, lipogenesis and lipolysis (Keuper et al., 2019; Kharitonenkov et al., 2005; Staiger et al., 2017). These seemingly contradictory effects are thought to be dependent on the nutritional state of the adipocyte and the mode of FGF21 induction, i.e. pharmacological administration or physiological secretion (BonDurant et al., 2017). In mice, FGF21 increases energy expenditure by inducing browning of WAT thus increasing thermogenesis (Bargut et al., 2017; Coskun et al., 2008). Some of the beneficial effects of FGF21 on glucose homeostasis and energy expenditure depend on the induction of adiponectin in adipose tissue and FGF21 was identified as a potent regulator of adiponectin secretion (Holland et al., 2013; Lin et al., 2013). FGF21 also plays a role in the brain where it regulates features of starvation, such as growth inhibition, and altered circadian

rhythm (Sarruf et al., 2010) and affects nutrient preference (Soberg et al., 2017; von Holstein-Rathlou et al., 2016).

Due to its beneficial effects on glucose/lipid homeostasis and the maintenance of body weight, FGF21 arose as a promising therapeutic candidate for the treatment of metabolic disorders (Gimeno and Moller, 2014). FGF21 itself has a very short half-life but analogs with improved pharmacokinetics have been designed and are tested in clinical trials (Gimeno and Moller, 2014). Results demonstrated that pharmacological application of FGF21 improves lipid and cholesterol metabolism, reduces insulin levels and induces modest weight loss (Sonoda et al., 2017). However, one of its side effects is a decrease in bone mass. Furthermore, no glucose lowering effects were detected in any trial making it less attractive as an anti-diabetic drug (BonDurant and Potthoff, 2018). Studies reporting contradictory results suggest that the physiological effects differ from the pharmacological (Lewis et al., 2019; Staiger et al., 2017).

1.2.2   Regulation by macronutrients

The nutrient-dependent regulation of FGF21 is summarized in the following. It should be noted, that most of the knowledge on FGF21 physiology is derived from animal studies, including feeding, knock-out and overexpression studies. However, considerable discrepancies in FGF21 regulation seem to exist between mice and men (Staiger et al., 2017).

A large body of evidence indicates that overfeeding of carbohydrates or simple sugars acutely induces hepatic *FGF21* expression and increases circulating FGF21 levels (Dushay et al., 2015; Lundsgaard et al., 2017; Soberg et al., 2017; von Holstein-Rathlou et al., 2016). The induction of FGF21 by sugar seems to be dependent on carbohydrate response element binding protein (ChREBP) (Fisher et al., 2017; Stamatikos et al., 2016). Recent evidence suggests that FGF21 is postprandially controlled by insulin rather than glucose *per se* (Samms et al., 2017). Moreover, FGF21 was shown to centrally affect appetite and macronutrient preference, e.g. in rodents and primates knock out of *FGF21* increases sugar intake while FGF21 injection reduces the preference for sweets (Talukdar et al., 2016; von Holstein-Rathlou et al., 2016). In humans, a SNP in the *FGF21* locus has been associated with increased consumption of candy (Soberg et al., 2017). The regulation of sweet preference by FGF21 was shown to be dependent on KLB expression in the brain (Talukdar et al., 2016). The data points towards FGF21 being involved in a negative feedback loop along the liver-brain axis regulating sugar consumption and possibly other reward systems (Staiger et al., 2017). It was suggested that FGF21 might be responsible for maintaining glucose homeostasis when a diet high in simple sugars is consumed (von Holstein-Rathlou and Gillum, 2019).

There are contradictory data regarding the effect of dietary fat on FGF21, but fat seems to only moderately influence serum FGF21 levels. *In vitro* experiments in HepG2-cells indicate that

FGF21 is directly regulated by FFA in a PPARα dependent manner (Mai et al., 2009). In the same study, lipid infusions in healthy subjects increased serum FGF21 concentrations (Mai et al., 2009). However, modest increases in FGF21 in response to high-fat overfeeding (Heilbronn et al., 2013) and decreased FGF21 serum concentrations after an oral fat load have also been reported (Matikainen et al., 2012). A short-term (3-day) high-fat diet did not significantly increase FGF21 levels in contrast to an 8-fold induction of FGF21 after a carbohydrate-enriched diet (Lundsgaard et al., 2017). It has been proposed that high-fat diet, or more specifically diet-induced obesity, leads to an FGF21-resistant state as KLB, the FGF21 co-receptor, was found to be downregulated with increasing FGF21 concentrations in obesity (Fisher et al., 2010; Gallego-Escuredo et al., 2015).

The role of FGF21 in the metabolic adaptation to starvation was narrowed down by Laeger et al. who postulated that FGF21 is an endocrine signal of protein restriction, not energy restriction (Laeger et al., 2014). Subsequent studies confirmed that FGF21 is potently induced in response to dietary protein restriction (DPR) and that it is required for the adaptive changes in metabolism and behavior (Hill et al., 2017; Laeger et al., 2016; Maida et al., 2016; Morrison and Laeger, 2015). Furthermore, mice on DPR increase their energy intake in an attempt to compensate for the lack in essential amino acids (Gosby et al., 2016).

Though the mechanisms inducing FGF21 in response to DPR have been extensively studied, the downregulation of FGF21 by high-protein diets has gained less attention. Markova and colleagues observed a pronounced decrease in circulating FGF21 in response to a 6-week high-protein diet in diabetic human subjects (Markova et al., 2017). Although others have reported similar responses, the decrease in circulating FGF21 after prolonged high-protein intake has rather been attributed to changes in glucose metabolism (Chalvon-Demersay et al., 2016) or alleviation of hepatic cell stress due to reduced steatosis (Garcia-Caraballo et al., 2013; Garcia Caraballo et al., 2017).

In an attempt to reconcile the conflicting data on FGF21, Solon-Biet and colleagues used a nutritional modeling platform to compare the effect of 25 diets varying in fat, protein, and carbohydrate content in mice (Solon-Biet et al., 2016). The results indicate that FGF21 is induced by both, states of starvation and hyperphagia, and that its metabolic effects differ dependent on the nutritional state. FGF21 induction was highest when a low-protein diet was combined with high carbohydrate intakes (Solon-Biet et al., 2016).

1.2.3 Response to metabolic stress

De Sousa-Coelho and coworkers revealed that amino acid deprivation increases FGF21 via activation of the GCN2-branch of the integrated stress response (ISR) (De Sousa-Coelho et al., 2012). This pathway of the ISR is initiated by uncharged tRNAs activating the amino acid

sensing kinase general control non-derepressible 2 (GCN2) which phosphorylates eukaryotic translation initiation factor 2α (eIF2α) (De Sousa-Coelho et al., 2012) (Figure 2). eIF2α leads to overall protein synthesis reduction and induction of activating transcription factor 4 (ATF4). The purpose of this response is to halt protein synthesis in the face of a lack of building blocks in order to maintain cell homeostasis (Proud, 2014). ATF4 is a key factor of the ISR as it modulates a variety of genes involved in the adaptation to dietary stress, including the apoptosis controlling protein CHOP (De Sousa-Coelho et al., 2012).
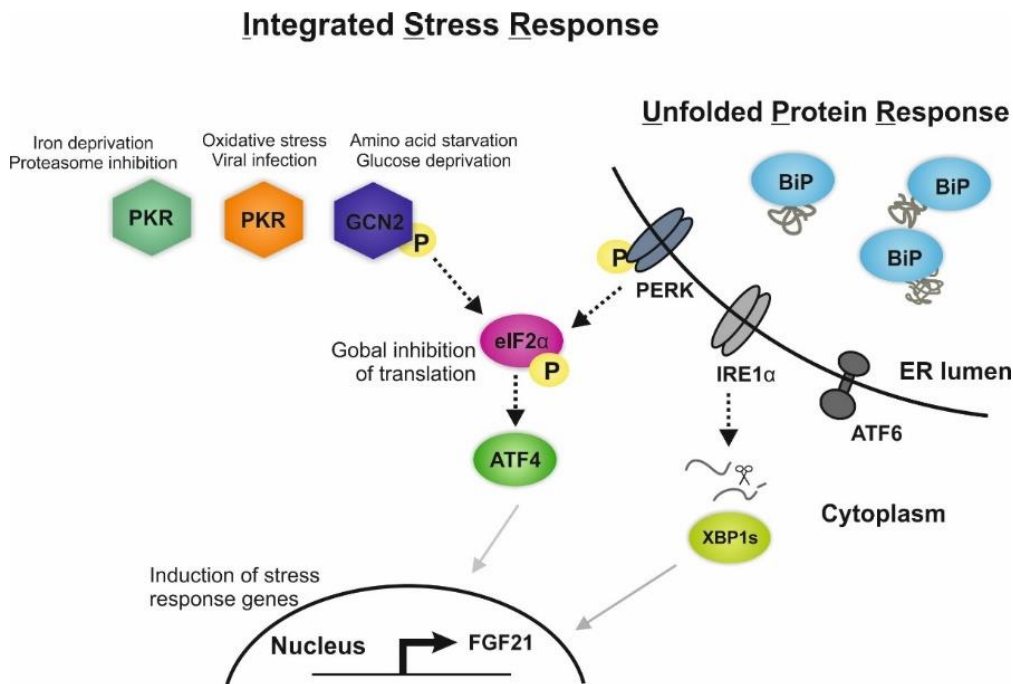
Figure 2 | Cellular stress pathways induce FGF21: Integrated stress response (ISR) and unfolded protein response (UPR). Figure modified from (Halliday and Mallucci, 2015; Way and Popko, 2016), produced with CorelDRAW®.

Organelle stress is another potent inducer of hepatic FGF21 expression through eIF2α/ATF4 signaling (Kim and Lee, 2014; Salminen et al., 2017a; Schaap et al., 2013). Kim and coworkers demonstrated that mitochondrial dysfunction, provoked by autophagy deficiency or inhibition of the mitochondrial respiratory chain, increased *Fgf21* expression via GCN2/ATF4 (Kim et al., 2013). An ISR related pathway is the unfolded protein response (UPR). Accumulation of unfolded proteins in the ER is sensed by the chaperone binding immunoglobulin protein (BiP, also known as GRP78), which mediates phosphorylation of eIF2a via the transmembrane kinase PERK (Figure 2). Furthermore, BiP activates splicing of X-box binding protein 1 (XBP1), a stress-induced transcription factor, via the kinase inositol-requiring enzyme 1 α (IRE1α) (Figure 2). Jiang and colleagues uncovered that FGF21 is induced by the IRE1α-XBP1s branch of the UPR and alleviates ER stress-induced hepatic steatosis (Jiang et al., 2014).

1.2.4   FGF21 and fatty liver disease

Liver fat content is the strongest BMI-independent determinant for circulating FGF21 concentrations (Liu et al., 2014; Staiger et al., 2017; Yilmaz et al., 2010). Conversely, FGF21 serves as an independent predictor for the development of fatty liver (Liu et al., 2014; Yan et al., 2011) and is consistently elevated in patients with NAFLD or steatohepatitis (Dushay et al., 2010; Maratos-Flier, 2017). Likewise, subjects with derailed glycaemia show increased FGF21 serum concentrations as fatty liver is strongly linked to the pathophysiology of T2DM (Keuper et al., 2019; Staiger et al., 2017). Genetic manipulations of *Fgf21* in mice indicate a causative link between FGF21 and liver fat (Garcia Caraballo et al., 2017; Maratos-Flier, 2017). *Fgf21* knock-down in mice consuming a ketogenic diet led to severe accumulation of TAG in blood and liver, reduced fatty acid oxidation and impaired hepatic clearance of TAG via VLDL particles, thus provoking fatty liver disease (Badman et al., 2009). Similarly, livers of *Fgf21* knockout mice fed a hepatotoxic high-fructose diet demonstrated signs of inflammation and fibrosis in their livers which were absent in controls (Fisher et al., 2017).

Mechanistically, a substrate oversupply, as present in obesity, may cause an accumulation of unfolded proteins in the ER, exceeding its capacity and leading to activation of ER stress pathways (Hotamisligil, 2010). Unresolved ER stress and more specifically the UPR were shown to contribute to the development of fatty liver disease by suppressing the expression of a subset of metabolic transcription factors involved in the regulation of lipid homeostasis in the liver (DeZwaan-McCabe et al., 2017; Rutkowski et al., 2008). Several lines of evidence point towards a role of FGF21 in linking ER stress with NAFLD. FGF21 deficiency is associated with higher expression of ER stress markers and the accumulation of excess hepatic lipids upon tunicamycin treatment. Similarly, ER stress and hepatic fat content were reduced by FGF21 overexpression (Kim et al., 2015; Maruyama et al., 2018).

Thus, apart from its potential utility as an antidiabetic drug, FGF21 has been contemplated for the treatment of NAFLD. Recently, Sanyal and colleagues published the results of a randomized, double-blind, phase 2a study examining the effect of pegbelfermin, a PEGylated FGF21 analogue in patients with NASH (Sanyal et al., 2019). The major finding was a significant reduction of hepatic fat content in the pegbelfermin treated group while the drug was well tolerated (Sanyal et al., 2019). However, liver fat content is considerably influenced by nutritional intakes, e.g. a Western style diet promotes hepatic TAG accumulation (Machado et al., 2015) while targeted nutritional intervention is highly effective in reducing liver fat (Barrera and George, 2014). Dietary strategies are needed and are to be preferred over pharmacological approaches (Rinella and Sanyal, 2016). Consequently, insights into the interplay between dietary protein, FGF21, and NAFLD pathogenesis in humans are of great interest (Ullah et al., 2019).

1.3 The adipokine chemerin

The chemerin cDNA was originally discovered as a tazarotene (a synthetic retinoid) responsive gene and accordingly termed *tazarotene-induced gene 2* (TIG2) and later *RARRES2* (Goralski et al., 2007; Martensson et al., 2005; Nagpal et al., 1997). Chemerin itself was isolated and characterized in a screening for ligands of the orphan G-protein coupled receptor CMKLR1 from human inflammatory fluids (Wittamer et al., 2003). Furthermore, it was shown to colocalize with immune cells in inflamed tissue and to have chemoattractant activity, recruiting leucocytes, in particular dendritic cells, macrophages and natural killer cells, to the site of inflammation (Parolini et al., 2007; Wittamer et al., 2003). Goralski and coworkers identified chemerin as a novel adipokine and demonstrated its role in adipogenesis and adipocyte metabolism (Goralski et al., 2007). Shortly after, Bozaoglu and colleagues published a study confirming chemerin's association with obesity and the metabolic syndrome in murine models and also human subjects (Bozaoglu et al., 2007).

Chemerin is highly expressed in WAT, liver and lung and is synthesized as an inactive precursor (Mattern et al., 2014). N-terminal truncation results in secretion of chemerin into the extracellular matrix or circulation but it requires further proteolytic C-terminal processing for chemerin to reach its full biological activity (Helfer and Wu, 2018; Mattern et al., 2014). A variety of proteases cleave chemerin thereby generating isoforms with different receptor affinity (Mattern et al., 2014). Thus, successive proteolytic processing provides a key regulatory mechanism affecting its localization and activity (Helfer and Wu, 2018).

Three receptors for chemerin have been identified: its main receptor chemokine-like receptor 1 (CMKLR1, also known as chemR23), C-C motif chemokine receptor-like 2 (CCRL2) and G protein-coupled receptor 1 (GPR1) (Mariani and Roncucci, 2015). CMKLR1 and GPR1 transduce a signal in response to chemerin binding but only CMKLR1 signaling mediates chemotaxis of immune cells via NFκB and MAPK pathways (Bozaoglu et al., 2007; Wittamer et al., 2003). Instead, CCRL2 functions to concentrate chemerin on the cell surface (Helfer and Wu, 2018).

Circulating chemerin concentrations have been shown to be moderately heritable (Bozaoglu et al., 2007; Bozaoglu et al., 2010; Mussig et al., 2009; Tonjes et al., 2014). In a meta-analysis of genome-wide association studies (GWAS) in three distinct cohorts, Tönjes and colleagues identified 4 SNPs with genome-wide significance to partly explain variation in serum chemerin levels (Tonjes et al., 2014).

1.3.1 Role as a metabolic regulator

Chemerin serum concentrations are positively associated with BMI, obesity and obesity-related biomarkers (Bozaoglu et al., 2007; Chakaroun et al., 2012; Sell et al., 2009; Tonjes et

al., 2014). In addition, positive correlation with the adipokines leptin and resistin but non or a negative association with adiponectin were reported (Chu et al., 2012; Weigert et al., 2010). Circulating levels have been implicated in the development of metabolic disease, including insulin resistance and fatty liver disease (Docke et al., 2013; Ernst et al., 2010; Helfer and Wu, 2018) and to be a weak predictor of T2DM (Bobbert et al., 2015). Treatment of NAFLD patients with metformin decreased serum chemerin concentrations concomitantly with improvements in NAFLD (Zhuang et al., 2015).

Loss of chemerin or CMKLR1 signaling almost completely blocks adipogenesis in *in vitro* models and alters expression of genes important for glucose and lipid metabolism (Goralski et al., 2007). In the murine 3T3-L1 adipocytes it has been demonstrated that *RARRES2* and *CMKLR1* expression increase during differentiation and reach their highest levels in mature adipocytes (Goralski et al., 2007; Roh et al., 2007). Ohers have reported decreasing *CMKLR1* expression in fully differentiated adipocytes (Bozaoglu et al., 2007). However, most studies have been conducted in murine cell culture models and evidence from primary human adipocytes is limited (Ferland and Watts, 2015).

Next to its chemoattractant activity, chemerin is suspected to promote angiogenesis. In co-culture studies chemerin induced the growth of capillary-like structures through ERK1/2 signaling (Nakamura et al., 2018). The angiogenic potential of chemerin was supported by another study in human endothelial cells (Kaur et al., 2010). These findings have led to the concept that chemerin promotes adipogenesis through the expansion of capillary blood flow in adipose tissue (Ferland and Watts, 2015). On the other hand, chemerin was reported to increase the generation of reactive oxygen species and to have proapoptotic, proinflammatory, and proliferative effects in human vascular cells indicating that chemerin contributes to obesity-related vascular injury (Neves et al., 2015).

Ernst and Sinal proposed a model in which elevated chemerin synthesis in obese WAT leads to increased release of pro-inflammatory, pro-diabetic adipokines, alters adipocyte function, fosters WAT inflammation, and negatively affects glucose uptake and vascular health thereby contributing to the development of metabolic disease (Ernst and Sinal, 2010).

1.3.2 Regulation by macronutrients

Only little is known about chemerin's regulation in response to diet, particularly in humans. In obese human subjects, dietary weight-loss strategies were reported to decrease serum chemerin concentrations (Chakaroun et al., 2012). In accordance, excessive weight loss after bariatric surgery significantly reduced chemerin expression in omental and subcutaneous fat depots (Chakaroun et al., 2012). Furthermore, weight-loss maintenance diets decreased circulating chemerin levels while there was no effect of macronutrient composition (Hron et al.,

2017). Evidence from animal studies indicate that nutritional status regulates chemerin expression in adipose tissue but not in liver (Stelmanska et al., 2013).

In mice, high-fat chow increased serum chemerin levels which was attenuated by exercise (Lloyd et al., 2015). Similarly, expression of chemerin and its receptor are up-regulated in adipose tissue of mice fed a high-fat diet (Roh et al., 2007). In obese patients chemerin was found to positively correlate with low-density lipoprotein (LDL) cholesterol and negatively with high-density lipoprotein (HDL) cholesterol (Lorincz et al., 2014). Recently, Markova and coworker reported that circulating chemerin is downregulated by a high-protein diet in human T2DM patients (Markova et al., 2017).

An epidemiological study in metabolically healthy obese adults categorized dietary patterns according to their inflammatory potential and found chemerin to be elevated in subjects with a high dietary inflammatory index (Mirmajidi et al., 2019). Subjects with a high dietary inflammatory index consumed more carbohydrates and less protein, less poly- and monounsaturated fats, less fiber, and more saturated fats (Mirmajidi et al., 2019).

In summary, prior studies in humans on the effect of diet, particularly on the role of macronutrient composition, are limited. Insights on the regulation of chemerin in serum and its mRNA expression within adipose tissue are lacking and there is a need for dietary intervention studies in humans.

1.3.3   Chemerin and adipose tissue inflammation

Apart from its role in metabolic disease, chemerin has been implicated in various disorders, including NAFLD, specific cancers, allergic asthma, reproductive disorders, inflammatory bowel disease, hypertension, atherosclerosis, CVD, Lupus nephritis, rheumatoid arthritis, and psoriasis (Helfer and Wu, 2018). A potential link between these different roles of chemerin are its association with a derailed or insufficient functioning of the immune system (Helfer and Wu, 2018).

Since its discovery, chemerin has consistently been associated with markers of inflammation or autoimmune disease and chemerin levels were found to be elevated in inflammatory fluids (Ernst and Sinal, 2010; Mariani and Roncucci, 2015). Its predicted structure differs from the typical chemokine structure but chemerin shows structural homology to cathelicidins which exhibit antimicrobial activity (Banas et al., 2013). Furthermore, two chemerin isoforms have been shown to inhibit the growth rate of *Escherichia coli* (Kulig et al., 2011). In humans, serum chemerin correlated with proinflammatory cytokines, such as tumor necrosis factor α (TNFα), interleukin 6 (IL6), and C-reactive protein (CRP) (Lehrke et al., 2009; Weigert et al., 2010) and chemerin expression was shown to be induced by TNFα (Sell et al., 2009). Within the tissue, active chemerin is proteolytically cleaved by proteases associated with coagulation or fibrolytic

cascades indicating that chemerin activation is the result of infectious or allergic inflammation (Zabel et al., 2005):

The chemerin receptor CMKLR1 is expressed on various immune cells, including dendritic cells, macrophages and natural killer cells (Parolini et al., 2007; Zabel et al., 2006). The available evidence suggests that chemerin/CMKLR1 signaling is involved in the recruitment of these cells to the site of inflammation and plays a role in the initiation and progression of inflammation (Ernst and Sinal, 2010). However, a role for chemerin in the resolution of inflammation has also been reported (Laranjeira et al., 2018; Luangsay et al., 2009; Mariani and Roncucci, 2015).

2   Hypotheses and aims of the study

The aim of this thesis was to investigate circulating levels and tissue-specific regulation of (1) FGF21 and (2) chemerin in a cohort of morbidly obese patients. The study participants were asked to adhere to a diet containing either high (HP: 30 EN%, n = 9) or low (LP: 10 EN%, n = 10) protein amounts for 3 weeks prior to bariatric surgery (the LEMBAS study, cohort 1). Before and after the intervention, subjects were anthropometrically assessed and routine parameters in serum as well as hepatic fat content were determined. Furthermore, tissue biopsies from liver, SAT, and VAT were collected during surgery. The results obtained in the metabolically stressed subjects of cohort 1 were compared to data from 92 healthy twins with normal glucose tolerance and liver fat content (cohort 2). In the first part of the thesis, the study participants are characterized, and outcomes of the dietary interventions on anthropometric and routine clinical parameters are presented.

The second part of the thesis aimed to investigate how FGF21 is regulated by acute and persistent high-protein intakes in metabolically stressed compared to healthy individuals. FGF21 is potently induced by various stressors, including nutrient deficiency or excess. Furthermore, previous results in diabetic human subjects indicate that not only low-protein but also protein-enriched diets may independently regulate FGF21. Considering that FGF21 has been implicated in the central regulation of appetite, it was hypothesized that the hepatokine might serve as a signal for both, the lack of essential amino acids and the accumulation of ammonia in order to restore macronutrient balance. Furthermore, elevated circulating FGF21 levels have been associated with liver fat content and are sought to be predictive for steatosis and NAFLD. In the patients undergoing bariatric surgery as a treatment for excessive obesity, serum FGF21 concentrations were expected to be elevated and to be positively correlated with the accumulation of hepatic lipids. The latter was histologically and molecularly assessed in the hepatic tissue biopsies.

In the third part of the thesis, the potential regulation of chemerin by diet and its association with metabolic disease was investigated. Chemerin has repeatedly been linked to inflammation and the pathogenesis of insulin resistance but discordant data exists on the potential role of chemerin in NAFLD. The collection of tissue biopsies from liver, SAT, and VAT during bariatric surgery allowed an analysis of chemerin not only in serum but within the tissue. It was hypothesized that chemerin is associated with inflammatory markers, particularly in the visceral depot. Furthermore, human primary adipocytes were isolated from the adipose biopsies and differentiated *in vitro* to gain mechanistic insights on chemerin's effects on this cell type.

3 Materials and methods

3.1 Material

3.1.1 Chemical compounds and solutions

Chemicals	Company
Basic	
BSA Standard	G-Biosciences, USA
Cell Lysis Buffer	Cell Signaling, Danvers, USA
Dimethyl sulfoxide (DMSO)	Sigma-Aldrich, St. Louis, USA
Ethanol	Carl Roth, Karlsruhe, Germany
Ethylene diamine tetraacetic acid (EDTA)	Carl Roth, Karlsruhe, Germany
Formaldehyde	Sigma-Aldrich, St. Louis, USA
Hydrogen chloride solution	Sigma-Aldrich, St. Louis, USA
2-Mercaptoethanol	Thermo Fisher Scientific, Waltham, USA
Polyoxyethylene (10) tridecyl ether	Sigma-Aldrich, St. Louis, USA
Phosphatase Inhibitor Cocktail	Roche Diagnostics, Basel, Switzerland
Protease Inhibitor Cocktail	Roche Diagnostics, Basel, Switzerland
Rnase/DNase-free Water	MP Biomedicals, Solon, USA
RNase Inhibitor, Applied Biosystems	Thermo Fisher Scientific, Waltham, USA
Sodium chloride (NaCl)	Merck, Darmstadt, Germany
Sodium dihydrogen phosphate monohydrate ($NaH_2PO_4 * H_2O$)	Carl Roth, Karlsruhe, Germany
Tween-20	AppliChem, Darmstadt, Germany
Tween-40	Sigma-Aldrich, St. Louis, USA
Cell culture	
Accutase detachment solution	Sigma-Aldrich, St. Louis, USA
Ammonium chloride	Merck, Darmstadt, Germany
Antibiotic Antimycotic Solution	Sigma-Aldrich, St. Louis, USA
Arachidonic acid	Sigma-Aldrich, St. Louis, USA
Biotin	Sigma-Aldrich, St. Louis, USA
Bovine serum albumin (BSA), fatty acid free, low endotoxin	Sigma-Aldrich, St. Louis, USA
Chemerin, human, recombinant	R&D Systems, Minneapolis, USA
Collagenase D from C. histolyticum	Sigma-Aldrich, St. Louis, USA
Dexamethasone	Sigma-Aldrich, St. Louis, USA

Dulbecco's Modified Eagle Medium (DMEM)	Thermo Fisher Scientific, Waltham, USA
Dulbecco's Phosphate Buffered Saline (DPBS)	Thermo Fisher Scientific, Waltham, USA
DMEM/F12	Thermo Fisher Scientific, Waltham, USA
Earl's Balanced Salt Solution (EBSS)	Thermo Fisher Scientific, Waltham, USA
Fatty Acid Supplement Mix	Sigma-Aldrich, St. Louis, USA
Fetal Bovine Serum (FBS)	Biochrom GmbH, Berlin, Germany
Hank's Balanced Salt Solution (HBSS)	Thermo Fisher Scientific, Waltham, USA
Hes6 siRNA and negative control	Qiagen, Hilden, Germany
HyClone FBS	Fisher Scientific, Waltham, USA
Hydrocortisone	Sigma-Aldrich, St. Louis, USA
Insulin, human, recombinant	Sigma-Aldrich, St. Louis, USA
3-Isobutyl-1-methylxanthine (IBMX)	Sigma-Aldrich, St. Louis, USA
L-glutamine solution	Thermo Fisher Scientific, Waltham, USA
Lipofectamine transfection reagent	Thermo Fisher Scientific, Waltham, USA
MEM Amino Acids	Thermo Fisher Scientific, Waltham, USA
MEM Non-essential Amino Acids (NEAA)	Thermo Fisher Scientific, Waltham, USA
Minimum Essential Medium (MEM)	Thermo Fisher Scientific, Waltham, USA
Oil Red O	Sigma-Aldrich, St. Louis, USA
Palmitic acid	Sigma-Aldrich, St. Louis, USA
Pantothenate	Sigma-Aldrich, St. Louis, USA
Phosphate Buffered Saline (PBS)	Thermo Fisher Scientific, Waltham, USA
Preadipocyte Growth Medium	Promo Cell, Heidelberg, Germany
Preadipocyte Supplement Mix	Promo Cell, Heidelberg, Germany
Red Blood Cell (RBC) Lysis Buffer	Sigma-Aldrich, St. Louis, USA
Rosiglitazone	Sigma-Aldrich, St. Louis, USA
Thapsigargin	Sigma-Aldrich, St. Louis, USA
Transferrin, human	Sigma-Aldrich, St. Louis, USA
Trichlormethan/ chloroform	Carl Roth, Karlsruhe, Germany
3,3′,5-triiodo-L-thyronine (T3)	Sigma-Aldrich, St. Louis, USA
Trypsin-EDTA	Thermo Fisher Scientific, Waltham, USA
Tunicamycin	Sigma-Aldrich, St. Louis, USA

3.1.2 Assays

Assay	Company
Routine parameters	

ABX Cholesterol 100	Horiba ABX Diagnostics, Montpellier, France
ABX Pentra ALT CP	Horiba ABX Diagnostics, Montpellier, France
ABX Pentra AST CP	Horiba ABX Diagnostics, Montpellier, France
ABX Pentra CREA	Horiba ABX Diagnostics, Montpellier, France
ABX Pentra CRP	Horiba ABX Diagnostics, Montpellier, France
ABX Pentra GGT CP	Horiba ABX Diagnostics, Montpellier, France
ABX Pentra Glucose HK CP	Horiba ABX Diagnostics, Montpellier, France
ABX Pentra HbA$_{1c}$	Horiba ABX Diagnostics, Montpellier, France
ABX Pentra HDL Direct CP	Horiba ABX Diagnostics, Montpellier, France
ABX Pentra NEFA C	Wako Chemicals, Neuss, Germany
ABX Pentra TAG CP	Horiba ABX Diagnostics, Montpellier, France
ABX Pentra URAC	Horiba ABX Diagnostics, Montpellier, France
ABX Pentra UREA	Horiba ABX Diagnostics, Montpellier, France

ELISA

Adiponectin, human	R&D Systems, Minneapolis, USA
Chemerin, human	BioVendor, Brno, Czech Republic
FGF21, human	R&D Systems, Minneapolis, USA
Insulin, human	Mercodia, Uppsala, Sweden
Leptin, human	R&D Systems, Minneapolis, USA
Omentin, human	BioVendor, Brno, Czech Republic

Kits

Agilent RNA 6000 Nano LabChip Kit	Agilent technologies, Böblingen, Germany
High Capacity cDNA Reverse Transcription Kit	Thermo Fisher Scientific, Waltham, USA
HumanOmniExpressExome BeadChips	Illumina, San Diego, USA
NucleoSpin DNA Kit	Macherey-Nagel, Düren, Germany
NucleoSpin RNA II Kit	Macherey-Nagel, Düren, Germany
Power SYBR Green PCR Master Mix	Thermo Fisher Scientific, Waltham, USA
Protein Assay Kit	Bio-Rad Laboratories, Hercules, USA
Primer Express 2.0, Applied Biosystems	Thermo Fisher Scientific, Waltham, USA
RNase-free DNase Set	Qiagen, Hilden, Germany
RNeasy Lipid Tissue Kit	Qiagen, Hilden, Germany
Triglyceride Determination Kit	Sigma-Aldrich, St. Louis, USA
U-PLEX Biomarker Group 1(hu) Multiplex Assays	Meso Scale Diagnostics, Rockville, USA
QIAzol Lysis Reagent	Qiagen, Hilden, Germany

3.1.3 Laboratory equipment

Instruments	Company
ABX Pentra 4000	Horiba ABX SAS, Montpellier, France
Agilent 2100 BioAnalyzer	Agilent technologies, Böblingen, Germany
Biometra TS1 Thermo Shaker	Biometra GmbH, Göttingen, Deutschland
Bio–Plex 200 Multiplex system	Bio-Rad Laboratories GmbH, Munich, Germany
BOD POD	COSMED, Rome, Italy
BX50 upright microscope, XC50 camera	Olympus, Tokyo, Japan
Calibrated digital scale	Soehnle Professional, Nassau, Germany
Infinite 200 PRO plate reader	Tecan AG, Männedorf, Switzerland
Labsonic homogenizer	Braun, Melsungen, Germany
MAGNETOM Avanto 1.5T MRI System	Siemens Healthcare, Erlangen, Germany
Mastercycler	Eppendorf AG, Hamburg, Germany
EON Microplate Spectrophotometer	Bio Tek Instruments, Winooski, USA
NanoDrop ND 1000 spectrophotometer	Thermo Fisher Scientific, Waltham, USA
QuickPlex SQ 120 ECL imager	Meso Scale Discovery, Rockville, USA
SpeedMill PLUS bead mill	Analytik Jena, Jena, Germany
Thermomixer Compact	Eppendorf AG, Hamburg, Germany
TissueLyser LT	Qiagen, Hilden, Germany
ViiA 7 real-time PCR system	Thermo Fisher Scientific, Waltham, USA

3.1.4 Software

Software	Company
2100 Expert Bioanakyzer software, version 2.5	Agilent Technologies, Santa Clara, USA
Bio-Plex Manager, version 6.0	Bio-Rad Laboratories GmbH. Munich, Germany
CorelDraw Graphics Suite X7	Corel, Ottawa, Canada
GraphPad Prism, version 6.0	GraphPad Prism Inc., La Jolla, USA
i-control plate reader software	Tecan AG, Männedorf, Switzerland
ImageJ, Adiposoft plug-in	Public Domain, BSD-2
NanoDrop 100 Operating Software	Thermo Fisher Scientific, Waltham, USA
PRODI nutritional software	Nutri-Science GmbH, Hausauch, Germany
SPSS Statistics, version 24.0	IBM, Armonk, USA
QuantStudio, Real-Time PCR Software	Thermo Fisher Scientific, Waltham, USA

3.1.5 Primers

Gene	Forward	Reverse
Human		
Inflammation		
_IL6_	TGACAGCCAGTCCACCACAAT	ATGGCTGGACGGTAACAGGAA
MCP1	GATGCGTGGAGAGTCGAAAT	CTATCCAGCTCACCGGTCTC
TNFA	GGCCAGGCTCTTCCTTGAAT	TAGAGGAGTGTTCCAGGGCA
Fibrosis		
ACTA2	TCAATGTCCCAGCCATGTAT	CAGCACGATGCCAGTTGT
COL1A1	GCCAAATATGTGTCTGTGACTCA	GGGCGAGTAGGAGCAGTTG
COL3A1	ACGAGCTGGTCAAGTTCGAG	AGGCTCTTGATGGCTTCCTT
COL6A1	CCGTGGACCTGATCAAGAG	TCGATGACGTGGACGGATACT
MMP9	TGGGTACAATGAGGAGTAGG	CCTACTCCTCATTGTACCCA
TGFB1	TCTCATTGCTGGAAAACTGC	AAACAGGGAAACACTGTGCAT
TIMP1	GGACCTCTCTCTAATCAGCCCTC	TCGAGAAGATGATCTGACTGCC
Lipid metabolism		
ACC1	TCGCTTTGGGGGAAATAAAGTG	ACCACCTACGGATAGACCGC
ATGL	AGCTCATCCAGGCCAATGTCT	GGTTGTCTGAAATGCCACCAT
ChREBP	CAGCTGCGGGATGAGATTGA	AAACGCTGGTGTGTGTGGGTA
FASN	ACTGGGCAGTGAAGGAATTG	CTAGCCATTGCGGATTTCAT
HSL	AGCCCTGAGAAAGGAGACATGTA	TCTGCCAGTGCCTCTTTGCT
LPL	CATAGCAGCCACCTTCATTCC	TCTGCAGTGAGATCTTCCTATTGG
PGC1A	CGAGGGCGATCTTGACAG	TCTTTGCTCTGCTCCTG
PPARA	GCTTTGGCTTTACGGAATACCA	TTCGATGTTCAATGCTCCACTG
PPARG	CTGGAGGAATTTCACAAGCACC	GCCTCACAAATATTCCAGCTGG
SCD1	CCACCGTTTCTTCGTGGAT	TGCTCGCTCTAAGAGATGTTCC
SREBP1c	AATTGAGGGCTTTCGCCTTAG	CCGGTAGTGAACCCGTTGAT
ER stress		
ATF4	GGGTTCTCCAGCGACAAGGCTAAG	AACAGGGCATCCAAGTCGAACTC
BiP	CGAGGAGGAGGACAAGAAGG	CACCTTGAACGGCAAGAACT
CHOP	CCTGCAAGAGGTCCTGTCTTCA	TCAGTCAGCCAAGCCAGAGAA
XBP1u	GTGAGCTGGAACAGCAAGTGGT	CCAAGCGCTGTCTTAACTCCTG
XBP1s	CCGCAGCAGGTGCAGG	GAGTCAATACCGCCAGAATCCA
FGF21 pathway		
FGF21	GGGAGTCAAGACATCCAGGT	GGCTTCGGACTGGTAAACAT
FGFR1	GAATTGGAGGCTACAAGGTCCG	TGCTGCCGTACTCATTCTCCAC
FGFR2	CCCGTGGAGGAACTTTTTAAGC	TGCCAACAGTCCCTCATCATC
KLB	CATTTACATCACCGCCAGTGG	GGTATGCTTTCAGCACCTCCTG

Chemerin pathway

CCRL2	TCGCCTGGTCAATGCTCTAAGT	TGAGGATCAAAGCAT
CMKLR1	ACGAAGACATCCCACCAATC	GGGCAGTTCTTGGTCTCGT
GPR1	GCGCCCTCCTTGGCTCAACA	ATGCCATCTGGCACCCGCAC
RARRES2	CATAACAGCAGGAGCTCATCGT	ACGAGCCCATTCATAGACATCA

Housekeeper

HPRT1	TGACACTGGCAAAACAATGCA	GGTCCTTTTCACCAGCAAGCT
RPLP0	GCTTCCTGGAGGGTGTCC	GGACTCGTTTGTACCCGTTG
Murine		
Atf4	GGAATGGCCGGCTATGG	TCCCGGAAAAGGCATCCT
Fgf21	ACCGCAGTCCAGAAAGTCTCCT	TGAGGCGATCCATAGAGAGCTC
Hes6	TGTTCACCTCTCCCTGCCTTT	TTCAGGTCAGGATTGCTGTGG
Hprt	TCCTCCTCAGACCGCTTTT	CCTGGTTCATCATCGCTAATC
Rplp0	CTGATCATCCAGCAGGTGTT	CCAGGAAGGCCTTGACCTTT

3.2 Clinical intervention studies

For the results of this thesis, data from three different human cohorts have been analyzed as described in the following sections. Participants were medically examined and supervised by the responsible study doctor as well as trained study nurses. Analysis of routine blood parameters was supported by technical assistants in the laboratory.

The human intervention studies were conducted in accordance with the Declaration of Helsinki. All participants provided written informed consent prior to study enrollment. Participants were informed about the study aim, physical examinations and associated risks. and had the right to resign from the study at any time point. Anthropometrical assessments and blood collections were performed at the clinical research center at the German Institute of Human Nutrition (DIfE), Department of Clinical Nutrition, Potsdam-Rehbruecke, Germany.

3.2.1 LEMBAS: Protein intervention prior to bariatric surgery (cohort 1)

For the LEMBAS study ("Diet-induced changes in liver fat and energy metabolism prior to bariatric surgery"), participants were recruited in cooperation with the Clinic for Nutritional Medicine of Dr. med. Anke Rosenthal, Berlin, Germany. Inclusion and exclusion criteria were as follows:

Table 1 | Inclusion and exclusion criteria.

Inclusion criteria	Exclusion criteria
• Age: 18 - 75 years • BMI > 30 kg/m² • Indication for bariatric surgery	• Glucocorticoid therapy • Immunosuppression • Anemia • Severe liver disease (liver cirrhosis, HCC) • Chemotherapy (last 8 weeks) • Coagulopathy • Heart attack / stroke (last 6 months) • Past organ transplantation • Mental or psychiatric disorder • Addiction • Pregnancy • Insulin or long acting insulin analogue therapy (metformin, DPP-IV inhibitors, and diuretics were accepted)

Subjects with an indication for bariatric surgery were recruited and randomized into two groups according to sex, age, and BMI. There were two hypocaloric diet groups: the low-protein (LP, 10 EN% protein) and high-protein (HP: 30 EN% protein) group. The protein content was balanced with carbohydrates (LP: 55-65 EN% carbohydrates, HP: 35-45 EN% carbohydrates) while fats accounted for 25-35 EN% in both diets. The diets lasted for 3 weeks prior to bariatric surgery and were moderately hypocaloric (1500-1600 kcal/day). The participants received detailed food plans given as 10-day rotating menus compiled with the software PRODI (Nutri-Science GmbH, Hausauch, Germany). Part of the foods (protein shakes in the HP group and vegan spreads in the LP group) were provided to the participants. The LP diet was rich in bread, rice, potatoes, fruits and vegetables, whereas the HP diet was high in low-fat dairy products, meat, eggs, fruits and vegetables and supplemented with protein shakes. Preparation of dietary plans and nutritional counselling was supported by the MSc student Kathleen Herz.

Before (week 0) and after (week 3) the intervention, study subjects were anthropometrically assessed, fasting blood was drawn, body composition was determined by Air Displacement Plethysmograph (BOD POD, Cosmed, Rome, Italy), and hepatic fat content was determined by proton magnetic resonance spectroscopy (MRI$_{spec}$). During surgery, blood as well as tissue biopsies from the subcutaneous adipose tissue (SAT), the visceral omental adipose tissue (VAT), and the liver were taken. Tissue collection during surgery was performed by one of two surgeons in a standardized manner. Processing of tissue biopsies was conducted within the surgery room maintaining sterility as far as possible. Tissue samples were immediately washed in ice cold PBS, aliquoted and either stored in liquid nitrogen (for RNA and protein isolation) or transported on ice in HBSS [for human mesenchymal stromal cell (hMSC) isolation] or 4% formaldehyde (for histology). There was a gap of approximately 3-5 days between completion

of the study and day of surgery during which participants were instructed to continue on the respective diet.

In total, 20 participants had been recruited, 10 in each group. 1 participant in the HP group was later excluded from the study due to low compliance resulting in 19 participants finally completing the study (LP: n = 10, HP: n = 9; mean BMI: 44.8 ± 0.9 kg/m², mean age: 47.9 ± 2.0 years). Baseline anthropometric and routine clinical measures are presented in Appendix Table A1. Furthermore, blood and tissue samples were collected during surgery only from 15 additional patients not participating in the dietary interventions, termed the reference protein group (RP, n = 15).

The LEMBAS study was approved by the Ethics Committee of the Charité-Universitätsmedizin Berlin (EA4/006/15) and was registered at the German Clinical Trials Register (Unique identifier: DRKS00009509). The study was supported by an EASD-grant "Identification of individual response criteria for reduction of hepatic fat by nutritional approaches and subsequent maintenance by dietary strategies" to Andreas F.H. Pfeiffer.

3.2.2 Reference cohorts 2 and 3

High protein intervention in heathy subjects (cohort 2)

As a reference cohort, data from 92 healthy, non-obese twins (mean BMI: 22.5 ± 0.3 kg/m², mean age: 31.5 ± 1.5 years, 58 female/ 34 male) was analyzed. Details of recruitment, phenotyping of study participants, as well as the dietary interventions were published previously (Schuler et al., 2017). Baseline characteristics of the study participants as well as changes in anthropometric and routine clinical measures in response to the interventions are presented in Appendix Table A3.

Study subjects followed an initial 6-week healthy diet (LF: 55 EN% carbohydrates, 30 EN% fat, 15 EN% protein), as recommended by the German Nutrition Society (DGE, Bonn, Germany), to standardize for different dietary habits. This was followed by a 6-week high-fat diet (HF: 40 EN% carbohydrates, 45 EN% fat, 15 EN% protein) high in saturated fats and animal fat products. A final 6-week high-protein diet (HP: 30 EN% carbohydrates, 40 EN% fat, 30 EN% protein) was completed by 24 subjects. Baseline characteristics of this smaller subcohort as well as changes in anthropometric and routine clinical measures are presented in Appendix Table A5. Clinical investigation days (CIDs) took place after 6 weeks of LF diet (LF6), 1 week of HF diet (HF1), 6 weeks of HF diet (HF6), and 6 weeks of HP diet (HP6). Study participants received standardized meals and snacks for one week before each CID.

On each CID, participants were anthropometrically characterized, fasting blood samples were collected, liver fat was determined by MRI$_{spec}$ (at LF6, HF1, HF6), body composition was determined by dual-energy X-ray absorptiometry (DEXA, at LF6, HF6), and SAT biopsies were

taken. Participants were recruited at the German Institute of Human Nutrition (DIfE). The study was approved by the Ethics Committee of the Charité-Universitätsmedizin Berlin (EA4/021/09) and was registered at ClinicalTrials.gov (Unique identifier: NCT01631123). The NUGAT study was funded by the German Federal Ministry of Education and Research (BMBF, grant no.0315424).

Short-term protein intervention (cohort 3)

To investigate regulation of FGF21 in the short-term, 21 healthy, elderly subjects (mean BMI: 25.6 ± 0.9 kg/m², mean age: 61.7 ± 1.5 years, 15 female/ 6 male) were randomized into two groups according to sex, age, and BMI. Baseline characteristics of the study participants as well as changes in anthropometric and routine clinical measures in response to the interventions are presented in Appendix Table A6. Dietary counselling and supervision of the study participants was supported by the MSc student Ulrike Hass.

All participants followed an initial 3-day low-protein diet (LP: 10 EN% from protein) for standardization. Subsequently participants consumed diets containing either normal (NP: 15 EN% from protein, n = 10) or high (HP: 30 EN% protein, n = 11) dietary protein for 3 consecutive days. The diets were balanced with dietary fat while carbohydrates were kept constant at 45 EN%. Every 24 h serum samples were collected after overnight fast.

Participants were recruited at the German Institute of Human Nutrition (DIfE). The study represents a subcohort of the NutriAct study which was approved by the Ethics Committee of the Landesärztekammer Brandenburg [AS 160(a)2015] and was registered at the German Clinical Trials Register (Unique identifier: DRKS00010049). The NutriAct study was supported by the NutriAct – Competence Cluster Nutrition Research Berlin-Potsdam funded by the Federal Ministry of Education and Research (grant no. FKZ: 01EA1408A).

3.3   Methods

3.3.1   Heritability

Heritability of FGF21 and chemerin was estimated based on the ACE structural equation model in the 34 monozygotic (MZ) and 12 dizygotic (DZ) twin pairs of cohort 2. The ACE algorithm is based on comparisons of the degree of concordance of a phenotypic trait within and between MZ and DZ twin pairs. By calculating the degree of correlation, it was determined which proportion of variance in serum protein concentrations is attributed to additive genetic effects (A), or due to common environmental (C) and non-shared environmental (E) effects. Heritability analyses were performed by Dr. Andreas Busjahn (Healthtwist, Berlin) and Dr. Martin Osterhoff [Department of Clinical Nutrition, German Institute of Human Nutrition (DIfE)].

3.3.2 Genotyping

Genotyping of the study participants in cohort 2 has been described previously (Schuler et al., 2017). In brief, genomic DNA was isolated from buffy coat and genotyped on HumanOmniExpressExome BeadChips (Illumina, San Diego, USA) at the Interdisciplinary Center for Clinical Research (IZKF, Leipzig, Germany).

3.3.3 Anthropometric measurements

At each CID (week 0, week 3), participants of the LEMBAS study were anthropometrically assessed. Body height was determined by a wall-mounted stadiometer and body weight was measured with a calibrated digital scale (Soehnle Professional, Nassau, Germany). BMI was calculated according to the following formula: BMI = body weight [kg] / body height^2 [m^2]. Waist and hip circumferences were recorded and the waist-to-hip-ratio (WHR) was calculated accordingly.

Body composition of the participants was determined by air displacement plethysmography (BOD POD, COSMED, Rome, Italy). The instrument consists of an airtight chamber and measures the volume of displaced air, recorded as a change in pressure, when a participant is seated inside. Based on body volume and body weight whole-body densitometry was calculated and the relative proportion of fat and fat-free mass was derived accordingly.

3.3.4 Determination of routine parameters in blood

Blood samples were collected after overnight fasting using a standard blood collection system (S-Monovette, Sarstedt, Germany). Depending on further analyses, plasma tubes contained EDTA or DPP4-inhibitors and were centrifuged (10 min, 3000 rpm, 4°C) immediately after blood sampling. Serum tubes contained a coagulation activator and were left to clot for 10 min before centrifugation. Samples were aliquoted and stored at -80°C until further use.

<u>Glucose and HbA1c</u>

Blood glucose concentrations were determined spectrophotometrically after 2-step enzymatic transformation to gluconate 6-phosphate and equimolar NADPH/H+. Absorption of NADPH was measured as 340 nm.

Glycated hemoglobin (HbA$_{1c}$) is expressed as a percentage of total hemoglobin and is determined spectrophotometrically in whole blood. The assay is based on the latex agglutination inhibition test. In this test, HbA1c prevents agglutination of latex particles covered with monoclonal mouse antibodies specific for HbA1c and thus reduced absorbance at 550 nm.

Insulin and estimates for insulin resistance

Insulin concentrations were determined by enzyme-linked immunosorbent assay (ELISA) (Mercodia, Uppsala, Sweden) according to the manufacturer's instructions.

Homeostasis Model Assessment for Insulin Resistance (HOMA-IR) index was calculated according to the formula: HOMA-IR = (fasting insulin in mU/l x fasting glucose in mmol/l) / 22.5. Index of adipose tissue insulin resistance (Adipo-IR) was calculated according to the formula: Adipo-IR = fasting insulin [mU/l] x fasting free fatty acids [mmol/l].

Blood lipids

Triacylglycerides (TAG), total cholesterol, high-density lipoprotein cholesterol (HDL), and free fatty acids (FFA) were spectrophotometrically determined on an ABX Pentra 4000 analyzer (HORIBA ABX SAS, Montpellier, France) using the respective commercially available kit as listed in section 3.1.2. The measurements are based on enzymatic, colorimetric assays. From the obtained values for total cholesterol, TAG, and HDL, the concentration of low-density lipoprotein cholesterol (LDL) was calculated according to (Friedewald et al., 1972).

C-reactive protein (CRP)

CRP was determined by immunoturbidimetric assay (Horiba ABX SAS, Montpellier). Antibody-labeled microbeads complex with CRP thus causing a change in light intensity due to the scattering effect of the dissolved particles. Turbidity was measured at 850 nm from which the CRP concentrations was calculated.

Hepato- and adipokines

Concentrations of chemerin, FGF21, omentin, leptin, and adiponectin were determined by commercially available ELISA kits (listed in section 3.1.2) according to the manufacturer's instructions.

Renal and hepatic biomarkers

Serum concentrations of urea, uric acid, and creatinine, as well as activity of the liver enzymes aspartate aminotransaminase (AST), alanine aminotransaminase (ALT), and gamma-glutamyl transferase (γ-GT) were determined by on the ABX Pentra 4000 analyzer (HORIBA ABX SAS, Montpellier, France) using commercially available kits as listed in section 3.1.2.

3.3.5 Histology

Small tissue pieces from SAT, VAT, and liver were immediately fixated in 4% formaldehyde (Sigma-Aldrich, St. Louis, USA) and transported to the laboratory. After 24 h, the tissue biopsies were embedded in paraffin after which sections were cut in 2 µm thick slices and stained on glass slides. Preparation and staining of histological tissue sections was conducted

by Elisabeth Meyer [Max Rubner Laboratory, German Institute of Human Nutrition (DIfE)]. Images were acquired with a BX46 Upright Microscope (Olympus Tokyo, Japan). Evaluation of tissue sections was supported by the MSc student Elisabeth Friedl [(Department of Clinical Nutrition, German Institute of Human Nutrition (DIfE)].

<u>Adipose tissue biopsies</u>

Hematoxylin and eosin (H&E) staining

For H&E staining, tissue sections were deparaffinized with Roti-Histol (Carl Roth, Karlsruhe, Germany) and stained according to standard protocols. Hematoxylin stains nuclei blue-purple while eosin stains the extracellular matrix and cytoplasm pink. Other cellular structures also become apparent taking on different shades between the two colors.

Adipocyte morphology was assessed using the software ImageJ with the Adiposoft plug-in (Parlee et al., 2014). From each tissue section, 5 representative images with 4X magnification were taken (calibrated to 1 pixel = 0.845 µm). The sections were analyzed fully automatically by the software avoiding any bias to be introduced by the user. Adipocyte diameter and area (in µm) were calculated and exported to Excel (Microsoft, Redmond, USA). Approximately 200 ± 100 cells/image were detected resulting in a total of at least 1000 cells assessed per subject in each depot. The average cell diameter and area from 5 representative images were taken for analyses.

Cluster of differentiation (CD) 68 staining

To assess adipose tissue macrophage infiltration, tissue sections were stained for CD68 (alias macrosialin). CD68 is a glycoprotein expressed on the cell surface of cells in the monocyte lineage such as tissue macrophages. Tissue sections were deparaffinized and incubated with anti-human CD68 primary antibody (monoclonal mouse, DAKO, Glostrup, Denmark) at a 1:100 dilution for 1 h at room temperature. Subsequently the slides were incubated with secondary horseradish peroxidase (HRP)-conjugated anti-mouse antibody (Nichirei Biosciences, Tokio, Japan) for 30 min at room temperature. The substrate 3,3'-diaminobenzidine (Sigma-Aldrich, St. Louis, USA) was added, which was catalyzed to a brown colored product by the HRP enzyme at the site of CD68 antigen. Finally, a hematoxylin staining was conducted to mark cell nuclei. Thereafter tissue sections were dehydrated and mounted.

Tissue sections were evaluated for crown-like structures (CLS), defined as >50% of an adipocyte surrounded by macrophages. Representative images at 4X magnification were taken and the number of CLS/ unit area were recorded. For data analysis, histological preparations were categorized into 4 categories according to 0, ≤ 1, ≤ 2, ≥ 3 CLS/ unit area.

Liver biopsies

Liver tissue was H&E stained as described above. Representative images at 20X magnification were taken. Each biopsy was scored for grade of steatosis, lobular inflammation, hepatocellular ballooning, and fibrosis according to histological scoring systems for NAFLD. Severity of NAFLD was assessed by summarizing the scores obtained in each category and calculation of the NAFLD Activity Score (NAS) (Kleiner et al., 2005), as presented in Appendix Table A7, and Steatosis-Fibrosis (SAS) Score (Bedossa et al., 2012), as presented in Appendix Table A8.

The NAS is an unweighted sum of scores of steatosis, lobular inflammation, and hepatocellular ballooning while fibrosis is assessed separately. NAS scores of 0 - 2 are categorized as not NASH, scores of 3-4 are borderline, and scores of 5-8 are considered diagnostic for NASH as assessed in a reference cohort (Kleiner et al., 2005). However, discrepancies between NAS and NASH diagnosis have been described (Rastogi et al., 2017).

The SAF score uses steatosis as an entry criterion for the algorithm as NAFLD is defined by steatosis in > 5% of hepatocytes (Machado et al., 2006), thus not considering steatosis to grade disease severity. All cases with at least grade 1 steatosis were considered NAFLD (steatosis). Hepatocyte ballooning and lobular inflammation were used to assess disease activity. When both scores were at least grade 1, then the lesion was classified as NASH (Bedossa et al., 2012).

3.3.6 Magnetic resonance imaging (MRI) and spectroscopy (^{1}H-MRS)

Intrahepatic lipids (IHL) were determined on a 1.5-T whole-body scanner (Magnetom Avanto, Siemens Healthcare, Erlangen, Germany) conducted at the Ernst von Bergmann Hospital (Department of Diagnostic and Interventional Radiology, Potsdam, Germany). Intrahepatic lipids (IHLs) were quantified by single voxel ^{1}H Magnetic Resonance Spectroscopy (^{1}H-MRS), given as the ratio of fat (methylene + methyl resonances) divided by water + fat.

3.3.7 Enzymatic determination of hepatic TAG content

HB-buffer

- 10 mM NaH2PO4 * H2O
- 1 mM EDTA (pH 7.4)
- 1% polyoxyethylene (10) tridecyl ether

Hepatic tissue was grinded in liquid nitrogen and dissolved in HB-buffer (10 μg/ 100 μl) followed by homogenization in the TissueLyser LT (Qiagen, Hilden, Germany). The tissue homogenate was centrifuged (30 min, 23100 xg, 4°C) and the lipid containing supernatant was collected. After incubation in the thermoshaker (5 min, 70°C) and cooling-down on ice (5 min), the

solution was centrifuged again, and the supernatant was collected. For normalization purposes, protein content of the sample was determined using the Protein Assay Kit (Bio-Rad Laboratories, Hercules, USA) which is based on the Lowry protein assay.

Tissue TAG content was determined using the Triglyceride Determination Kit (Sigma-Aldrich, St. Louis, USA) according to the manufacturer's manual. The assay is based on the enzymatic cleavage of TAG into glycerol and NEFAs by addition of the enzyme lipase. Absorption at 540 nm was measured before and after addition of lipase. The TAG content was normalized to total protein content determined in the sample.

3.3.8   Gene expression analysis

<u>RNA isolation from adipose tissue</u>

RNA was isolated from adipose tissue using the RNeasy Lipid Tissue Kit (Qiagen, Hilden, Germany) according to the manufacturer's instructions. The Approximately 300 mg tissue each from SAT and VAT were used. Tissues were homogenized in the bead mill (SpeedMill, Analytik Jena, Jena, Germany) by addition of a guanidinium thiocyanate-based reagent (QIAzol, Qiagen, Hilden, Germany). After addition of chloroform (Carl Roth GmbH, Karlsruhe, Germany) and centrifugation, the homogenate separated into aqueous and organic phases. The aqueous phase was extracted, and RNA precipitated in ethanol (Carl Roth GmbH, Karlsruhe, Germany) prior to binding to the membrane of the provided columns. DNA, salts, and macromolecular contaminants were removed by several washing steps and inclusion of an incubation step with rDNase (Qiagen, Hilden, Germany). Pure RNA was eluted using RNase free water (MP Biomedicals, Solon, USA).

<u>RNA isolation from liver</u>

For RNA isolation from liver, the NucleoSpin RNA II Kit (Macherey-Nagel, Düren, Germany) was used according to the manufacturer's recommendations. The tissue was homogenized by grinding in liquid nitrogen and subsequent mechanical shearing in the bead mill with added zirconium beads (SpeedMill, Analytik Jena, Jena, Germany). RNA preparation using this kit is based on adsorption of RNA to the silica membrane of a column, followed by two washing steps to remove salts, metabolites, and contaminants. An incubation step with rDNase was included to remove residual DNA. Pure RNA was eluted using RNase/DNase free water.

<u>RNA isolation from cell cultures</u>

For RNA isolation from cell cultures (HepG2, primary murine hepatocytes, primary human adipocytes) the NucleoSpin RNA II Kit (Macherey-Nagel, Düren, Germany) was used according to the manufacturer's manual. Cells were harvested by addition of the provided Lysis Buffer supplemented with freshly added β-mercaptoethanol (Thermo Fisher Scientific,

Waltham, USA) and mechanical removal of adherent cells using cell scrapers. An incubation step with rDNase was included to remove residual DNA

Determination of RNA quantity and quality

RNA concentration and purity were estimated by spectrophotometric analysis using NanoDrop ND 1000 (Thermo Scientific, Wilmington, USA). The absorption of the sample was determined at 260 nm (RNA, DNA), 280 nm (protein, phenolic compounds or other contaminants), and 230 nm (carbohydrates, phenols). A 260/280 ratio above 1.8 together with a 260/230 ratio between 2.0 - 2.2 was considered as "pure" RNA.

For sensitive applications, quality and quantity of RNA was determined by capillary electrophoresis (Bioanalyzer, Agilent technologies, Böblingen, Germany) according to the manufacturer's manual. After a denaturation step (2 min, 70°C), RNA was loaded onto the gel containing chip and separated by application of an electrical field. The resulting electropherogram, the RNA integrity number [(RIN, ranging from 1 (completely degraded) to 10 (intact RNA)] and RNA quantity were provided by the instrument. A RIN value of above 7 was considered sufficient for high-throughput RNA sequencing.

cDNA synthesis

For cDNA synthesis the High Capacity cDNA Reverse Transcription Kit (Thermo Fisher Scientific, Wilmington, USA) was used according to the manufacturer's instructions. In brief, a mix consisting of provided buffer, random primers, RNase inhibitor, the enzyme reverse transcriptase and deoxyribonucleotide triphosphates (dNTPs) was produced and combined with 1µg of RNA. Synthesis of cDNA was performed in the Mastercycler (Eppendorf, Hamburg, Germany) as follows: enzyme activation for 10 min at 25°C, cDNA synthesis for 120 min at 37°C, enzyme inactivation at 85°C for 5 min, cooling down to 4°C after which the samples were removed and stored at -20°C.

Quantitative real-time polymerase chain reaction (qRT-PCR)

Quantification of gene expression was performed using Power SYBR Green PCR Master Mix (Thermo Fisher Scientific, Waltham, USA) according to the manufacturer's instructions. SYBR Green is a double-stranded DNA binding dye that emits a fluorescent signal upon intercalating with DNA. Apart from the dye, the provided Master Mix contained a hot-start DNA-polymerase, dNTPs, and a passive internal reference used to normalize non-PCR-related fluorescence fluctuations. cDNA samples were diluted in RNase/DNase free water. Standards were prepared by pooling cDNA from the respective tissue or cell type and subsequent serial 1:4 dilutions.

Appropriately diluted cDNA was combined with the provided SYBR Green Master Mix as well as forward and reverse primers depending on the gene to be analyzed. Primers (Invitrogen, Carlsbad, USA) were designed using the software Primer Express 2.0 (Applied Biosystems, Thermo Fisher Scientific, Waltham, USA). Water was used as a no-template control to detect extraneous nucleic acid contaminations. Furthermore, a no-reverse transcriptase control was included to detected DNA contamination in the samples. Samples were measured in triplicates. The qRT-PCR reactions were run on the ViiA 7 Real-Time PCR System (Thermo Fisher Scientific, Waltham, USA). The PCR program were as follows: polymerase activation for 10 min at 95 °C followed by 45 cycles denaturation for 15 s at 95°C, annealing and elongation for 1 min at 60°C.

Gene expression was quantified by the PCR software according to the standard curve method. Melt curves were analyzed for possible unspecific PCR products. Relative gene expression was normalized to the geometric mean of expression of the housekeeping genes *RPLP0* and *HPRT*. Primer sequences are listed in section 3.1.5.

3.3.9   Multiplex assay

Wash Buffer

- 1 ml 10X protease inhibitor
- 1 ml 10X phosphatase inhibitor
- 8 ml 1X PBS

Lysis Buffer

- 100 µl 10X protease inhibitor
- 100 µl 10X phosphatase inhibitor
- 100 µl 10X Cell Lysis Buffer
- 700 µl 1x PBS

IFNγ, IL1ß, IL6, IL10, MCP1, and TNFα were determined in serum and tissue lysates by MSD multiplex assay (Meso Scale Diagnostics, Rockville, USA). This technique is based on the ELISA principle and allows parallel measurement of up to 10 biomarkers. In principle, biotinylated capture antibodies are coupled with specific linkers that self-assemble onto unique spots on a 96-well plate. Analytes in the sample bind to the capture antibody and are detected with electrochemiluminescent (ECL) labeled antibodies. The intensity of the emitted light, which is proportional to the analyte present in the sample, is finally measured on the ECL plate reader (Meso Scale Diagnostics, Rockville, USA) .

Serum samples were measured directly while adipose tissue lysates were prepared as follows. 500 – 800 mg tissue was washed twice in Wash Buffer separated from any visible blood clots and centrifuged (5 min, 2000 xg, 4°C). Subsequently, Lysis Buffer was added (1:1) and

homogenized by mechanical disruption (SpeedMill, Analytik Jena, Jena, Germany) (2 x 3 min) and probe sonicator (Labsonic, Braun, Melsungen, Germany) (2 x 5 sec). Finally, the tissue homogenate was rotated for 30 min, centrifuged (5 min, 2000 xg, 4°C), and the supernatant was collected.

The multiplex assay was conducted according to the manufacturer's instructions. In brief, individually prepared linker-antibody-solutions were combined and coated on a 96-well plate. After overnight incubation and washing, samples and standards were added to the plate and incubated for 1 h at room temperature. The plate was washed 3 times and Read Buffer (provided) was added. The plate was analyzed on the MSD ECL imager (Meso Scale Diagnostics, Rockville, USA).

3.3.10 Culture and treatment of HepG2 and primary murine hepatocytes

HepG2

HepG2 Growth Medium

In MEM (without glutamine)
- 2 mM glutamine
- 10% FBS
- 1% NEAA
- 1% antibiotic/antimycotic solution

Human hepatoma cells (HepG2, a gift from Christiane Bumke-Vogt, Department of Endocrinology, Diabetes and Nutrition, Charité-Universitätsmedizin Berlin, Berlin, Germany) were cultivated in HepG2 Growth Medium in a CO2-incubator (37°C, 5% CO_2) (Heraeus, Hanau, Germany). Before confluence, cells were seeded in 6-well TPP plates (Techno Plastic Products, Trasadingen, Switzerland) at a density of 6 x 10^5/well and left to attach overnight. To study the effect of nitrogenous metabolites on *FGF21* expression serum-free MEM medium (Thermo Fisher Scientific, Waltham, USA) was supplemented with different concentrations of ammonium chloride (Merck, Darmstadt, Germany) or glutamine (Thermo Fisher Scientific, Waltham, USA) as indicated in the results. During the last 6 h of the experiment, 5 µg/ml tunicamycin (Sigma-Aldrich, St.Louis, USA) or vehicle control (DMSO, Sigma-Aldrich) were added to induce *FGF21* mRNA.

Primary Hepatocytes

Hepatocyte Complete Medium (HCM)

In MEM:
- 10% FBS
- 1% penicillin-streptomycin

Isolation and treatment of primary hepatocytes was conducted by Steffi Heidenreich (Schupp lab, Institute of Pharmacology, Charité-Universitätsmedizin Berlin, corporate member of Freie Universität Berlin, Humboldt-Universität zu Berlin, and Berlin Institute of Health, Berlin, Germany).

Primary hepatocytes were isolated from healthy male C57BL/6J mice by perfusing livers with EBSS (Thermo Fisher Scientific, Waltham, USA) followed by digestion buffer [5000 U/ml collagenase, type I (Worthington Biochemical, Lakewood, USA) in HBSS (Thermo Fisher Scientific, Waltham, USA)]. Hepatocytes were released from excised livers by carefully applying pressure on the liver lobes. The obtained cell suspension was filtered through a 100-µm-mesh and separated by Percoll gradient centrifugation (Biochrom, Berlin, Germany). Cells were seeded at a density of 2.5 x 105 cells/well on 12-well collagen I-coated plates (BD Biosciences, San Jose, USA) Hepatocyte Complete Medium (HCM). For experiments, cells were allowed to settle down for 5 h in HCM, after which medium was changed to serum-free MEM overnight. One day after isolation, increasing concentrations of ammonium chloride or glutamine were added to the media for 24 h after which cells were harvested.

<u>RNA interference and adenoviral delivery</u>

To study the effect of Hes6 on *Fgf21* expression, Hes6 was silenced using small interfering RNAs (siRNA) and overexpressed by means of an adenoviral vector. For siRNA experiments, isolated primary hepatocytes were allowed to settle down for 4 h in complete medium after which medium was changed to serum-free MEM (Thermo Fisher Scientific, Waltham, USA). Cells were transfected overnight with siRNA directed against *Hes6* or negative controls (all Qiagen, Hilden, Germany) using lipofectamine transfection reagent (Thermo Fisher Scientific, Waltham, USA) according to the manufacturer's recommendations. The next morning, medium was changed to hepatocyte complete medium and cells were harvested 48 h after transfection.

For overexpression experiments, primary hepatocytes were transduced with adenoviral-associated viral particles overexpressing *Hes6* or *GFP* control. Viral load for Adeno-mHes6 and Adeno-GFP was 1.1×10^{11} and 1.2×10^{11} infectious units/ml, respectively, which was diluted 1:100 and added to the wells at increasing concentrations (0.1 µl, 1 µl, and 10 µl). Hepatocytes were harvested 48h after transduction and expression of Hes6 and Fgf21 mRNA was determined by qRT-PCR.

3.3.11 Culture, differentiation, and treatment of human primary adipocytes

<u>Isolation of human mesenchymal stromal cells (hMSCs)</u>

After transportation to the laboratory, SAT and VAT biopsies were repeatedly washed with PBS and cut with a scalpel into small pieces. Visible connective tissue or blood clots were

removed. Isolation of hMSCs was conducted based on the protocol provided by (Lee and Fried, 2014) with minor modifications.

The minced tissue was weighed and digested with collagenase D (Sigma-Aldrich, St. Louis, USA) to create a single cell suspension (30 min – 2 h, 37°C). Progress of tissue disaggregation was checked regularly. Under the cell culture bench tissue was further homogenized by shaking and gentle pipetting. If needed, the digested tissue was filtered through a sterilized funnel with an attached 250 µm nylon mesh and washed with PBS. The flow-through was transferred to a 50 ml tube and centrifuged (6 min, 350 xg, room temperature).

After centrifugation three layers became visible: a fat layer on the top, medium in the middle and a cell pellet on the bottom. After aspiration of the upper layers, the cell pellet was resuspended in red RBC lysis buffer (Sigma-Aldrich, St. Louis, USA) and incubated for 10 min in the dark. After centrifugation (6 min, 350 xg) the cell pellet was resuspended in complete Preadipocyte Growth Medium (Promo Cell, Heidelberg, Germany), cells were counted using a hemocytometer and plated accordingly on Primaria cell culture plates (Corning, New York, USA). After overnight attachment, cells were washed twice with PBS and refed with Preadipocyte Growth Medium. Thereafter cells were washed as needed and refed twice a week. Before confluence, cells were either split or frozen in liquid nitrogen [5 x 10^5 cells/tube in 70% medium, 20% HyClone (Fisher Scientific, Waltham, USA), 10% DMSO].

Primary adipocyte differentiation

Adipocyte Differentiation Medium

In DMEM/F12:
- 500 µM IBMX
- 25 nM dexamethasone
- 0.2 nM T3
- 8 µg/ml biotin
- 5 mM panthothenat
- 100 nM hydrocortisone
- 20 nM human insulin
- 0.01 µg/ml transferrin
- 2 µM rosiglitazone

Adipocyte Maintenance Medium

In DMEM:
- 10% FBS (HyClone)

Preadipocytes were plated on 6-well Primaria plates (Corning, New York, USA) at a density of 3 x 10^5 cells/well. Postconfluent cells were induced to differentiate by the addition of Adipocyte

Differentiation Medium. The medium was replenished twice per week for 14 days. Thereafter cells were washed twice with PBS and cultured in Adipocyte Maintenance Medium for at least 5-7 days prior to an experiment. Degree of differentiation was determined by analysis of mRNA expression of adipocyte marker genes and Oil Red O staining (Sigma-Aldrich, St. Louis, USA) according to the manufacturer's manual. The dye Oil Red O specifically stains triglycerides which can be quantified by measuring the absorbance at 518 nm.

<u>Stimulation of mature adipocytes</u>
Fully differentiated adipocytes from SAT were treated with increasing concentrations (0.1 nM – 30 nM) of recombinant human chemerin (R&D systems, Minneapolis, USA) or vehicle control (PBS with 0.1% BSA). Furthermore, mature adipocytes were treated with palmitic acid (350 µM), arachidonic acid (200 µM), a fatty acid mixture (1%) (all Sigma-Aldrich, St. Louis, USA), or vehicle control [1% Tween-40 (Sigma-Aldrich, St. Louis, USA)]. After 24 h cells were harvested, and mRNA expression was determined by qRT-PCR.

3.3.12 Animal studies

Samples from a previously published study in ten-week old male C57BL/6 mice (Charles River, Sulzfeld, Germany) fed for 20 weeks with semisynthetic HF diets (20% w/w of fat) containing either an adequate (AP: 8.9 EN% protein) or high (HP: 44.8 EN% protein) amount of whey protein, or an AP diet supplemented with L-leucine corresponding to the leucine content of the HP diet (AP+L: 6% w/w leucine) (Freudenberg et al., 2012) were reanalyzed for expression of *Fgf21* and *Atf4*. Furthermore, gene expression was assessed in samples from a 1-week trial conducted under the same conditions (Freudenberg et al., 2013). Here, the diet was supplemented with equimolar L-leucine or L-alanine to separate leucine specific effects (n = 7-8 per group). The experiments were performed in accordance with the guidelines of the ethics committee of the Ministry for Environment, Health and Consumer Protection (State Brandenburg, Germany, Permission No. 23-2347-8-3-2008).

3.3.13 Statistics

Before data analysis, parameters were tested for plausibility by identifying outliers defined as a data point whose distance from the median exceeds 1.5 times the interquartile range of a box-and-whiskers plot. In view of the high variability of human data and the small cohort sizes, data points obtained in cohort 1 and 3 were only excluded if reasonable. In respective cases, findings were reanalyzed, and divergent results were reported.

Variables were tested for normal distribution with the Shapiro-Wilk (cohort 1, cohort 3) or Kolmogorov-Smirnov (cohort 2) test depending on cohort size. Non-normally distributed variables were transformed with the natural logarithm (ln) and reassessed for normality. Paired

Student's t-test or non-parametric Wilcoxon test were used to test for differences between two time points with a group. Unpaired Student's t-test or non-parametric Mann-Whitney-U test were used to test for differences between two different groups. Multiple comparisons were performed by 1-way (> 2 groups) or repeated-measures ANOVA (> 2 time points) followed by *post-hoc* analysis (Bonferroni). 2-way ANOVA was applied to test for differences between groups defined by multiple independent variables. Pearson's coefficient or Spearman's rank correlation coefficient was used for correlation analysis of variables with normal and skewed distribution, respectively. For the primary cell culture experiments representative results of at least three independent experiments are shown.

All statistical analyses were performed with SPSS software, version 24.0 (IBM SPSS. Chicago, IL, USA). Values are expressed as mean ± SEM unless otherwise stated. Statistical significance was designated at $P < 0.05$ and significant results were indicated with asterisks (*$P < 0.05$, **$P < 0.01$, ***$P < 0.001$).

4 Results

4.1 The LEMBAS intervention study

4.1.1 Baseline characteristics of the study participants

For the LEMBAs study (cohort 1), morbidly obese subjects were recruited and randomly assigned to the low-protein (LP, 10 EN%) or high-protein (HP, 30 EN%) group. 20 participants completed the study, 10 in each group. One participant in the HP group was excluded from the study for reasons of noncompliance resulting in ultimately 9 subjects in the HP group. The randomization parameters are outline in Table 2. There were no significant differences in these parameters between the groups.

Table 2 ǀ Randomization parameters.

Parameter	LP	HP	P_{LPvsHP}
Participants [n]	10	9	
Sex [f/m]	6 / 4	6 / 3	
Age [y]	47.2 ± 8.7	48.7 ± 9.1	0.188
BMI [kg/m^2]	45.2 ± 1.2	44.5 ± 1.3	0.693

Data are mean ± SEM.

The dietary interventions lasted for 3 weeks prior to bariatric surgery. At baseline and after the intervention serum was taken (LP: n = 10, HP: n = 7) and the participants were anthropometrically characterized (LP: n = 10, HP: n = 9). During bariatric surgery, serum as well as liver and abdominal adipose tissue biopsies from the subcutaneous and visceral (omental) fat depot were obtained (LP: n = 10, HP: n = 9).

Furthermore, serum and tissue samples were collected from 15 additional subjects during surgery only. This group did not participate in the dietary interventions and was termed the reference protein (RP: n = 15) group.

Table 3 ǀ Basic parameters of the RP group.

Parameter	RP
Participants [n]	15
Sex [f/m]	2 / 13
Age [y]	45.6 ± 3.5
BMI [kg/m^2]	41.5 ± 1.1

The RP group did not participate in the dietary interventions. However, serum and tissue samples were collected during surgery. Data are mean ± SEM.

4.1.2 Anthropometry and body composition

The dietary interventions were moderately hypocaloric (1500-1600 kcal/d) aiming for a weight and particularly liver fat reduction in preparation for bariatric surgery. The LP and HP diet differed in the amount of protein which was balanced by carbohydrates while keeping fat intake constant at 25-35 EN% (the study design is depicted in Figure 3A). The intervention groups received detailed food plans as well as dietary counseling before the intervention (the documents were prepared and provided to the study subjects by the MSc student Kathleen Herz).

After three weeks on the respective diet, participants in both groups significantly lost body weight (LP: -5.31 ± 0.99 kg, HP: -4.69 ± 0.98 kg, P_{LPvsHP} = 0.860). In accordance, BMI reduced in both groups in response to the hypocaloric interventions (LP: -1.73 ± 0.28 kg/m², HP: -1.54 ± 0.32 kg/m², P_{LPvsHP} = 0.842) (Figure 3B).

A
          B
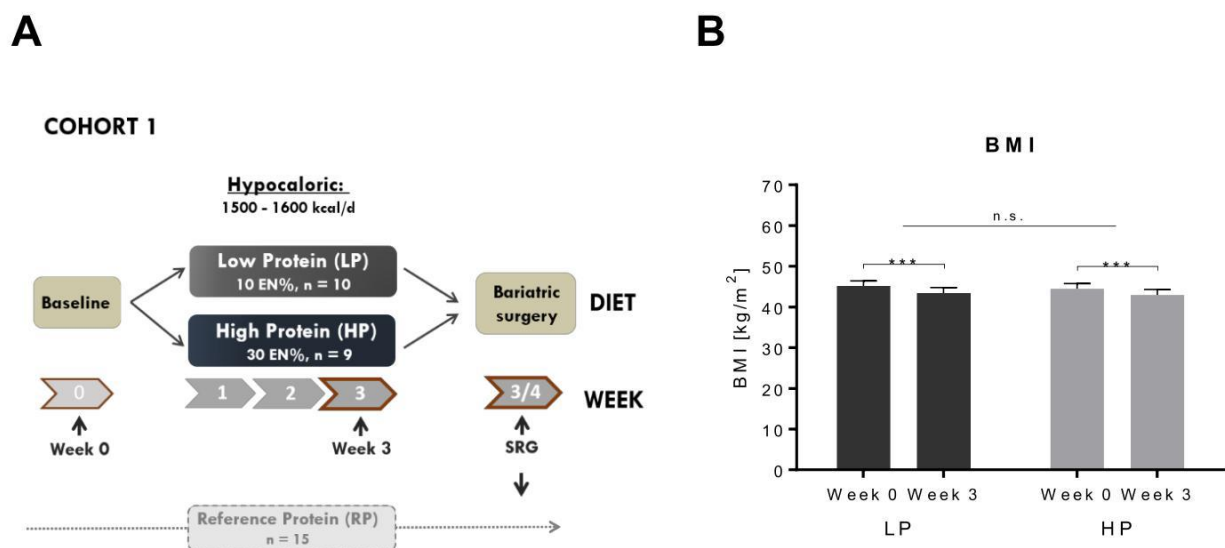
Figure 3 I Design of the LEMBAS study and changes in BMI. A, Morbidly obese subjects consumed hypocaloric low-protein (LP, 10 EN%) or high-protein (HP, 30 EN%) diets 3 weeks prior to bariatric surgery. Subjects in the RP group did not participate in the dietary interventions. However, blood and tissue samples from these participants were collected during surgery. **B,** Body weight and body height were assessed before and after the 3-week dietary interventions. BMI = kg/m². SRG indicates surgery. n.s., not significant. ***$P < 0.001$ different from week 0.

Participants in both groups effectively reduced their waist circumference (P_{LP} = 0.004, P_{HP} = 0.009), while the changes in hip circumference were only significant in the LP group (P_{LP} = 0.019) (Table 4). The reductions in waist-to-hip ratio (WHR) remained not significant as well as the changes in fat mass which were determined by BOD POD measurement (Table 4). There were no significant differences between the groups in the anthropometric measures assessed.

Table 4 ı Diet induced changes in anthropometric measures.

Parameter	Low Protein			High Protein			
	Week 0	Week 3	P_{LP}	Week 0	Week 3	P_{HP}	P_{HPvsLP}
Waist circumf. [cm]	134.5 ± 4.4	129.9 ± 4.1	**0.004**	134.4 ± 5.4	127.7 ± 5.5	**0.009**	0.369
Hip circumf. [cm]	136.0 ± 3.8	134.1 ± 3.9	**0.019**	139.8 ± 3.6	138.0 ± 3.8	0.444	0.548
WHR	1.00 ± 0.04	0.97 ± 0.04	0.058	0.97 ± 0.04	0.93 ± 0.28	0.081	0.904
Fat mass [kg]	69.8 ± 5.9	65.0 ± 4.9	0.052	77.4 ± 9.6	77.8 ± 8.8	0.252	0.898
Fat mass [%]	53.0 ± 2.6	51.6 ± 2.1	0.421	54.8 ± 2.7	55.6 ± 2.8	0.839	0.873
Lean mass [kg]	61.0 ± 4.5	60.9 ± 4.2	0.978	62.2 ± 5.2	60.6 ± 4.9	0.203	1.000
Lean mass [%]	47.0 ± 2.6	48.4 ± 2.1	0.910	45.2 ± 2.7	44.4 ± 2.8	0.839	0.841

Before (week 0) and after (week 3) the intervention participants were anthropometrically assessed. Fat mass and lean mass were determined by air displacement plethysmography (BOD POD) in the fasted state. Data are mean ± SEM. *P*-values refer to differences between the groups in absolute change from week 0 to week 3. Significant values (*P* < 0.05) are marked in bold. Circumf. indicates circumference, WHR, waist-to-hip ratio.

4.1.3 Routine parameters in blood

Changes in indicators of glucose metabolism are shown in Figure 4. Fasting glucose and insulin levels at baseline were not significantly different between the groups (Appendix Table A1). In both groups, LP and HP, participants significantly reduced their fasting insulin levels in response to the intervention (P_{LP} = 0.007, P_{HP} = 0.042, P_{LPvsHP} not significant) while the reduction in fasting glucose was only significant in the LP group (P_{LP} = 0.005, P_{LPvsHP} = 0.029) (Figure 4). Mean glycated haemoglobin (HbA1c) was 6.3% [categorized as impaired fasting glycaemia (2009)] in the LP and 5.6% [categorized as normal glycaemia (2009)] in the HP group (P_{LPvsHP} not significant). HbA1c, a long-term indicator of blood glucose levels, did not change in either group in response to the 3-week intervention.

Two indicators of insulin sensitivity were calculated. The Homeostatic Model Assessment of Insulin Resistance (HOMA-IR) (Matthews et al., 1985) and the adipose tissue insulin resistance (Adipo-IR) (Gastaldelli et al., 2017). In the LP group, HOMA-IR decreased markedly from 11.7 ± 2.4 to 4.3 ± 0.6 (- 62.8%, P_{LP} = 0.007) (Figure 4). In the HP group HOMA-IR decreased in response to the dietary intervention being marginally significant (- 40.0%, P_{HP} = 0.081). The improvements in HOMA-IR were not significantly different between the groups. Furthermore, the mean HOMA-IR in both groups was still in the range of severe insulin resistance (Salgado et al., 2010). Adipo-IR improved in both groups. However, statistical significance was only reached in the LP group (LP: - 40.6%, *P* = 0.034; HP: - 36.3 %, *P* = 0.576) (Figure 4). The changes from week 0 to week 3 were not significantly different between the LP and HP group.
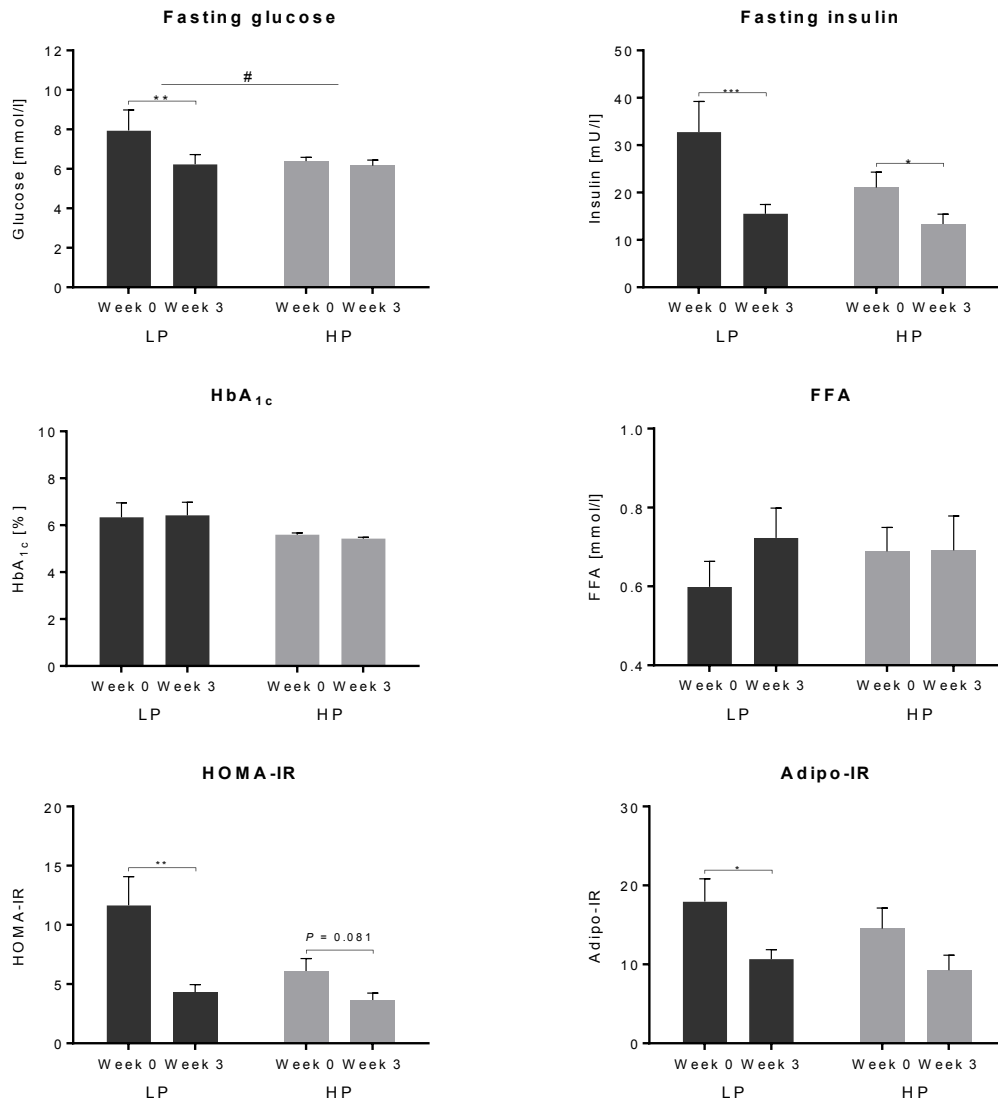
Figure 4 ǀ Diet induced changes in indicators of glucose homeostasis. Glucose, insulin, and FFA were measured in serum, HbA1c in whole blood, collected in the fasted state. Measures of insulin resistance were calculated as follows: HOMA-IR = (fasting insulin in mU/l x fasting glucose in mmol/l) / 22.5, Adipo-IR = fasting insulin in mU/l x fasting free fatty acids in mmol/l. *P < 0.01, **P < 0.01, P < 0.001 different from week 0. #P < 0.05 difference in relative change in time between the groups.

As an indicator for compliance, urea concentrations in serum were measured. Baseline urea levels were not significantly different between the groups (Appendix Table A1). In response to the intervention, urea strongly decreased in the LP group (P = 0.001) while it increased in the HP group (P = 0.031, P_{HPvsLP} < 0.001) indicating compliance of the study participants (Table 5).

Serum creatinine was measured as an indicator for renal function. The creatinine levels of all participants, except one man in the LP group, were within the normal range [women: 45 to 90 µmol/l, men: 60 to 110 µmol/l (Delanaye et al., 2017)]. Serum creatinine increased slightly in response to the LP diet with no effect on the number of participants being outside the normal range. Furthermore, hyperuricemia is often associated with obesity (Lin et al., 2006). In total,

eight participants (four in each group) had higher than normal serum uric acid levels [women: 140–360 µmol/l, men: 200–430 µmol/l (Desideri et al., 2014)] at baseline. In response to the intervention creatinine levels in the LP group increased significantly (P_{LP} = 0.013) such that one additional participant was characterized with abnormal creatinine levels (Table 5). In contrast, circulating creatinine concentrations declined insignificantly in the HP group which caused one participant to switch into the normal range category (Table 5). The changes in creatinine were significantly different between the groups (P_{LPvsHP} = 0.015).

There were little changes in blood lipids in response to the 3-week dietary interventions. In the HP group, serum TAG, HDL cholesterol and FFA remained unchanged while total cholesterol and LDL cholesterol decreased in response to the HP diet (HP: P = 0.040 and P = 0.033, respectively) (Table 5). In the LP group, LDL cholesterol showed a trend to decline in response to the diet (P_{LP} = 0.052) while other blood lipids remained unchanged (Table 5). The absolute changes in blood lipids were not different between the groups.

The liver enzyme aspartate aminotransferase (AST), alanine aminotransferase (ALT), and gamma-glutamyl transferase (γ-GT) were measured to assess hepatic function. There were no significant differences in AST. Before the intervention, γ-GT activity in serum was considerably but insignificantly higher in the LP group. In response to the LP diet, γ-GT levels were effectively reduced (- 24.3 U/l, P_{LP} < 0.001) (Table 5). ALT activity was higher after the HP diet (P_{HP} = 0.006) but still within the normal range [7 – 55 U/l (Giannini et al., 2005)] (Table 5).

Table 5 ı Diet induced changes in routine parameters in blood.

Parameter	Low Protein			High Protein			
	Week 0	Week 3	P_{LP}	Week 0	Week 3	P_{HP}	P_{LPvsHP}
<u>Renal</u>							
Urea [mmol/l]	5.26 ± 0.39	3.17 ± 0.26	**< 0.001**	4.69 ± 0.47	6.04 ± 0.62	**0.031**	**< 0.001**
Creatinine [µmol/l]	77.6 ± 7.7	85.2 ± 8.7	**0.013**	77.1 ± 6.1	75.6 ± 5.3	0.473	**0.015**
Uric acid [µmol/l]	362 ± 30	390 ± 18	**0.050**	390 ± 39	362.8 ± 23.9	0.120	**0.012**
<u>Cardiovascular</u>							
TAG [mmol/l]	2.11 ± 0.22	2.31 ± 0.28	0.515	1.48 ± 0.11	1.23 ± 0.08	0.077	0.172
Cholesterol [mmol/l]	4.81 ± 0.35	4.46 ± 0.21	0.121	4.87 ± 0.44	4.17 ± 0.41	**0.040**	0.470
HDL [mmol/l]	0.98 ± 0.07	0.92 ± 0.04	0.138	1.11 ± 0.10	1.02 ± 0.06	0.578	0.979
LDL [mmol/l]	2.87 ± 0.30	2.50 ± 0.25	0.052	3.09 ± 0.38	2.58 ± 0.38	**0.033**	0.967
FFA [mmol/l]	0.60 ± 0.06	0.72 ± 0.08	0.214	0.69 ± 0.06	0.69 ± 0.09	0.956	0.477
<u>Hepatic</u>							
AST [U/l]	32.3 ± 6.6	34.7 ± 5.0	0.240	24.4 ± 3.4	36.6 ± 11.8	0.375	0.887
ALT [U/l]	44.3 ± 10.8	43.8 ± 5.6	0.444	36.7 ± 8.3	50.3 ± 9.8	**0.006**	0.154
γ-GT [U/l]	66.2 ± 24.1	41.8 ± 12.7	**0.001**	34.6 ± 10.9	56.1 ± 31.3	0.375	**0.003**

All parameters were measured in serum in the fasted state. Data are mean ± SEM. P_{LPvsHP}-values refer to differences between the groups in absolute change from week 0 to week 3. Significant values ($P < 0.05$) are marked in bold.

4.1.4 Liver fat and progression of NAFLD

In preparation for bariatric surgery patients are routinely advised to consume an energy-restricted diet aiming to reduce liver fat content due to its association with increased risks during surgery (Alami et al., 2007; Schouten et al., 2016). In order to assess whether the LP or HP diet were more effective in improving hepatic steatosis in the 3-week interventions preceding bariatric surgery several analyses to assess the degree of NAFLD in the morbidly obese study subjects were employed.

First, the fatty liver index (FLI) (Bedogni et al., 2006), an algorithm based on waist circumference, BMI, TAG, and γ-GT for the prediction of fatty liver, was calculated. Both study groups had a baseline FLI of over 60% indicating hepatic steatosis (Bedogni et al., 2006). The FLI improved in the LP group by -16.8% (P_{LP} = 0.010, n = 10) and in the HP group by -20.5% (P_{HP} = 0.043, n = 7). Thus, both diets effectively improved FLI with no significant differences, neither in the absolute nor relative change, between the groups.

Second, before and after the intervention intrahepatic lipids (IHL) were assessed by MRI$_{spec}$ (LP: n = 6, HP: n = 5). Hepatic fat content of all participants was considerably higher than the threshold of 5.56% for NAFLD definition (Szczepaniak et al., 2005). Baseline IHL levels were higher in the LP compared to the HP group (LP: 22.7 ± 3.5%, HP: 12.4 ± 2.2%, P_{LPvsHP} = 0.032) (Appendix Table A1). In response to the protein enriched diet, IHL content in livers of the HP participants was extensively reduced, resulting in an overall decrease of - 42.6% (P_{HP} = 0.014). In contrast, in the LP group, the IHL reduction (-11.5%) was not significant and two participants even had higher IHL content after the intervention. Comparison of the change in response to diet between the groups confirmed a significantly higher reduction of IHL in the HP group (absolute and relative change both P_{LPvsHP} < 0.001).

After the dietary interventions, liver tissue samples were collected from the participants undergoing bariatric surgery, including those of the RP group. Hepatic TAG content of the biopsies was determined enzymatically and compared to the MRI$_{spec}$ measurements. Both methods for determining hepatic lipids (*in vivo* by MRI$_{spec}$ or *ex vivo* in the tissue samples via enzymatic digestion) highly correlated (r = 0.790, P = 0.004) indicating that the data is robust. The *ex vivo* results confirmed that lipid content was considerably lower in the livers collected from the HP participants (1-way ANOVA P = 0.002, *post-hoc* Bonferroni P_{LPvsHP} = 0.002, P_{LPvsRP}= 0.031) (Figure 5C). However, it should be noted, that the MRI$_{spec}$ measurements already indicated that hepatic lipid contents of the LP participants were very high already before the intervention (Figure 5B). Hence, the lower hepatic TAG content in the HP group at week 3, as determined enzymatically, may not reflect a diet-specific effect.

In order to assess if the strong reduction of IHL in the HP group was due to either increased lipid oxidation or decreased lipid uptake, mRNA expression of genes involved in hepatic lipid metabolism were measured. Genes regulating fat uptake (LPL, P_{LPvsHP} = 0.006), *de novo* lipogenesis (FASN: P_{LPvsHP} = 0.005; SREBP1c: P_{LPvsHP} = 0.025; ChREBP: P_{LPvsHP} = 0.049), and synthesis of monounsaturated fatty acids (SCD1: P_{LPvsHP} = 0.007) were significantly lower expressed in the HP than in the LP group (Figure 5D). However, lipid catabolism remained unaffected by the diets as no change in expression of genes involved in fatty acid β-oxidation (ACOX1 and PPARα both P_{LPvsHP} not significant) were detected (Figure 5B).
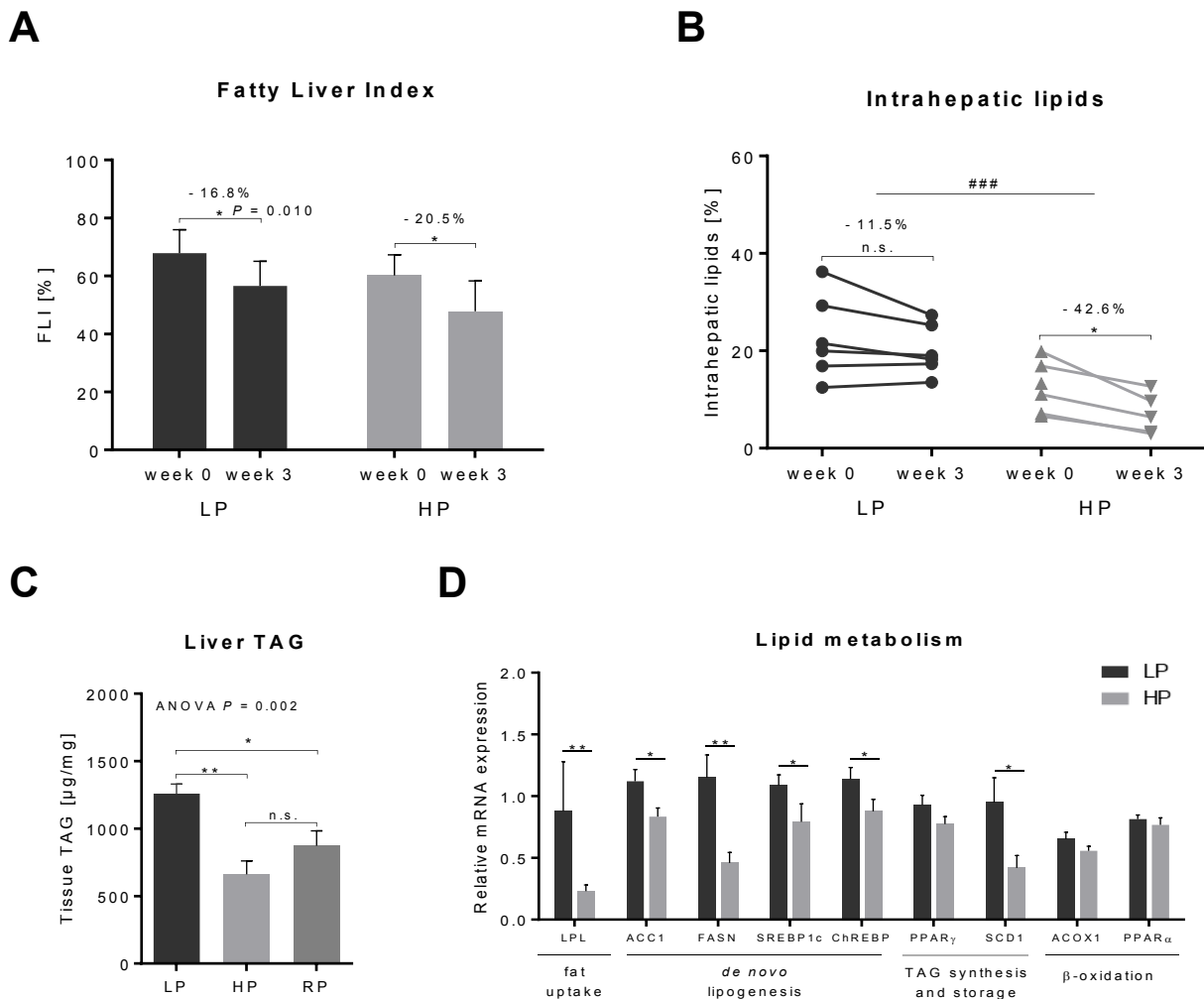
Figure 5 ǀ Assessment of hepatic lipid content. A, FLI was calculated according to Bedogni et al. (Bedogni et al., 2006). **B,** IHL content was determined by MRI_spec (LP: n = 6, HP: n = 5) before and after the intervention. **C,** Liver TAG content was determined *ex vivo* in the liver biopsies collected during surgery. **D,** Expression of genes involved in hepatic lipid metabolism as determined by qRT-PCR in the liver biopsies. Asterisks indicate statistical significance as follows *P < 0.05, **P < 0.01. *P < 0.05, ** P < 0.01. ##P < 0.01 difference in relative change between the groups. n.s. indictes not significant; LPL, lipoprotein lipase; ACC1, acetyl-CoA carboxylase; FASN, fatty acid synthase; SREBP1c, sterol regulatory element-binding protein 1; ChREBP, carbohydrate-response element-binding protein; PPARγ, peroxisome proliferator-activated receptor gamma; SCD1, stearoyl-CoA desaturase-1; ACOX1, peroxisomal acyl-coenzyme A oxidase; PPARα, peroxisome proliferator-activated receptor alpha

Histological preparations of the tissue samples were produced and stained with hematoxylin and eosin (HE) by Elisabeth Meyer [Max Rubner Laboratory, German Institute of Human

Nutrition (DIfE)]. Liver biopsies were histologically assessed for severity of NAFLD in four categories: steatosis, hepatocellular ballooning, lobular inflammation, and stage of fibrosis (Figure 7). Based on the histological assessment, the SAF (Steatosis, Activity and Fibrosis) score and the NAS (NAFLD activity score, range: 0-8) were calculated.

The NAS is intended to be used to grade disease activity after confirmed NAFLD diagnosis (Kleiner et al., 2005). However, Bedossa and colleagues argue that grade of steatosis should not be considered for grading disease severity as no detrimental effects of liver fat *per se* have been proven The authors developed a modified algorithm, the SAF score (Bedossa et al., 2012). The SAF score differentiates between "normal", "steatosis" (NAFLD), and "NASH", whereas the NAS grades disease activity and includes the category "borderline" [for details see methods (section 3.3.5) and Appendix Table A7 and Table A8]. The histological scores obtained for the LEMBAS cohort are presented in Table 6.

Table 6 I Classification of study participants according to SAF and NAS score.

Parameter	LP	HP	RP
SAF score			
Normal	0	3	5
Steatosis	7	5	7
NASH	3	1	3
NAS			
Normal	0	3	5
Steatosis	7	5	4
Borderline	2	1	6
NASH	1	0	0

Scores are calculated based on histological assessment of liver biopsies used to determine severity of NAFLD (according to Appendix Table A7 and Table A8). Data are absolute number of participants.
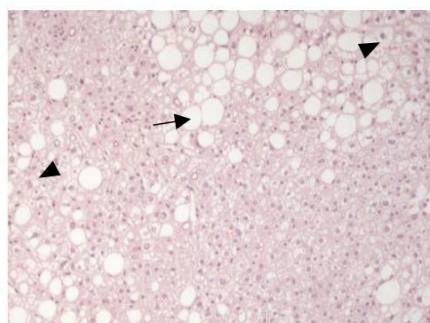
Figure 6 I Histological preparation of liver tissue. Exemplary histological preparation of liver biopsy of a patient diagnosed as "NASH" according to SAF score. Arrow indicates steatosis, arrowhead indicates ballooning.

As expected, a higher histological NAFLD score was associated with a higher TAG content (Figure 7A-B, both scores 1-way ANOVA $P < 0.001$). Biopsies categorized as "normal" according to SAF score had a mean TAG content of 422.7 ± 48.0 µg/mg protein in the tissue whereas the mean TAG content of those samples categorized as "NASH" was 1142.1 ± 119.2 µg/mg (*post-hoc* Bonferroni $P < 0.001$ different from "normal") (Figure 7A). Application of NAS instead of SAF resulted in only one participant being grouped in the "NASH" category while most samples were "borderline" (Figure 7B and Table 6).

The histological scoring systems, SAF and NAS score, have been reported to be positively correlated with liver enzymes (Rastogi et al., 2017). In the present study, only a weak positive correlation between NAS and γ-GT was found ($\rho = 0.352$, $P = 0.044$). Furthermore, correlation of γ-GT with NAS was mainly driven by the one participant categorized as "NASH".

A

B

C

D
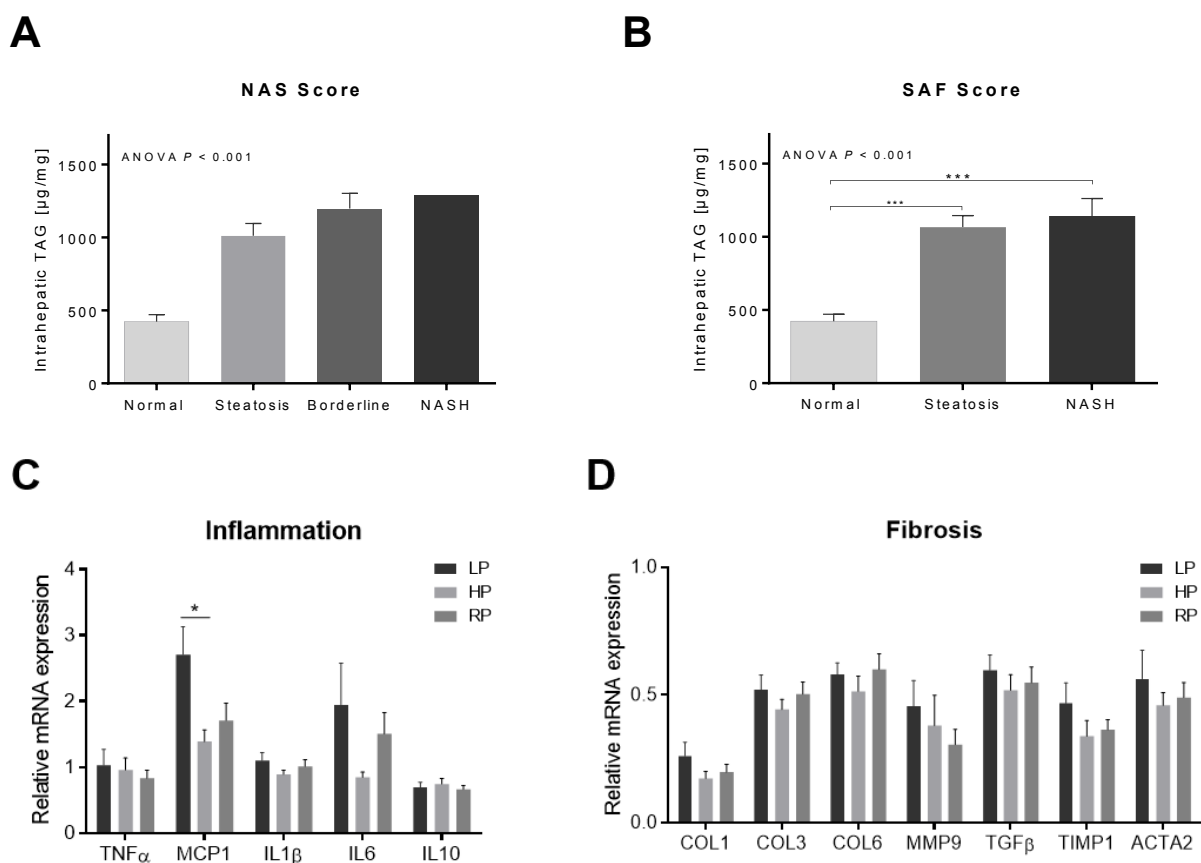
Figure 7 ǀ Histological and molecular assessment of hepatic tissue biopsies. A-B, SAF and NAS scores, as determined histologically, are highly associated with the enzymatically determined TAG content in the tissue. **C,** mRNA expression of cytokines in hepatic tissue biopsies, **D,** mRNA expression of fibrosis-associated genes in hepatic tissue biopsies. ***$P < 0.001$ different from "normal" (B), *$P < 0.05$ difference between the groups (C).

In addition, hepatic mRNA expression of inflammatory and fibrosis markers was assessed. Mean expression of the pro-inflammatory cytokines *tumor necrosis factor α* (TNFα), *monocyte chemoattractant protein-1* (MCP1), *interleukin 1β* (IL1β), and *interleukin 6* (IL6) were higher in the LP than in the HP or RP group though only *MCP1* reached statistical significance (1-way ANOVA $P = 0.023$, *post-hoc* Bonferroni $P_{LPvsHP} = 0.034$) (Figure 7C). There were no differences in hepatic expression of the anti-inflammatory cytokine *interleukin 10* (IL10) (Figure 7C).

As an indicator for fibrosis, mRNA expression of the *collagens type 1, 3* and *6* (COL1, COL3, COL6), as well as *transforming growth factor β* (TGFβ), *metalloproteinase 9* (MMP9), *tissue inhibitor of metalloproteinase 1* (TIMP1), and *α-smooth muscle actin* (ACTA2) were analyzed in the liver biopsies. Mean mRNA expression of all fibrosis-associated genes was higher in the LP than in the HP group though not being statistically significant (Figure 7D).

4.1.5   Adipocyte morphology and adipose lipid metabolism

Paired adipose tissue biopsies from SAT and VAT were collected during surgery. Small tissue pieces were histologically assessed by hematoxylin and eosin (HE-) staining to visualize adipocyte morphology and by CD68 staining (also known as Gp110 or macrosialin), a

transmembrane glycoprotein that specifically marks macrophages and monocytes within the tissue. Analysis of the histological adipose tissue preparations was supported by the MSc student Elisabeth Friedl.

Already macroscopically SAT differed from VAT in terms of structure and color. SAT had a higher degree of pervading blood vessels and appeared tighter in its constitution (Figure 8A). In contrast, VAT biopsies were whiter and seemed almost semi-liquid (Figure 8B). Histological preparations and HE-staining made the mature adipocytes and their nuclei visible. As described in the literature (Green and Kehinde, 1975), adipocytes had a unilocular morphology with a large lipid droplet in the middle, displacing the cytoplasm and nucleus to the side (Figure 8D) .

A

B

C

D
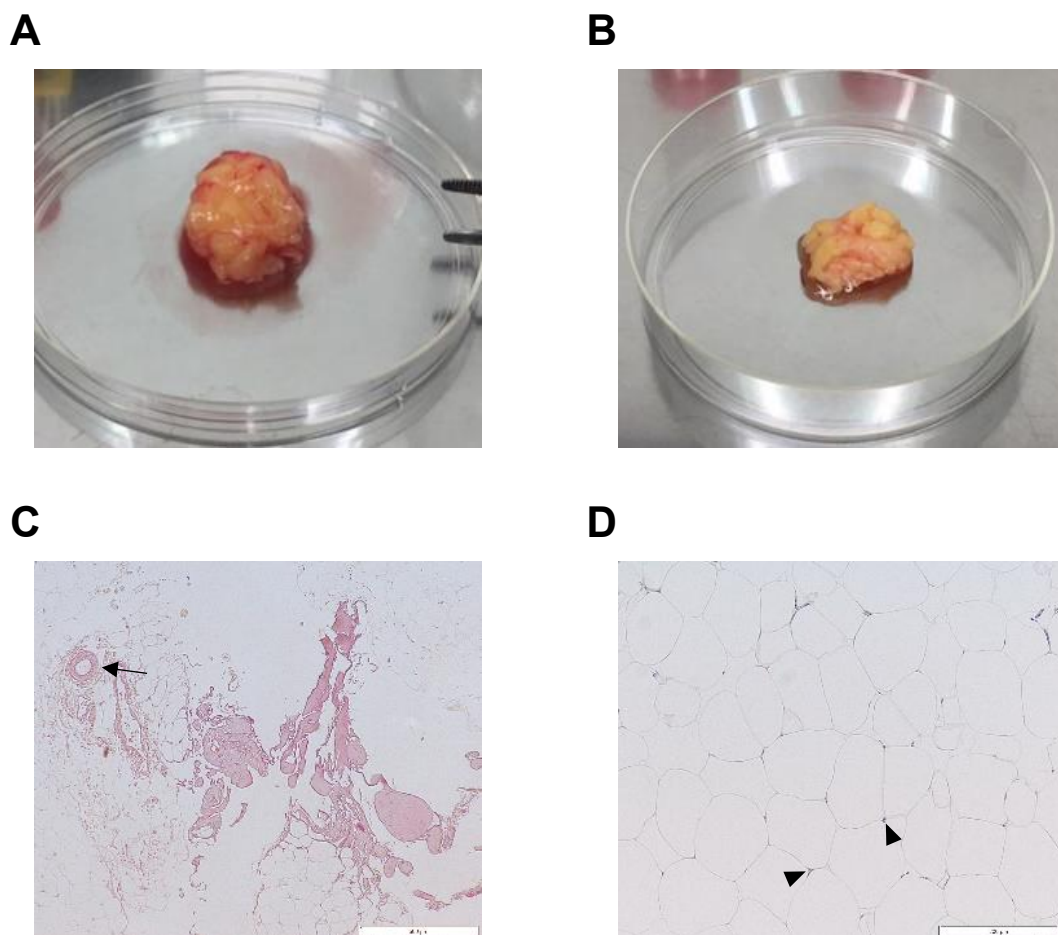
Figure 8 ı Representative images of adipose tissue biopsies and HE-stained histological preparations. A-B, Paired adipose tissue biopsies from subcutaneous (A) and visceral (B) fat depot collected during bariatric surgery (LP: n = 10, HP: n = 9, RP: n = 15). **C,** Representative microscopical image (4X magnification) of VAT showing blood vessels (arrow) and tissue segmentation by connective tissue. **D,** Microscopical image from SAT (10x magnification) showing lipid-filled adipocytes with peripheral nuclei (arrowheads).

The adipocytes from the subcutaneous fat depot were significantly larger than those in the visceral depot (SAT: 87.1 ± 0.99 µm, VAT: 79.89 ± 0.90 µm, P_{SATvsVAT} < 0.001) (Figure 9A, left panel). However, there were no differences in cell size between the intervention groups in

either depot (Figure 9A, right panel). The same results were obtained for adipocyte area, which was calculated based on cell size ($P_{SATvsVAT}$ < 0.001) (data not shown).

Next, the data were assessed for differences in the distribution of cell size between the fat depots. As already indicated by the mean adipocyte diameter, a higher ratio of large cells was detected in the histological preparations of SAT (Figure 9B, left panel). There were no differences in mean cell size as well as cell size distribution between diabetic (n = 8) and non-diabetic (n = 26) subjects in either fat depot (Figure 9B, right two panels). Selection of participants with the highest and lowest HbA1c resulted in significantly larger adipocytes in SAT in the high-HbA1c group compared to the low-HbA1c group (P = 0.032) (not shown), whereas there was no difference detected in VAT.

A

B
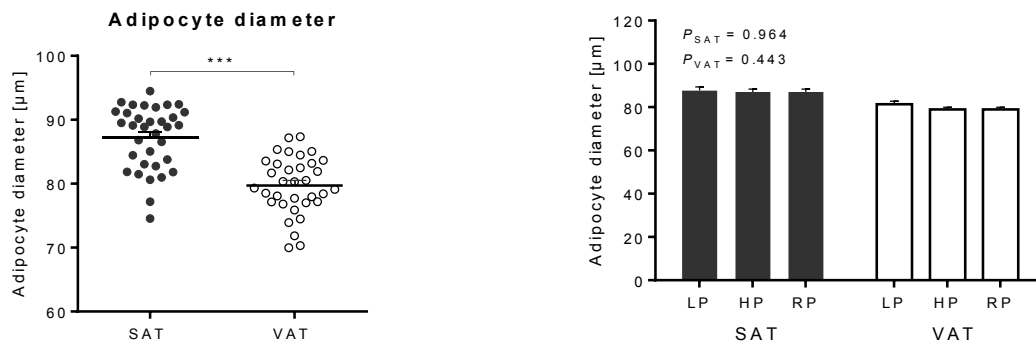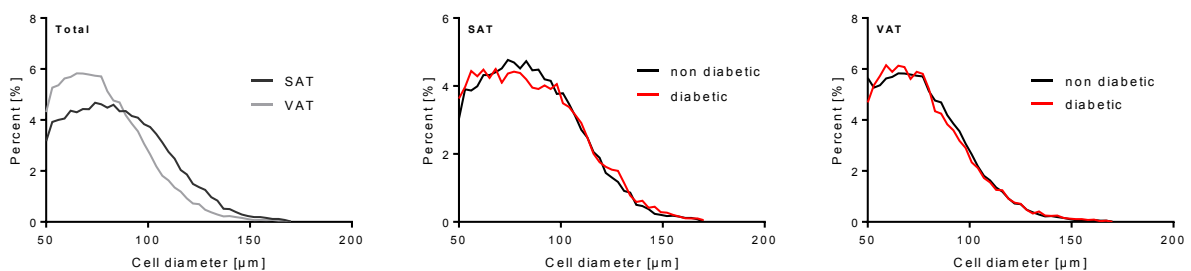
Figure 9 ι Analysis of adipocyte morphology. Histological preparations were assessed for cell size in an automated manner using the software ImageJ. **A,** Adipocyte diameter was significantly higher in SAT compared to VAT (left panel) though no difference were detected between the groups in either fat depot (right panel). **B,** Relative share of cell diameter measurements in 3 μm intervals was calculated. A higher share of smaller cells and concomitantly a lower proportion of larger cells were detected in VAT (left panel). No differences in cell size distribution between subjects previously diagnosed with T2DM (n = 8) and non-diabetic subjects (n = 26) in SAT or VAT (middle and right panel, respectively). ***P < 0.001 for difference between adipose tissue depots.

The data were then tested for an association between adipocyte morphology and anthropometric and clinical measures. No significant correlation between cell size and BMI, waist circumference, or waist-to-hip ratio in either fat depot was detected. Furthermore, no correlations in either depot were found between adipocyte size and fasting glucose, or HbA1c.

There was a weak correlation between fasting insulin and adipocyte size in VAT (ρ = 0.400, *P* = 0.021).

Furthermore, the expression of genes involved in fat uptake (LPL), *de novo* lipogenesis (*ACC1, FASN, SREBP1c*), lipid storage (*PPARγ, PGC1α, SCD1*) and lipolysis (*ATGL, HSL*) were analyzed in the adipose tissue biopsies. In the subcutaneous fat depot, expression of *LPL, FASN*, and *PPARγ* were significantly different between the LP, HP, and RP group (1-way ANOVA, *LPL*: *P* = 0.047; *FASN*: *P* = 0.038, *PPARγ*: *P* = 0.047) (Figure 10). However, *post-hoc* tests did not reach statistical significance. In VAT, lipid metabolizing genes were not differentially expressed.
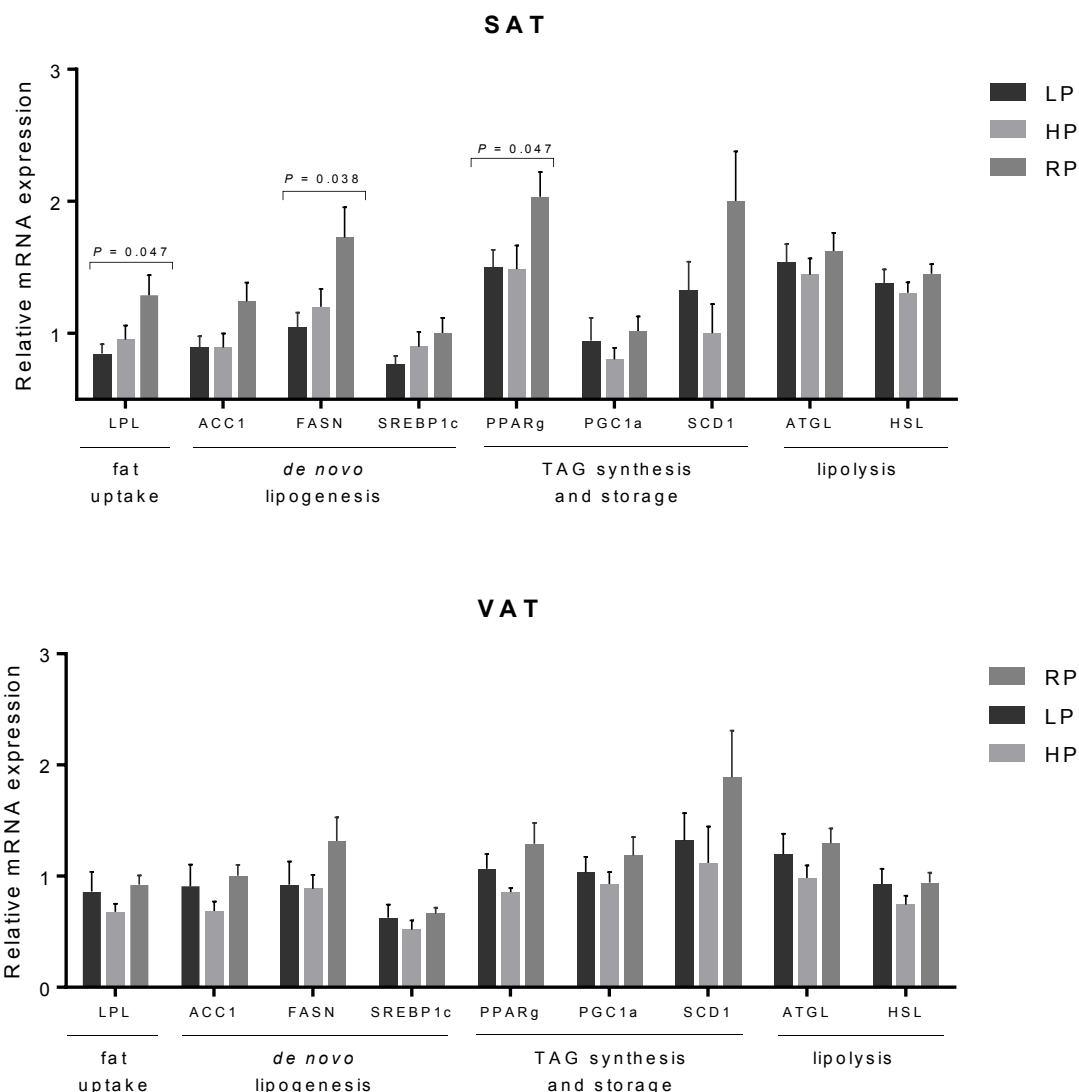
Figure 10 ׀ Diet induced changes in expression of lipid metabolizing genes in adipose tissue. RNA was isolated from paired SAT and VAT biopsies collected during surgery. Gene expression was determined by qRT-PCR. LPL indicates lipoprotein lipase; ACC1, acetyl-CoA carboxylase; FASN, fatty acid synthase; SREBP1c, sterol regulatory element-binding protein 1; PPARγ, peroxisome proliferator-activated receptor gamma; PGC1α, PPAR-gamma coactivator 1 alpha; SCD1, stearoyl-CoA desaturase-1; ATGL, adipose triglyceride lipase; HSL, hormone-sensitive lipase. P-values indicate significant differences between the groups as tested by 1-way ANOVA.

4.1.6   Systemic and adipose tissue inflammation

In order to analyze the effect of the interventions on systemic inflammation, changes in the acute-phase protein CRP and pro-inflammatory cytokines MCP1, TNFα, IFNy, IL6 as well as the anti-inflammatory cytokine IL10 were analyzed in serum (Figure 11). Baseline values of these markers were not significantly different between the groups. Remarkably, in the morbidly obese subjects, baseline CRP levels were considerably elevated with more than 10 mg/l in both intervention groups indicating chronic metabolic inflammation (Frohlich et al., 2000).

All inflammatory markers tended to decrease over the 3-week intervention but mostly without reaching statistical significance. There were no significant changes in MCP1, TNFα, IL10, and IFNγ in response to either diet (Figure 11). Circulating IL6 and CRP levels dropped slightly in the LP group (P_{LP} = 0.024 and P_{LP} = 0.020, respectively) (Figure 11). For none of these markers significant differences between the intervention groups were detected.
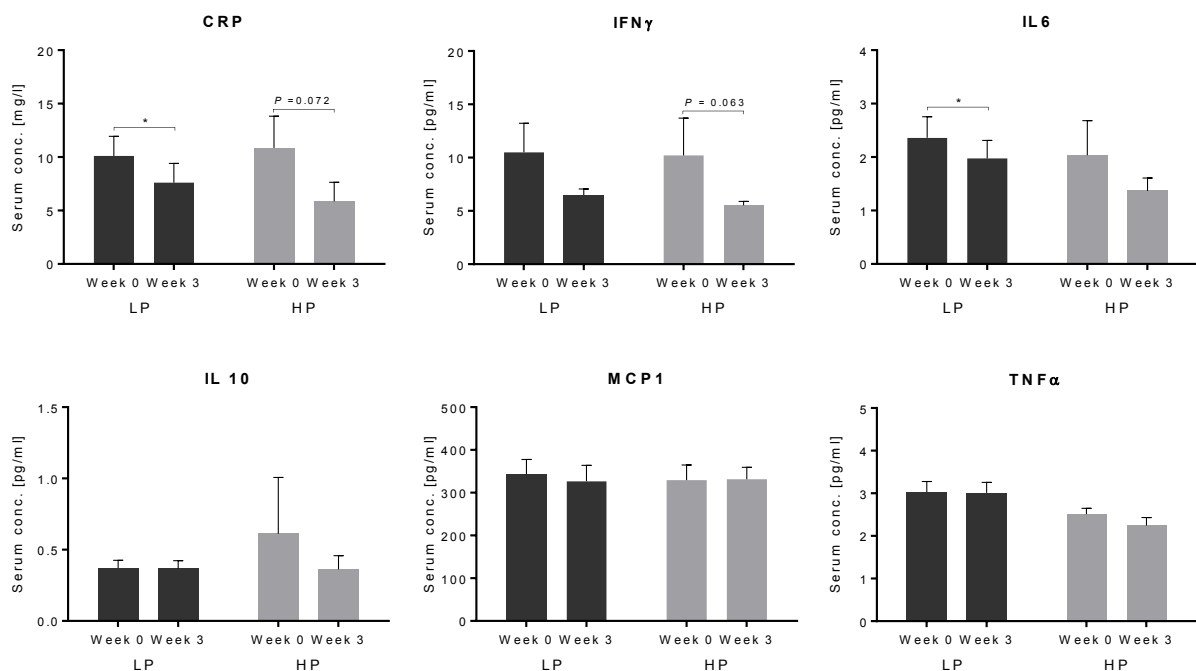
Figure 11 ∣ Diet induced changes in circulating cytokines and CRP. All parameters were measured in serum in the fasted state. There were no significant differences in diet-induced changes in serum inflammatory markers between the intervention groups. Conc. indicates concentration *P < 0.05 different from week 0.

Furthermore, *MCP1, TNFα,* and *IL6* expression in the adipose tissue biopsies were analyzed. mRNA expression of all three cytokines was significantly higher in the subcutaneous depot (all P < 0.001) (Figure 12A) Similarly, MCP1 and IL6 protein levels were higher in lysates from SAT though only IL6 reached statistical significance (IL6: $P_{SATvsVAT}$ = 0.031) (Figure 12A). TNFα protein levels were extremely low in the lysed biopsies and only analyzable in 6 participants in SAT and 4 participants in VAT. Variation in TNFα data was therefore high. MCP1 protein levels

in the adipose tissue lysates were approximately 50x higher than the other markers assessed which was in accordance with MCP1 serum concentrations (Figure 11).

There were no significant differences between the intervention groups in *MCP1, TNFα*, or *IL6* mRNA expression in either fat depot (all: 1-way ANOVA $P > 0.05$, thus no *post-hoc* analyses were conducted) (Figure 12C).
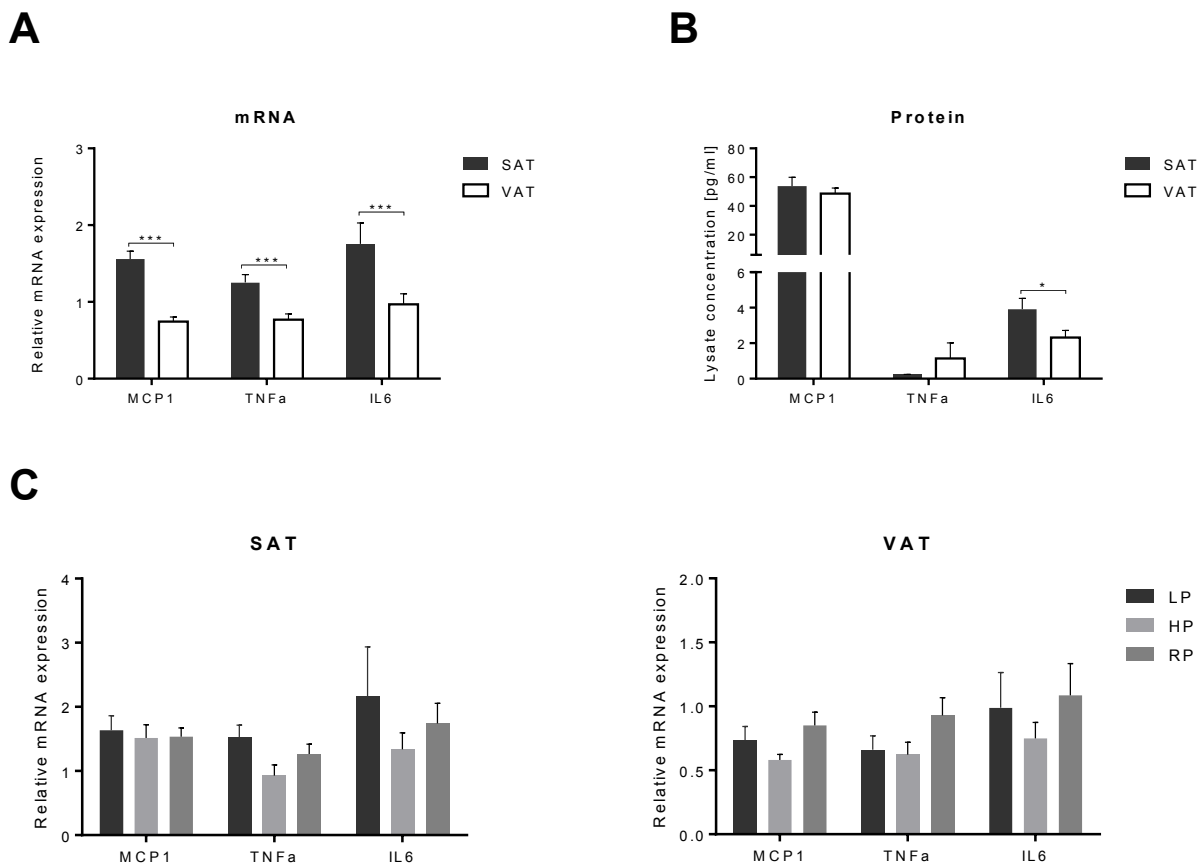
Figure 12 ǀ Cytokine mRNA and protein expression in adipose tissue. Paired adipose tissue biopsies were collected during surgery from participants in the LP (n = 10), HP (n = 9), and RP (n = 15) group. **A-B,** Cytokine mRNA (A) and protein (B) expression were measured in SAT and VAT tissue lysates. **C,** mRNA expression of cytokines in SAT (left panel) and VAT (right panel). *$P < 0.05$, ***$P < 0.001$ difference SAT *versus* VAT.

To assess tissue inflammation the presence of macrophages was histologically analyzed by CD68 staining. Quantified were the number of crown-like structures (CLS) per unit area of adipose tissue in SAT and VAT (Figure 13A). CLS are stained macrophages that surround dead or dying adipocytes and are a marker of chronic inflammation (Murano et al., 2008).

In the histological preparations, significantly more CLS were detected in SAT than in VAT (SAT: 1.53 ± 0.16 CLS per unit area, VAT: 0.82 ± 0.141 CLS per unit area; $P < 0.001$ (Figure 13B). Furthermore, in SAT density of CLS was significantly different between the intervention groups with participants in the LP group having the most and those in the HP group having the least CLS (LP: 2.22 ± 0.22, HP: 1.00 ± 0.24 CLS per unit area; 1-way ANOVA $P = 0.010$) (Figure 13C).

Participants were then categorized as CLS⁻ or CLS⁺ in each fat depot based on the absence or presence, respectively, of CLS. In VAT, 12 participants (36.4%) were CLS⁻ whereas in SAT only 4 participants (12.5%) had no CLS. In contrast in SAT, ≥3 CLS were found in the histological preparations of 5 subjects (15.6%) compared to only 2 (6.1%) in VAT (Figure 13D). No difference between CLS⁻ and CLS⁺ participants were detected in the clinical parameters fasting insulin, fasting glucose, HbA1c, or HOMA-IR in either depot (data not shown).

A

B

C

D
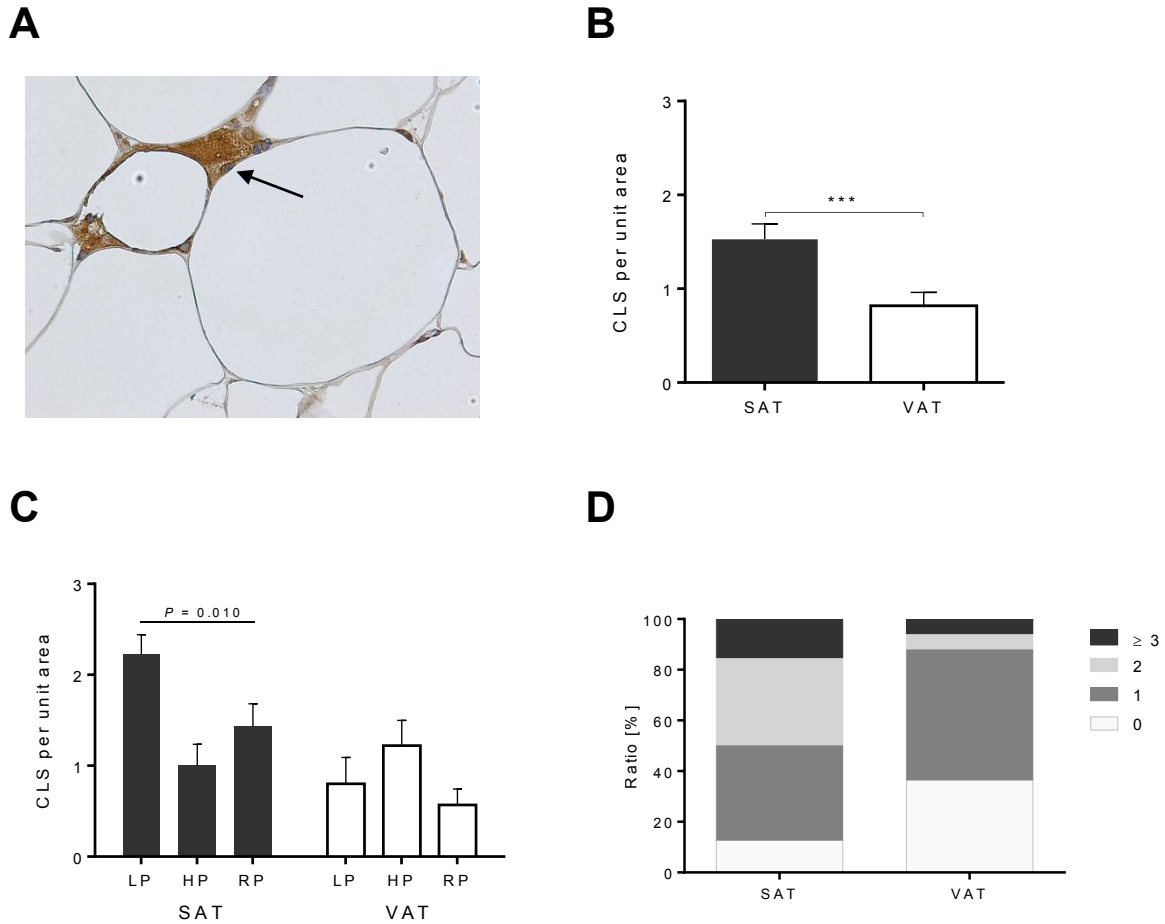
Figure 13 ׀ Analysis of CD68 stained crown-like-structure in adipose tissue biopsies. A, Representative picture of a CLS, tissue macrophages surrounding a dead adipocyte in SAT. **B,** Significantly more CLS in SAT *versus* VAT. **C,** Differences in number of CLS in SAT and VAT between the intervention groups (LP: n= 10, HP: n= 9, RP: n= 15). **D,** Ratio of respective number of CLS in SAT compared to VAT. ***$P < 0.001$ difference between adipose tissue depots.

4.2   FGF21 is a metabolic integrator of protein metabolism

In the following the results on the regulation of FGF21 by diet, particularly by protein, and its association with hepatic steatosis as assessed in the morbidly obese subjects (cohort 1) are presented. For comparison and for heritability estimates, data from a previously published dietary intervention study conducted in metabolically healthy twins (Schuler et al., 2017) (cohort 2, section 4.2.1 and 4.2.4) were analyzed. Furthermore, a short-term intervention study was conducted evaluating the acute regulation of FGF21 by dietary protein within 3 days (cohort 3, section 4.2.5). If not otherwise indicated, tables and figures refer to results of the LEMBAS study (cohort 1).

4.2.1   Circulating FGF21 levels are heritable

Heritability of circulating FGF21 was calculated using data obtained in the healthy, lean twins of cohort 2. Correlation of serum FGF21 in monozygotic twin pairs was high (ρ = 0.654, $P <$ 0.001) (Figure 14A) whereas there was no significant correlation of circulating FGF21 levels in dizygotic twin pairs (Figure 14B). Heritability of serum FGF21 was estimated based on the ACE structural equation model (He et al., 2016). The ACE model evaluates the degree of concordance of a phenotypic trait in monozygous compared to dizygous twins. It was applied to estimate the relative contribution of 'A' additive genetic, 'C' common environmental, and 'E' constant unique environmental components (Figure 14C). Based on this algorithm, heritability of circulating FGF21 was calculated to be 79.5%.
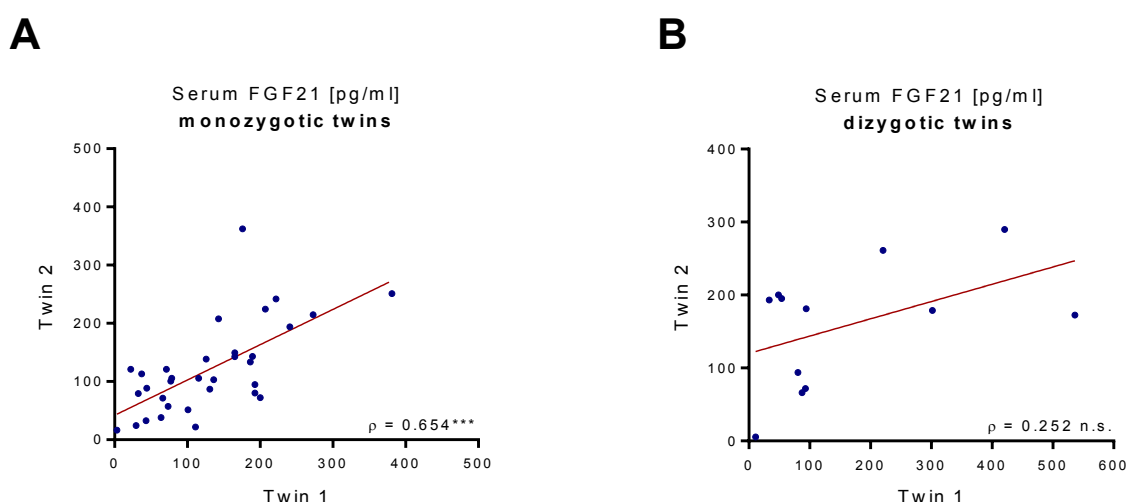
Figure 14 ǀ Heritability estimates for circulating FGF21 levels. **A-B,** Correlation of serum FGF21 in monozygotic (A) and dizygotic (B) twin pairs (cohort 2, n = 92). High correlation of serum FGF21 in monozygotic twin pairs and no correlation in dizygotic twin pairs indicate high heritability which was estimated to be 79.5% based on the ACE structural equation model. Asterisks indicate statistical significance of correlation coefficients as follows: ***$P <$ 0.001. n.s. indicates not significant.

4.2.2 Serum FGF21 strongly correlates with the amount of intrahepatic lipids

Associations of FGF21 with anthropometric and clinical measures were evaluated in the LEMBAS study (cohort 1). In the morbidly obese study subjects, FGF21 was not correlated with age, BMI, fat mass, or WHR neither at baseline nor after the intervention (Appendix Table A2). Furthermore, there were no correlations between FGF21 and markers of lipid or glucose metabolism in the serum samples collected before the intervention. It should be noted though that anthropometric measurements as well as indices based on these were only collected from subjects of the two intervention groups, LP and HP group.

Serum samples collected on the day of surgery include subjects of the RP group. Moderate positive correlations between FGF21 and TAG ($\rho = 0.505$, $P = 0.003$), NEFA ($\rho = 0.456$, $P = 0.008$) and HbA1c ($\rho = 0.455$, $P = 0.020$) were detected in serum collected during surgery. Furthermore, FGF21 serum concentrations were higher in subjects previously diagnosed with T2DM ($FGF21_{T2DM} = 491.4 \pm 90.5$ pg/ml, $FGF21_{noT2DM} = 280.2 \pm 35.9$ pg/ml; $P = 0.014$).

The strongest correlation was detected between circulating FGF21 concentrations and IHL after the intervention ($\rho = 0.9$; $P < 0.001$). There was a weak, positive correlation between baseline circulating FGF21 and AST ($\rho = 0.527$, $P = 0.025$) but not between FGF21 and ALT or γ-GT at either time point. A detailed analysis of the association of FGF21 with hepatic fat content is presented in the following section.

4.2.3 FGF21 is associated with progression of NAFLD

FGF21 was shown to be elevated in patients with fatty liver and has been proposed as a potential blood marker for NAFLD (Rusli et al., 2016). As outlined, circulating FGF21 concentrations and hepatic fat content were highly correlated (Figure 15A and Appendix Table A2) in the obese study subjects with high prevalence of fatty liver. Furthermore, the TAG content determined enzymatically in the hepatic tissue biopsies was highly correlated with serum FGF21 ($\rho = 0.606$, $P = 0.00186$) (Figure 15B).

Circulating FGF21 concentrations were significantly higher in patients previously diagnosed with NASH ($FGF21_{NASH} = 475.5 \pm 70.0$ pg/ml, $FGF21_{nonNASH} = 259.33 \pm 36.8$; $P = 0.009$). Furthermore, FGF21 concentrations in serum increased with severity of NAFLD according to histological SAF score (Figure 15C). Mean FGF21 levels in the "normal" group (n = 8) were 130.6 ± 21.7 pg/ml whereas in the "NASH" group (n = 7) circulating FGF21 was 454.0 ± 104.0 pg/ml (1-way ANOVA $P = 0.004$, *post-hoc* Bonferroni $P = 0.007$). Participants histologically diagnosed with "steatosis" (n = 18) had medium FGF21 levels of 372.9 ± 43.0 pg/ml (*post-hoc* Bonferroni $P = 0.014$ different from "normal").

Application of the NAS instead if the SAF score resulted in only one participant categorized as "NASH". FGF21 in serum of this patient was extraordinarily high with an astonishing 931.8 pg/ml (the highest value in the cohort), which is in comparison to the mean FGF21 concentrations in the "normal" subjects an increase of more than +700% (data not shown).
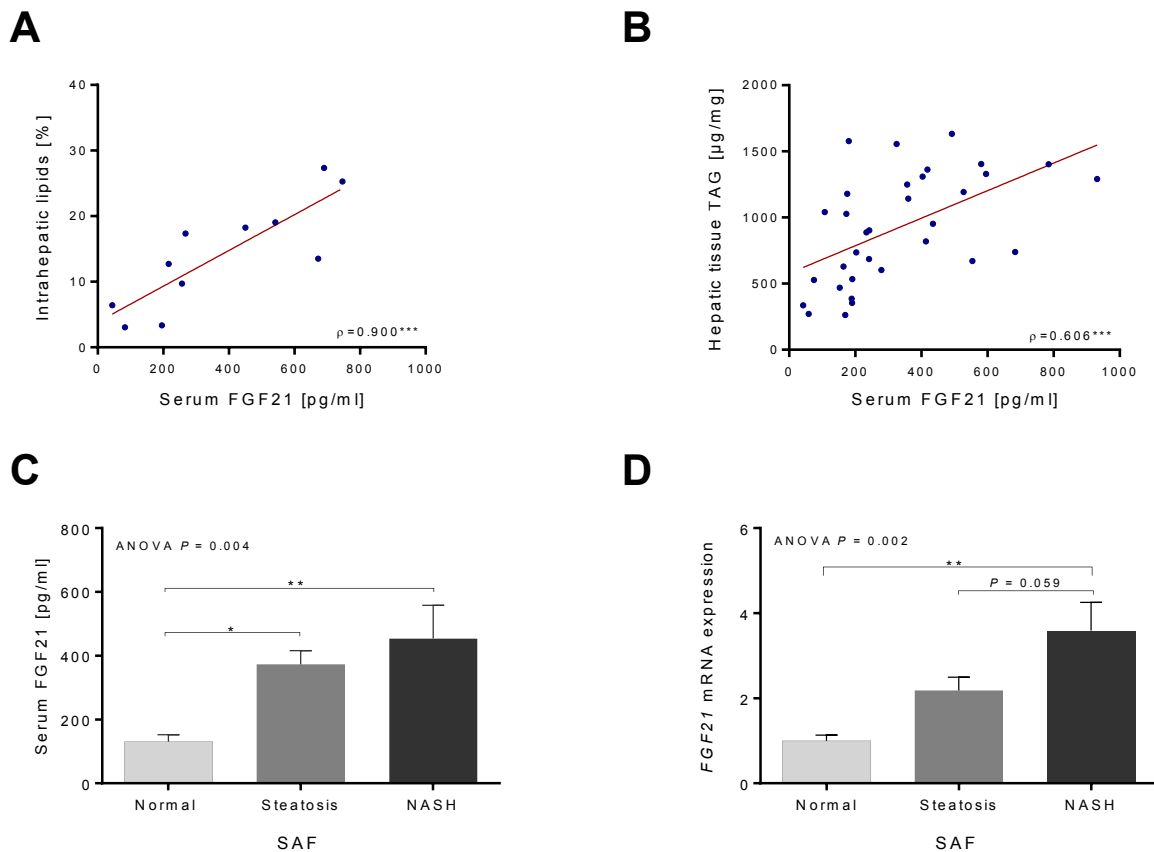
Figure 15 ǀ Association of FGF21 with fatty liver disease. A-B, Serum FGF21 is highly correlated with hepatic fat content as determined by MRI (A) and enzymatically (B). **C-D,** Serum FGF21 (C) and hepatic expression (B) increase with severity of NALFD according to the histological SAF score. FGF21 mRNA expression in the "normal" group was normalized to a value of 1 (D). *$P < 0.05$, **$P < 0.01$ different from "normal".

Based on these results the same analysis was conducted for *FGF21* mRNA expression in the collected liver biopsies. Indeed, the same pattern was observed (Figure 15D). *FGF21* mRNA expression in liver increased with severity of NAFLD and was highest in the "NASH" group (1-way ANOVA $P = 0.002$, *post-hoc* Bonferroni $P = 0.002$ different from "normal"). Mean *FGF21* mRNA detected in livers of subjects histologically categorized as "NASH" was more than 4-times higher than in the "normal" subjects. The difference between "steatosis" and "NASH" in hepatic *FGF21* expression was borderline significant ($P = 0.059$) when *post-hoc* correcting with the stringent Bonferroni test (for comparison: *post-hoc* LSD $P = 0.005$). Again, the one participant diagnosed as "NASH" by applying the NAS score had extremely high hepatic *FGF21* mRNA expression, which was over 4 times higher than the average *FGF21* expression in the "normal" group. As serum concentrations and hepatic mRNA expression of this patient

were in accordance, both being extraordinarily high, the data seem to be the results of the (patho-) physiology and were not considered outliers.

Separate analysis of the histological score components revealed that FGF21 serum concentrations, *FGF21* mRNA expression, and *FGFR2* mRNA were associated with "steatosis" (FGF21$_{serum}$: *P* < 0.001, *FGF21$_{mRNA}$*: *P* = 0.026, *FGFR2$_{mRNA}$*: *P* = 0.057) and "ballooning" (FGF21$_{serum}$: *P* < 0.001, *FGF21$_{mRNA}$*: *P* < 0.001, *FGFR2$_{mRNA}$*: *P* = 0.036) but not with "inflammation" or "fibrosis". In contrast, *FGFR1* mRNA was not associated with any of the histological score components.

Finally, correlations between FGF21 and mRNA expression of fibrosis/inflammation markers were assessed. Hepatic *FGF21* mRNA was positively associated with expression collagenases 1 and 3 (COL1: ρ = 0.346, *P* = 0.049; *COL3:* ρ = 0.393, *P* = 0.024) and α-smooth muscle actin (*ACTA2*: ρ = 0.497, *P* < 0.001) but not with *MMP9*, its inhibitor *TIMP1*, or *TGFβ*. Furthermore, there was no correlation between *FGF21* mRNA and cytokines except for a weak correlation with *TNFα* (ρ = 0.401, *P* = 0.021). Interestingly, circulating FGF21 concentrations were strongly associated with TIMP1 concentrations in blood (ρ = 0.761, *P* < 0.001).

4.2.4   A protein-enriched diet suppresses FGF21

Before and after the dietary intervention, circulating FGF21 levels were measured in serum. The LP diet provoked an increase in FGF21 concentrations from 342.25 ± 76.36 pg/ml to 486.52 ± 29.66 pg/ml (P_{LP} = 0.049) (Figure 16A). In the HP group, circulating FGF21 fell by 24.7% from 172.95 ± 36.76 pg/ml to 130.29 ± 29.25 pg/ml without significance. The difference between the groups in terms of the respective change in FGF21 was significant (P_{LPvsHP} = 0.014) (Figure 16A). The data indicates that serum FGF21 concentrations are bi-directionaly regulated by dietary protein. Notably, serum FGF21 levels varied widely between subjects and baseline FGF21 levels were almost twice as high in the LP group compared to the HP group (week 0: P_{LPvsHP} = 0.052) (Figure 16A).

A

Serum FGF21
cohort 1

B

Serum Urea
cohort 1
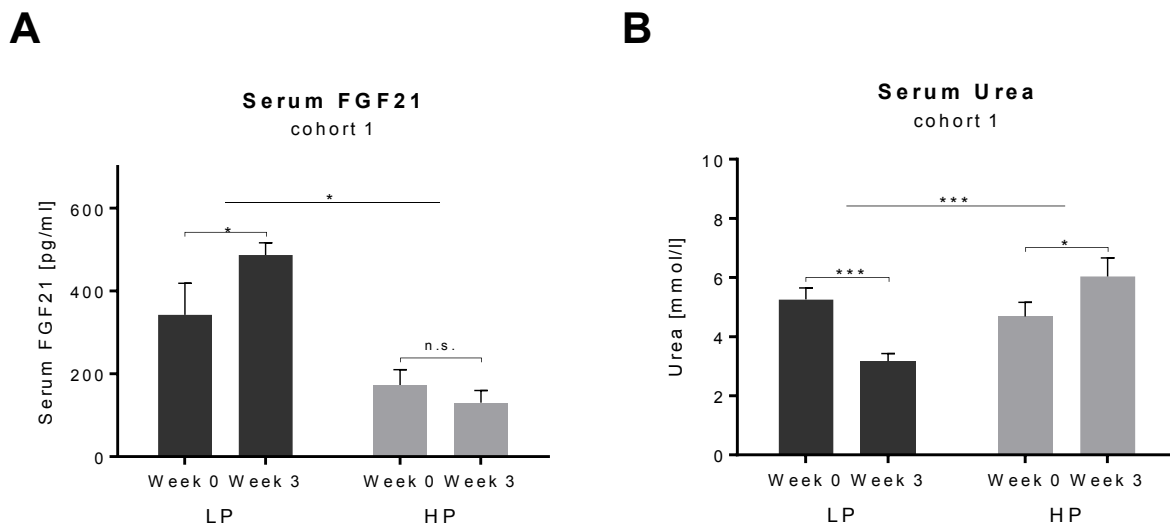
Figure 16 ǀ Response of FGF21 to differing dietary protein content in obese subjects. FGF21 is bi-directionally regulated by dietary protein. **A,** FGF21 concentrations were measured in serum in the fasted state. **B,** Urea concentrations were measured in serum in the fasted state. *$P < 0.05$, ***$P < 0.001$ difference as indicated by brackets.

As expected and outlined in section 4.1.4, serum urea decreased markedly in the LP group (-2.09 mmol/l, $P < 0.001$) indicating decreased ureagenesis in response to the lower protein nitrogen intake (Figure 16B). Similarly, but less pronounced, urea levels increased in the HP group (+ 1.35 mmol/l, $P = 0.031$) corresponding to the increase in dietary protein (Figure 16B and Table 4).

The results obtained in the obese subjects were compared to the reference cohort 2 for several reasons: (1) to see if the responses are specific to metabolically stressed subjects with considerably elevated FGF21 levels or can be replicated in lean, healthy subjects, (2) to examine the effect of a long-term (6 weeks) HP diet, and (3) to assess data from a larger cohort with fewer variation in FGF21 concentrations. Mean BMI of the study participants in cohort 2 was 22.5 kg/m² and mean age was 31 years while glucose tolerance, lipoprotein levels and hepatic fat content were normal (for other anthropometric and routine blood parameters see Appendix Table A3).

A total of 92 study participants were standardized for 6 weeks on a low-fat, carbohydrate-rich, normal-protein healthy diet (LF: 55 EN% carbohydrate, 30 EN% fat, 15 EN% protein) as recommended by the German Nutrition Society after which they switched to a high-fat diet enriched in saturated fatty acids for 6 weeks (HF: 40 EN% carbohydrate, 45 EN% fat, 15 EN% protein). Finally, they continued for another 6 weeks on a high-protein diet by exchanging 15 EN% of fat with protein while keeping carbohydrates constant (HP: 40 EN% carbohydrates, 30 EN% fat, 30 EN% protein). The intervention was isocaloric to the individual energy requirements. Clinical investigation days (CIDs) took place after the low-fat diet (LF6), after 1 and 6 weeks of the high-fat diet (HF1, HF6), and after 6 weeks on the HP diet (HP6). The

participants received standardized diets 1 week before each CID. A graphical abstract of the study design is depicted in Figure 17. From the full cohort (n = 92), 24 subjects continued on the HP diet. The mean age of this subcohort (n = 24) was 39 years. BMI, lipoprotein levels, liver fat content and glucose tolerance were within the normal range (Appendix Table A5).

COHORT 2

Isocaloric
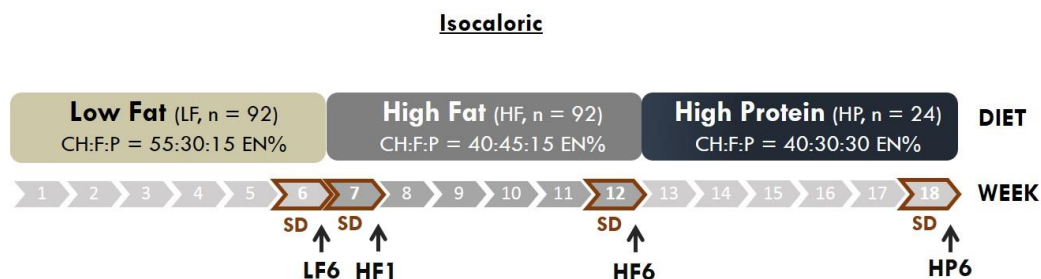
Figure 17 | Study design of the dietary intervention in cohort 2. Clinical investigation days took place after 6 weeks on a low-fat diet (LF6), after 1 (HF1), and 6 (HF6) weeks on an unhealthy high-fat diet, and after 6 weeks on a high-protein diet (HP6). CH indicates carbohydrates; F, fat; P, protein, SD, standardized diet.

At screening participants had circulating FGF21 levels of 170.5 ± 20.5 pg/ml. After standardization on the healthy LF diet for 6 weeks FGF21 was 126.6 ± 21.9 pg/ml which rose back to baseline levels in response to the HF diet to 171.1 ± 20.0 pg/ml ($P_{LF6vsHF6}$ = 0.005). In contrast, the HP diet induced a marked decrease of FGF21 from 160.3 ± 26.0 pg/ml to 60.6 ± 11.3 pg/ml (P_{HP} < 0.001), representing a -62.1% decrease from HF6 and - 64.5% from baseline FGF21 levels (Figure 18A). Serum urea levels rose in correspondence to the higher protein intake confirming compliance of the study participants (Figure 18B).

A

B
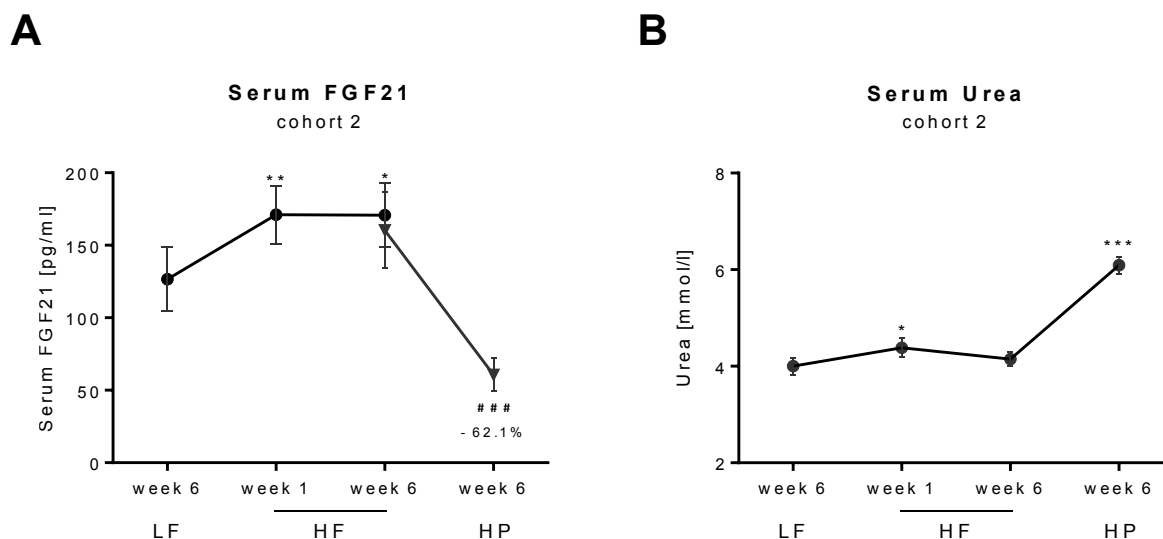
Figure 18 | Response of FGF21 to a HP diet in lean, healthy subjects (cohort 2, n = 24). HP diet potently decreases serum FGF21 concentrations. **A,** FGF21 concentrations were measured in serum in the fasted state on ELISA plates. Data for LF1, HF1 and HP6 were measured on the same plate (dots, analyzed by repeated measures ANOVA, statistical significance indicated by asterisks). Values for HP6 were measured on a separate plate together with reanalysis of the HF6 data (triangles, analyzed by T-test, statistical significance indicated by hashtags). The two measurements of FGF21 at HF6 were highly correlated (P < 0.001). **B,** Urea concentrations were measured in serum in the fasted state. *P < 0.05, **P < 0.01, ***P < 0.001 different from LF6; ###P < 0.001 different from HF6.

4.2.5 The protein-mediated downregulation of FGF21 is an acute response

In order to test whether the observed downregulation of FGF21 requires long-term high-protein intake, a 3-day dietary study contrasting normal protein (NP: 15 EN%, n = 10) with high protein (HP: 30 EN%, n = 11) was conducted (cohort 3). The mean age of the participants was 61.7 ± 1.5 years indicating "elderly" subjects in this cohort. Mean BMI (25.6 ± 0.90 kg/m²) was slightly above normal, which is assumed to be advantageous at higher age (Kvamme et al., 2012; Weiss et al., 2008). All baseline characteristics of the participants are summarized in Appendix Table A6. Recruitment and nutritional counseling of the study participants in cohort 3 was supported by the MSc student Ulrike Hass.

Participants were randomized into the NP or HP group by age, sex, and BMI. All participants consumed an initial 3 days of low protein (LP: 10 EN%) after which they switched to either the NP or HP diet for another 3 days. The diets were balanced with dietary fat while carbohydrates were kept constant at 45 EN%. On each CID participants were weighed, and blood and urine were sampled. The study design is depicted in Figure 19A.
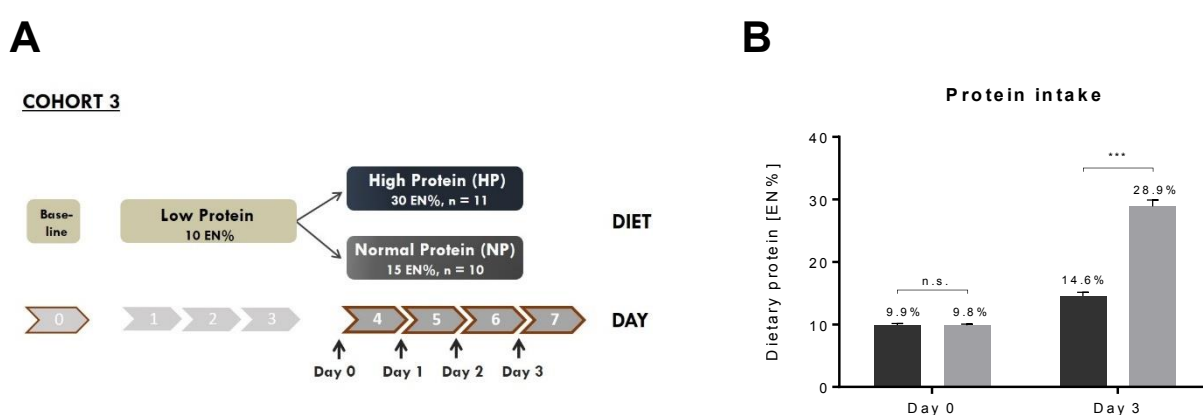
Figure 19 ı Study design of the short-term protein intervention in cohort 3. A, Twenty-one healthy subjects consumed an initial 3-day low-protein diet (LP, 10EN%) after which they switched for 3-days each to either a diet with normal (NP, 15 EN%) or high (HP, 30 EN%) dietary protein content. **B,** Protein intake according to nutritional journals. NP, dark grey; HP, light grey.

In order to monitor dietary intakes, participants were asked to fill out nutritional journals. Habitual protein intake in the NP group was 15.9 ± 1.6 EN% and in the HP group 16.1 ± 1.0 EN% (P_{NPvsHP} not significant).

Baseline urea levels differed between the groups as the NP group had significantly higher urea concentrations in blood compared to the HP group (NP: 5.27 ± 0.32 mmol/l, HP: 4.38 ± 0.26 mmol/l, P_{NPvsHP}= 0.040). As expected, the two diets significantly and oppositely affected serum urea concentrations (2-way ANOVA P_{Time} < 0.001, $P_{TimexGroup}$ < 0.001) (Figure 20A). The initial LP diet led to a decline in urea in both groups.

Following this standardization period, the participants received dietary plans with either high or normal protein according to their respective group. In the NP group, urea modestly rose back to 4.79 ± 0.32 mmol/l in response to the 3-day 15 EN% protein (*post-hoc* Bonferroni P_{d3vsd0} not significant). In contrast, in the HP group serum urea increased strongly to 6.56 ± 0.38 mmol/l (ANOVA repeated measures $P < 0.001$, *post-hoc* Bonferroni $P_{d3vsd0} < 0.001$) reflecting the higher protein intake of 30 EN% (Figure 20A). Already within 24 h urea levels were significantly different from day 0 (*post-hoc* Bonferroni $P_{d1vsd0} = 0.003$). The data indicates that the participants were compliant to the dietary protein instructions.

Next, changes in serum FGF21 levels during the short-term protein interventions were analyzed. FGF21 serum concentrations were dose-dependently affected by the protein content of the diets (2-way ANOVA $P_{Time} < 0.001$, $P_{TimexGroup} < 0.008$). As expected, the initial 10 EN% protein phase led to a modest increase in circulating FGF21 to 295.3 ± 32.0 pg/ml in the NP group and 294.3 ± 65.6 pg/ml in the HP group (both not significant, P_{NPvsHP} not significant) (Figure 20B). A modest increase in dietary protein to 15 EN% in the NP group induced an insignificant decrease in serum FGF21 to 200.7 ± 24.6 pg/ml within 24 h after which it increased slightly to 229.9 ± 20.0 pg/ml over the next two days (Figure 20B). On day 3, FGF21 levels were not significantly different from neither the values at baseline nor after the LP diet (day 0). Protein intake in the control group resembled habitual protein intake.

In contrast, in the HP group circulating FGF21 levels fell sharply within 24 h (ANOVA repeated measures $P < 0.001$, *post-hoc* Bonferroni $P_{d1vsd0} < 0.001$) (Figure 20B). After 3 days on the HP diet FGF21 levels were lowest with 111.9 ± 20.1 pg/ml (*post-hoc* Bonferroni $P_{d3vsd0} < 0.001$) which is less than half of baseline FGF21 serum concentrations and a reduction of -62.0% compared to serum concentrations after the initial protein-reduced phase (day 0) (Figure 20B). On day 2, serum FGF21 levels were significantly different between the groups. The difference between the groups was highest at day 3 ($P_{NPvsHP} < 0.001$) (Figure 20B). The results indicate that FGF21 dose-dependently responds to the protein content of the diet.

A

Serum FGF21
cohort 3

B

Serum Urea
cohort 3

C

D

E

F
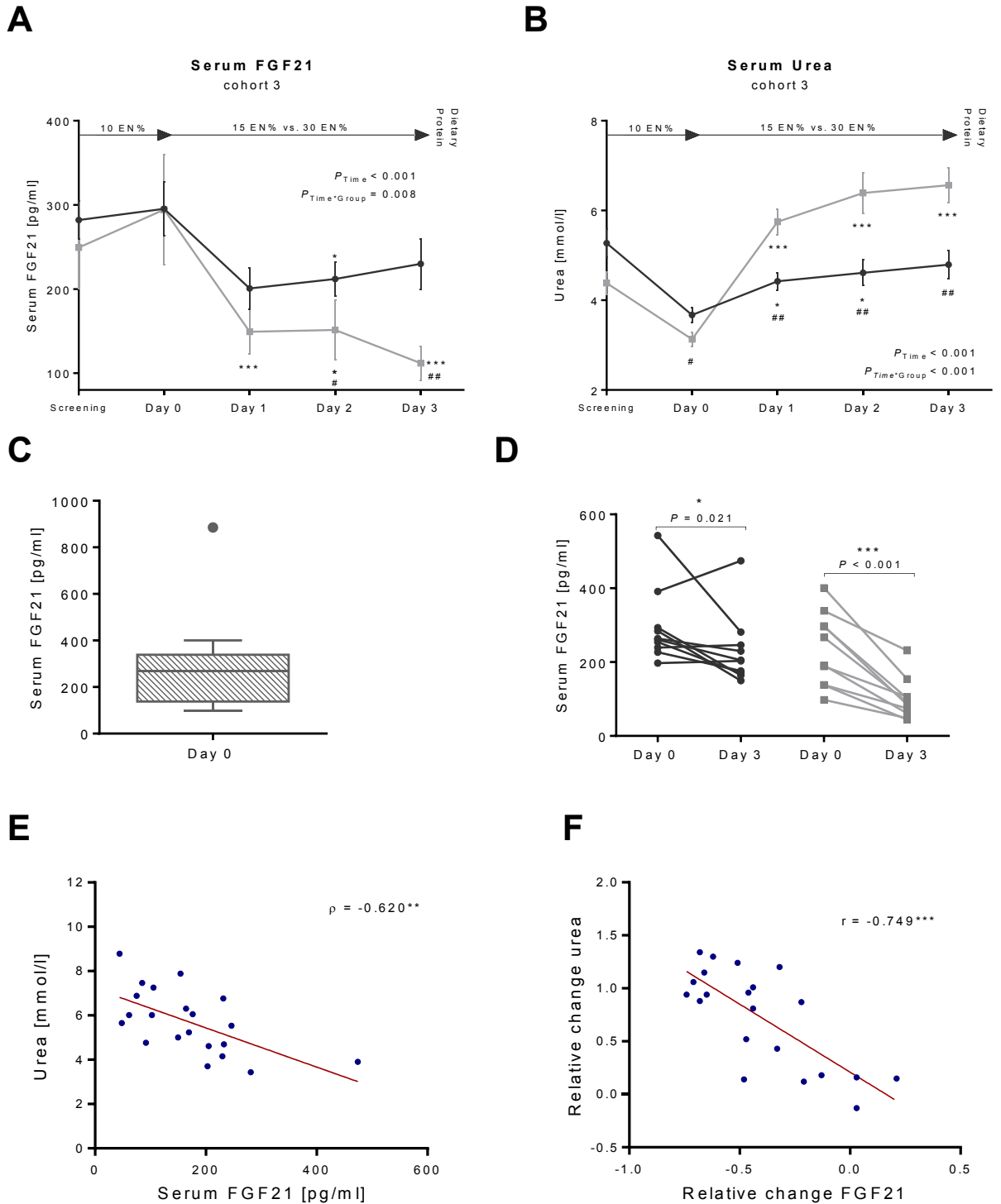
Figure 20 I Changes in FGF21 and urea in response to a short-term HP diet (cohort 3). A-B, Serum FGF21 and urea concentrations were measured in the 21 healthy subjects at baseline, after the initial 3-days with 10 EN% protein, and on each day during the intervention with either 15 EN% protein in the NP (n = 10, dark line) or 30 EN% in the HP (n = 11, grey line) group. Raising the dietary protein content slightly decreased circulating FGF21 in the NP group (A). However, serum FGF21 decreased markedly in the HP group which was twice as high compared to the 15 EN% protein group. The amount of dietary protein consumed is reflected by the changes in serum urea (B). *$P < 0.05$, **$P < 0.01$, and ***$P < 0.001$ difference from day 0. #$P < 0.05$, ##$P < 0.01$ difference between groups at the respective time point. **C,** Box-and-whiskers plot of serum FGF21 concentrations identifying one measurement as an outlier. **D,** Individual changes in serum FGF21 concentrations after 3-days of the intervention. Serum FGF21 concentrations decreased in every single participant in the HP group (light grey) while individual changes in the NP group (dark grey) varied. *$P < 0.05$, ***$P < 0.001$ difference from day 0. **E-F,** Negative correlation between baseline serum FGF21 and urea (E) as well as between the relative change of serum FGF21 and urea concentrations (F) after the 3-day intervention. **$P < 0.01$, ***$P < 0.001$ correlation coefficient.

One participant in the HP group had extraordinarily high baseline serum FGF21 levels of 885.6 pg/ml. The value qualified as an outlier, defined as a data point whose distance from the median exceeds 1.5 times the interquartile range of a box-and-whiskers plot (Figure 20C). However, reanalysis of the data after eliminating this point still confirmed the above results; the decline in FGF21 levels in response to the HP diet was highly significant (1-way ANOVA P_{HP} < 0.001, *post-hoc* Bonferroni P_{d3vsd0} < 0.001). Furthermore, it is questionable if the data point can be considered an outlier taking into consideration the high variation of FGF21 concentrations in humans. However, as both analyses led to the same conclusion the observed effect can be considered robust.

Looking at the individual data, it stands out that serum FGF21 concentrations of every single participant in the HP group declined in response to the protein-enriched diet (Figure 20D, right panel). In contrast, mean FGF21 levels of the NP group fell slightly in response to the 15 EN% protein diet but FGF21 levels were even higher in some individuals after the 3-day intervention (Figure 20D, left panel).

Next, the association of circulating FGF21 levels with serum urea, a marker of protein intake was tested. Indeed, at day 3 of the intervention circulating FGF21 levels were highly and negatively correlated with serum urea (ρ = -0.620, P = 0.003) (Figure 20E). In addition, the relative change of FGF21 during the intervention correlated strongly with the relative change of urea in the opposite direction (r = -0.689, P < 0.001) (Figure 20F).

Changes in routine renal and cardiovascular parameters were not significant, neither within nor between the groups (Appendix Table A6). In consideration of the shortness of the intervention, changes in weight and BMI were not assessed. The liver enzymes and the inflammatory marker CRP remained unchanged during the 3-day intervention (Figure 21).
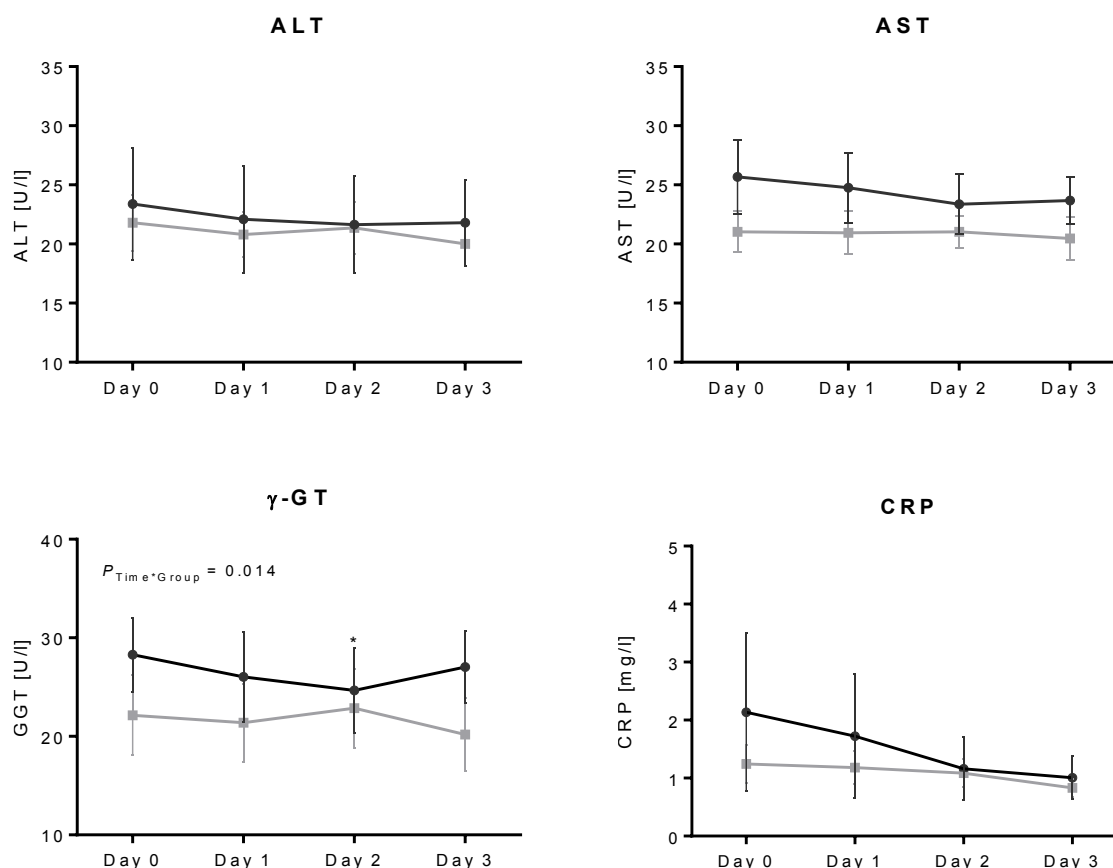
Figure 21 I Changes of liver enzymes and CRP during the short-term protein intervention. No effect of dietary protein content on concentrations of liver enzymes and CRP during the 3-day interventions in serum. NP, dark line; HP, grey line. *$P < 0.05$ different from day 0. *P*-values for Time and Time*Group effects were calculated by repeated measures ANOVA, post-hoc tests were not significant.

The following table summarizes the results for baseline FGF21 serum concentrations as well as the respective changes during HP intervention obtained in the different cohorts (Table 7). FGF21 serum concentrations were elevated in metabolically stressed or elderly individuals. In all three cohorts, FGF21 serum levels were substantially reduced in response to a protein-rich diet, varying between -51% to -64%.

Table 7 I Summary of changes in serum FGF21 concentrations in response to dietary protein.

Parameter	Morbidly obese (Cohort 1)	Healthy, young (Cohort 2)	Healthy, old (Cohort 3)
n (whole / HP group)	19/ 8	24	21/ 11
Protein [EN%]	30	30	30
Duration diet [weeks]	3	6	3 days
Baseline FGF21 [pg/ml] – whole cohort	267.0 ± 48.8	170.5 ± 20.5	264.9 ± 27.2
FGF21 before intervention [pg/ml] – HP group	173.0 ± 36.8	160.3 ± 26.0	249.4 ± 48.6
FGF21 after intervention [pg/ml] – HP group	130.3 ± 29.2	60.6 ± 11.3	111.9 ± 20.1

Data are mean ± SEM.

4.2.6   Dietary protein alters expression of the FGF21 pathway in liver but not in fat

After evaluating the changes in FGF21 serum concentrations in response to dietary protein, tissue expression of *FGF21* and its receptors were analyzed in the collected liver and adipose tissue biopsies from the subjects undergoing bariatric surgery.

In accordance with serum levels, hepatic *FGF21* mRNA expression was different between the intervention groups (1-way ANOVA P = 0.020) (Figure 22A). Relative *FGF21* expression was lowest in the HP group and highest in the LP group (*post-hoc* Bonferroni P_{LPvsHP}= 0.019) (Figure 22A). However, in both groups *FGF21* mRNA levels were not significantly different from that measured in the RP group.

It is well established that amino acid deficiency or single amino acid deprivation potently induce *FGF21* via the kinase GCN2 and activation of the integrated stress response (ISR) involving phosphorylation of eIF2α and induction of the transcription factor ATF4 (De Sousa-Coelho et al., 2012; Laeger et al., 2014). In order to assess involvement of this pathway, mRNA expression of genes involved in the ISR were analyzed in the liver biopsies. Expression of the downstream IRS factors *ATF4* was not significantly different between the intervention groups. There was also no difference in *ATF4* expression when directly comparing the HP and LP group, not taking the RP group into consideration. The ER stress markers *BiP*, *XBP1s* and *CHOP* tended to be lower expressed in the HP condition though *BiP* only reached statistical significance when directly compared to the LP condition [BiP: P_{LPvsHP} = 0.047 (T-test); 1-way ANOVA P = 0.128; XBP1s: 1-way ANOVA P = 0.026, *post-hoc* Bonferroni P_{HPvsRP} = 0.023; CHOP: 1-way ANOVA P = 0.032, *post-hoc* Bonferroni P_{HPvsRP} = 0.049] (Figure 22B). The XBP1s/*XBP1u* ratio remained unaffected by the protein content of the diet (Figure 22B).

A   **B**
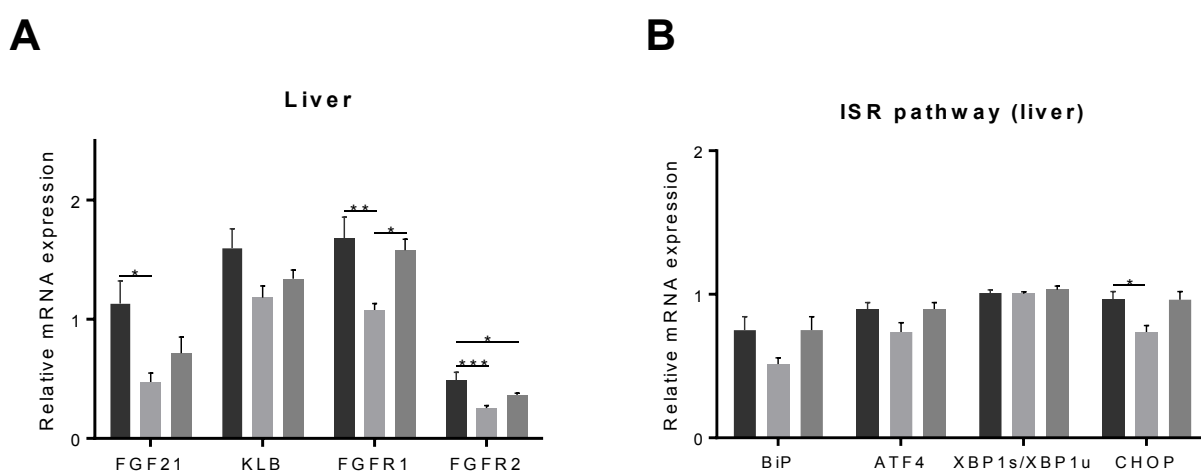
Figure 22 ׀ Expression of FGF21 pathway and ISR genes in liver biopsies. A, Hepatic expression of *FGF21* and its receptors measured in liver lysates. **B,** Hepatic expression of genes involved in the integrated stress response. LP, dark column, HP, grey column, RP, medium shaded column. *P < 0.05, **P < 0.01, ***P < 0.001.

In humans, FGF21 expression is almost exclusively restricted to the liver under basal conditions (Petryszak et al., 2016). Large data repositories such as the Human Protein Atlas (HPA) or the Expression Atlas (EMBL-EBI, 2019: ID: ensg00000105550) confirm the predominant expression of *FGF21* in the liver. In accordance, in the SAT and VAT tissue biopsies expression of *FGF21* was not detectable but its receptors were well expressed. However, the interventions had no significant effect on *KLB, FGFR1*, or *FGFR2* mRNA levels in both SAT and VAT (Figure 23A-B).

Downregulation of the FGF21 receptor KLB has been described to compromise the action of FGF21 in metabolic disease (Fisher et al., 2010; Rusli et al., 2016). However, in the morbidly obese subjects *KLB* expression was not different among the intervention groups neither in adipose tissue nor in liver (Figure 22A and Figure 23). Furthermore, hepatic regulation of *FGFR1* and *FGFR2* was similar to *FGF21* with their expression being lowest in the HP and highest in the LP group *(1-way* ANOVA *FGFR1: P* = 0.004, FGFR2: *P* = 0.001) (Figure 22A). Thus, no indications of a counter-regulation of FGF21 and its receptors were observed in this 3-week intervention.

A   **B**
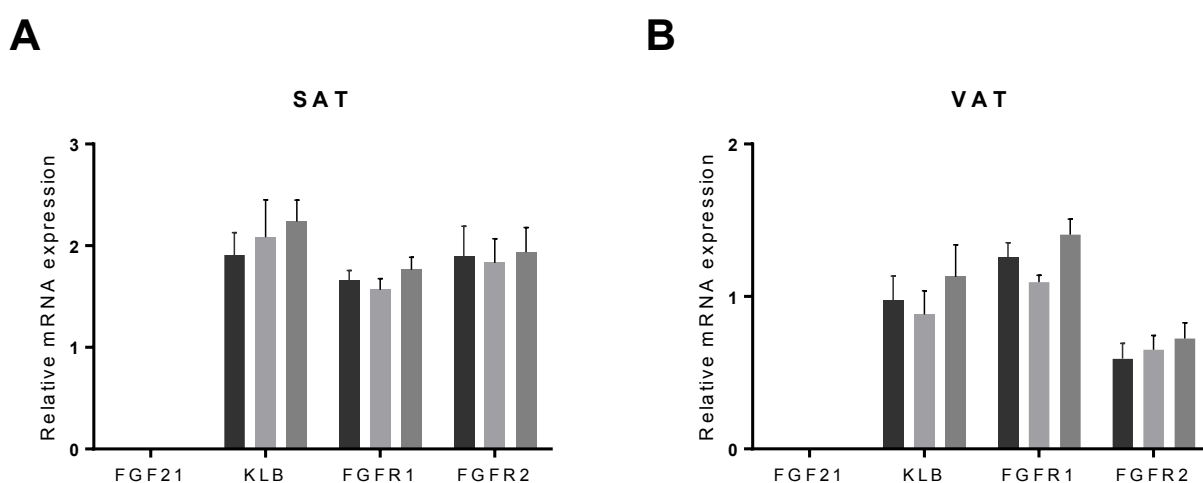
Figure 23 ᛁ Expression of FGF21 pathway in adipose tissue biopsies. A-B, Hepatic expression of FGF21 and its receptors measured in SAT (A) and VAT (B). FGF21 mRNA was not detectable in the adipose tissue biopsies.

4.2.7 Nitrogen metabolites suppress FGF21 in a hepatocyte-autonomous manner

To test whether the downregulation of *FGF21* in response to high protein is a hepatocyte-autonomous response experiments in the hepatoma cell line HepG2 were conducted. HepG2 cells are an immortalized cell line derived from human liver carcinoma cells. They are routinely used for *in vitro* studies with liver cells as they grow well and deliver reproducible data (Donato et al., 2015).

Basal *FGF21* expression is extremely low in HepG2 cells but extensively inducible by various stressors including ER stress (Kim et al., 2015; Schaap et al., 2013). Two ER stress inducers

that are commonly used to study ER stress in an *in vitro* setting were evaluated in terms of *FGF21* induction. First, thapsigargin, a non-competitive inhibitor of the sarco/endoplasmic reticulum Ca^{2+} ATPase. Second, tunicamycin, an antibiotic that inhibits N-linked glycosylation and thereby blocks protein folding and transit through the ER. Both drugs effectively induced *FGF21* expression in HepG2 while tunicamycin resulted in an almost 100-fold induction (Figure 24A-B). Further experiments were conducted with tunicamycin only as previous experiences with handling tunicamycin already existed in the laboratory, e.g. the optimal dose in HepG2 cells had been determined previously.
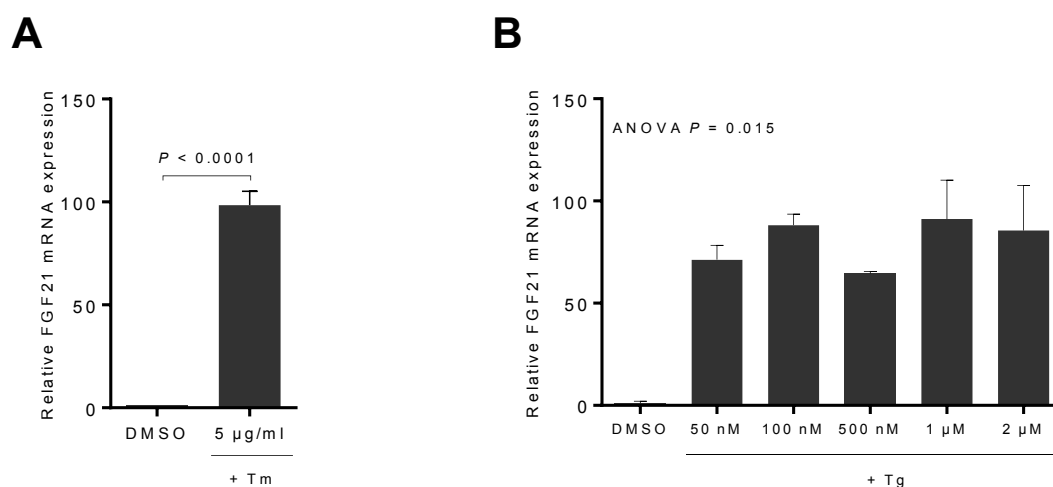
Figure 24 I ER stress-related *FGF21* induction in HepG2 cells. *FGF21* mRNA in hepatocytes is potently increased by chemicals known to induce cellular ER stress. **A,** HepG2 cells were treated with tunicamycin or vehicle control (DMSO) for 4 h after which *FGF21* mRNA expression was determined. **B,** HepG2 cells were treated with increasing concentrations of thapsigargin or DMSO for 4 h after which *FGF21* mRNA expression was determined. *FGF21* expression in the DMSO condition was normalized to a value of 1. Differences between thapsigargin concentrations were not significant. Tm indicates tunicamycin; Tg, thapsigargin; DMSO, dimethylsulfoxid.

The strong correlation between FGF21 and urea in the human intervention studies pointed towards an association of FGF21 with the urea cycle (section 4.2.4 and 4.2.5). The cycle functions to detoxify ammonia by converting it into harmless urea which is excreted via the kidneys. Incubation of HepG2 cells with ammonium (NH_4Cl), dose-dependently prevented the tunicamycin-induced rise in FGF21 expression up to over 50% compared to control ($P = 0.001$) (Figure 25A).

Furthermore, glutamine, a more physiologic supplier of ammonia, effectively blunted the ER-stress-related FGF21 induction (1-way ANOVA $P = 0.0495$) (Figure 25B). Glutamine is the main vehicle to transport amino groups from peripheral oxidation to the liver for ureagenesis as levels of toxic ammonia are physiologically carefully controlled. Thus, the data indicates that the downregulation of *FGF21* in response to HP intakes is regulated in a cell-autonomous manner.

Lastly, the expression of UPR genes was assessed. Tunicamycin leads to an accumulation of unfolded proteins in the ER which activates the UPR. As expected, tunicamycin treatment strongly induced expression of *BiP, XBP1s,* and *ATF4* confirming activation of the UPR (Figure 25C). Increasing ammonia concentrations prevented full induction of *BiP* and *ATF4* expression (Figure 25C). However, this was not the case with the *XBP1s/XBP1u* ratio. *XBP1* expression and the *XBP1s/XBP1u* ratio remained high with tunicamycin treatment even with increasing ammonia concentrations (Figure 25C).

Finally, it was tested whether the responses obtained in HepG2 cells were reproducible in primary hepatocytes. Primary murine hepatocytes were isolated from C57BL/6J mice and treated with ammonium and glutamine by Steffi Heidenreich (Schupp lab, Institute of Pharmacology, Charité-Universitätsmedizin Berlin, Berlin, Germany). *Fgf21* was well expressed in this cell type. Again, ammonium dose-dependently reduced basal *Fgf21* expression within 24 h (Figure 25E). Similarly, glutamine led to substantially decreased *Fgf21* mRNA levels when supplied in excess amounts to primary hepatocytes (Figure 25F). In summary the data indicates that the hepatic increase in ureagenesis and thus the flux of ammonia to the liver drives the decrease of FGF21.

A

B

C

D

E
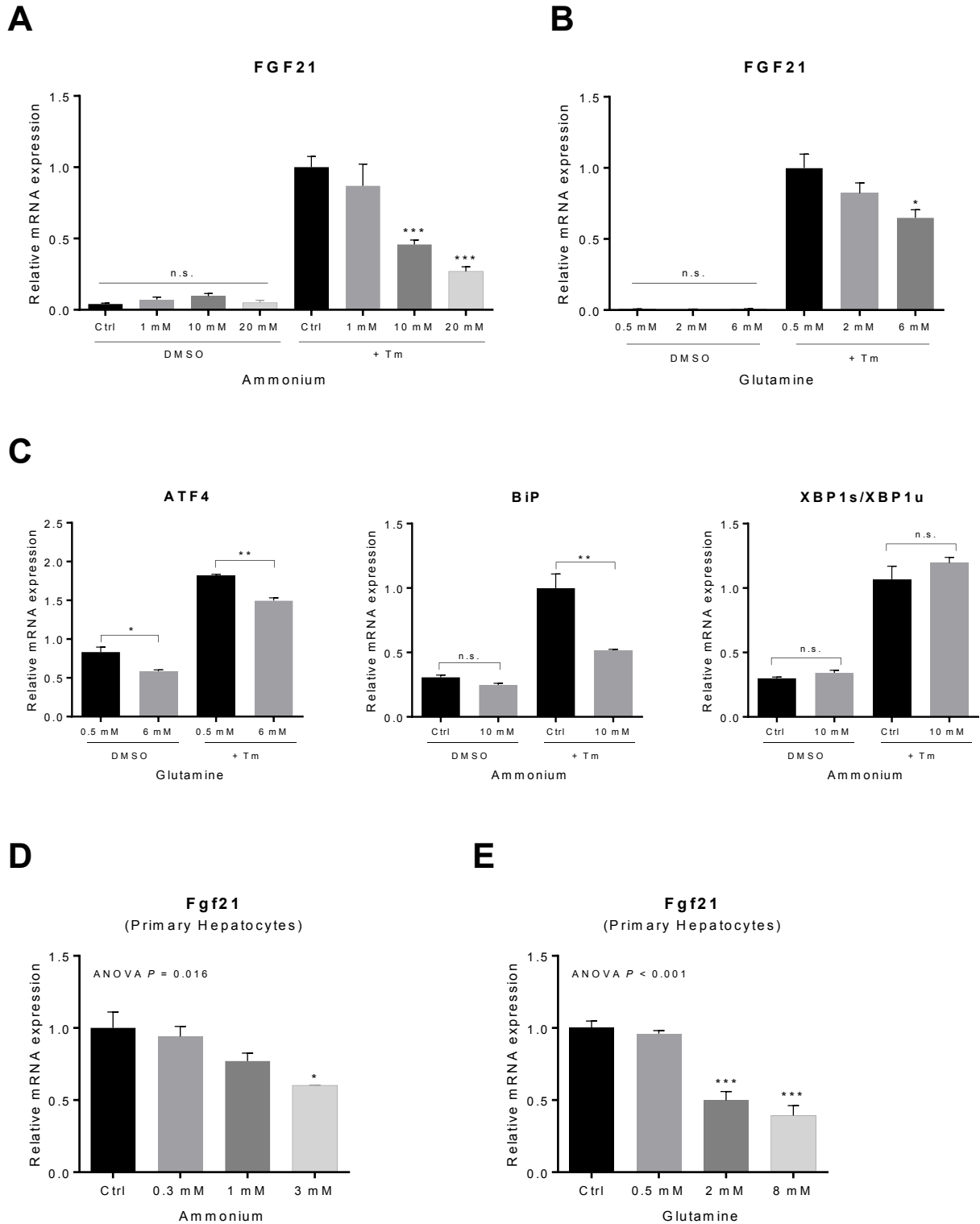
Figure 25 I Nitrogen metabolites suppress *FGF21* in hepatocytes. **A-B,** Human HepG2 cells were cultivated with increasing concentrations of NH$_4$Cl (A) or glutamine (B) in the media and stimulated with tunicamycin for 4 h after which *FGF21* expression was analyzed. **C,** Expression of genes involved in the cellular UPR in the glutamine (left panel) and NH$_4$Cl (middle and right panel) treated cells stimulated with tunicamycin or vehicle control. **D-E**, In primary hepatocytes, addition of increasing concentrations of NH$_4$Cl (D) and glutamine (E) to the cell culture media for 24 h decreased *Fgf21* mRNA expression in a dose-dependent manner. *$P < 0.05$, **$P < 0.01$, ***$P < 0.001$ differences from control condition. Ctrl indicates control; n.s., not significant.

Lastly, samples from two previously published studies in C57BL/6 mice were reanalyzed for *Fgf21* expression in order to assess in mice the regulation of FGF21 by diets enriched in

protein as well as single amino acids only. In the first study mice were fed for 20 weeks *ad-libitum* high-fat diets with either adequate protein (AP: 8.9 EN% protein), high-protein (HP: 44.8 EN%), or an AP diet supplemented with L-leucine corresponding to the leucine content of the HP diet (AP+L: 6% w/w leucine, 14.2 EN% protein) (Freudenberg et al., 2012). In a short-term follow-up study, the same diets as well as an additional condition consisting of an AP diet supplemented with equimolar L-alanine (AP+A) were fed for 1 week (Freudenberg et al., 2013). Indeed, in the obese mice hepatic *Fgf21* expression was potently reduced in the HP group compared to AP controls (Figure 26A). This effect was already observed after 1 week (Figure 26B). Interestingly, both leucine and alanine supplementation of an AP diet were sufficient to induce a suppression of *Fgf21*. While hepatic *Atf4* expression was moderately reduced in response to long-term intake of HP chow (or the single amino acid supplemented AP diet), *Atf4* expression measured after 1 week remained unchanged by the diets (Figure 26A-B, right panels). The data indicates that HP intake or amino acid supplementation similarly reduce hepatic *Fgf21* expression in mice. Furthermore, the HP-related suppression of *Fgf21* was not dependent on changes in *Atf4*.

A
B
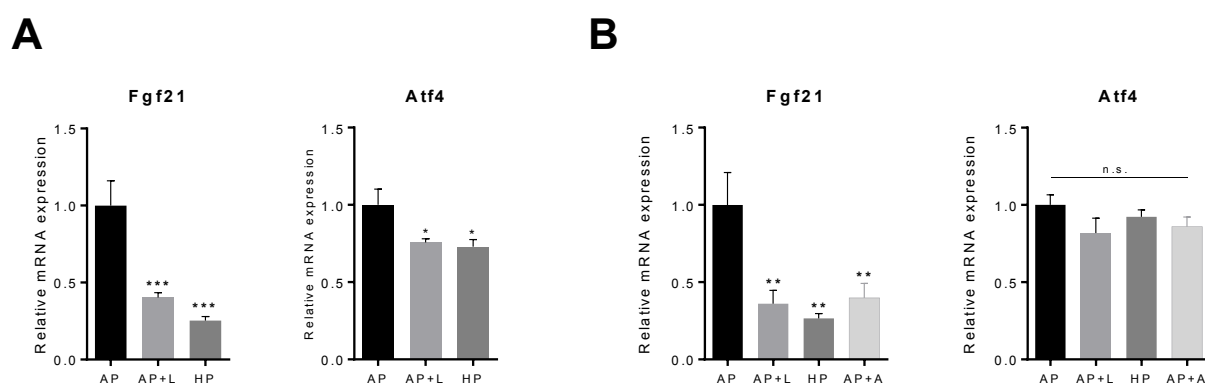
Figure 26 ı Hepatic *Fgf21* expression in mice fed a HP or amino acid supplemented diet. **A,** *Fgf21* and *Atf4* mRNA were measured in 30 weeks old C57BL/6 mice fed 20 weeks high-fat diets with adequate protein (AP: 8.9 EN% protein), high-protein (HP: 44.8 EN%) or an AP diet supplemented with L-leucine corresponding to the leucine content of the HP diet (AP+L: 6% w/w leucine) (n = 9-10). **B,** In a 1-week short-term feeding study 11 weeks old male C57BL/6 mice were fed high-fat diets with AP, HP or AP supplemented with leucine (AP+L) or equimolar alanine (AP+A) (n = 7-8). Hepatic *Fgf21* and *Atf4* mRNA was determined by qRT-PCR. *$P < 0.05$, **$P < 0.01$, ***$P < 0.001$ different from AP.

4.2.8   Identification of potential molecular pathways

Promoter elements of the human FGF21 gene (Pubmed gene ID: 26291) were analyzed by an *in-silico* search for transcription factor binding sites using MatInspextor (Genomatix, Intrexon Bioinformatics GmbH, Germany) resulting in 497 hits. The results were narrowed down by selecting only repressors with hepatic expression. This approach yielded 5 hits, though 4 of them encode for functionally related binding sites with only slight variations in their sequence (Table 8). The respective DNA-binding transcription factor is human insulinoma-associated protein 1 (INSM1, also known as Zinc finger protein IA-1). In addition, MYC associated factor

X (MAX), a ubiquitously expressed transcriptional regulator that acts in complex with MYC or MAD, was identified. The MYC:MAX complex is a transcriptional activator, whereas the MAD:MAX complex acts as a repressor.

Table 8 ⁞ Identification of *FGF21* promoter elements.

Family information	Matrix information	Tissue	Sequence
Insulinoma associated factors	Zinc finger protein insulinoma-associated 1 (IA-1) functions as a transcriptional REPRESSOR	Digestive System, Endocrine System, Liver, Pancreas	tggctGGGGaggt
Insulinoma associated factors	Zinc finger protein insulinoma-associated 1 (IA-1) functions as a transcriptional REPRESSOR	Digestive System, Endocrine System, Liver, Pancreas	tgagtGGGGcagt
Insulinoma associated factors	Zinc finger protein insulinoma-associated 1 (IA-1) functions as a transcriptional REPRESSOR	Digestive System, Endocrine System, Liver, Pancreas	ttccaGGGGcggc
Insulinoma associated factors	Zinc finger protein insulinoma-associated 1 (IA-1) functions as a transcriptional REPRESSOR	Digestive System, Endocrine System, Liver, Pancreas	tgtcgGGGGccga
REPRESSOR	MYC associated factor X	ubiquitous	ctggcCACGccccagcg

Results are from MatInspector. DNA binding sites are marked with capital letters in sequence.

However, this approach for identifying repressor binding sites in the *FGF21* promotor misses out on those transcription factors that are not labeled as "repressors" whereas inclusion of all cases leads to an extensively long list of results.

When trying to identify a potential molecular pathway, one faces the challenge that the enzymes involved in the urea cycle are still poorly elaborated and their regulation is rather complex (Morris, 2002). Similarly, a literature search for candidate transcription factors which are upregulated by high protein diets resulted in a variety of candidates. However, Martinez-Jimenez et al. identified the HES6/HNF4α protein complex (Martinez-Jimenez et al., 2010), which coordinates a set of metabolizing enzymes during fasting and feeding conditions, as a putative negative regulator of *Fgf21* expression. Although no HES6/ HNF4α binding sites were identified in the promotor analysis above, it might indirectly control *FGF21* expression. Stimulation of HepG2 cells with ammonium (the cell culture model described in section 4.2.7.), dose-dependently increased *HES6* mRNA expression while *HNF4A* mRNA expression remained unchanged (data not shown). Furthermore, Hes6 mRNA and protein were upregulated by dietary protein in the mice fed high-protein diets for 1 and 20 weeks (Figure 26) confirming HES6 as an interesting candidate repressor of FGF21.

In order to assess its effect on hepatic *Fgf21* expression, Hes6 was overexpressed and silenced in primary murine hepatocytes. The respective experiments were carried out by Steffi Heidenreich (Schupp lab, Institute of Pharmacology, Charité-Universitätsmedizin Berlin,

Berlin, Germany). As expected, transfection of primary murine hepatocytes with Hes6-targeting small interfering RNA (siRNA) effectively blunted *Hes6* mRNA expression, already at the lowest siRNA concentration (1-way ANOVA *P* = 0.005) (Figure 27A). However, no effect on *Fgf21* mRNA levels compared to control was observed (Figure 27A, right panel). Similarly, overexpression of *Hes6* using an adenoviral vector did not reduce *Fgf21* mRNA expression (Figure 27B) compared to GFP control. In the condition with the highest viral load, *Fgf21* expression was even increased (1-way ANOVA *P* = 0.012, *post-hoc* Bonferroni *P* = 0.015 compared to control). The data indicates that Hes6 most likely is not a repressor of *Fgf21*.

A

B
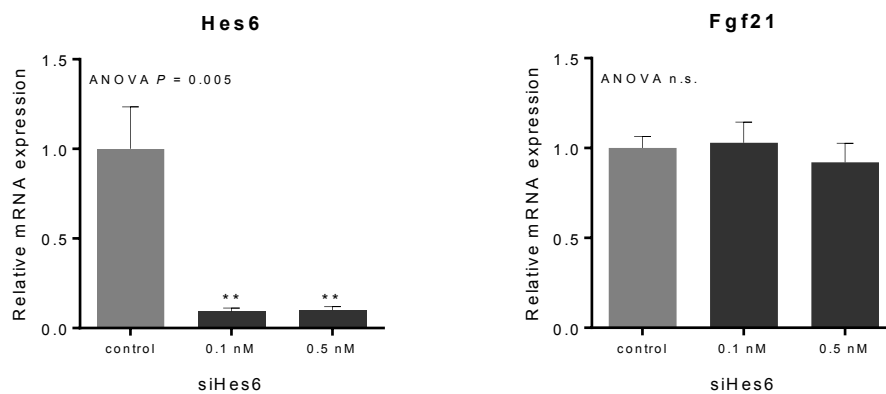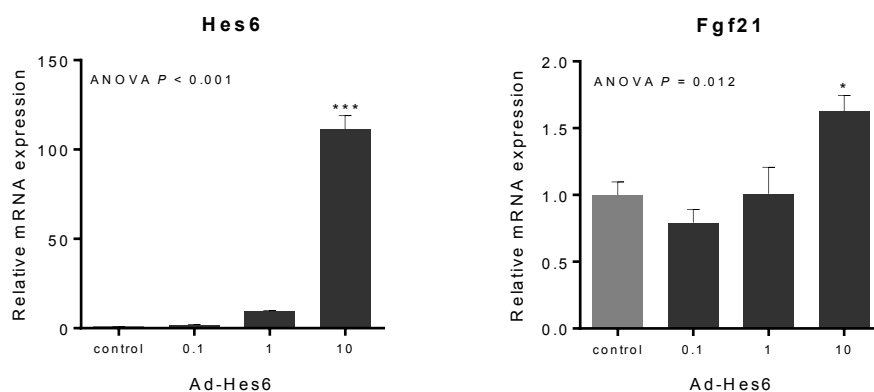
Figure 27 ǀ *Hes6* silencing and overexpression in primary murine hepatocytes. A-B, Hepatocytes isolated from C57BL/6J mice were treated with siRNA against *Hes6* (A) or an adenoviral vector overexpressing *Hes6* (Ad-Hes6) for 48 h before cell harvest (B). Subsequently *Hes6* (left panel) and *Fgf21* expression (right panel) was analyzed by qRT-PCR. RNAi indicates RNA interference, OX, overexpression., Hes6, hes family bHLH transcription factor 6.

4.3 Chemerin is regulated by diet and associated with adipose tissue inflammation

4.3.1 Circulating chemerin levels are elevated in obesity

The third part of this thesis addresses the regulation of chemerin in morbidly obese and healthy human subjects, its response to diet, and its association with NAFLD and adipose tissue inflammation. First, associations of serum chemerin with clinical parameters were assessed in both, the morbidly obese study subjects undergoing bariatric surgery (cohort 1) and the healthy reference cohort (cohort 2). If not otherwise indicated, tables and figures refer to results of the LEMBAS study (cohort 1).

Circulating chemerin has been reported to increase with BMI and body fat mass and has repeatedly been linked to metabolic disorders, including T2DM and NAFLD (Bobbert et al., 2015; Bozaoglu et al., 2007; Docke et al., 2013; Sell et al., 2009). However, in the morbidly obese subjects, chemerin in blood did not correlate with the anthropometric measures BMI, WHR or fat mass. Chemerin was also not associated with TAG, cholesterols, or FFA. Furthermore, chemerin did not correlate with clinical measures for insulin sensitivity, i.e. fasting glucose, fasting insulin, HbA1c, HOMA-IR, or Adipo-IR. In the samples collected during surgery, weak correlations between chemerin and total cholesterol (r = 0.422, P = 0.014) as well as fasting insulin (ρ = 0.391, P = 0.025) were detected. In this cohort of metabolically stressed patients, confirmed diagnosis of T2DM did not affect serum chemerin levels (chemerin$_{T2DM}$ = 191.2 ± 13.5 ng/ml, chemerin$_{nonT2DM}$ = 182.9 ± 9.0 ng/ml; P = 0.604).

In summary, the reported associations of chemerin with obesity-related measures could not be replicated in cohort 1. However, most clinical measures assessed were shifted towards the diseased state. Thus, the parameters were rather representing the extreme than a normal distribution. All participants met the criteria for bariatric surgery, amongst others due to the abnormal serum parameters. Therefore, the correlation analysis was repeated in the healthy, normal weight, and insulin sensitive study subjects of cohort 2 (for details see section 3.2.2 and Appendix Table A3). In addition, the greater cohort size (n = 92) enhanced the data.

In the healthy, lean study subjects, baseline chemerin levels were considerably lower than those measured in the obese subjects of cohort 1 (cohort 2: 134.1 ± 2.5 ng/ml, n = 85; cohort 1: 195.9 ± 9.3 ng/ml, n = 19). Correlation coefficients between chemerin and clinical characteristics measured in cohort 2 are presented in Table 9. Circulating chemerin significantly correlated with age and BMI at all 3 clinical investigation days (CIDs) (age: P_{LF} = 0.010, P_{HF1} = 0.001, P_{HF6} = 0.040; BMI: P_{LF} = 0.032, P_{HF1} = 0.001, P_{HF6} = 0.024). Furthermore, chemerin was positively associated with absolute and relative fat mas (fat mass: P_{LF} = 0.001, P_{HF6} = 0.023; % fat mass P_{LF} = 0.018, P_{HF6} = 0.034). Similarly, chemerin correlated with WHR, a measure of central obesity (P_{LF} = 0.017, P_{HF1} = 0.024).

Interestingly, circulating chemerin was positively associated with TAG, total cholesterol and LDL cholesterol after the high-carbohydrate, low-fat (LF) diet and after 1 week on the high-fat (HF) diet (all: $P_{LF} < 0.01$, $P_{HF1} < 0.05$) but not after 6 weeks on the same diet. Chemerin was not associated with HDL cholesterol or FFA at any CID. Hepatic lipids (IHL) correlated with chemerin before ($P_{LF} = 0.005$) and after the HF intervention ($P_{HF6} = 0.244$) (Table 9). Regarding parameters of glucose metabolism, a weak positive association between circulating chemerin and HbA1c at LF6 ($P = 0.026$) and with fasting glucose at HF1 ($P = 0.003$) was detected. Furthermore, serum chemerin weakly and positively correlated with the adipokine leptin during the HF intervention ($P_{HF1} = 0.018$, $P_{HF6} = 0.018$), with visfatin before and after the HF diet ($P_{LF} = 0.021$, $P_{HF6} = 0.073$), but not with adiponectin (Table 9).

Table 9 | Correlation of chemerin with clinical measures in the healthy subjects of cohort 2.

Correlation of chemerin with	LF	HF1	HF6
Anthropometry			
Age	**0.278****	**0.354****	**0.222***
BMI	**0.232***	**0.341****	**0.244***
WHR	**0.258***	**0.245***	0.073
Absolute fat mass	**0.340***	NA	**0.266**
Relative fat mass	**0.256***	NA	**0.229**
Lipid metabolism			
TAG	**0.303***	**0.240***	0.204
Cholesterol	**0.289****	**0.263***	0.127
LDL-c	**0.288****	**0.222***	0.105
HDL-c	0.032	-0.073	-0.080
FFA	0.046	-0.133	0.015
IHL	**0.316****	0.166	**0.244***
Glucose metabolism			
Glucose	0.186	**0.314****	0.156
Insulin	0.113	0.148	0.115
HbA1c	**0.262***	0.133	0.023
HOMA-IR	0.129	0.175	0.161
Adipo-IR	0.180	0.093	0.124
Organokines			
Adiponectin	-0.157	0.080	-0.087
Leptin	0.212	**0.258***	**0.256***
FGF21	0.123	0.053	0.133
Visfatin	**0.252***	0.016	**0.227***

Data are Pearson or Spearman correlation coefficients dependent on a normal or skewed distribution, respectively. Blood parameters were measured in the fasted state. IHL content was determined by MRI$_{spec}$. Asterisks indicate statistical significance as follows *$P < 0.05$, **$P < 0.01$. Significant correlations ($P < 0.05$) are marked in bold. LF6 indicates clinical investigation day (CID) after 6 weeks on the low-fat, high-carbohydrate diet; HF1, CID after 1 week on the high-saturated fat diet; HF6, CID after 6 weeks on the HF diet; NA, not assessed.

4.3.2 Serum chemerin concentrations have a genetic determinant

Next, it was investigated in the 46 twin pairs of cohort 2 whether serum chemerin levels are genetically determined. Based on the ACE structural equation model, over 55% of variation in serum chemerin can be explained by additive genetic effects. In accordance, intrapair correlation of serum chemerin was high in monozygous twins (r = 0.745, P < 0.001) but chemerin values did not correlate in dizygous twins (r = 0.306, not significant) (Figure 28).
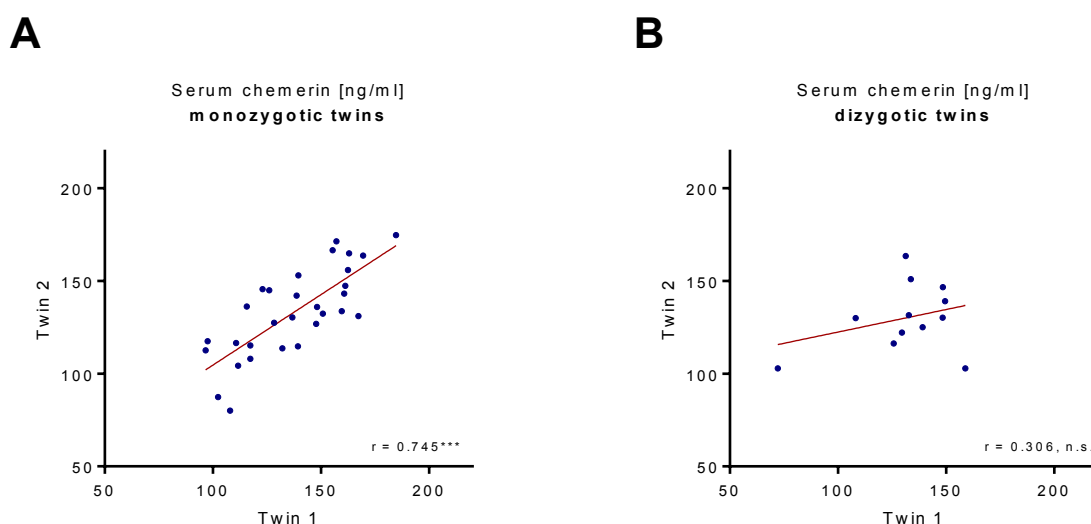
Figure 28 ∣ Heritability estimates for circulating chemerin levels. **A-B,** Correlation of serum chemerin in monozygotic (A) and dizygotic (B) twin pairs (cohort 2, n = 85). High correlation of serum chemerin in monozygotic twin pairs and no correlation in dizygotic twin pairs indicates high heritability which was estimated to be 55% based on the ACE structural equation model. Asterisks indicate statistical significance of correlation coefficients as follows: ***P < 0.001. n.s. indicates not significant.

In cohort 2, genomic DNA had been isolated from blood cells and genotype information for a variety of genes was available. The association of serum chemerin with selected single nucleotide polymorphisms (SNPs) was investigated in order to identify genetic factors explaining the high heritability of serum chemerin. The SNP rs3735167 is located in the 5'UTR of *RARRES2* and has previously been associated with circulating chemerin levels (Tonjes et al., 2014). Genotype frequencies in the study cohort were AA (homozygous carrier) = 1, AG (heterozygous carrier) = 31, and GG (homozygous non-carriers) = 59.

At all clinical investigation days, carriers of the SNP had significantly higher serum chemerin levels than non-carriers (HF1; AA/AG: 142.5 ± 3.6 ng/ml, GG: 129.2 ± 3.1 ng/ml; 2-way ANOVA P_{SNP} = 0.004, $P_{Time*SNP}$ not significant) (Figure 29A). Concomitantly, carriers had higher *RARRES2* expression in SAT at HF1 and HF6 (2-way ANOVA P_{SNP} = 0.019, $P_{Time*SNP}$ not significant). However, the rs3735167 polymorphism had no effect on response to the HF diet in terms of serum chemerin or *RARRES2* expression in adipose tissue (Figure 29A-B).

Interestingly, carriers of the SNP had a significantly lower ratio of body fat mass (dominant model, P = 0.010), while the relative contribution of VAT mass was higher in these subjects (P_{VAT} = 0.038, $P_{\%VAT}$ = 0.007) (Figure 29C-E). The SNP had no effect on SAT mass indicating that the higher body fat mass in SNP carriers is attributable to a higher ratio of interorgan fat. Furthermore, no difference in BMI, glucose tolerance or blood lipids were detected between carriers and non-carriers (data not shown).
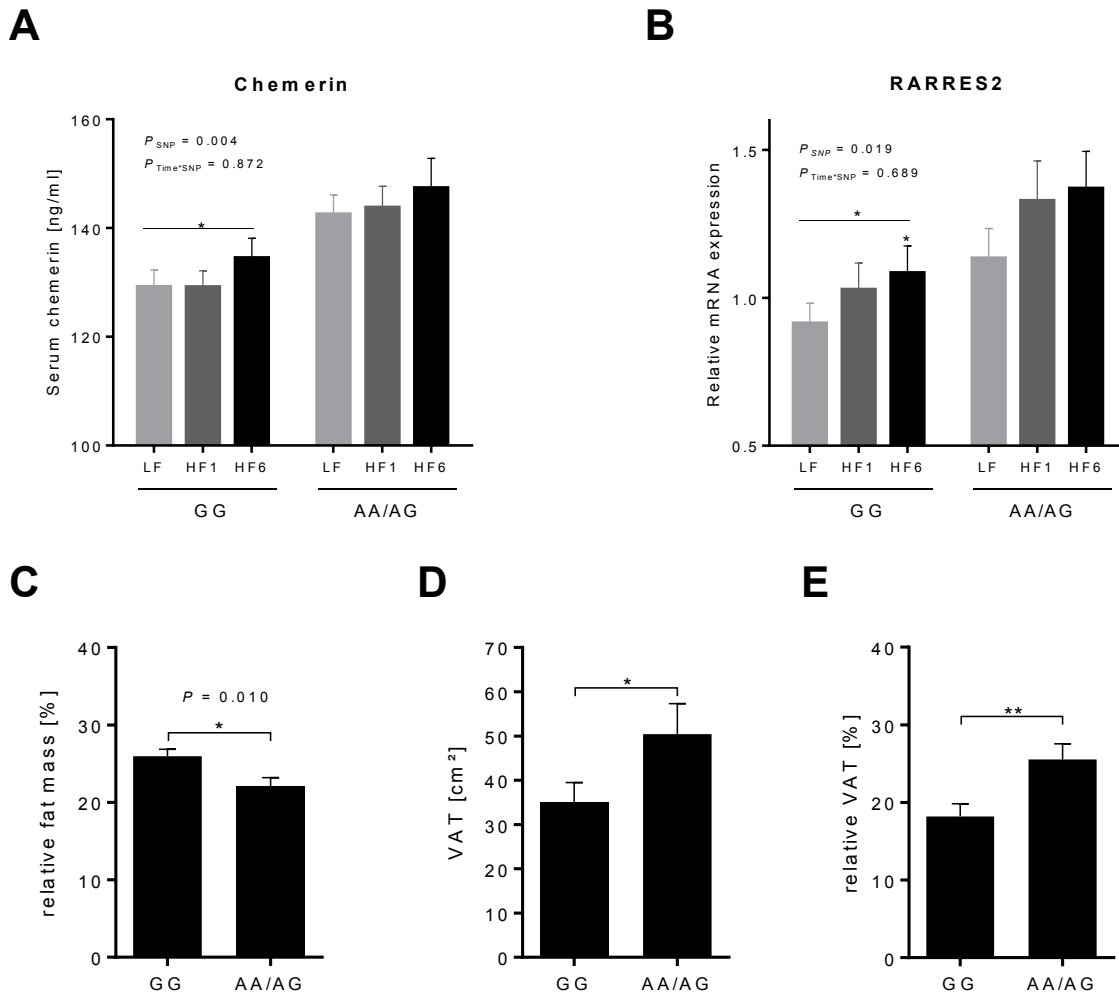
Figure 29 ∣ Effect of a SNP in the *RARRES2* locus on chemerin concentrations. SNP rs3735167 is located in the 5'UTR of RARRES2 and is associated with circulating chemerin in cohort 2. **A-B,** Carriers of the SNP (AA/AG) had significantly higher serum chemerin (A), paralleled by higher RARRES2 expression in SAT (B) than homozygous non-carriers (dominant model). However, the SNP did not affect response to diet. *P < 0.05 different from LF6. **C-E,** Significantly lower total fat mass (C) but higher visceral fat mass (D-E) in homozygous or heterozygous carriers of SNP rs3735167. *P < 0.05, **P < 0.01 difference between carriers and non-carriers.

4.3.3 Chemerin is responsive to dietary interventions

Subsequently it was investigated if and how serum chemerin levels are regulated by diet. In the morbidly obese study subjects of cohort 1, baseline chemerin levels were 193.6 ± 14.6 ng/ml in the LP group and 198.7 ± 11.1 ng/ml in the HP group (P_{LpvsHP} not significant). The hypocaloric interventions induced a drop in circulating chemerin in both groups (P_{LP} = 0.018,

P_{HP} = 0.061, P_{LPvsHP} not significant) (Figure 31A). However, serum chemerin levels were not affected by the protein content of the diet as the changes in serum chemerin in response to the interventions were not different between the groups (Figure 30A).

Expression of chemerin mRNA was analyzed in SAT, VAT and liver. *RARRES2* was well expressed in all analyzed tissues. Contrary to expectations, tissue *RARRES2* expression did not correlate with circulating chemerin concentrations neither from SAT, VAT nor liver. There was a modest association of *RARRES2* expression between the two adipose tissue depots (r = 0.394, *P* = 0.021).

Similar to serum chemerin, expression of *RARRES2* in adipose tisse (Figure 33) or liver (Figure 30B) was not affected by the the dietary protein content as mRNA expression in these tissues was not significantly different between the intervention groups. In accordance with the decrease in circulating chemerin in response to the calorie restriction, *RARRES2* expression in SAT and liver was lower in the LP and HP groups compared to the RP group. Interestingly, hepatic expression of CM*KLR1*, the primary chemerin receptor, was significantly upregulated in the LP group (CMKLR1: 1-way ANOVA *P* = 0.029, *post-hoc* Bonferroni P_{LPvsHP} = 0.042, CCRL2: 1-way ANOVA *P* = 0.481) (Figure 30B).

A

B
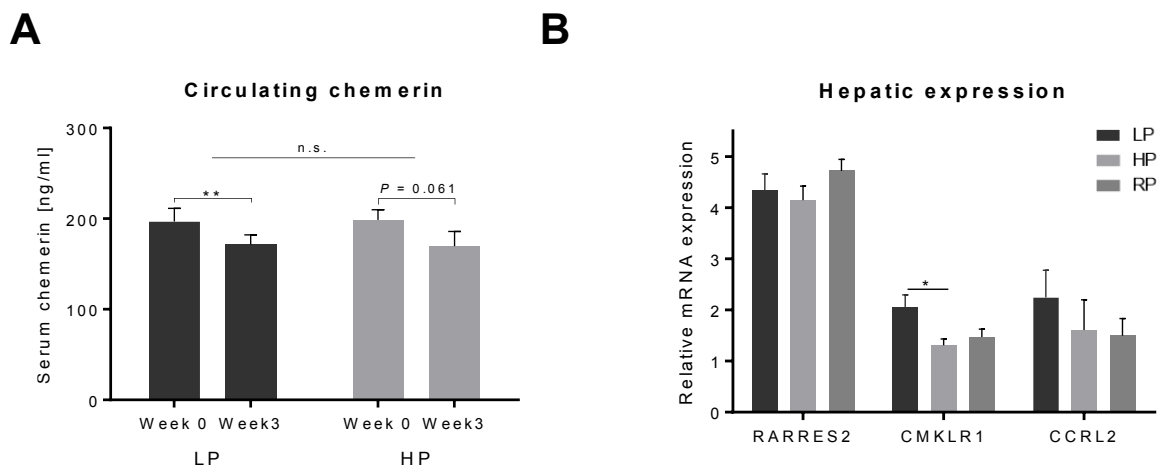
Figure 30 I Response of chemerin to differing dietary protein content. Serum chemerin concentrations and hepatic mRNA levels were measured before and after the LP and HP interventions in the morbidly obese subjects (cohort 1). **A,** Serum chemerin concentrations decrease in response to the hypocaloric diet but are not affected by dietary protein content. **P < 0.01 different from week 0. **B,** Hepatic *CMKLR1* expression is higher in the LP compared to the HP group. *P < 0.05 difference between groups determined by 1-way ANOVA followed by *post-hoc* Bonferroni correction. n.s. indicates not significant.

Elevated circulating chemerin concentrations have been associated with a sedentary lifestyle and high-fat chow in rats (Kaur et al., 2018; Lloyd et al., 2015; Roh et al., 2007). The effect of an unhealthy high-fat (HF) diet on serum chemerin was investigated in the metabolically healthy subjects of cohort 2. Furthermore, as the dietary intervention was isocaloric to the

individual energy requirements, the influence of changes in caloric intake could be eliminated which presumably accounted for the main effect in in cohort 1.

In the healthy study subjects, a 1-week unhealthy HF diet enriched in saturated fatty acids induced a modest increase in circulating chemerin concentrations. After 6 weeks on the unhealthy HF diet, circulating chemerin levels were significantly elevated with 139.5 ± 3.1 ng/ml (ANOVA repeated measures $P = 0.035$) (Figure 31A). In accordance, adipose tissue *RARRES2* expression increased during the HF intervention (ANOVA repeated measures $P = 0.006$, *post-hoc* Bonferroni $P_{HF6vsLF6} = 0.003$) (Figure 31B). Interestingly, the chemerin receptor, *CMKLR1*, was acutely downregulated after 1 week on the HF diet (ANOVA repeated measures $P = 0.003$, *post-hoc* Bonferroni $P_{HF1vsLF6} = 0.012$) but returned to baseline levels after the full 6 weeks on the HF diet (Figure 31C).

A   **B**   **C**
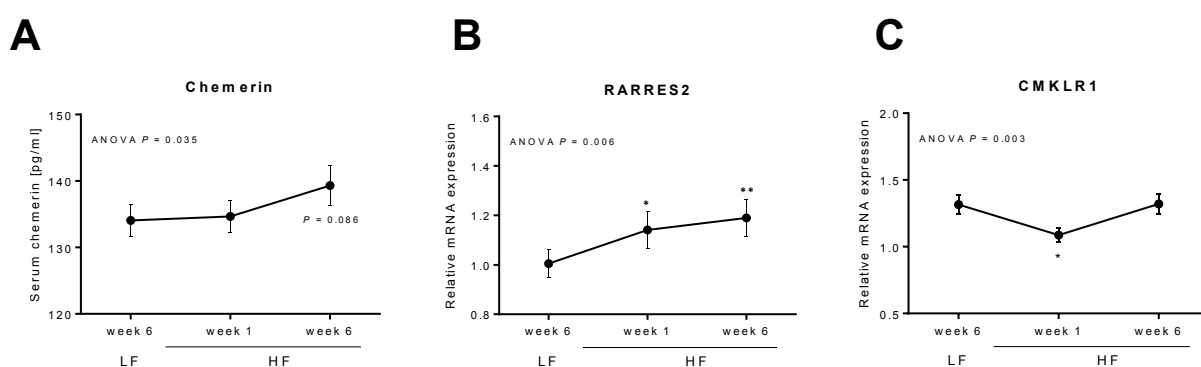
Figure 31 ᴵ Response of chemerin to a high-fat diet (cohort 2). Serum chemerin concentrations and adipose tissue mRNA expression were measured before (LF6), after 1 week (HF1), and after 6 weeks (HF6) on the HF diet in the healthy, lean subjects (cohort 2). **A,** Serum chemerin increases significantly in response to the HF diet, **B-C,** *RARRES2* expression in SAT is upregulated (B) in response to the HF diet while its receptor, *CMKLR1*, is transitionally downregulated (C), returning to baseline levels after prolonged HF intake. *$P < 0.05$, **$P < 0.01$ different from LF6.

4.3.4 Expression of *CMKLR1* correlates with markers of hepatic fibrosis

Reports on the role of chemerin in fatty liver disease are not concordant (Docke et al., 2013; Kajor et al., 2017; Krautbauer et al., 2013; Pohl et al., 2017; Wolfs et al., 2015). Associations of serum and hepatic chemerin were assessed in the obese subjects (cohort 1) with high prevalence of hepatic steatosis (described in section 4.1.4.).

In cohort 1, correlation of chemerin with IHL, as determined by MRI$_{spec}$, did not reach statistical significance, despite a moderate correlation coefficient (week 0: r = 0.458, $P = 0.156$; week 3: r = 0.392, $P = 0.233$). Furthermore, chemerin did not correlate with hepatic TAG content as assessed enzymatically. Although circulating chemerin increased with severity of NAFLD the data was statistically not significant. Lastly, serum chemerin concentrations were not significantly higher in patients previously diagnosed with NASH (chemerin$_{NASH}$ = 196.6 ± 9.6 ng/ml, chemerin$_{nonNASH}$ = 177.9 ± 10.1 ng/ml; $P = 0.248$).

In accordance, no associations were found between serum chemerin and the histological assessment of steatosis, fibrosis, ballooning, or inflammation, neither with serum concentrations nor hepatic expression of *RARRES2* or its receptors. However, *RARRES2* expression in SAT was weakly associated with liver fibrosis (*P* = 0.016) and inflammation (*P* = 0.031). Chemerin in serum and hepatic mRNA were weakly correlated with expression of fibrosis-associated genes in liver. Circulating chemerin negatively correlated with *collagenase 6* mRNA in liver (COL6: r = - 0.389, *P* = 0.025) while hepatic *RARRRES2* expression was negatively associated with TIMP1 concentrations in blood (ρ = -0.406, *P* = 0.019). Interestingly, hepatic *CMKLR1* expression strongly and positively correlated with mRNA expression of *COL1* (ρ = 0.653, *P* < 0.001), *COL3* (r = 0.511, *P* = 0.002), *COL6* (r = 0.453, *P* = 0.008), *ACTA2* (r = 0.685, *P* < 0.001), *MMP9* (ρ = 0.644, *P* < 0.001), *TGFβ* (r = 0.632, *P* < 0.001), and *TIMP1* (r = 0.700, *P* < 0.001), but not with TIMP1 serum concentrations.

4.3.5 Serum chemerin and tissue *RARRES2* expression are differentially associated with markers of inflammation

In the following, associations of chemerin with markers of inflammation are presented as assed in serum and tissue biopsies collected from (1) the morbidly obese and metabolically-stressed subjects of cohort 1 (serum, SAT, VAT, and liver), and (2) the healthy subjects of cohort 2 (serum and SAT). As presented in section 4.1.6, circulating CRP levels in in the obese subjects were considerably elevated indicating chronic low-grade inflammation. In serum collected during surgery, circulating chemerin correlated with MCP1 (r = 0.381, *P* = 0.029), TNFα (r = 0.409, *P* = 0.018), and, highly significantly, with IL6 (ρ = 0.665, *P* < 0.001) (Figure 32) but not with CRP, IFNγ, IL1β, or IL10.
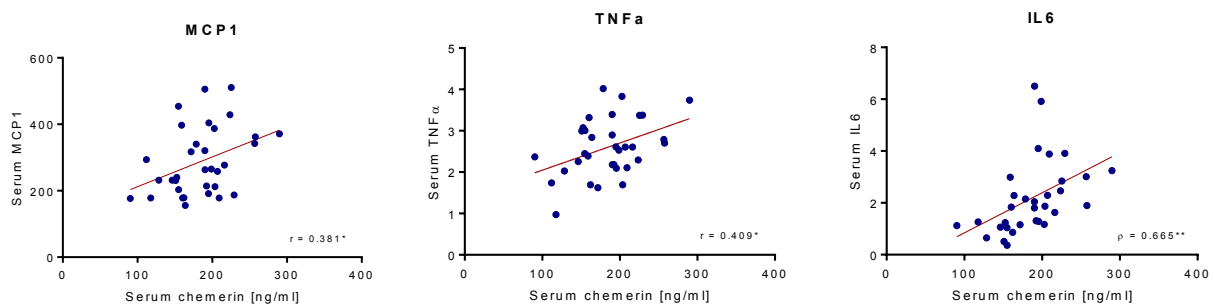
Figure 32 ɪ Correlation of chemerin with cytokines in serum. Chemerin, MCP1, TNFα, and IL6 were measured in serum collected during bariatric surgery. Asterisks indicate statistical significance of correlation coefficients: **P* < 0.05, ***P* < 0.01.

In contrast to the circulating chemerin, *RARRES2* did not correlate with any of the inflammatory markers analyzed in the obese subjects, neither in SAT nor in VAT. However, *CMKLR1* expression was strongly and positively associated with *TNFα* and *MCP1* mRNA in SAT (*TNFα*:

$\rho = 0.615$, $P < 0.001$; MCP1: $r = 0.539$, $P = 0.001$) as well as *TNFα* mRNA in VAT ($\rho = 0.520$, $P = 0.002$).

Next, the association of chemerin expression with infiltration of adipose tissue macrophages as assessed histologically (section 4.1.6) was investigated. Serum chemerin concentrations increased with number of CLS in VAT (no CLS: 186.8 ± 13.5 ng/ml; 1 CLS: 191.3 ± 12.1 ng/ml; 2 CLS: 206.5 ng/ml; ≥ 3 CLS: 236.4 ± 52.5 ng/ml). However, this association remained insignificant. No difference between CLS$^-$ and CLS$^+$ participants in chemerin serum concentrations or *RARRES2* mRNA expression were detected in either SAT or VAT. However, there were only 4 participants categorized as CLS$^-$ in SAT.

In liver, serum chemerin or hepatic mRNA did not correlate with histologically determined inflammation (section 4.3.1). In patients whose tissue sections showed hepatic inflammation (histological score ≥ 1), SAT expression of *RARRES2* was elevated ($P = 0.031$). In accordance with adipose tissue, expression of the chemerin receptor *CMKLR1* was positively correlated with *TNFα* ($\rho = 0.386$, $P = 0.026$) and *MCP1* ($\rho = 0.410$, $P = 0.020$) mRNA in liver. Furthermore, hepatic *CMKLR1* levels were positively associated with *TNFα* expression in SAT ($\rho = 0.457$, $P = 0.007$) but not in VAT. No associations between hepatic *RARRES2* expression and mRNA quantity of any cytokine analyzed were found.

In summary, chemerin was only weakly associated with markers of inflammation in serum, liver and adipose tissue in the morbidly obese subjects. Chemerin serum concentrations increased with macrophage infiltration in adipose tissue but no statistical significance was reached which might be due to the low number of observations.

In the healthy subjects of cohort 2, circulating CRP concentrations were considerably lower than in the extremely overweight subjects of cohort 1. CRP levels in blood increased significantly in response to the unhealthy HF diet (LF: 0.29 ± 0.05 mg/l, HF1: 0.46 ± 0.06 mg/l, HF6: 0.64 ± 0.10 mg/l; ANOVA repeated measures $P < 0.001$) reflecting the high intake of saturated fats. In serum, chemerin was moderately and positively associated with circulating CRP concentrations at HF1 ($\rho = 0.230$, $P = 0.034$), with IL6 concentrations before and after the HF diet (LF6: $\rho = 0.226$, $P = 0.038$; HF6: $\rho = 0.240$, $P = 0.026$), as well as with the anti-inflammatory cytokine IL1RA at LF6 ($r = 0.284$, $P = 0.008$) but not with serum concentrations of MCP1, TNFα, or IL10.

In SAT, *RARRES2* mRNA levels were strongly and positively associated with expression of *TNFα* (all CIDs $r > 0.3$ and $P < 0.001$), *MCP1*, the inflammasome component *NLRP3 and* with the macrophage markers *CD14* (all CIDs $P < 0.001$) and *CD68* (all CIDs $P < 0.001$) (Appendix Table A4). Interestingly *RARRES2* mRNA levels were negatively associated with mRNA expression of *NFkB*, *IL1β* and *EMR1* (Appendix Table A4).

Finally, a potential association with mRNA levels of the main chemerin receptor *CMKLR1* and cytokine expression in SAT was assessed. *CMKLR1* mRNA levels were positively associated with expression of *TNFα*, *MCP1*, and *NLRP3* (all CIDs $P < 0.001$) but not with *IL1β* and only at HF6 with *NFκB* (Appendix Table A4). Furthermore, *CMKLR1* expression was associated with *CD14* (all CIDs $P < 0.001$) and *CD68* expression (all CIDs $P < 0.001$) but not with EMR1 (Appendix Table A4).

In summary, chemerin is inconsistently associated with inflammatory cytokines depending on the study cohort, time point, and tissue analyzed. Furthermore, a negative association was found between *RARRES2* and pro-inflammatory mediators, i.e. the cytokine *IL1β* and the transcription factor *NFκB*, as well as macrophage marker *EMR1* in the healthy subjects pointing towards a role of chemerin not only in the onset but also the resolution of inflammation. Interestingly, mRNA expression of the chemerin receptor, *CMKLR1*, was consistently associated with expression of *TNFα,* a marker of systemic inflammation.

4.3.6   Chemerin is associated with adipocyte cell size and lipid metabolism

Chemerin has been shown to play a role in adipogenesis and adipocyte function (Goralski et al., 2007). In the paired adipose tissue biopsies, mRNA levels of *RARRES2, CMKLR1*, and *CCRL2* were significantly higher in the subcutaneous fat depot (all $P_{SATvsVAT} < 0.001$) whereas *GPR1* expression was higher in the visceral fat depot ($P_{SATvsVAT} = 0.016$) (Figure 33A). Furthermore, expression of *RARRES2* was weakly correlated between the two adipose tissue depots (r = 0.394, *P* = 0.021).

Next, potential differences between the intervention groups were analyzed. In accordance with the circulating chemerin, *RARRES2* expression in fat was not significantly regulated by dietary protein. However, expression of *CMKLR1* was downregulated in the HP group in both fat depots (SAT: ANOVA *P* = 0.032, *post-hoc* Bonferroni $P_{LPvsHP} = 0.028$; VAT: ANOVA *P* = 0.040, *post-hoc* Bonferroni $P_{HPvsRP} = 0.040$) (Figure 33B). *GPR1* was regulated in a similar direction but without reaching statistical significance (Figure 33B).

A

B
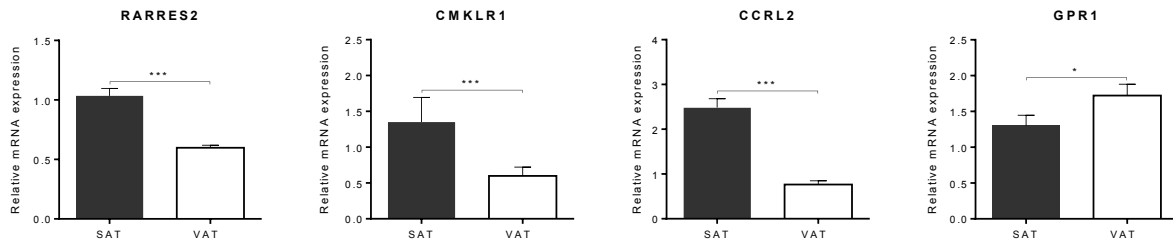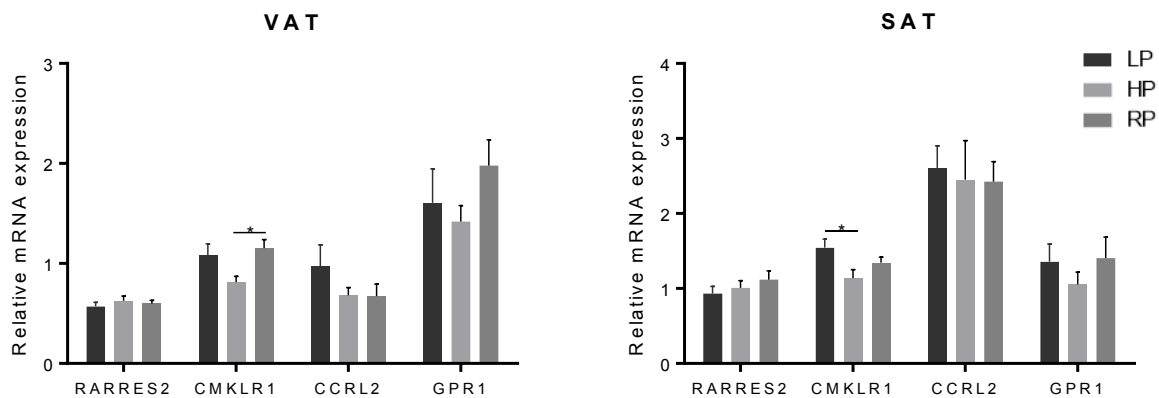
Figure 33 ǀ Expression of *RARRES2* and the chemerin receptors in adipose tissue. A, mRNA expression in SAT *versus* VAT. *$P < 0.05$, ***$P < 0.001$ difference between fat depot. **B,** Adipose tissue mRNA expression of chemerin pathway in VAT (left panel) and SAT (right panel). Differences between groups were assessed by 1-way ANOVA with *post-hoc* Bonferroni correction. *$P < 0.05$ difference between groups.

As described previously (section 4.1.5), the adipocytes of cohort 1 were relatively large, as was expected from the obese study subjects. A positive association between adipocyte cell size and serum chemerin was found. Indeed, serum chemerin concentrations were positively correlated with adipocyte diameter (r = 0.438, *P* = 0.010) and area (r = 0.448, *P* = 0.009) in VAT but not in SAT. There were no significant associations between adipocyte cell size and *RARRES2* expression in either tissue.

As indicated by the murine data of Goralski and colleagues, chemerin seems to play a role in adipocyte lipid metabolism (Goralski et al., 2007). In SAT, *RARRES2* mRNA levels were strongly associated with the expression of genes involved in lipid metabolism (Table 10). However, as these genes are participating in the same enzymatic processes, correlation among the genes was also high. In VAT, *RARRES2* was moderately associated with genes involved in fat uptake and storage (*PPARγ*, *PGC1α*, *LPL*) but not with those involved in *de novo* lipogenesis (*ACC1, FASN, SREBP1c*) or lipolysis (*ATGL, HSL*) (Table 10).

Table 10 ı Correlation of *RARRES2* with adipose tissue lipid metabolism in obese subjects.

Correlation of *RARRES*2 with	SAT	VAT
De novo lipogenesis		
ACC1	**0.555*****	0.173
FASN	**0.659*****	0.289
SREBP1c	**0.634*****	0.219
Fat uptake and storage		
PPARγ	**0.634*****	**0.487****
PGC1α	**0.345***	**0.370***
SCD1	**0.392***	0.311
LPL	**0.475****	**0.460****
Lipolysis		
ATGL	**0.547*****	0.319
HSL	**0.505****	0.293

Data are Pearson or Spearman correlation coefficients dependent on a normal or skewed distribution, respectively. ACC1 indicates acetyl-CoA carboxylase; ATGL, adipose triglyceride lipase; FASN, fatty acid synthase; HSL, hormone-sensitive lipase; LPL, lipoprotein lipase; PGC1α, peroxisome proliferator-activated receptor gamma coactivator 1-alpha; PPARγ, peroxisome proliferator-activated receptor gamma; SCD1, stearoyl-CoA desaturase-1; SREBP1c, sterol regulatory element-binding protein 1. Asterisks indicate statistical significance as follows *$P < 0.05$, **$P < 0.01$.

Correlation of *RARRES2* with genes involved in lipid metabolism was also confirmed in the healthy subjects of cohort 2. Here, *RARRES2* strongly and positively correlated with *FASN, PPARα, PPARγ, PGC1α* (only at LF6 and HF1), *LPL,* and *ADIPOQ* (encoding adiponectin) (all: r > 0.36, *P* < 0.001 at all CIDs) (Figure 34). Remarkably, the association between *ADIPOQ* and *RARRES2* expression in SAT was highly significant at all time points with correlation coefficients of > 0.8 at LF6 and > 0.6 for both CIDs of the HF diet (Figure 34, lower right panel). Despite this strong correlation at the gene expression level, circulating chemerin and adiponectin were not associated at any time point.
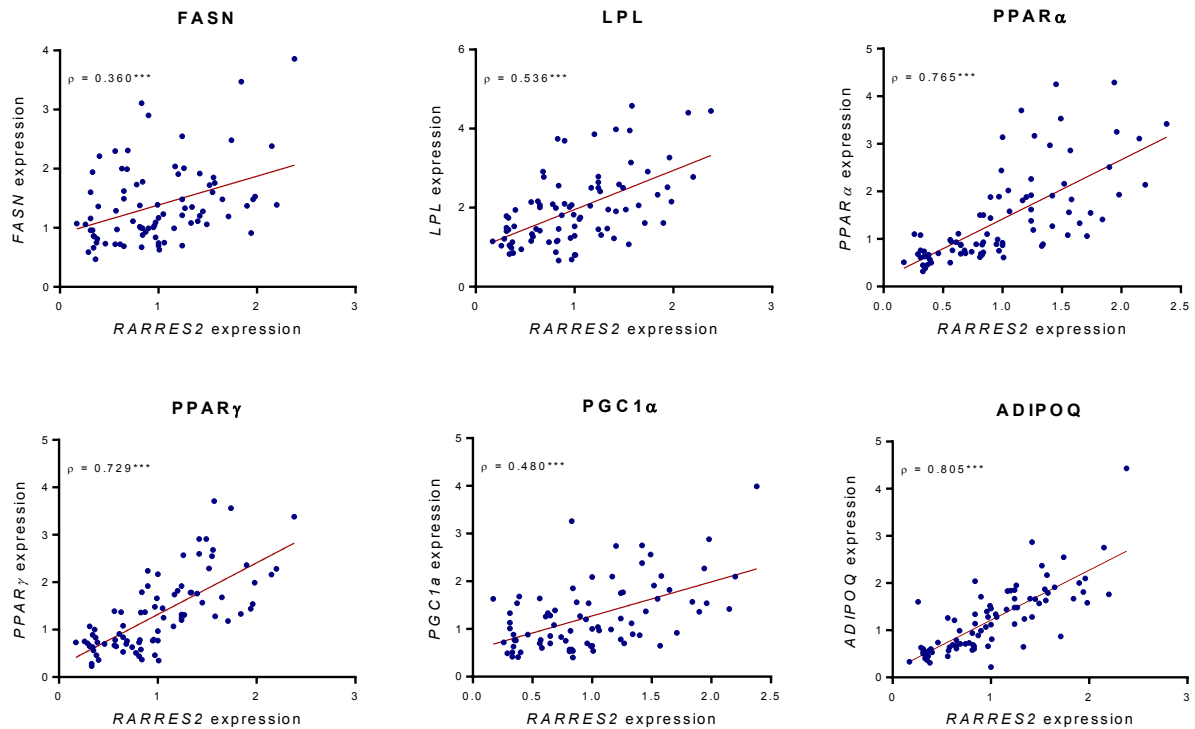
Figure 34 ı Correlation of *RARRES2* with lipid metabolism in SAT of lean subjects (cohort 2). Shown are mRNA concentrations measured at LF6 in SAT of the lean, healthy subjects. Asterisks indicate statistical significance of correlation coefficients as follows: ****P* < 0.001.

4.3.7   Mechanistic studies in differentiating and mature primary human adipocytes

The collected adipose tissue biopsies from cohort 1 allowed it to study the expression of chemerin during differentiation as well as its effects on the mature cell in primary, human adipocytes. In order to isolate preadipocytes from the adipose tissue biopsies, the stromal vascular fraction was separated from the mature adipocytes, blood vessels, and connective tissue by enzymatic digestion and centrifugation (Figure 35A). Under cell culture conditions, mesenchymal stromal cells (MSCs) were isolated from the stromal vascular fraction and cultured in selective preadipocyte medium. Differentiation into adipocytes was induced by adding a hormonal cocktail (amongst others including insulin, rosiglitazone, dexamethasone and triiodothyronine) to the cell culture medium. During differentiation the typical adipocyte morphology became apparent with large, rounded, lipid-droplet filled cells (Figure 35A). Preadipocytes isolated from SAT grew fast and reliably differentiated into mature adipocytes whereas the successful differentiation of preadipocytes isolated from VAT seemed to be donor dependent. For the following experiments adipocytes isolated from SAT were used only.

Degree of differentiation was determined microscopically and by qRT-PCR of the mature adipocyte markers *GLUT4, FASN,* and *PPARγ* (Figure 35B). Only well differentiated adipocytes were used for further experiments.

A

B
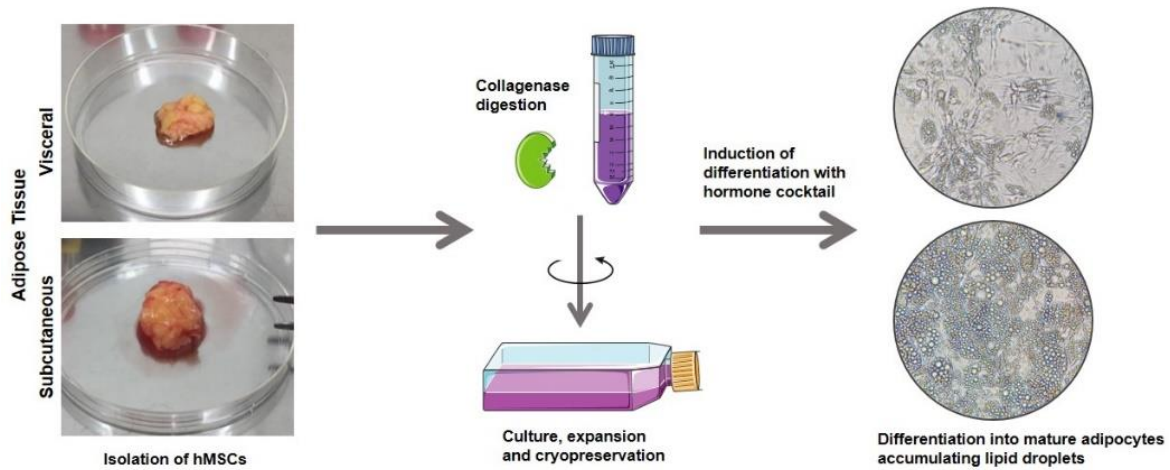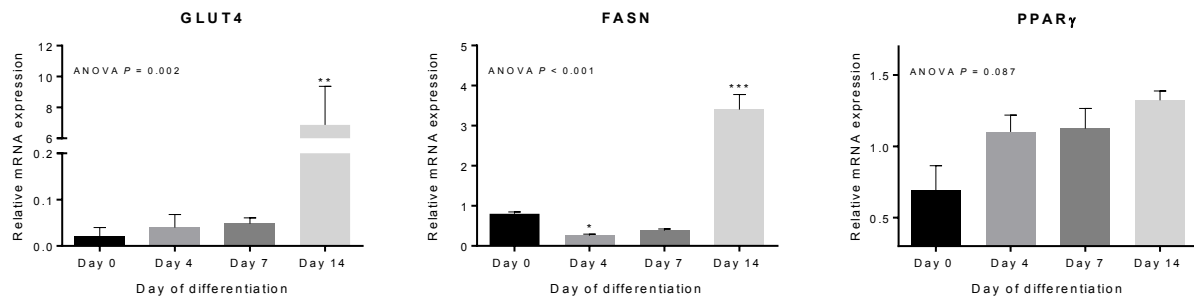
Figure 35 ǀ Differentiation of human mesenchymal stromal cells (MSCs) into mature adipocytes. A, Primary human MSCs were isolated from SAT and VAT biopsies by enzymatic digestion and expanded in selective preadipocyte medium. Differentiation was induced by addition of a hormonal cocktail to the cell culture medium. Successful differentiated adipocytes were round and filled with lipid droplets while preadipocytes had a fibroblast-like morphology. **B,** Significant increases in mRNA expression of adipocyte markers during differentiation. $**P < 0.01$, $P < 0.001$ different from day 0.

RARRES2 expression was extremely low in proliferating preadipocytes and increased among induction of differentiation. At day 14 of differentiation, mature adipocytes had over 10x higher *RARRES2* expression levels than at day 0 (1-way ANOVA $P < 0.001$, *post-hoc* Bonferroni $P_{d14vsd0} < 0.001$) (Figure 36A). The chemerin receptors are predominantly expressed on immune cells but *CMKLR1* is also expressed on adipocytes (Mariani and Roncucci, 2015; Wargent et al., 2015). As expected, mRNA expression of *CMKLR1* was low in both, preadipocytes as well as mature adipocytes. Changes in *CMKLR1* expression during differentiation were not significant (Figure 36B).

A

B
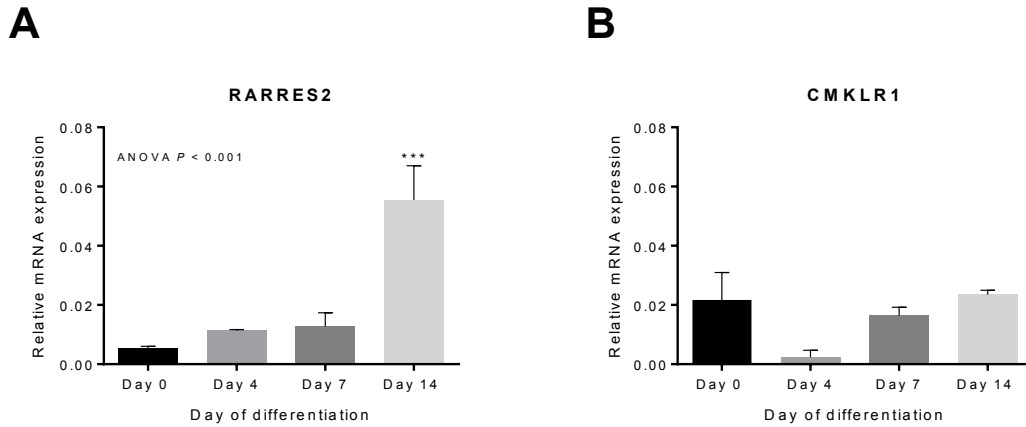
Figure 36 ı Expression of *RARRES2* and *CMKLR1* during adipocytes differentiation. Human MSCs were isolated from SAT and differentiated for 14 days into mature adipocytes by hormonal induction. *RARRES2* and *CMKLR1* expression were determined during differentiation by qRT-PCR. ***P < 0.001 different from day 0.

To study the effect of chemerin on primary human adipocytes, fully differentiated cells were treated with increasing concentrations of recombinant human chemerin. Subsequently, mRNA expression of cytokines and lipid metabolizing genes was assessed.

Treatment of *in vitro* differentiated adipocytes with recombinant chemerin did not affect *IL6* or *MCP1* expression (Figure 37A). Changes in *TNFa* and *CCL3* could not be analyzed due to the low expression in this cell type. Furthermore, expression of genes involved in lipid metabolism were measured in chemerin treated cells. Recombinant chemerin had no effect on the expression of *FASN*, *PPARγ*, *LPL*, or ADIPOQ even at the highest concentration of 30 nM (Figure 37B).

A
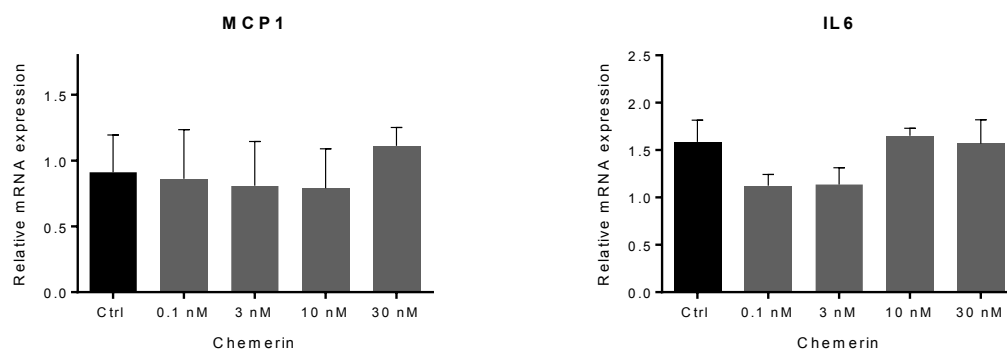
B
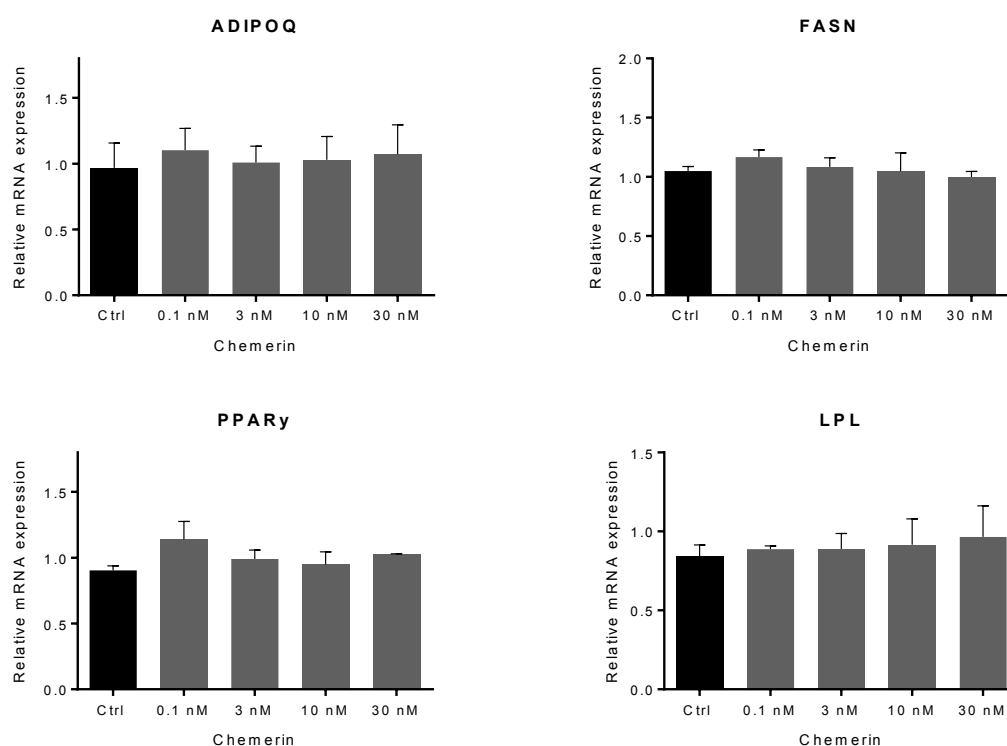
Figure 37 ׀ Treatment of mature adipocytes with recombinant chemerin. Fully differentiated primary human adipocytes were treated with increasing concentrations of recombinant chemerin or vehicle control for 24 h. Addition of chemerin to the cell culture media had no effect on mRNA expression of cytokines (A), the adipokine adiponectin, or genes involved in lipid metabolism (B).

As presented in the previous sections, serum chemerin levels increased in response to a HF diet 4.3.2). In order to test, whether FFA might trigger chemerin mRNA expression in adipocytes, fully differentiated adipocytes were treated with the saturated fatty acid palmitic acid (350 µM), the unsaturated fatty acid arachidonic acid (200 µM), or a commercially available fatty acid mixture. After 24 h cells were harvested and *RARRES2* expression was analyzed. However, treatment of primary adipocytes with fatty acids did not induce *RARRES2* expression compared to vehicle control (data not shown).

5 Discussion

5.1 The LEMBAS intervention study

5.1.1 Low *versus* high dietary protein intakes prior to bariatric surgery

The LEMBAS study evaluated the effects of a LP compared to a HP dietary intervention 3 weeks prior to bariatric surgery. Both diets were effective in reducing body weight while the reduction in hepatic fat content was more pronounced in the HP group. Changes in serum parameters of glucose and lipid metabolism were not markedly different between the intervention groups.

The mean BMI of the participants was in the range of class III obesity, the category with the highest associated risk to develop adiposity-related diseases, according to the WHO classification. Indeed, the prevalence of disease, especially diabetes, thyroid disease, hypertension, and hepatic steatosis, was high in the study cohort. Patients undergoing bariatric surgery are usually advised to follow a preoperative very low-calorie diet (VLCD, usually < 1000 kcal/d) in order to achieve a short-term weight loss and to reduce related complications such as bleeding and infections (Alami et al., 2007; Schouten et al., 2016; Van Nieuwenhove et al., 2011). The VLCD is supposed to cut-down on liver size and intra-abdominal fat thus reducing the difficulty of the procedure (Cassie et al., 2011). Here, the dietary intervention was moderately hypocaloric (~ 1500 kcal/d). Both diets induced a significant reduction in body weight and BMI.

In the LP group the loss in body weight tended to be attributable to a decrease in total fat mass (P_{LP} = 0.052) while fat-free mass remained stable. In the HP group the data indicated an insignificant loss in lean mass. However, only 5 participants could be analyzed by BodPod in this group. It is well established that high protein intake during weight loss therapy supports maintenance of lean mass (Arentson-Lantz et al., 2015; Larsen et al., 2010; Paddon-Jones and Leidy, 2014). Furthermore, protein and particularly branched-chain amino acids (BCAA) are thought to increase muscle protein synthesis by activation of the mammalian target of rapamycin (mTOR) pathway and are therefore routinely consumed by athletes to build up muscle mass (Foure and Bendahan, 2017; Petzke et al., 2014). Due to its satiation effects, HP diets are often advised to support weight maintenance after weight reduction while conserving lean mass (Steenackers et al., 2018).

Despite the well described beneficial effects of HP diets on lean body mass, satiety and weight maintenance, increased protein intakes have also been linked to unfavorable outcomes. In epidemiological studies an increase in the protein content of the diet has been associated with risk of T2DM (Asghari et al., 2018; Sluijs et al., 2010). Murine and human intervention studies

indicate that protein, particularly BCAA, induce hepatic lipogenesis and impair insulin sensitivity by activation of mTOR and phosphorylation of the insulin receptor substrate 1 (IRS1) (Newgard, 2012; Rietman et al., 2014; Weickert et al., 2011; Zoncu et al., 2011). Furthermore, a diet enriched in protein was shown to abolish the improvements in insulin action related to a body weight reduction (Smith et al., 2016). Lastly, high-protein diets have been linked to various kidney complications including renal dysfunction in susceptible individuals (Ahmed, 1991; Blachley, 1984).

In the present study, no adverse effects on glucose metabolism were observed in the HP group. Instead, improvements in fasting glucose as well as tissue insulin resistance, as assessed by HOMA-IR and Adipo-IR, were noted in both groups though the results of the HP group were not statistically significant. Unfortunately, whole body insulin sensitivity was not assessed in this cohort. However, the results are in line with findings in diabetic subjects demonstrating improved metabolic parameters after a 6-week HP intervention despite high BCAA intake in the animal protein group (Markova et al., 2017). Others reported improvements in glycemic control and blood lipids after elevated protein intakes (Dong et al., 2013; Gannon and Nuttall, 2004). In addition, dietary protein is known to stimulate pancreatic insulin secretion as well as hepatic insulin sensitivity (Layman et al., 2008; Smith et al., 2016).

Furthermore, no adverse effects on renal parameters were detected in the HP group as assessed by serum uric acid and creatinine concentrations. Both dietary strategies had a positive influence on the low-grade inflammation present in the obese subjects as serum concentrations of CRP and pro-inflammatory cytokines were lower after the interventions. However, statistical significance was only reached in the LP group for CRP and IL6. In addition, some of the observed beneficial effects in the present study are likely related to the low energy content of the diets and the associated marked weight loss in both groups.

5.1.2 Effects on hepatic fat content

One of the main aims of the LEMBAS study was to compare the efficiency of a 3-week LP *versus* HP diet in eliminating liver fat in morbidly obese patients. The sole accumulation of lipids in the liver is considered benign but hepatic steatosis may progress to more severe forms of NAFLD (Younossi et al., 2018). Furthermore, NAFLD affects extrahepatic tissues and increases the risk to develop T2DM, CVD and chronic kidney disease (Byrne and Targher, 2015). Thus, apart from the general aim to lose weight, a reduction in hepatic fat content is desirable for obese patients. Furthermore, liver fat content should be reduced in preparation for bariatric surgery as described above.

Both intervention groups reduced their liver fat during the hypocaloric interventions. However, hepatic fat content decreased remarkably in every single participant in the HP group whereas

the loss in hepatic fat in the LP group was not significant. It should be noted that baseline IHL levels were higher in the LP than in the HP group, but all study participants analyzed had a hepatic fat content above the threshold for NAFLD.

Parry and Hodson reviewed the existing literature on the influence of dietary macronutrients on the accumulation of liver fat (Parry and Hodson, 2017). Despite mixed results, one consistent finding was that a hypocaloric diet reduces hepatic TAG content (Parry and Hodson, 2017). The present study indicates that among the hypocaloric diets, a HP strategy is more effective than a LP strategy in alleviating fatty liver in obese patients. This conclusion is supported by previous findings in mice (Freudenberg et al., 2013; Garcia-Caraballo et al., 2013; Garcia Caraballo et al., 2017; Pichon et al., 2006) and men (Arciero et al., 2008; Markova et al., 2017). In addition, protein deficiency has been associated with hepatic steatosis and NASH (Meghelli-Bouchenak et al., 1989).

The expression of genes involved in lipid metabolism were analyzed in the liver biopsies to gain mechanistic insights in regard to the pronounced loss of liver fat in the HP group. The liver accumulates TAGs when there is an imbalance between lipid supply (impaired FFA oxidation, increased FFA uptake, enhanced hepatic *de novo* lipogenesis) and lipid disposal via release of VLDL particles (Leclercq and Horsmans, 2008). Chronic nutrient oversupply may cause the storage capacity of adipose tissue to be exceeded leading to inflammation, insulin resistance and increased lipolysis within the tissue (Fabbrini et al., 2008). This causes an increased flux of FFA to be taken up by the liver (Donnelly et al., 2005). In the LEMBAS study the LP strategy induced only an insignificant increase in circulating FFA while there were no changes in FFA in the HP condition. Furthermore, in the HP condition, genes involved in fat uptake, *de novo* lipogenesis and lipid storage were lower expressed. However, the expression of genes involved in the break down and oxidation of fatty acids were not increased in the HP study subjects. In summary, the results indicate that the utilization of lipids in the liver was similar among the groups but that less fat was taken up by the liver in the HP condition.

The differing amount of energy received from protein (10 EN% *versus* 30 EN%) in the two intervention groups was balanced by carbohydrates while dietary fat was kept constant. Carbohydrates are known to induce hepatic lipogenesis by activating ChREBP (Sevastianova et al., 2012). Indeed, *ChREBP* mRNA expression was found to be elevated in the LP compared to the HP group. Furthermore, consumption of simple sugars, particularly fructose is known to contribute to NAFLD (Softic et al., 2017; Stamatikos et al., 2016). However, independent from macronutrient composition, several rodent studies indicate a downregulation of genes involved in *de novo* lipogenesis and lipid storage upon HP feeding (Freudenberg et al., 2012; Marsset-Baglieri et al., 2004; Noguchi et al., 2010). In summary, an exchange of dietary carbohydrates

with protein-rich foods seems to be advisable for patients with NAFLD (Kargulewicz et al., 2014).

Lastly, adipokines and hepatokines were shown to be dysregulated in obesity and fatty liver disease. The association of FGF21 and chemerin with hepatic lipid content and their potential role in the pathogenesis of NAFLD are discussed below (section 5.2.2 and 5.3.2, respectively).

5.2   FGF21

5.2.1   Regulation of FGF21 by dietary protein

In the second part of this thesis, the regulation of FGF21 by dietary protein was analyzed in serum, liver, and adipose tissue. The main finding was that FGF21 is potently downregulated by high protein intakes as demonstrated in three different human dietary intervention studies as well as hepatic cell cultures. The data indicates that the decrease in FGF21 in response to HP intake occurs in both, metabolically healthy (cohort 2, cohort 3) and metabolically stressed individuals (cohort 1). Therefore, the FGF21 lowering effect of dietary protein seems to be robust and able to counteract the stress-related induction of FGF21 observed in the obese subjects. Furthermore, the data obtained in the short-term HP intervention study (cohort 3) demonstrates that the FGF21-decreasing effect of dietary protein is an acute response occurring within 24 h. Indeed, analyses of meal tolerance tests conducted in another intervention study confirmed that circulating FGF21 levels were reduced already within 3 h after a HP load (Seebeck et al., manuscript under revision). The response persisted upon prolonged HP intake as serum FGF21 concentrations remained low after 3 weeks (cohort 1) and 6 weeks (cohort 2) on the HP diet. The protein induced downregulation of FGF21 was also observed in different strains of mice being on either a high-fat or normal-chow diet background (Seebeck et al., manuscript under revision).

Similar findings were reported from a human intervention study comparing *ad-libitum* diets containing either 10 EN%, 15 EN% or 25 EN% of protein. Consumption of a low protein diet led to a 1.6-fold induction of circulating FGF21 compared to the 15 EN% protein diet. Nevertheless, the HP diet decreased circulating FGF21 levels almost 4-fold compared to the control diet (Gosby et al., 2016). However, one might argue that the drop in FGF21 in response to a HP diet only reflects the reversal of the LP-related induction of FGF21. It is well established that FGF21 is an endocrine signal of protein restriction (Laeger et al., 2014). FGF21 is potently induced by low-protein diets and required for mediating the effects of DPR (De Sousa-Coelho et al., 2012; Laeger et al., 2014; Maida et al., 2016). However, in the morbidly obese subjects FGF21 levels dropped by 25% in response to the HP diet while there was no protein deficiency before the intervention.

Still there are some concerns with the data obtained in cohort 1. First, statistical significance was only reached in direct comparison to the LP group possibly due to the high inter-individual variation in FGF21 levels. Second, FGF21 was shown to be increased by energy restriction (Crujeiras et al., 2017) and metabolic stress (Waluga et al., 2017) which might have modulated the effect of the HP intervention on FGF21 concentrations in the obese subjects. Third, in the LP condition, it cannot be excluded that the increase in FGF21 was induced by a shortage in single amino acids in view of the hypocaloric interventions and the high body weight of the study participants, though 10 EN% protein is generally considered protein-sufficient for humans (DRI 2005). Lastly, baseline FGF21 concentrations were almost twice as high in the LP than in the HP group. Considering the above-mentioned confounding factors in cohort 1, data from two additional intervention studies were analyzed to assess the robustness of the HP-induced downregulation of FGF21.

In response to the short-term protein intervention conducted in cohort 3, FGF21 responded dose-dependently to the change in protein intake within 24 h. Habitual protein intake was approximately 16 EN% and reducing protein in the diet to 10 EN% led to a modest, insignificant increase in FGF21. However, the 30 EN% HP diet induced an acute and pronounced decrease in FGF21 which was twice as high as the change in FGF21 serum concentrations in the 15 EN% control diet, as well as compared to baseline FGF21 concentrations. In accordance, in the healthy and lean twins of cohort 2, increasing protein intake from 15 EN% to 30 EN% induced a pronounced and highly significant decrease in FGF21 serum concentrations that remained low for the duration of the study (6 weeks). The data supports the conclusion that the rapid and persistent decrease of FGF21 in response to high-protein happens independently from the low-protein induced increase in FGF21. As 15 EN% reflects habitual protein intake and are more than protein sufficient an undersupply in essential amino acids is very unlikely in this condition. In line with this conclusion, hepatic mRNA expression of *ATF4* and *PPARα* were not significantly different between the intervention groups in the liver biopsies obtained during surgery. The induction of FGF21 during protein restriction requires both, activation of the GCN2-ATF4 branch of the ISR and PPARα signaling (Laeger et al., 2014).

The FGF21 lowering effect of dietary protein has previously been attributed to differences in carbohydrate content (Chalvon-Demersay et al., 2016). Indeed, FGF21 is acutely induced by overfeeding carbohydrates or simple sugars (Lundsgaard et al., 2017; Soberg et al., 2017; von Holstein-Rathlou and Gillum, 2019). In the present study, the protein content of the diet was balanced with carbohydrates, which constituted about 40 EN% in the HP and 60 EN% in the LP condition. Although the study subjects were advised to abstain from sugary products, there is still a bias introduced by the differing amount of carbohydrates in cohort 1. However, in the short-term intervention study (cohort 3) carbohydrates were kept constant at 45 EN%. Still, FGF21 was potently downregulated in a dose dependent manner upon increasing protein

content. Similarly, in the healthy subjects of cohort 2, FGF21 decreased by over 60% after switching from a HF to a HP diet while carbohydrates remained constant at 40 EN%. Therefore, the consistent and dose-dependent decrease in FGF21 in response to increasing protein occurred independently from changes in carbohydrate intake.

In all cohorts analyzed, FGF21 was negatively correlated with serum urea pointing towards an association of FGF21 with the regulation of protein catabolism. Proteins are degraded to amino acids or simple derivative compounds by enzymatic hydrolysis of the peptide bond (Schutz, 2011). Subsequently, amino acids are further broken down to intermediates of the citric acid cycle in order to obtain the stored energy. This requires removal of the amino group, i.e. oxidative deamination, resulting in the release of ammonia. Ammonia is a highly toxic compound that needs to be excreted by the organism for which it is converted to urea in a series of enzymatic reactions termed the urea cycle (Shambaugh, 1977). In support of an association of FGF21 with the urea cycle, the liver, where FGF21 is mainly produced, is the central tissue for amino acid catabolism and urea synthesis (Walker, 2014). Furthermore, a dysregulation of the urea cycle has been associated with fatty liver disease, a disorder tightly associated with circulating FGF21 concentrations (De Chiara et al., 2018).

Ammonia and glutamine, which is readily degraded to ammonia (Li et al., 2016), dose-dependently decreased *Fgf21* expression as demonstrated in primary murine hepatocytes and HepG2 cell cultures. Indeed, the downregulation occurred even in the presence of the strong ER stress (and thus FGF21) inducer tunicamycin in the HepG2 cultures. In line with this data, previous studies have reported that non-essential amino acid supply affects *Fgf21* expression and secretion at the hepatocyte level (Maida et al., 2016). Nevertheless, it remains to be resolved how ammonia or intermediates of the urea cycle are molecularly linked to the regulation of FGF21 expression.

One might only speculate what the biological function of the HP induced downregulation of FGF21 is. Morrison and colleagues proposed that FGF21 senses nutrient intake and acts as a hepatic signal of nutrient imbalance, particularly protein deficiency (Hill et al., 2018; Morrison and Laeger, 2015). FGF21 is mainly secreted by the liver which is a critical regulator of energy and nutrient homeostasis and uniquely positioned to sense dietary protein intake via the portal circulation (Hill et al., 2018). In the context of a low protein diet, FGF21 is essential for mediating adaptive responses to protein restriction thereby mitigating its consequences (Morrison and Laeger, 2015). However, excessive protein intake likewise causes metabolic stress on the organism. Failure to excrete nitrogenous waste may lead to increased blood ammonia levels which are associated with a variety of clinical symptoms, including CNS abnormalities (Auron and Brophy, 2012). Apart from a scenario of protein excess, the organism benefits from noticing the abundancy of nitrogen metabolites as in this case anabolic

processes, such as muscle formation and synthesis of hormones and neurotransmitters, can be intensified while catabolic processes, such as autophagy, are blocked.

Emerging data supports the notion that FGF21 senses nutrient status and serves as a signal to the brain and other tissues to adapt metabolically and behaviorally (Hill et al., 2018). It has been demonstrated in mice that FGF21 affects macronutrient intake via centrally modulating appetite and dietary preferences (Gillum, 2018; Soberg et al., 2017; Talukdar et al., 2016; von Holstein-Rathlou and Gillum, 2019). Furthermore, dietary protein restriction increases food consumption and triggers a preference for protein in the diet (BonDurant and Potthoff, 2018; Morrison and Laeger, 2015). Therefore, it was further investigated if decreased FGF21 serum concentration might likewise alter feeding behavior. Indeed, FGF21 deficient mice preferred the low-protein chow over the high-protein chow when given the choice between two isocaloric diets with different macronutrient composition while wildtype mice consumed similar amounts of both diets (Seebeck et al., manuscript under revision). Low FGF21 levels might therefore be indicative for a nitrogen-rich diet independently from fat and total energy intake and, in cooperation with classical energy balance signals (leptin, insulin, ghrelin, etc.), serves the organism to adjust accordingly (Hill et al., 2018).

5.2.2 FGF21 and hepatic steatosis

The strongest correlation between FGF21 and any parameter analyzed was with intrahepatic lipids (r = 0.9). Furthermore, severity of NAFLD, as assessed histologically, was associated with higher circulating FGF21 levels.

Previously, HP chow was shown to decrease hepatic TAG content and to be able to reverse pre-existing diet-induced steatosis in mice (Freudenberg et al., 2012; Garcia-Caraballo et al., 2013; Garcia Caraballo et al., 2017). Furthermore, circulating FGF21 levels and hepatic *Fgf21* mRNA expression were significantly reduced by HP feeding and plasma FGF21 correlated tightly with hepatic TAG content (Garcia-Caraballo et al., 2013; Garcia Caraballo et al., 2017). In line with the mouse data and the results of this study, Markova et. al. demonstrated in human diabetic subjects that prolonged HP intake reduced intrahepatic lipids by 36%-48% independently from the protein source and from changes in body weight (Markova et al., 2017). Concomitantly, FGF21 concentrations decreased by almost 50%, and correlated with the loss in IHL (Markova et al., 2017).

Garcia-Caraballo and colleagues suspected that the downregulation of FGF21 upon HP feeding was provoked by the reduction in hepatic ER stress related to the loss in hepatic fat (Garcia-Caraballo et al., 2013). Markers of chronic ER stress were found in liver tissue of subjects with obesity and T2DM (Boden et al., 2008; Ozcan et al., 2004), metabolic disorders in which serum FGF21 levels are consistently elevated. Excessive ER stress signaling has

been shown to initiate a programmed cell-death pathway, involving *CHOP* and other pro-apoptotic factors, leading to the removal of impaired hepatocytes thereby contributing to hepatic disorders such as NASH and NAFLD (Brenner et al., 2013). Jiang and co-workers demonstrated that the ER-stress dependent induction of FGF21 is mediated by the IRE1α/XBP1 branch of the unfolded protein response (UPR) (Jiang et al., 2014). In this murine model, pharmacologically triggered ER stress induced hepatic steatosis and an increase in FGF21 expression. FGF21 in turn ameliorated ER-stress induced TAG overload in the liver, which was shown by applying recombinant FGF21 to tunicamycin-treated mice (Jiang et al., 2014).

In the present study, the amount of spliced XBP1 was lower in the HP compared to the RP group. However, the *XBP1s/XBP1u* ratio (XBP1-spliced /XBP1-unspliced ratio) remained unaffected by the protein content of the diet. As IRE1α mediates splicing of *XBP1* upon UPR activation, one would expect an increase in the active, spliced form relative to the unspliced form. However, expression of the ER chaperone *BiP* and the transcriptional repressor *CHOP* were also decreased in the HP condition. Similarly, in the *in vitro* studies, *ATF4* and *BiP* were concomitantly reduced by stimulation with ammonia or glutamine while the *XBP1/XBP1s* ratio remained unaffected. Hence, a reduction or blockade of ER stress pathways by nitrogen metabolites might play a role in repressing *FGF21*. Indeed, free amino acids and derivatives have been implicated to function as unspecific chemical chaperones in the ER lumen by increasing the stability of native proteins (Welch and Brown, 1996). Furthermore, the decrease in *BiP* might reflect the reduction of unfolded proteins in the ER, the amount of which BiP is tightly correlated with (Halliday and Mallucci, 2015). Interestingly, the drug 4-phenylbutyric acid acts as a chemical chaperone approved by the US Food and Drug Administration for the treatment of urea-cycle disorders in humans (Engin and Hotamisligil, 2010).

However, in the murine study by Garcia-Caraballo the reduction in ER stress was deduced from the phosphorylation status of eIF2α and the lower hepatic expression of *Clec2* and *Asns* mRNA. These changes were only significant in comparison to the LP diet (which is well known to activate this pathway). In contrast, the classical ER stress markers *Atf4*, *Chop* (*Ddit3*), *BiP*, and *Xbp1s* were not differentially expressed (Garcia-Caraballo et al., 2013). In the study conducted by Markova et al. in diabetic subjects no signs of reduced ER stress were found in SAT biopsies in response to the HP intervention as determined by *ATF4* and *XBP1s* though no liver biopsies were available (Markova et al., 2017).

An additional key mechanism to restore homeostasis upon cellular stress is the induction of autophagy (Brenner et al., 2013). Autophagy contributes to the degradation of intracellular lipids (also known as "lipophagy") and autophagic defects have been linked to the accumulation of TAGs in the liver (Singh et al., 2009). In the LEMBAS study, hepatic autophagy

was analyzed by the medical doctoral student Chenchen Xu. In brief, autophagic flux was upregulated by the LP diet but remained unchanged in the HP group. Thus, upregulation of autophagy did not concomitantly reduce hepatic fat content as has been hypothesized. However, autophagic flux was positively correlated with FGF21 concentrations (Xu, Markova, Seebeck et al, manuscript under revision).

In summary, the results indicate that prolonged ER stress in the morbidly obese subjects may have been, at least in part, alleviated by the HP diet thus leading to decreased UPR signaling and autophagy. However, the downregulation of FGF21 upon HP intake seems to be controlled by other pathways than the GCN2/eIF2α/ATF4 mediated upregulation of FGF21 as *ATF4* remained unchanged and cannot explain the pronounced drop in *FGF21* mRNA expression and circulating levels in the human cohorts. In addition, the mouse data showed that *Atf4* remained unchanged in the short-term (1 week) feeding study (Figure 26). In contrast, FGF21 was immediately and potently downregulated in mice and humans (within 24 h). However, suppression of *CHOP* upon HP intake might have contributed to the significantly lower hepatic TAG content in the HP group. Unfortunately, hepatic expression of *CHOP* and other ER stress markers could not be analyzed in the remaining cohorts as liver biopsies were only collected in cohort 1.

Interpretation of the results is further complicated by the fact that the HP group had lower IHL content already at baseline which decreased in response to the intervention. In addition, serum transaminases, indicators for liver stress, increased in the HP group (γ-GT significantly) while they decreased in the LP group, contradicting the conclusion that hepatic stress was lower after the HP than the LP intervention. Lastly, morbidly obese subjects have elevated ER stress *per se* and the hypocaloric diets together with a loss in IHL in both intervention groups caused a relieve of metabolic stress independent from the dietary protein content.

5.2.3 FGF21: A potential biomarker for metabolic disease?

FGF21 is a versatile metabolic regulator with pleiotropic effects in various organs. Pharmacological application of FGF21 provides multiple metabolic benefits including a reduction in body weight and glucose levels, improvements in blood lipids as well as insulin and leptin sensitivity, and a decrease in hepatic steatosis (Gimeno and Moller, 2014; Keuper et al., 2019). Therefore, several studies aimed to investigate mechanisms to induce endogenous FGF21 production and an increase in serum FGF21 concentrations generally is considered as a positive study outcome regarding metabolic health.

In contrast, FGF21 levels are considerably and consistently elevated in conditions of metabolic stress (Keuper et al., 2019; Kralisch et al., 2013; Liu et al., 2014; Maratos-Flier, 2017) and FGF21 was even suggested as a biomarker for disease (Lewis et al., 2019). Recently it has

been demonstrated that serum FGF21 levels are increased in old patients with cachexia (Franz et al., 2019), which was also observed in the elderly subjects of cohort 3. Reviewing FGF21 physiology, BonDurant and Potthoff suggest that the paradoxically high FGF21 levels in pathological states may fail to mediate metabolic improvements due to nonfunctional, proteolytically cleaved FGF21 which requires further investigation (BonDurant and Potthoff, 2018; Zhen et al., 2016). Others proposed that a downregulation of *KLB* impairs FGF21 signaling, similar to leptin or insulin resistance (Fisher et al., 2010). However, the connection of FGF21 secretion with hepatic steatosis, diabetes, alcohol, nutrient deprivation/excess and hepatotoxic agents has led to a broader view of FGF21 as a signal of metabolic or cellular stress (Hill et al., 2018). Indeed, various conditions of cellular or organelle stress induce FGF21 even in tissues where FGF21 expression is normally low such as skeletal muscle (Itoh, 2014; Keipert et al., 2014; Kim et al., 2013). In addition, serum FGF21 reduced concomitantly with removal of the stressor, weight loss, or alleviation of hepatic steatosis. Therefore, changes in FGF21 levels are not easily interpreted as being either good or bad but may reflect a status of metabolic imbalance. In line with this interpretation, the action of FGF21 seems to be less needed after the HP intervention due to the diet-related improvements, e.g. in hepatic fat content.

Interestingly, transgenic overexpression of FGF21 has been found to increase lifespan in mice (Zhang et al., 2012). In conditions of chronic stress FGF21 might act as metabolic regulator enhancing cellular resistance (Salminen et al., 2017a, b). Due to its interorgan action on energy metabolism, both peripheral and central, FGF21 alleviates many age-related metabolic disorders (Salminen et al., 2017b). Others argue that FGF21 is a starvation hormone and powerful caloric restriction mimetic in the liver (Fujii et al., 2019; Gokarn et al., 2018; Mendelsohn and Larrick, 2012; Solon-Biet et al., 2015). FGF21 overexpression or exogenous administration reproduces many of the beneficial effects achieved by fasting or dietary restriction, possibly by acting on growth hormones and attenuating IGF1 signaling (Inagaki et al., 2008; Mendelsohn and Larrick, 2012). In summary, FGF21 might on the one hand reflect metabolic stress or nutrient imbalance but on the other hand, when the dose of stress is tolerable, FGF21 induces adaptive responses overall strengthening the organism.

5.3 Chemerin

5.3.1 Genotype, obesity, and diet regulate circulating chemerin

The major findings of the third part of this thesis are that chemerin levels are heritable, responsive to diet and dysregulated in obesity. While chemerin has consistently been linked

to obesity-related inflammation, it seems to be differently regulated in obese and lean human subjects.

Chemerin serum concentrations were found to be considerably heritable, with 55% of the variation in circulating chemerin concentrations determined by additive genetic effects as calculated by the ACE structural equation model in monozygotic and dizygotic twin pairs (cohort 2). Others have reported moderate heritability of serum chemerin concentrations with an estimated 25% in a cohort with Mexican-Americans (n = 1354) (Bozaoglu et al., 2010) and 16% in a cohort from Germany (n = 824) (Tonjes et al., 2014). The differences in estimated heritability might be explained by the methodology, i.e. genome-wide association studies (GWAS) in large cohorts compared to analysis of concordance of a trait between monozygotic and dizygotic twin pairs in a smaller cohort, which was the case in the present study.

The SNP rs3735167 within in the *RARRES2* locus was identified to be positively associated with serum chemerin concentrations, *RARRES2* mRNA expression in adipose tissue, as well as visceral fat mass, though it did not affect the response to diet. Previously, Tönjes and colleagues identified the SNP rs7806429 with the strongest evidence for an association with serum chemerin levels as assessed in a GWAS meta-analysis of three independent human cohorts (Tonjes et al., 2014). While this SNP was not covered by the Illumina Chip used to genotype cohort 2, both SNPs, rs3735167 and rs7806429, are in strong linkage disequilibrium. In addition, the rs3735167 SNP was identified by GWAS in a Taiwanese population (n = 2197) as the lead *RARRES2* polymorphism determining chemerin concentrations (Er et al., 2019). However, serum chemerin concentrations but not rs3735167 genotype were predictive for the long-term outcome of coronary artery disease in this study (Er et al., 2019). Nevertheless, SNPs in the *RARRES2* locus have previously been associated with body fat distribution (Mussig et al., 2009) which was also observed in the present study. In two other GWAS studies, associations between *RARRES2* polymorphisms and chemerin levels in blood did not reach genome-wide significance (Bozaoglu et al., 2010; Leiherer et al., 2016). In summary, the data indicates that serum chemerin levels are at least in part determined by genetic variation within the *RARRES2* promotor region.

Chemerin has repeatedly been shown to be associated with measures of obesity (Bozaoglu et al., 2007; Chakaroun et al., 2012; Docke et al., 2013; Sell et al., 2009). In the 92 healthy subjects of cohort 2, serum chemerin concentrations positively correlated with anthropometric measures including BMI, WHR, and fat mass. Furthermore, circulating chemerin levels were associated with cholesterol and TAG concentrations as well as markers of glucose homeostasis in blood. In contrast, no associations of serum chemerin with the above clinical parameters were found in the morbidly obese subjects of cohort 1. However, chemerin levels in blood were substantially elevated in the obese participants as were total fat mass and other

obesity-related measures. Thus, no correlation might have been determined in this relatively small cohort due to its particular characteristics, i.e. the clinical and anthropometric measures reflecting extreme obesity.

Regulation of chemerin by diet was assessed in both, the healthy and the morbidly obese subjects. In the latter (cohort 1), chemerin concentrations decreased in response to the hypocaloric diets while the differing protein intake had no effect on serum chemerin or *RARRES2* mRNA levels in adipose tissue or liver. In line with this data, both chemerin serum concentrations and mRNA expression have been demonstrated to decrease in rats fed a calorie restricted diet. In the same study, chemerin was upregulated in response to refeeding (Stelmanska et al., 2013) pointing towards regulatory mechanism depending on energy status. In accordance, chemerin levels dropped after overnight fast in mice (Wargent et al., 2015).

In lean, healthy subjects (cohort 2), the 6-week HF diet enriched in saturated fatty acids induced a modest but significant increase in serum chemerin concentrations. The increase in blood chemerin levels was paralleled by a 20% upregulation of adipose tissue *RARRES2* expression. In contrast, Hansen and coworkers reported that plasma chemerin concentrations remained unchanged in mice fed a high-fat or cafeteria diet (Hansen et al., 2014). However, others demonstrated that plasma chemerin concentrations were elevated in the genetically obese *ob/ob* mice (Ernst 2010) or in diet-induced obese mice (Wargent et al., 2015). Knockout studies of the chemerin receptors *Gpr1* (Rourke 2014, Ernst 2010) and *Cmklr1* (Ernst et al., 2012) (Wargent et al., 2015) in mice fed HF chow provided mixed results on chemerin's effect on body weight, glucose homeostasis and energy expenditure. Interestingly, in the present study *CMKLR1* was acutely downregulated after 1 week on the HF diet but returned to baseline levels after 6 weeks on the same diet.

Apart from differences between mice and men, differences in the respective strain, sex, or age of mice or the duration and composition of diet (Helfer et al., 2016) might have contributed to the discordant results. Helfer and coworkers demonstrated that direct injection of a chemerin bolus in the murine brain had a bimodal effect on body weight and food intake (Helfer et al., 2016). An acute chemerin injection decreased while chronic chemerin infusion increased body weight (Helfer et al., 2016). Furthermore, the timeframe dependent regulation of the chemerin receptor might as well contribute to the varying effects of chemerin.

Interestingly, in both cohorts assessed, circulating chemerin did not correlate with adipose tissue or hepatic *RARRES2* expression at any CID. Others have reported similar (Huang et al., 2012; Kajor et al., 2017) though adipose tissue and liver are considered the main contributors to chemerin concentrations in blood (Helfer and Wu, 2018). This observation might be explained by the extensive processing of chemerin which affects its localization and bioactivity (Mattern et al., 2014). Mass spectrometry analyses revealed that chemerin isoforms

in serum differed from those found in adipose tissue, and even among different fat depots (Chang et al., 2016). Increases in local chemerin concentrations have been shown to remain unparalleled by changes in serum chemerin (Huang et al., 2012). Dependent on the isoform, chemerin might be locally activated to act in an autocrine or paracrine manner without being secreted as has been shown to be the case at early stages of inflammation (Wittamer et al., 2005).

5.3.2   Chemerin and hepatic steatosis

Serum chemerin increased with severity of NAFLD, as assessed histologically, though not reaching statistical significance. Circulating chemerin levels were also not significantly elevated in patients previously diagnosed with NASH. Furthermore, chemerin concentrations were not associated with hepatic fat content as determined by MRI$_{spec}$. Neither hepatic chemerin mRNA nor serum levels were associated with histologically assessed grade of steatosis, fibrosis, or inflammation. Thus, in the morbidly obese subjects, no robust association of chemerin with hepatic steatosis and progression of NAFLD could be determined. In cohort 2, there was a moderate positive correlation between circulating chemerin and IHL before and after the HF diet. Unfortunately, no hepatic tissue or information on the prevalence of NAFLD were available in this cohort but expected to be low in the lean participants.

Studies evaluating the role of chemerin in NAFLD provided discordant results. Döcke and colleagues reported that serum chemerin and hepatic *RARRES2* expression are elevated in livers of NASH patients (Docke et al., 2013). Others found chemerin expression to be independently associated with liver fibrosis, steatosis, and inflammation (Krautbauer et al., 2013). In contrast, in a cohort of severely obese patients no association of hepatic *RARRES2* expression with features of NAFLD were found (Wolfs et al., 2015) which is in accordance with the results of the present study. Furthermore, in a study with moderately overweight subjects, hepatic chemerin mRNA was even reduced in livers of NASH patients and negatively associated with hepatic inflammation, fibrosis, and NASH score (Pohl et al., 2017). Animal studies also reported discordant findings with either increased (Krautbauer et al., 2013) or reduced (Deng et al., 2013) hepatic chemerin expression when fed a NASH-inducing diet. However, chemerin expression in SAT of the heavily obese subjects was found to be associated with hepatic fibrosis and inflammation which is in accordance with previous results (Wolfs et al., 2015).

To reconcile the conflicting data, Pohl et al. suggest that NAFLD patients tend to have a higher BMI, are often insulin resistant, and prescribed with multiple medications, and that these factors might have interfered with the reported results (Pohl et al., 2017). Serum chemerin levels are associated with body weight, BMI, and waist-to-hip ratio, and those factors often

differ between patients with NAFLD and healthy controls (Bozaoglu et al., 2007; Pohl et al., 2017).

In the present study, BMI, body weight, and hepatic fat content were all elevated but comparable between subjects with or without NASH diagnosis. Furthermore, serum chemerin has been shown to remain unaffected in NAFLD or borderline NASH but to be elevated in confirmed NASH cases, the number of which was often low in respective studies (Docke et al., 2013; Pohl et al., 2017; Ye et al., 2014). In the present study, only one of the 34 subjects were histologically categorized as NASH according to NAS score, 8 according to SAF score, and 12 subjects had previously been diagnosed with NASH.

Interestingly, while *CMKLR1* mRNA levels were not elevated in NASH patients or associated with NAS score, there was a strong and consistent positive correlation between *CMKLR1* expression and fibrosis-associated genes indicating increased chemerin signaling in NAFLD. An association of *CMKLR1* with liver fibrosis has previously been reported (Docke et al., 2013; Kajor et al., 2017; Krautbauer et al., 2013; Wanninger et al., 2012). In contrast, Gruben and co-workers demonstrated that genetic *Cmklr1* deletion in mice did not affect development of fatty liver or insulin resistance. In *Cmklr1* deficient mice, the upregulation of chemerin signaling might have be compensated by the remaining chemerin receptors, *Ccrl2* and *Gpr1* (Gruben et al., 2014).

5.3.3 Chemerin and inflammation

In both study cohorts, chemerin was associated with markers of inflammation though it was differentially regulated in the obese and lean subjects. In the morbidly obese participants (cohort 1), circulating chemerin was positively associated with serum MCP1, TNFα, and IL6, whereas in the healthy and lean subjects (cohort 2) serum chemerin was only associated with IL6 and the anti-inflammatory cytokine IL1RA but with none of the other cytokines assessed. Furthermore, in the obese subjects no association of *RARRES2* expression in either SAT, VAT or liver with inflammatory factors was detected. In contrast, data obtained in the lean subjects indicate strong correlation of *RARRES2* with expression of several cytokines, the macrophage markers *CD14* and *CD68* and the inflammasome component *NLRP3* but also a negative association with mRNA levels of *NFκB*, *IL1β and EMR1*.

The positive association of *RARRES2* with the two macrophage markers *CD14* and *CD68* on the one hand and the negative associated with *EMR1* (the human homolog of F4/80) on the other hand, seems contradictory. However, Khazen et al. demonstrated that *CD14* and *CD68* are not macrophage-specific markers and are also highly expressed on human adipocytes (Khazen et al., 2005). The authors suggest EMR1 to be the most specific macrophage marker.

As chemerin has been shown to play a role in adipocyte differentiation and function, the strong correlation with *CD14* and *CD68* mRNA might be independent from inflammatory processes.

It is well accepted that chronic nutrient overload induces adipose tissue inflammation (Solinas and Karin, 2010). Hypertrophic, apoptotic adipocytes induce resident macrophages to release chemokines and cytokines further amplifying the inflammatory response through the recruitment of immune cells to adipose tissue (Kloting and Bluher, 2014; Solinas and Karin, 2010). Chronically inflamed adipose tissue is causally linked to obesity-induced insulin resistance (Xu et al., 2003). Klöting and colleagues investigated what distinguishes insulin-resistant from insulin-sensitive obese subjects and identified macrophage infiltration and altered adipokine release, including chemerin, to be the best predictors for insulin resistance in obesity (Kloting et al., 2010). Insulin-resistant obese subjects had significantly higher circulating chemerin concentrations independently from total body fat mass (Kloting et al., 2010). Furthermore, a causal role of chemerin in the induction of skeletal muscle insulin resistance has been demonstrated (Sell et al., 2009).

However, in the present study chemerin serum concentrations were not significantly different between subjects previously diagnosed with T2DM compared to insulin-sensitive subjects. While chemerin concentrations in serum increased with number of crown-like structures (CLS) in VAT the data was not statistically significant. Furthermore, *RARRES2* expression was not different between CLS$^-$ and CLS$^+$ study subjects as determined in both adipose tissue depots. In cohort 2, serum chemerin and adipose tissue expression of *RARRES2* and *CMKLR1* were not or even negatively associated with expression of the macrophage marker *EMR1*. Lastly, visceral fat mass and adipokine release from VAT are mainly associated with metabolic disease while SAT is considered benign (Ibrahim, 2010). Here, *RARRES2* expression in VAT was relatively low and did not correlate with chemerin levels measured in serum. In support, Weigert and coworkers demonstrated that the contribution of chemerin release from VAT to circulating levels is neglectable (Weigert et al., 2010). In summary, an association of chemerin with macrophage infiltration and a clearly pro-inflammatory role of chemerin cannot be deduced from the available data. Nevertheless, the lack of statistical significance might be due to the small cohort size of the LEMBAS study.

Interestingly, in the lean subjects *RARRES2* expression in SAT was negatively associated with gene expression of *NFκB*, *IL1β* and *EMR1*. Indeed, emerging data indicates that chemerin is involved in both, the onset and resolution of inflammation (Mariani and Roncucci, 2015). Dranse and colleagues demonstrated that inhibition of chemerin increases macrophage recruitment and NFκB signaling pointing towards an anti-inflammatory role of chemerin. However, discordant data have also been reported. Yamawaki and coworkers demonstrated that chemerin inhibits NFκB activation in human vascular endothelial cells (Yamawaki et al.,

2012) while others reported increased NFκB signaling in skeletal muscle cells (Sell et al., 2009) and human microvascular endothelial cells (Kaur et al., 2010) in response to chemerin. Thus, chemerin post-receptor signaling might differ depending on the respective site within the body.

5.3.4 Chemerin and adipocyte function

In the adipose tissue biopsies of the obese human subjects, *RARRES2* as well as the chemerin receptors *CMKLR1* and *CCRL2* were markedly higher expressed in SAT than in VAT. In contrast, a higher mRNA level of *GPR1* was detected in the visceral fat depot. No differences in chemerin pathway expression were found between the intervention groups, except for *CMKLR1*. *CMKLR1* was lower expressed in the HP compared to the LP group in both adipose tissue depots, as well as liver. However, as tissue biopsies were collected during bariatric surgery, no data was available on chemerin pathway expression before the intervention. Thus, the downregulation of the chemerin receptor in the HP group might not represent a diet-induced effect but a consequence of the inherent characteristics of the participants, e.g. hepatic fat content was significantly higher in the LP group already at baseline which may affect chemerin expression as discussed above (section 5.3.2).

RARRES2 and *CMKLR1* expression were strongly associated with *ADIPOQ* mRNA levels in SAT. Furthermore, strong associations between *RARRES2* and expression of lipid metabolizing genes were detected in SAT in both, the obese and lean subjects. These results are in line with previous reports demonstrating that chemerin is required for normal adipocyte function and stimulates lipolysis in adipocytes (Bozaoglu et al., 2007; Goralski et al., 2007). An induction of chemerin and its receptor by adiponectin has also been reported (Reverchon et al., 2014; Wanninger et al., 2012). However, in this and previous studies circulating chemerin was not associated with adiponectin concentrations in blood pointing towards a tissue-specific function.

In vitro differentiation of primary human preadipocytes revealed that *RARRES2* expression increases during differentiation and is highest in the mature adipocyte. Similar data has also been reported in 3T3-L1 adipocytes (Bozaoglu et al., 2007; Goralski et al., 2007), murine primary adipocytes (Dranse et al., 2016), and human primary adipocytes (Roh et al., 2007). In contrast, contradictory reports exists regarding changes in mRNA expression of the chemerin receptor, *CMKLR1*, upon induction of differentiation. In the present study, *CMKLR1* mRNA was not significantly different before and after differentiation. Others reported increased (Bozaoglu et al., 2007; Dranse et al., 2016; Roh et al., 2007) or decreased (Goralski et al., 2007) expression in mature adipocytes. Sell and colleagues reported increased *CMKLR1* expression during the first 3 days upon induction of differentiation in human adipocytes after which *CMKLR1* mRNA returned to baseline levels. This observation might explain discordant

data of previous studies in 3T3-L1 adipocytes and is in line with the results obtained in the present study. In summary, there is agreement that chemerin release and signaling via its own receptor is essential for adipocyte differentiation and metabolic function (Goralski et al., 2007). It has also been proposed that chemerin promotes healthy expansion of adipose tissue by favoring adipocyte hyperplasia *versus* hypertrophy (Dranse et al., 2016).

The addition of recombinant chemerin to the cell culture media of fully differentiated adipocytes had no effect on *RARRES2* expression. Furthermore, it did not alter the expression of key cytokines and genes involved in lipid metabolism. While treatment of murine adipocytes with oleic acid and palmitic acid has been shown to induce chemerin (Bauer et al., 2011) this was not the case in the present study. Stimulation of mature human adipocytes with saturated or unsaturated fatty acids or a commercially available fatty acid mixture did not change chemerin expression. The *in vitro* experiments indicate that other factors within the tissue are essential for mediating chemerin's action. These results might also be explained by the existence of multiple chemerin isoforms in adipose tissue and the observation that substantial differences exist between endogenous and synthetic chemerin (Dranse et al., 2016). Thus, properties of the recombinant chemerin used in this study, for which activity has been proven in a chemotaxis assay, might differ from native chemerin isoforms synthesized in adipose tissue.

In summary, efforts to elucidate the physiology of chemerin are hampered by the complex regulation and various isoforms of chemerin. Chemerin levels differ depending on time of the day, eating habits, and level of satiety/starvation (Parlee et al., 2010). Furthermore, fundamental differences exist between species and most studies have been conducted in mice, e.g. homology between the murine and human CMKLR1 receptor is estimated to be 80% (Ferland and Watts, 2015). In addition, sex, age, and body composition were shown to affect chemerin concentrations. Most importantly, chemerin is extensively processed by different proteases and the resulting chemerin isoforms differ in function and localization, even showing opposing effects. Lastly, there are vast differences in chemerin and CMKLR1 expression depending on location within the body and tissue *RARRES2* expression does not correlate with circulating chemerin levels. Thus, results on chemerin regulation and physiology need to be interpreted according to the specific experimental design and study circumstances and may not be generalized. Future studies should consider the complexity of chemerin regulation and investigators need to carefully plan their methodology.

5.4   Study limitations

The LEMBAS study assessed the effect of a 3-week low *versus* high protein diet on serum parameters and associated molecular changes in visceral and subcutaneous adipose tissue as well as liver of morbidly obese human subjects. Particularly paired adipose and hepatic

tissue samples are difficult to obtain and hence there is a lack of molecular studies in human tissue. Thus, the LEMBAS study provides unique and most valuable data adding to the understanding of human physiology.

However, the study also has some limitations that should be mentioned. First, the study subjects were morbidly obese and in part multiply medicated which might have interfered with the results. Together with the small cohort size and heterogeneity of the study participants this caused high variation in some parameters assessed. Statistical significance was often not reached in the HP group which might in part be explained by the above factors. Second, although participants were randomized into the two intervention groups, subjects in the HP group had lower hepatic fat content, less severe NAFLD score, and lower FGF21 and γ-GT concentrations in serum. Third, interpretation of the results in terms of the dietary protein content is complicated by (1) the low energy content and (2) the differing amounts of carbohydrates in the diets. Both factors contribute own, independent effects that cannot be fully detangled from the protein effect.

Lastly, the high protein content in the HP diet was achieved by supplementing the diet with protein shakes which were shown to be less accepted and tolerated than a standard diet (Schouten et al., 2016). However, compliance of the study participants was assessed by means of serum urea levels which reflect dietary protein intake. As expected, serum urea significantly decreased in the LP group and increased in the HP group. The differences in serum urea between the groups were highly significant at the end of the intervention. Furthermore, the findings on FGF21 regulation by HP diet are supported by evidence obtained in cohort 2 and 3 as well as the cell culture data. Nevertheless, additional long-term studies in large cohorts are needed to be able to generalize results, to evaluate the durability of the induced changes, and to detect group differences.

6 Summary

The hepatokine FGF21 and the adipokine chemerin have been implicated as metabolic regulators and mediators of inter-tissue crosstalk. While FGF21 is associated with beneficial metabolic effects and is currently being tested as an emerging therapeutic for obesity and diabetes, chemerin is linked to inflammation-mediated insulin resistance. However, dietary regulation of both organokines and their role in tissue interaction needs further investigation.

The LEMBAS nutritional intervention study investigated the effects of two diets differing in their protein content in obese human subjects with non-alcoholic fatty liver disease (NAFLD). The study participants consumed hypocaloric diets containing either low (LP: 10 EN%, n = 10) or high (HP: 30 EN%, n = 9) dietary protein 3 weeks prior to bariatric surgery. Before and after the intervention the participants were anthropometrically assessed, blood samples were drawn, and hepatic fat content was determined by MRS. During bariatric surgery, paired subcutaneous and visceral adipose tissue biopsies as well as liver biopsies were collected. The aim of this thesis was to investigate circulating levels and tissue-specific regulation of (1) FGF21 and (2) chemerin in the LEMBAS cohort. The results were compared to data obtained in 92 metabolically healthy subjects with normal glucose tolerance and normal liver fat content.

(1) Serum FGF21 concentrations were elevated in the obese subjects, and strongly associated with intrahepatic lipids (IHL). In accordance, FGF21 serum concentrations increased with severity of NAFLD as determined histologically in the liver biopsies. Though both diets were successful in reducing IHL, the effect was more pronounced in the HP group. FGF21 serum concentrations and mRNA expression were bi-directionally regulated by dietary protein, independent from metabolic improvements. In accordance, in the healthy study subjects, serum FGF21 concentrations dropped by more than 60% in response to the HP diet. A short-term HP intervention confirmed the acute downregulation of FGF21 within 24 hours. Lastly, experiments in HepG2 cell cultures and primary murine hepatocytes identified nitrogen metabolites (NH_4Cl and glutamine) to dose-dependently suppress *FGF21* expression.

(2) Circulating chemerin concentrations were considerably elevated in the obese *versus* lean study participants and differently associated with markers of obesity and NAFLD in the two cohorts. The adipokine decreased in response to the hypocaloric interventions while an unhealthy high-fat diet induced a rise in chemerin serum levels. In the lean subjects, mRNA expression of *RARRES2*, encoding chemerin, was strongly and positively correlated with expression of several cytokines, including MCP1, TNFα, and IL6, as well as markers of macrophage infiltration in the subcutaneous fat depot. However, *RARRES2* was not associated with any cytokine assessed in the obese subjects and the data indicated an involvement of chemerin not only in the onset but also resolution of inflammation. Analyses of

the tissue biopsies and experiments in human primary adipocytes point towards a role of chemerin in adipogenesis while discrepancies between the *in vivo* and *in vitro* data were detected.

Taken together, the results of this thesis demonstrate that circulating FGF21 and chemerin levels are considerably elevated in obesity and responsive to dietary interventions. FGF21 was acutely and bi-directionally regulated by dietary protein in a hepatocyte-autonomous manner. Given that both, a lack in essential amino acids and excessive nitrogen intake, exert metabolic stress, FGF21 may serve as an endocrine signal for dietary protein balance. Lastly, the data revealed that chemerin is derailed in obesity and associated with obesity-related inflammation. However, future studies on chemerin should consider functional and regulatory differences between secreted and tissue-specific isoforms.

7   References

Ahmed, F.E. (1991). Effect of diet on progression of chronic renal disease. Journal of the American Dietetic Association *91*, 1266-1270.

Alami, R.S., Morton, J.M., Schuster, R., Lie, J., Sanchez, B.R., Peters, A., and Curet, M.J. (2007). Is there a benefit to preoperative weight loss in gastric bypass patients? A prospective randomized trial. Surgery for obesity and related diseases : official journal of the American Society for Bariatric Surgery *3*, 141-145; discussion 145-146.

Arciero, P.J., Gentile, C.L., Pressman, R., Everett, M., Ormsbee, M.J., Martin, J., Santamore, J., Gorman, L., Fehling, P.C., Vukovich, M.D.*, et al.* (2008). Moderate protein intake improves total and regional body composition and insulin sensitivity in overweight adults. Metabolism: clinical and experimental *57*, 757-765.

Arentson-Lantz, E., Clairmont, S., Paddon-Jones, D., Tremblay, A., and Elango, R. (2015). Protein: A nutrient in focus. Applied physiology, nutrition, and metabolism = Physiologie appliquee, nutrition et metabolisme *40*, 755-761.

Asghari, G., Farhadnejad, H., Teymoori, F., Mirmiran, P., Tohidi, M., and Azizi, F. (2018). High dietary intake of branched-chain amino acids is associated with an increased risk of insulin resistance in adults. Journal of diabetes *10*, 357-364.

Auron, A., and Brophy, P.D. (2012). Hyperammonemia in review: pathophysiology, diagnosis, and treatment. Pediatric nephrology (Berlin, Germany) *27*, 207-222.

Badman, M.K., Koester, A., Flier, J.S., Kharitonenkov, A., and Maratos-Flier, E. (2009). Fibroblast growth factor 21-deficient mice demonstrate impaired adaptation to ketosis. Endocrinology *150*, 4931-4940.

Badman, M.K., Pissios, P., Kennedy, A.R., Koukos, G., Flier, J.S., and Maratos-Flier, E. (2007). Hepatic fibroblast growth factor 21 is regulated by PPARalpha and is a key mediator of hepatic lipid metabolism in ketotic states. Cell metabolism *5*, 426-437.

Banas, M., Zabieglo, K., Kasetty, G., Kapinska-Mrowiecka, M., Borowczyk, J., Drukala, J., Murzyn, K., Zabel, B.A., Butcher, E.C., Schroeder, J.M.*, et al.* (2013). Chemerin is an antimicrobial agent in human epidermis. PloS one *8*, e58709.

Bargut, T.C.L., Souza-Mello, V., Aguila, M.B., and Mandarim-de-Lacerda, C.A. (2017). Browning of white adipose tissue: lessons from experimental models. Hormone molecular biology and clinical investigation *31*.

Barrera, F., and George, J. (2014). The role of diet and nutritional intervention for the management of patients with NAFLD. Clinics in liver disease *18*, 91-112.

Bauer, S., Wanninger, J., Schmidhofer, S., Weigert, J., Neumeier, M., Dorn, C., Hellerbrand, C., Zimara, N., Schaffler, A., Aslanidis, C.*, et al.* (2011). Sterol regulatory element-binding protein 2 (SREBP2) activation after excess triglyceride storage induces chemerin in hypertrophic adipocytes. Endocrinology *152*, 26-35.

Bedogni, G., Bellentani, S., Miglioli, L., Masutti, F., Passalacqua, M., Castiglione, A., and Tiribelli, C. (2006). The Fatty Liver Index: a simple and accurate predictor of hepatic steatosis in the general population. BMC gastroenterology *6*, 33.

Bedossa, P., Poitou, C., Veyrie, N., Bouillot, J.L., Basdevant, A., Paradis, V., Tordjman, J., and Clement, K. (2012). Histopathological algorithm and scoring system for evaluation of liver lesions in morbidly obese patients. Hepatology (Baltimore, Md) *56*, 1751-1759.

Blachley, J.D. (1984). The role of dietary protein in the progression and symptomatology of chronic renal failure. The American journal of the medical sciences *288*, 228-234.

Bluher, M. (2013). Adipose tissue dysfunction contributes to obesity related metabolic diseases. Best practice & research Clinical endocrinology & metabolism *27*, 163-177.

Bobbert, T., Schwarz, F., Fischer-Rosinsky, A., Maurer, L., Mohlig, M., Pfeiffer, A.F., Mai, K., and Spranger, J. (2015). Chemerin and prediction of Diabetes mellitus type 2. Clinical endocrinology *82*, 838-843.

References

Boden, G., Duan, X., Homko, C., Molina, E.J., Song, W., Perez, O., Cheung, P., and Merali, S. (2008). Increase in endoplasmic reticulum stress-related proteins and genes in adipose tissue of obese, insulin-resistant individuals. Diabetes *57*, 2438-2444.

BonDurant, L.D., Ameka, M., Naber, M.C., Markan, K.R., Idiga, S.O., Acevedo, M.R., Walsh, S.A., Ornitz, D.M., and Potthoff, M.J. (2017). FGF21 Regulates Metabolism Through Adipose-Dependent and -Independent Mechanisms. Cell metabolism *25*, 935-944.e934.

BonDurant, L.D., and Potthoff, M.J. (2018). Fibroblast Growth Factor 21: A Versatile Regulator of Metabolic Homeostasis. Annual review of nutrition *38*, 173-196.

Bozaoglu, K., Bolton, K., McMillan, J., Zimmet, P., Jowett, J., Collier, G., Walder, K., and Segal, D. (2007). Chemerin is a novel adipokine associated with obesity and metabolic syndrome. Endocrinology *148*, 4687-4694.

Bozaoglu, K., Curran, J.E., Stocker, C.J., Zaibi, M.S., Segal, D., Konstantopoulos, N., Morrison, S., Carless, M., Dyer, T.D., Cole, S.A.*, et al.* (2010). Chemerin, a novel adipokine in the regulation of angiogenesis. The Journal of clinical endocrinology and metabolism *95*, 2476-2485.

Brenner, C., Galluzzi, L., Kepp, O., and Kroemer, G. (2013). Decoding cell death signals in liver inflammation. Journal of hepatology *59*, 583-594.

Bril, F., Lomonaco, R., Orsak, B., Ortiz-Lopez, C., Webb, A., Tio, F., Hecht, J., and Cusi, K. (2014). Relationship between disease severity, hyperinsulinemia, and impaired insulin clearance in patients with nonalcoholic steatohepatitis. Hepatology (Baltimore, Md) *59*, 2178-2187.

Bugianesi, E., Gastaldelli, A., Vanni, E., Gambino, R., Cassader, M., Baldi, S., Ponti, V., Pagano, G., Ferrannini, E., and Rizzetto, M. (2005). Insulin resistance in non-diabetic patients with non-alcoholic fatty liver disease: sites and mechanisms. Diabetologia *48*, 634-642.

Byrne, C.D., and Targher, G. (2015). NAFLD: a multisystem disease. Journal of hepatology *62*, S47-64.

Cassie, S., Menezes, C., Birch, D.W., Shi, X., and Karmali, S. (2011). Effect of preoperative weight loss in bariatric surgical patients: a systematic review. Surgery for obesity and related diseases : official journal of the American Society for Bariatric Surgery *7*, 760-767; discussion 767.

Chakaroun, R., Raschpichler, M., Kloting, N., Oberbach, A., Flehmig, G., Kern, M., Schon, M.R., Shang, E., Lohmann, T., Dressler, M.*, et al.* (2012). Effects of weight loss and exercise on chemerin serum concentrations and adipose tissue expression in human obesity. Metabolism: clinical and experimental *61*, 706-714.

Chalasani, N., Younossi, Z., Lavine, J.E., Diehl, A.M., Brunt, E.M., Cusi, K., Charlton, M., and Sanyal, A.J. (2012). The diagnosis and management of non-alcoholic fatty liver disease: practice Guideline by the American Association for the Study of Liver Diseases, American College of Gastroenterology, and the American Gastroenterological Association. Hepatology (Baltimore, Md) *55*, 2005-2023.

Chalvon-Demersay, T., Even, P.C., Tome, D., Chaumontet, C., Piedcoq, J., Gaudichon, C., and Azzout-Marniche, D. (2016). Low-protein diet induces, whereas high-protein diet reduces hepatic FGF21 production in mice, but glucose and not amino acids up-regulate FGF21 in cultured hepatocytes. The Journal of nutritional biochemistry *36*, 60-67.

Chang, S.S., Eisenberg, D., Zhao, L., Adams, C., Leib, R., Morser, J., and Leung, L. (2016). Chemerin activation in human obesity. Obesity (Silver Spring, Md) *24*, 1522-1529.

Choi, K.M. (2016). The Impact of Organokines on Insulin Resistance, Inflammation, and Atherosclerosis. Endocrinology and metabolism (Seoul, Korea) *31*, 1-6.

Chu, S.H., Lee, M.K., Ahn, K.Y., Im, J.A., Park, M.S., Lee, D.C., Jeon, J.Y., and Lee, J.W. (2012). Chemerin and adiponectin contribute reciprocally to metabolic syndrome. PloS one *7*, e34710.

Coskun, T., Bina, H.A., Schneider, M.A., Dunbar, J.D., Hu, C.C., Chen, Y., Moller, D.E., and Kharitonenkov, A. (2008). Fibroblast growth factor 21 corrects obesity in mice. Endocrinology *149*, 6018-6027.

Crujeiras, A.B., Gomez-Arbelaez, D., Zulet, M.A., Carreira, M.C., Sajoux, I., de Luis, D., Castro, A.I., Baltar, J., Baamonde, I., Sueiro, A.*, et al.* (2017). Plasma FGF21 levels in obese patients undergoing energy-restricted diets or bariatric surgery: a marker of metabolic stress? International journal of obesity (2005) *41*, 1570-1578.

References

Dasarathy, S., Yang, Y., McCullough, A.J., Marczewski, S., Bennett, C., and Kalhan, S.C. (2011). Elevated hepatic fatty acid oxidation, high plasma fibroblast growth factor 21, and fasting bile acids in nonalcoholic steatohepatitis. European journal of gastroenterology & hepatology *23*, 382-388.

De Chiara, F., Heeboll, S., Marrone, G., Montoliu, C., Hamilton-Dutoit, S., Ferrandez, A., Andreola, F., Rombouts, K., Gronbaek, H., Felipo, V.*, et al.* (2018). Urea cycle dysregulation in non-alcoholic fatty liver disease. Journal of hepatology *69*, 905-915.

De Sousa-Coelho, A.L., Marrero, P.F., and Haro, D. (2012). Activating transcription factor 4-dependent induction of FGF21 during amino acid deprivation. The Biochemical journal *443*, 165-171.

Delanaye, P., Cavalier, E., and Pottel, H. (2017). Serum Creatinine: Not So Simple! Nephron *136*, 302-308.

Deng, Y., Wang, H., Lu, Y., Liu, S., Zhang, Q., Huang, J., Zhu, R., Yang, J., Zhang, R., Zhang, D.*, et al.* (2013). Identification of chemerin as a novel FXR target gene down-regulated in the progression of nonalcoholic steatohepatitis. Endocrinology *154*, 1794-1801.

Desideri, G., Castaldo, G., Lombardi, A., Mussap, M., Testa, A., Pontremoli, R., Punzi, L., and Borghi, C. (2014). Is it time to revise the normal range of serum uric acid levels? European review for medical and pharmacological sciences *18*, 1295-1306.

DeZwaan-McCabe, D., Sheldon, R.D., Gorecki, M.C., Guo, D.F., Gansemer, E.R., Kaufman, R.J., Rahmouni, K., Gillum, M.P., Taylor, E.B., Teesch, L.M.*, et al.* (2017). ER Stress Inhibits Liver Fatty Acid Oxidation while Unmitigated Stress Leads to Anorexia-Induced Lipolysis and Both Liver and Kidney Steatosis. Cell reports *19*, 1794-1806.

Docke, S., Lock, J.F., Birkenfeld, A.L., Hoppe, S., Lieske, S., Rieger, A., Raschzok, N., Sauer, I.M., Florian, S., Osterhoff, M.A.*, et al.* (2013). Elevated hepatic chemerin mRNA expression in human non-alcoholic fatty liver disease. European journal of endocrinology *169*, 547-557.

Domingo, P., Gallego-Escuredo, J.M., Domingo, J.C., Gutierrez Mdel, M., Mateo, M.G., Fernandez, I., Vidal, F., Giralt, M., and Villarroya, F. (2010). Serum FGF21 levels are elevated in association with lipodystrophy, insulin resistance and biomarkers of liver injury in HIV-1-infected patients. AIDS (London, England) *24*, 2629-2637.

Domouzoglou, E.M., and Maratos-Flier, E. (2011). Fibroblast growth factor 21 is a metabolic regulator that plays a role in the adaptation to ketosis. The American journal of clinical nutrition *93*, 901s-905.

Donato, M.T., Tolosa, L., and Gomez-Lechon, M.J. (2015). Culture and Functional Characterization of Human Hepatoma HepG2 Cells. Methods in molecular biology (Clifton, NJ) *1250*, 77-93.

Dong, J.Y., Zhang, Z.L., Wang, P.Y., and Qin, L.Q. (2013). Effects of high-protein diets on body weight, glycaemic control, blood lipids and blood pressure in type 2 diabetes: meta-analysis of randomised controlled trials. The British journal of nutrition *110*, 781-789.

Donnelly, K.L., Smith, C.I., Schwarzenberg, S.J., Jessurun, J., Boldt, M.D., and Parks, E.J. (2005). Sources of fatty acids stored in liver and secreted via lipoproteins in patients with nonalcoholic fatty liver disease. The Journal of clinical investigation *115*, 1343-1351.

Dranse, H.J., Muruganandan, S., Fawcett, J.P., and Sinal, C.J. (2016). Adipocyte-secreted chemerin is processed to a variety of isoforms and influences MMP3 and chemokine secretion through an NFkB-dependent mechanism. Molecular and cellular endocrinology *436*, 114-129.

Dushay, J., Chui, P.C., Gopalakrishnan, G.S., Varela-Rey, M., Crawley, M., Fisher, F.M., Badman, M.K., Martinez-Chantar, M.L., and Maratos-Flier, E. (2010). Increased fibroblast growth factor 21 in obesity and nonalcoholic fatty liver disease. Gastroenterology *139*, 456-463.

Dushay, J.R., Toschi, E., Mitten, E.K., Fisher, F.M., Herman, M.A., and Maratos-Flier, E. (2015). Fructose ingestion acutely stimulates circulating FGF21 levels in humans. Molecular metabolism *4*, 51-57.

Ebert, T., Gebhardt, C., Scholz, M., Wohland, T., Schleinitz, D., Fasshauer, M., Bluher, M., Stumvoll, M., Kovacs, P., and Tonjes, A. (2018). Relationship Between 12 Adipocytokines and Distinct Components of the Metabolic Syndrome. The Journal of clinical endocrinology and metabolism *103*, 1015-1023.

Engin, F., and Hotamisligil, G.S. (2010). Restoring endoplasmic reticulum function by chemical chaperones: an emerging therapeutic approach for metabolic diseases. Diabetes, obesity & metabolism *12 Suppl 2*, 108-115.

Er, L.K., Hsu, L.A., Juang, J.J., Chiang, F.T., Teng, M.S., Tzeng, I.S., Wu, S., Lin, J.F., and Ko, Y.L. (2019). Circulating Chemerin Levels, but not the RARRES2 Polymorphisms, Predict the Long-Term Outcome of Angiographically Confirmed Coronary Artery Disease. International journal of molecular sciences *20*.

Ernst, M.C., Haidl, I.D., Zuniga, L.A., Dranse, H.J., Rourke, J.L., Zabel, B.A., Butcher, E.C., and Sinal, C.J. (2012). Disruption of the chemokine-like receptor-1 (CMKLR1) gene is associated with reduced adiposity and glucose intolerance. Endocrinology *153*, 672-682.

Ernst, M.C., Issa, M., Goralski, K.B., and Sinal, C.J. (2010). Chemerin exacerbates glucose intolerance in mouse models of obesity and diabetes. Endocrinology *151*, 1998-2007.

Ernst, M.C., and Sinal, C.J. (2010). Chemerin: at the crossroads of inflammation and obesity. Trends in endocrinology and metabolism: TEM *21*, 660-667.

Fabbrini, E., Mohammed, B.S., Magkos, F., Korenblat, K.M., Patterson, B.W., and Klein, S. (2008). Alterations in adipose tissue and hepatic lipid kinetics in obese men and women with nonalcoholic fatty liver disease. Gastroenterology *134*, 424-431.

Fasshauer, M., and Bluher, M. (2015). Adipokines in health and disease. Trends in pharmacological sciences *36*, 461-470.

Fazeli, P.K., Lun, M., Kim, S.M., Bredella, M.A., Wright, S., Zhang, Y., Lee, H., Catana, C., Klibanski, A., Patwari, P.*, et al.* (2015). FGF21 and the late adaptive response to starvation in humans. The Journal of clinical investigation *125*, 4601-4611.

Ferland, D.J., and Watts, S.W. (2015). Chemerin: A comprehensive review elucidating the need for cardiovascular research. Pharmacological research *99*, 351-361.

Fisher, F.M., Chui, P.C., Antonellis, P.J., Bina, H.A., Kharitonenkov, A., Flier, J.S., and Maratos-Flier, E. (2010). Obesity is a fibroblast growth factor 21 (FGF21)-resistant state. Diabetes *59*, 2781-2789.

Fisher, F.M., Kim, M., Doridot, L., Cunniff, J.C., Parker, T.S., Levine, D.M., Hellerstein, M.K., Hudgins, L.C., Maratos-Flier, E., and Herman, M.A. (2017). A critical role for ChREBP-mediated FGF21 secretion in hepatic fructose metabolism. Molecular metabolism *6*, 14-21.

Foure, A., and Bendahan, D. (2017). Is Branched-Chain Amino Acids Supplementation an Efficient Nutritional Strategy to Alleviate Skeletal Muscle Damage? A Systematic Review. Nutrients *9*.

Franz, K., Ost, M., Otten, L., Herpich, C., Coleman, V., Endres, A.S., Klaus, S., Muller-Werdan, U., and Norman, K. (2019). Higher serum levels of fibroblast growth factor 21 in old patients with cachexia. Nutrition (Burbank, Los Angeles County, Calif) *63-64*, 81-86.

Freudenberg, A., Petzke, K.J., and Klaus, S. (2012). Comparison of high-protein diets and leucine supplementation in the prevention of metabolic syndrome and related disorders in mice. The Journal of nutritional biochemistry *23*, 1524-1530.

Freudenberg, A., Petzke, K.J., and Klaus, S. (2013). Dietary L-leucine and L-alanine supplementation have similar acute effects in the prevention of high-fat diet-induced obesity. Amino acids *44*, 519-528.

Friedewald, W.T., Levy, R.I., and Fredrickson, D.S. (1972). Estimation of the concentration of low-density lipoprotein cholesterol in plasma, without use of the preparative ultracentrifuge. Clinical chemistry *18*, 499-502.

Frohlich, M., Imhof, A., Berg, G., Hutchinson, W.L., Pepys, M.B., Boeing, H., Muche, R., Brenner, H., and Koenig, W. (2000). Association between C-reactive protein and features of the metabolic syndrome: a population-based study. Diabetes care *23*, 1835-1839.

Fujii, N., Uta, S., Kobayashi, M., Sato, T., Okita, N., and Higami, Y. (2019). Impact of aging and caloric restriction on fibroblast growth factor 21 signaling in rat white adipose tissue. Experimental gerontology *118*, 55-64.

Gallego-Escuredo, J.M., Gomez-Ambrosi, J., Catalan, V., Domingo, P., Giralt, M., Fruhbeck, G., and Villarroya, F. (2015). Opposite alterations in FGF21 and FGF19 levels and disturbed expression

of the receptor machinery for endocrine FGFs in obese patients. International journal of obesity (2005) *39*, 121-129.

Galman, C., Lundasen, T., Kharitonenkov, A., Bina, H.A., Eriksson, M., Hafstrom, I., Dahlin, M., Amark, P., Angelin, B., and Rudling, M. (2008). The circulating metabolic regulator FGF21 is induced by prolonged fasting and PPARalpha activation in man. Cell metabolism *8*, 169-174.

Gannon, M.C., and Nuttall, F.Q. (2004). Effect of a high-protein, low-carbohydrate diet on blood glucose control in people with type 2 diabetes. Diabetes *53*, 2375-2382.

Garcia-Caraballo, S.C., Comhair, T.M., Verheyen, F., Gaemers, I., Schaap, F.G., Houten, S.M., Hakvoort, T.B., Dejong, C.H., Lamers, W.H., and Koehler, S.E. (2013). Prevention and reversal of hepatic steatosis with a high-protein diet in mice. Biochimica et biophysica acta *1832*, 685-695.

Garcia Caraballo, S.C., Comhair, T.M., Dejong, C.H.C., Lamers, W.H., and Koehler, S.E. (2017). Dietary treatment of fatty liver: High dietary protein content has an antisteatotic and antiobesogenic effect in mice. Biochimica et biophysica acta Molecular basis of disease *1863*, 1789-1804.

Gastaldelli, A., Gaggini, M., and DeFronzo, R.A. (2017). Role of Adipose Tissue Insulin Resistance in the Natural History of Type 2 Diabetes: Results From the San Antonio Metabolism Study. Diabetes *66*, 815-822.

Giannini, E.G., Testa, R., and Savarino, V. (2005). Liver enzyme alteration: a guide for clinicians. CMAJ : Canadian Medical Association journal = journal de l'Association medicale canadienne *172*, 367-379.

Gillum, M.P. (2018). Parsing the Potential Neuroendocrine Actions of FGF21 in Primates. Endocrinology *159*, 1966-1970.

Gimeno, R.E., and Moller, D.E. (2014). FGF21-based pharmacotherapy--potential utility for metabolic disorders. Trends in endocrinology and metabolism: TEM *25*, 303-311.

Goetz, R., Beenken, A., Ibrahimi, O.A., Kalinina, J., Olsen, S.K., Eliseenkova, A.V., Xu, C., Neubert, T.A., Zhang, F., Linhardt, R.J.*, et al.* (2007). Molecular insights into the klotho-dependent, endocrine mode of action of fibroblast growth factor 19 subfamily members. Molecular and cellular biology *27*, 3417-3428.

Gokarn, R., Solon-Biet, S.M., Cogger, V.C., Cooney, G.J., Wahl, D., McMahon, A.C., Mitchell, J.R., Mitchell, S.J., Hine, C., de Cabo, R.*, et al.* (2018). Long-term Dietary Macronutrients and Hepatic Gene Expression in Aging Mice. The journals of gerontology Series A, Biological sciences and medical sciences *73*, 1618-1625.

Goralski, K.B., McCarthy, T.C., Hanniman, E.A., Zabel, B.A., Butcher, E.C., Parlee, S.D., Muruganandan, S., and Sinal, C.J. (2007). Chemerin, a novel adipokine that regulates adipogenesis and adipocyte metabolism. The Journal of biological chemistry *282*, 28175-28188.

Gosby, A.K., Lau, N.S., Tam, C.S., Iglesias, M.A., Morrison, C.D., Caterson, I.D., Brand-Miller, J., Conigrave, A.D., Raubenheimer, D., and Simpson, S.J. (2016). Raised FGF-21 and Triglycerides Accompany Increased Energy Intake Driven by Protein Leverage in Lean, Healthy Individuals: A Randomised Trial. PloS one *11*, e0161003.

Green, H., and Kehinde, O. (1975). An established preadipose cell line and its differentiation in culture. II. Factors affecting the adipose conversion. Cell *5*, 19-27.

Gregor, M.F., and Hotamisligil, G.S. (2011). Inflammatory mechanisms in obesity. Annual review of immunology *29*, 415-445.

Gruben, N., Aparicio Vergara, M., Kloosterhuis, N.J., van der Molen, H., Stoelwinder, S., Youssef, S., de Bruin, A., Delsing, D.J., Kuivenhoven, J.A., van de Sluis, B.*, et al.* (2014). Chemokine-like receptor 1 deficiency does not affect the development of insulin resistance and nonalcoholic fatty liver disease in mice. PloS one *9*, e96345.

Haas, J.T., Francque, S., and Staels, B. (2016). Pathophysiology and Mechanisms of Nonalcoholic Fatty Liver Disease. Annual review of physiology *78*, 181-205.

Halliday, M., and Mallucci, G.R. (2015). Review: Modulating the unfolded protein response to prevent neurodegeneration and enhance memory. Neuropathology and applied neurobiology *41*, 414-427.

Hansen, I.R., Jansson, K.M., Cannon, B., and Nedergaard, J. (2014). Contrasting effects of cold acclimation versus obesogenic diets on chemerin gene expression in brown and brite adipose tissues. Biochimica et biophysica acta *1841*, 1691-1699.

He, L., Sillanpaa, M.J., Silventoinen, K., Kaprio, J., and Pitkaniemi, J. (2016). Estimating Modifying Effect of Age on Genetic and Environmental Variance Components in Twin Models. Genetics *202*, 1313-1328.

Heianza, Y., Arase, Y., Tsuji, H., Fujihara, K., Saito, K., Hsieh, S.D., Tanaka, S., Kodama, S., Hara, S., and Sone, H. (2014). Metabolically healthy obesity, presence or absence of fatty liver, and risk of type 2 diabetes in Japanese individuals: Toranomon Hospital Health Management Center Study 20 (TOPICS 20). The Journal of clinical endocrinology and metabolism *99*, 2952-2960.

Heilbronn, L.K., Campbell, L.V., Xu, A., and Samocha-Bonet, D. (2013). Metabolically protective cytokines adiponectin and fibroblast growth factor-21 are increased by acute overfeeding in healthy humans. PloS one *8*, e78864.

Helfer, G., Ross, A.W., Thomson, L.M., Mayer, C.D., Stoney, P.N., McCaffery, P.J., and Morgan, P.J. (2016). A neuroendocrine role for chemerin in hypothalamic remodelling and photoperiodic control of energy balance. Scientific reports *6*, 26830.

Helfer, G., and Wu, Q.F. (2018). Chemerin: a multifaceted adipokine involved in metabolic disorders. The Journal of endocrinology *238*, R79-r94.

Hill, C.M., Berthoud, H.R., Munzberg, H., and Morrison, C.D. (2018). Homeostatic sensing of dietary protein restriction: A case for FGF21. Frontiers in neuroendocrinology *51*, 125-131.

Hill, C.M., Laeger, T., Albarado, D.C., McDougal, D.H., Berthoud, H.R., Munzberg, H., and Morrison, C.D. (2017). Low protein-induced increases in FGF21 drive UCP1-dependent metabolic but not thermoregulatory endpoints. Scientific reports *7*, 8209.

Holland, W.L., Adams, A.C., Brozinick, J.T., Bui, H.H., Miyauchi, Y., Kusminski, C.M., Bauer, S.M., Wade, M., Singhal, E., Cheng, C.C.*, et al.* (2013). An FGF21-adiponectin-ceramide axis controls energy expenditure and insulin action in mice. Cell metabolism *17*, 790-797.

Hotamisligil, G.S. (2010). Endoplasmic reticulum stress and the inflammatory basis of metabolic disease. Cell *140*, 900-917.

Hotta, Y., Nakamura, H., Konishi, M., Murata, Y., Takagi, H., Matsumura, S., Inoue, K., Fushiki, T., and Itoh, N. (2009). Fibroblast growth factor 21 regulates lipolysis in white adipose tissue but is not required for ketogenesis and triglyceride clearance in liver. Endocrinology *150*, 4625-4633.

Hron, B.M., Ebbeling, C.B., Feldman, H.A., and Ludwig, D.S. (2017). Hepatic, adipocyte, enteric and pancreatic hormones: response to dietary macronutrient composition and relationship with metabolism. Nutrition & metabolism *14*, 44.

Huang, K., Du, G., Li, L., Liang, H., and Zhang, B. (2012). Association of chemerin levels in synovial fluid with the severity of knee osteoarthritis. Biomarkers : biochemical indicators of exposure, response, and susceptibility to chemicals *17*, 16-20.

Ibrahim, M.M. (2010). Subcutaneous and visceral adipose tissue: structural and functional differences. Obesity reviews : an official journal of the International Association for the Study of Obesity *11*, 11-18.

Inagaki, T., Dutchak, P., Zhao, G., Ding, X., Gautron, L., Parameswara, V., Li, Y., Goetz, R., Mohammadi, M., Esser, V.*, et al.* (2007). Endocrine regulation of the fasting response by PPARalpha-mediated induction of fibroblast growth factor 21. Cell metabolism *5*, 415-425.

Inagaki, T., Lin, V.Y., Goetz, R., Mohammadi, M., Mangelsdorf, D.J., and Kliewer, S.A. (2008). Inhibition of growth hormone signaling by the fasting-induced hormone FGF21. Cell metabolism *8*, 77-83.

International Expert Committee (2009). International Expert Committee report on the role of the A1C assay in the diagnosis of diabetes. Diabetes care 32, 1327-1334.

Ito, S., Kinoshita, S., Shiraishi, N., Nakagawa, S., Sekine, S., Fujimori, T., and Nabeshima, Y.I. (2000). Molecular cloning and expression analyses of mouse betaklotho, which encodes a novel Klotho family protein. Mechanisms of development *98*, 115-119.

Itoh, N. (2014). FGF21 as a Hepatokine, Adipokine, and Myokine in Metabolism and Diseases. Frontiers in endocrinology *5*, 107.

Jiang, S., Yan, C., Fang, Q.C., Shao, M.L., Zhang, Y.L., Liu, Y., Deng, Y.P., Shan, B., Liu, J.Q., Li, H.T., *et al.* (2014). Fibroblast growth factor 21 is regulated by the IRE1alpha-XBP1 branch of the unfolded protein response and counteracts endoplasmic reticulum stress-induced hepatic steatosis. The Journal of biological chemistry *289*, 29751-29765.

Kajor, M., Kukla, M., Waluga, M., Liszka, L., Dyaczynski, M., Kowalski, G., Zadlo, D., Berdowska, A., Chapula, M., Kostrzab-Zdebel, A., *et al.* (2017). Hepatic chemerin mRNA in morbidly obese patients with nonalcoholic fatty liver disease. Polish journal of pathology : official journal of the Polish Society of Pathologists *68*, 117-127.

Kargulewicz, A., Stankowiak-Kulpa, H., and Grzymislawski, M. (2014). Dietary recommendations for patients with nonalcoholic fatty liver disease. Przeglad gastroenterologiczny *9*, 18-23.

Kaur, J., Adya, R., Tan, B.K., Chen, J., and Randeva, H.S. (2010). Identification of chemerin receptor (ChemR23) in human endothelial cells: chemerin-induced endothelial angiogenesis. Biochemical and biophysical research communications *391*, 1762-1768.

Kaur, J., Mattu, H.S., Chatha, K., and Randeva, H.S. (2018). Chemerin in human cardiovascular disease. Vascular pharmacology *110*, 1-6.

Keipert, S., Ost, M., Johann, K., Imber, F., Jastroch, M., van Schothorst, E.M., Keijer, J., and Klaus, S. (2014). Skeletal muscle mitochondrial uncoupling drives endocrine cross-talk through the induction of FGF21 as a myokine. American journal of physiology Endocrinology and metabolism *306*, E469-482.

Keuper, M., Haring, H.U., and Staiger, H. (2019). Circulating FGF21 Levels in Human Health and Metabolic Disease. Experimental and clinical endocrinology & diabetes : official journal, German Society of Endocrinology [and] German Diabetes Association.

Kharitonenkov, A., Shiyanova, T.L., Koester, A., Ford, A.M., Micanovic, R., Galbreath, E.J., Sandusky, G.E., Hammond, L.J., Moyers, J.S., Owens, R.A., *et al.* (2005). FGF-21 as a novel metabolic regulator. The Journal of clinical investigation *115*, 1627-1635.

Khazen, W., M'Bika J, P., Tomkiewicz, C., Benelli, C., Chany, C., Achour, A., and Forest, C. (2005). Expression of macrophage-selective markers in human and rodent adipocytes. FEBS letters *579*, 5631-5634.

Kim, J.B. (2016). Dynamic cross talk between metabolic organs in obesity and metabolic diseases. Experimental & molecular medicine *48*, e214.

Kim, K.H., Jeong, Y.T., Oh, H., Kim, S.H., Cho, J.M., Kim, Y.N., Kim, S.S., Kim, D.H., Hur, K.Y., Kim, H.K., *et al.* (2013). Autophagy deficiency leads to protection from obesity and insulin resistance by inducing Fgf21 as a mitokine. Nature medicine *19*, 83-92.

Kim, K.H., and Lee, M.S. (2014). FGF21 as a Stress Hormone: The Roles of FGF21 in Stress Adaptation and the Treatment of Metabolic Diseases. Diabetes & metabolism journal *38*, 245-251.

Kim, K.H., and Lee, M.S. (2015). FGF21 as a mediator of adaptive responses to stress and metabolic benefits of anti-diabetic drugs. The Journal of endocrinology *226*, R1-16.

Kim, S.H., Kim, K.H., Kim, H.K., Kim, M.J., Back, S.H., Konishi, M., Itoh, N., and Lee, M.S. (2015). Fibroblast growth factor 21 participates in adaptation to endoplasmic reticulum stress and attenuates obesity-induced hepatic metabolic stress. Diabetologia *58*, 809-818.

Kleiner, D.E., Brunt, E.M., Van Natta, M., Behling, C., Contos, M.J., Cummings, O.W., Ferrell, L.D., Liu, Y.C., Torbenson, M.S., Unalp-Arida, A., *et al.* (2005). Design and validation of a histological scoring system for nonalcoholic fatty liver disease. Hepatology (Baltimore, Md) *41*, 1313-1321.

Kloting, N., and Bluher, M. (2014). Adipocyte dysfunction, inflammation and metabolic syndrome. Reviews in endocrine & metabolic disorders *15*, 277-287.

Kloting, N., Fasshauer, M., Dietrich, A., Kovacs, P., Schon, M.R., Kern, M., Stumvoll, M., and Bluher, M. (2010). Insulin-sensitive obesity. American journal of physiology Endocrinology and metabolism *299*, E506-515.

Kralisch, S., Tonjes, A., Krause, K., Richter, J., Lossner, U., Kovacs, P., Ebert, T., Bluher, M., Stumvoll, M., and Fasshauer, M. (2013). Fibroblast growth factor-21 serum concentrations are associated with metabolic and hepatic markers in humans. The Journal of endocrinology *216*, 135-143.

References

Krautbauer, S., Wanninger, J., Eisinger, K., Hader, Y., Beck, M., Kopp, A., Schmid, A., Weiss, T.S., Dorn, C., and Buechler, C. (2013). Chemerin is highly expressed in hepatocytes and is induced in non-alcoholic steatohepatitis liver. Experimental and molecular pathology *95*, 199-205.

Kulig, P., Kantyka, T., Zabel, B.A., Banas, M., Chyra, A., Stefanska, A., Tu, H., Allen, S.J., Handel, T.M., Kozik, A.*, et al.* (2011). Regulation of chemerin chemoattractant and antibacterial activity by human cysteine cathepsins. Journal of immunology (Baltimore, Md : 1950) *187*, 1403-1410.

Kvamme, J.M., Holmen, J., Wilsgaard, T., Florholmen, J., Midthjell, K., and Jacobsen, B.K. (2012). Body mass index and mortality in elderly men and women: the Tromso and HUNT studies. Journal of epidemiology and community health *66*, 611-617.

Lade, A., Noon, L.A., and Friedman, S.L. (2014). Contributions of metabolic dysregulation and inflammation to nonalcoholic steatohepatitis, hepatic fibrosis, and cancer. Current opinion in oncology *26*, 100-107.

Laeger, T., Albarado, D.C., Burke, S.J., Trosclair, L., Hedgepeth, J.W., Berthoud, H.R., Gettys, T.W., Collier, J.J., Munzberg, H., and Morrison, C.D. (2016). Metabolic Responses to Dietary Protein Restriction Require an Increase in FGF21 that Is Delayed by the Absence of GCN2. Cell reports *16*, 707-716.

Laeger, T., Henagan, T.M., Albarado, D.C., Redman, L.M., Bray, G.A., Noland, R.C., Munzberg, H., Hutson, S.M., Gettys, T.W., Schwartz, M.W.*, et al.* (2014). FGF21 is an endocrine signal of protein restriction. The Journal of clinical investigation *124*, 3913-3922.

Laranjeira, S., Regan-Komito, D., Iqbal, A.J., Greaves, D.R., Payne, S.J., and Orlowski, P. (2018). A model for the optimization of anti-inflammatory treatment with chemerin. Interface focus *8*, 20170007.

Larsen, T.M., Dalskov, S.M., van Baak, M., Jebb, S.A., Papadaki, A., Pfeiffer, A.F., Martinez, J.A., Handjieva-Darlenska, T., Kunesova, M., Pihlsgard, M.*, et al.* (2010). Diets with high or low protein content and glycemic index for weight-loss maintenance. The New England journal of medicine *363*, 2102-2113.

Layman, D.K., Clifton, P., Gannon, M.C., Krauss, R.M., and Nuttall, F.Q. (2008). Protein in optimal health: heart disease and type 2 diabetes. The American journal of clinical nutrition *87*, 1571s-1575s.

Leclercq, I.A., and Horsmans, Y. (2008). Nonalcoholic fatty liver disease: the potential role of nutritional management. Current opinion in clinical nutrition and metabolic care *11*, 766-773.

Lee, M.J., and Fried, S.K. (2014). Optimal protocol for the differentiation and metabolic analysis of human adipose stromal cells. Methods in enzymology *538*, 49-65.

Lee, S., Choi, J., Mohanty, J., Sousa, L.P., Tome, F., Pardon, E., Steyaert, J., Lemmon, M.A., Lax, I., and Schlessinger, J. (2018). Structures of beta-klotho reveal a 'zip code'-like mechanism for endocrine FGF signalling. Nature *553*, 501-505.

Lehrke, M., Becker, A., Greif, M., Stark, R., Laubender, R.P., von Ziegler, F., Lebherz, C., Tittus, J., Reiser, M., Becker, C.*, et al.* (2009). Chemerin is associated with markers of inflammation and components of the metabolic syndrome but does not predict coronary atherosclerosis. European journal of endocrinology *161*, 339-344.

Leiherer, A., Muendlein, A., Kinz, E., Vonbank, A., Rein, P., Fraunberger, P., Malin, C., Saely, C.H., and Drexel, H. (2016). High plasma chemerin is associated with renal dysfunction and predictive for cardiovascular events - Insights from phenotype and genotype characterization. Vascular pharmacology *77*, 60-68.

Lewis, J.E., Ebling, F.J.P., Samms, R.J., and Tsintzas, K. (2019). Going Back to the Biology of FGF21: New Insights. Trends in endocrinology and metabolism: TEM *30*, 491-504.

Li, H., Wu, G., Fang, Q., Zhang, M., Hui, X., Sheng, B., Wu, L., Bao, Y., Li, P., Xu, A.*, et al.* (2018). Fibroblast growth factor 21 increases insulin sensitivity through specific expansion of subcutaneous fat. Nature communications *9*, 272.

Li, Z., Ji, X., Wang, W., Liu, J., Liang, X., Wu, H., Liu, J., Eggert, U.S., Liu, Q., and Zhang, X. (2016). Ammonia Induces Autophagy through Dopamine Receptor D3 and MTOR. PloS one *11*, e0153526.

References

Lin, S.D., Tsai, D.H., and Hsu, S.R. (2006). Association between serum uric acid level and components of the metabolic syndrome. Journal of the Chinese Medical Association : JCMA *69*, 512-516.

Lin, Z., Tian, H., Lam, K.S., Lin, S., Hoo, R.C., Konishi, M., Itoh, N., Wang, Y., Bornstein, S.R., Xu, A.*, et al.* (2013). Adiponectin mediates the metabolic effects of FGF21 on glucose homeostasis and insulin sensitivity in mice. Cell metabolism *17*, 779-789.

Liu, W.Y., Huang, S., Shi, K.Q., Zhao, C.C., Chen, L.L., Braddock, M., Chen, Y.P., Feng, W.K., and Zheng, M.H. (2014). The role of fibroblast growth factor 21 in the pathogenesis of liver disease: a novel predictor and therapeutic target. Expert opinion on therapeutic targets *18*, 1305-1313.

Lloyd, J.W., Zerfass, K.M., Heckstall, E.M., and Evans, K.A. (2015). Diet-induced increases in chemerin are attenuated by exercise and mediate the effect of diet on insulin and HOMA-IR. Therapeutic advances in endocrinology and metabolism *6*, 189-198.

Lorincz, H., Katko, M., Harangi, M., Somodi, S., Gaal, K., Fulop, P., Paragh, G., and Seres, I. (2014). Strong correlations between circulating chemerin levels and lipoprotein subfractions in nondiabetic obese and nonobese subjects. Clinical endocrinology *81*, 370-377.

Luangsay, S., Wittamer, V., Bondue, B., De Henau, O., Rouger, L., Brait, M., Franssen, J.D., de Nadai, P., Huaux, F., and Parmentier, M. (2009). Mouse ChemR23 is expressed in dendritic cell subsets and macrophages, and mediates an anti-inflammatory activity of chemerin in a lung disease model. Journal of immunology (Baltimore, Md : 1950) *183*, 6489-6499.

Lundasen, T., Hunt, M.C., Nilsson, L.M., Sanyal, S., Angelin, B., Alexson, S.E., and Rudling, M. (2007). PPARalpha is a key regulator of hepatic FGF21. Biochemical and biophysical research communications *360*, 437-440.

Lundsgaard, A.M., Fritzen, A.M., Sjoberg, K.A., Myrmel, L.S., Madsen, L., Wojtaszewski, J.F.P., Richter, E.A., and Kiens, B. (2017). Circulating FGF21 in humans is potently induced by short term overfeeding of carbohydrates. Molecular metabolism *6*, 22-29.

Luo, Y., and McKeehan, W.L. (2013). Stressed Liver and Muscle Call on Adipocytes with FGF21. Frontiers in endocrinology *4*, 194.

Machado, M., Marques-Vidal, P., and Cortez-Pinto, H. (2006). Hepatic histology in obese patients undergoing bariatric surgery. Journal of hepatology *45*, 600-606.

Machado, M.V., Michelotti, G.A., Xie, G., Almeida Pereira, T., Boursier, J., Bohnic, B., Guy, C.D., and Diehl, A.M. (2015). Mouse models of diet-induced nonalcoholic steatohepatitis reproduce the heterogeneity of the human disease. PloS one *10*, e0127991.

Mai, K., Andres, J., Biedasek, K., Weicht, J., Bobbert, T., Sabath, M., Meinus, S., Reinecke, F., Mohlig, M., Weickert, M.O.*, et al.* (2009). Free fatty acids link metabolism and regulation of the insulin-sensitizing fibroblast growth factor-21. Diabetes *58*, 1532-1538.

Maida, A., Zota, A., Sjoberg, K.A., Schumacher, J., Sijmonsma, T.P., Pfenninger, A., Christensen, M.M., Gantert, T., Fuhrmeister, J., Rothermel, U.*, et al.* (2016). A liver stress-endocrine nexus promotes metabolic integrity during dietary protein dilution. The Journal of clinical investigation *126*, 3263-3278.

Maratos-Flier, E. (2017). Fatty liver and FGF21 physiology. Experimental cell research *360*, 2-5.

Mariani, F., and Roncucci, L. (2015). Chemerin/chemR23 axis in inflammation onset and resolution. Inflammation research : official journal of the European Histamine Research Society [et al] *64*, 85-95.

Markan, K.R., and Potthoff, M.J. (2016). Metabolic fibroblast growth factors (FGFs): Mediators of energy homeostasis. Seminars in cell & developmental biology *53*, 85-93.

Markova, M., Pivovarova, O., Hornemann, S., Sucher, S., Frahnow, T., Wegner, K., Machann, J., Petzke, K.J., Hierholzer, J., Lichtinghagen, R.*, et al.* (2017). Isocaloric Diets High in Animal or Plant Protein Reduce Liver Fat and Inflammation in Individuals With Type 2 Diabetes. Gastroenterology *152*, 571-585 e578.

Marsset-Baglieri, A., Fromentin, G., Tome, D., Bensaid, A., Makkarios, L., and Even, P.C. (2004). Increasing the protein content in a carbohydrate-free diet enhances fat loss during 35% but not 75% energy restriction in rats. The Journal of nutrition *134*, 2646-2652.

References

Martensson, U.E., Bristulf, J., Owman, C., and Olde, B. (2005). The mouse chemerin receptor gene, mcmklr1, utilizes alternative promoters for transcription and is regulated by all-trans retinoic acid. Gene *350*, 65-77.

Martinez-Jimenez, C.P., Kyrmizi, I., Cardot, P., Gonzalez, F.J., and Talianidis, I. (2010). Hepatocyte nuclear factor 4alpha coordinates a transcription factor network regulating hepatic fatty acid metabolism. Molecular and cellular biology *30*, 565-577.

Maruyama, R., Shimizu, M., Hashidume, T., Inoue, J., Itoh, N., and Sato, R. (2018). FGF21 Alleviates Hepatic Endoplasmic Reticulum Stress under Physiological Conditions. Journal of nutritional science and vitaminology *64*, 200-208.

Matikainen, N., Taskinen, M.R., Stennabb, S., Lundbom, N., Hakkarainen, A., Vaaralahti, K., and Raivio, T. (2012). Decrease in circulating fibroblast growth factor 21 after an oral fat load is related to postprandial triglyceride-rich lipoproteins and liver fat. European journal of endocrinology *166*, 487-492.

Mattern, A., Zellmann, T., and Beck-Sickinger, A.G. (2014). Processing, signaling, and physiological function of chemerin. IUBMB life *66*, 19-26.

Matthews, D.R., Hosker, J.P., Rudenski, A.S., Naylor, B.A., Treacher, D.F., and Turner, R.C. (1985). Homeostasis model assessment: insulin resistance and beta-cell function from fasting plasma glucose and insulin concentrations in man. Diabetologia *28*, 412-419.

Meex, R.C.R., and Watt, M.J. (2017). Hepatokines: linking nonalcoholic fatty liver disease and insulin resistance. Nature reviews Endocrinology *13*, 509-520.

Meghelli-Bouchenak, M., Belleville, J., and Boquillon, M. (1989). Hepatic steatosis and serum very low density lipoproteins during two types of protein malnutrition followed by balanced refeeding. Nutrition (Burbank, Los Angeles County, Calif) *5*, 321-329.

Mendelsohn, A.R., and Larrick, J.W. (2012). Fibroblast growth factor-21 is a promising dietary restriction mimetic. Rejuvenation research *15*, 624-628.

Mirmajidi, S., Izadi, A., Saghafi-Asl, M., Vahid, F., Karamzad, N., Amiri, P., Shivappa, N., and Hebert, J.R. (2019). Inflammatory Potential of Diet: Association With Chemerin, Omentin, Lipopolysaccharide-Binding Protein, and Insulin Resistance in the Apparently Healthy Obese. Journal of the American College of Nutrition *38*, 302-310.

Morris, S.M., Jr. (2002). Regulation of enzymes of the urea cycle and arginine metabolism. Annual review of nutrition *22*, 87-105.

Morrison, C.D., and Laeger, T. (2015). Protein-dependent regulation of feeding and metabolism. Trends in endocrinology and metabolism: TEM *26*, 256-262.

Moschen, A.R., Wieser, V., and Tilg, H. (2012). Adiponectin: key player in the adipose tissue-liver crosstalk. Current medicinal chemistry *19*, 5467-5473.

Murano, I., Barbatelli, G., Parisani, V., Latini, C., Muzzonigro, G., Castellucci, M., and Cinti, S. (2008). Dead adipocytes, detected as crown-like structures, are prevalent in visceral fat depots of genetically obese mice. Journal of lipid research *49*, 1562-1568.

Mussig, K., Staiger, H., Machicao, F., Thamer, C., Machann, J., Schick, F., Claussen, C.D., Stefan, N., Fritsche, A., and Haring, H.U. (2009). RARRES2, encoding the novel adipokine chemerin, is a genetic determinant of disproportionate regional body fat distribution: a comparative magnetic resonance imaging study. Metabolism: clinical and experimental *58*, 519-524.

Nagpal, S., Patel, S., Jacobe, H., DiSepio, D., Ghosn, C., Malhotra, M., Teng, M., Duvic, M., and Chandraratna, R.A. (1997). Tazarotene-induced gene 2 (TIG2), a novel retinoid-responsive gene in skin. The Journal of investigative dermatology *109*, 91-95.

Nakamura, N., Naruse, K., Kobayashi, Y., Miyabe, M., Saiki, T., Enomoto, A., Takahashi, M., and Matsubara, T. (2018). Chemerin promotes angiogenesis in vivo. Physiological reports *6*, e13962.

Neves, K.B., Nguyen Dinh Cat, A., Lopes, R.A., Rios, F.J., Anagnostopoulou, A., Lobato, N.S., de Oliveira, A.M., Tostes, R.C., Montezano, A.C., and Touyz, R.M. (2015). Chemerin Regulates Crosstalk Between Adipocytes and Vascular Cells Through Nox. Hypertension (Dallas, Tex : 1979) *66*, 657-666.

Newgard, C.B. (2012). Interplay between lipids and branched-chain amino acids in development of insulin resistance. Cell metabolism *15*, 606-614.

Nishimura, T., Nakatake, Y., Konishi, M., and Itoh, N. (2000). Identification of a novel FGF, FGF-21, preferentially expressed in the liver. Biochimica et biophysica acta *1492*, 203-206.

Noguchi, Y., Nishikata, N., Shikata, N., Kimura, Y., Aleman, J.O., Young, J.D., Koyama, N., Kelleher, J.K., Takahashi, M., and Stephanopoulos, G. (2010). Ketogenic essential amino acids modulate lipid synthetic pathways and prevent hepatic steatosis in mice. PloS one *5*, e12057.

Ogawa, Y., Kurosu, H., Yamamoto, M., Nandi, A., Rosenblatt, K.P., Goetz, R., Eliseenkova, A.V., Mohammadi, M., and Kuro-o, M. (2007). BetaKlotho is required for metabolic activity of fibroblast growth factor 21. Proceedings of the National Academy of Sciences of the United States of America *104*, 7432-7437.

Oh, K.J., Lee, D.S., Kim, W.K., Han, B.S., Lee, S.C., and Bae, K.H. (2016). Metabolic Adaptation in Obesity and Type II Diabetes: Myokines, Adipokines and Hepatokines. International journal of molecular sciences *18*.

Oulion, S., Bertrand, S., and Escriva, H. (2012). Evolution of the FGF Gene Family. International journal of evolutionary biology *2012*, 298147.

Ozcan, U., Cao, Q., Yilmaz, E., Lee, A.H., Iwakoshi, N.N., Ozdelen, E., Tuncman, G., Gorgun, C., Glimcher, L.H., and Hotamisligil, G.S. (2004). Endoplasmic reticulum stress links obesity, insulin action, and type 2 diabetes. Science (New York, NY) *306*, 457-461.

Paddon-Jones, D., and Leidy, H. (2014). Dietary protein and muscle in older persons. Current opinion in clinical nutrition and metabolic care *17*, 5-11.

Parlee, S.D., Ernst, M.C., Muruganandan, S., Sinal, C.J., and Goralski, K.B. (2010). Serum chemerin levels vary with time of day and are modified by obesity and tumor necrosis factor-{alpha}. Endocrinology *151*, 2590-2602.

Parlee, S.D., Lentz, S.I., Mori, H., and MacDougald, O.A. (2014). Quantifying size and number of adipocytes in adipose tissue. Methods in enzymology *537*, 93-122.

Parolini, S., Santoro, A., Marcenaro, E., Luini, W., Massardi, L., Facchetti, F., Communi, D., Parmentier, M., Majorana, A., Sironi, M.*, et al.* (2007). The role of chemerin in the colocalization of NK and dendritic cell subsets into inflamed tissues. Blood *109*, 3625-3632.

Parry, S.A., and Hodson, L. (2017). Influence of dietary macronutrients on liver fat accumulation and metabolism. Journal of investigative medicine : the official publication of the American Federation for Clinical Research *65*, 1102-1115.

Petryszak, R., Keays, M., Tang, Y.A., Fonseca, N.A., Barrera, E., Burdett, T., Fullgrabe, A., Fuentes, A.M., Jupp, S., Koskinen, S.*, et al.* (2016). Expression Atlas update--an integrated database of gene and protein expression in humans, animals and plants. Nucleic acids research *44*, D746-752.

Petzke, K.J., Freudenberg, A., and Klaus, S. (2014). Beyond the role of dietary protein and amino acids in the prevention of diet-induced obesity. International journal of molecular sciences *15*, 1374-1391.

Pichon, L., Huneau, J.F., Fromentin, G., and Tome, D. (2006). A high-protein, high-fat, carbohydrate-free diet reduces energy intake, hepatic lipogenesis, and adiposity in rats. The Journal of nutrition *136*, 1256-1260.

Pischon, T., Boeing, H., Hoffmann, K., Bergmann, M., Schulze, M.B., Overvad, K., van der Schouw, Y.T., Spencer, E., Moons, K.G., Tjonneland, A.*, et al.* (2008). General and abdominal adiposity and risk of death in Europe. The New England journal of medicine *359*, 2105-2120.

Pohl, R., Haberl, E.M., Rein-Fischboeck, L., Zimny, S., Neumann, M., Aslanidis, C., Schacherer, D., Krautbauer, S., Eisinger, K., Weiss, T.S.*, et al.* (2017). Hepatic chemerin mRNA expression is reduced in human nonalcoholic steatohepatitis. European journal of clinical investigation *47*, 7-18.

Proud, C.G. (2014). Control of the translational machinery by amino acids. The American journal of clinical nutrition *99*, 231s-236s.

Rastogi, A., Shasthry, S.M., Agarwal, A., Bihari, C., Jain, P., Jindal, A., and Sarin, S. (2017). Non-alcoholic fatty liver disease - histological scoring systems: a large cohort single-center, evaluation study. APMIS : acta pathologica, microbiologica, et immunologica Scandinavica *125*, 962-973.

Reverchon, M., Bertoldo, M.J., Rame, C., Froment, P., and Dupont, J. (2014). CHEMERIN (RARRES2) decreases in vitro granulosa cell steroidogenesis and blocks oocyte meiotic progression in bovine species. Biology of reproduction *90*, 102.

Rietman, A., Schwarz, J., Tome, D., Kok, F.J., and Mensink, M. (2014). High dietary protein intake, reducing or eliciting insulin resistance? European journal of clinical nutrition *68*, 973-979.

Rinella, M.E., and Sanyal, A.J. (2016). Management of NAFLD: a stage-based approach. Nature reviews Gastroenterology & hepatology *13*, 196-205.

Roh, S.G., Song, S.H., Choi, K.C., Katoh, K., Wittamer, V., Parmentier, M., and Sasaki, S. (2007). Chemerin--a new adipokine that modulates adipogenesis via its own receptor. Biochemical and biophysical research communications *362*, 1013-1018.

Rusli, F., Deelen, J., Andriyani, E., Boekschoten, M.V., Lute, C., van den Akker, E.B., Muller, M., Beekman, M., and Steegenga, W.T. (2016). Fibroblast growth factor 21 reflects liver fat accumulation and dysregulation of signalling pathways in the liver of C57BL/6J mice. Scientific reports *6*, 30484.

Rutkowski, D.T., Wu, J., Back, S.H., Callaghan, M.U., Ferris, S.P., Iqbal, J., Clark, R., Miao, H., Hassler, J.R., Fornek, J.*, et al.* (2008). UPR pathways combine to prevent hepatic steatosis caused by ER stress-mediated suppression of transcriptional master regulators. Developmental cell *15*, 829-840.

Salgado, A.L., Carvalho, L., Oliveira, A.C., Santos, V.N., Vieira, J.G., and Parise, E.R. (2010). Insulin resistance index (HOMA-IR) in the differentiation of patients with non-alcoholic fatty liver disease and healthy individuals. Arquivos de gastroenterologia *47*, 165-169.

Salminen, A., Kaarniranta, K., and Kauppinen, A. (2017a). Integrated stress response stimulates FGF21 expression: Systemic enhancer of longevity. Cellular signalling *40*, 10-21.

Salminen, A., Kaarniranta, K., and Kauppinen, A. (2017b). Regulation of longevity by FGF21: Interaction between energy metabolism and stress responses. Ageing research reviews *37*, 79-93.

Saltiel, A.R., and Kahn, C.R. (2001). Insulin signalling and the regulation of glucose and lipid metabolism. Nature *414*, 799-806.

Samms, R.J., Lewis, J.E., Norton, L., Stephens, F.B., Gaffney, C.J., Butterfield, T., Smith, D.P., Cheng, C.C., Perfield, J.W., 2nd, Adams, A.C.*, et al.* (2017). FGF21 Is an Insulin-Dependent Postprandial Hormone in Adult Humans. The Journal of clinical endocrinology and metabolism *102*, 3806-3813.

Sanyal, A., Charles, E.D., Neuschwander-Tetri, B.A., Loomba, R., Harrison, S.A., Abdelmalek, M.F., Lawitz, E.J., Halegoua-DeMarzio, D., Kundu, S., Noviello, S.*, et al.* (2019). Pegbelfermin (BMS-986036), a PEGylated fibroblast growth factor 21 analogue, in patients with non-alcoholic steatohepatitis: a randomised, double-blind, placebo-controlled, phase 2a trial. Lancet (London, England) *392*, 2705-2717.

Sarruf, D.A., Thaler, J.P., Morton, G.J., German, J., Fischer, J.D., Ogimoto, K., and Schwartz, M.W. (2010). Fibroblast growth factor 21 action in the brain increases energy expenditure and insulin sensitivity in obese rats. Diabetes *59*, 1817-1824.

Schaap, F.G., Kremer, A.E., Lamers, W.H., Jansen, P.L., and Gaemers, I.C. (2013). Fibroblast growth factor 21 is induced by endoplasmic reticulum stress. Biochimie *95*, 692-699.

Schmid, A., Leszczak, S., Ober, I., Karrasch, T., and Schaffler, A. (2015). Short-term and divergent regulation of FGF-19 and FGF-21 during oral lipid tolerance test but not oral glucose tolerance test. Experimental and clinical endocrinology & diabetes : official journal, German Society of Endocrinology [and] German Diabetes Association *123*, 88-94.

Schouten, R., van der Kaaden, I., van 't Hof, G., and Feskens, P.G. (2016). Comparison of Preoperative Diets Before Bariatric Surgery: a Randomized, Single-Blinded, Non-inferiority Trial. Obesity surgery *26*, 1743-1749.

Schuler, R., Osterhoff, M.A., Frahnow, T., Seltmann, A.C., Busjahn, A., Kabisch, S., Xu, L., Mosig, A.S., Spranger, J., Mohlig, M*., et al.* (2017). High-Saturated-Fat Diet Increases Circulating Angiotensin-Converting Enzyme, Which Is Enhanced by the rs4343 Polymorphism Defining Persons at Risk of Nutrient-Dependent Increases of Blood Pressure. J Am Heart Assoc *6*.

Schutz, Y. (2011). Protein turnover, ureagenesis and gluconeogenesis. International journal for vitamin and nutrition research Internationale Zeitschrift fur Vitamin- und Ernahrungsforschung Journal international de vitaminologie et de nutrition *81*, 101-107.

Sell, H., Laurencikiene, J., Taube, A., Eckardt, K., Cramer, A., Horrighs, A., Arner, P., and Eckel, J. (2009). Chemerin is a novel adipocyte-derived factor inducing insulin resistance in primary human skeletal muscle cells. Diabetes *58*, 2731-2740.

Seppala-Lindroos, A., Vehkavaara, S., Hakkinen, A.M., Goto, T., Westerbacka, J., Sovijarvi, A., Halavaara, J., and Yki-Jarvinen, H. (2002). Fat accumulation in the liver is associated with defects in insulin suppression of glucose production and serum free fatty acids independent of obesity in normal men. The Journal of clinical endocrinology and metabolism *87*, 3023-3028.

Sevastianova, K., Santos, A., Kotronen, A., Hakkarainen, A., Makkonen, J., Silander, K., Peltonen, M., Romeo, S., Lundbom, J., Lundbom, N*., et al.* (2012). Effect of short-term carbohydrate overfeeding and long-term weight loss on liver fat in overweight humans. The American journal of clinical nutrition *96*, 727-734.

Shambaugh, G.E., 3rd (1977). Urea biosynthesis I. The urea cycle and relationships to the citric acid cycle. The American journal of clinical nutrition *30*, 2083-2087.

Singh, R., Kaushik, S., Wang, Y., Xiang, Y., Novak, I., Komatsu, M., Tanaka, K., Cuervo, A.M., and Czaja, M.J. (2009). Autophagy regulates lipid metabolism. Nature *458*, 1131-1135.

Sluijs, I., Beulens, J.W., van der, A.D., Spijkerman, A.M., Grobbee, D.E., and van der Schouw, Y.T. (2010). Dietary intake of total, animal, and vegetable protein and risk of type 2 diabetes in the European Prospective Investigation into Cancer and Nutrition (EPIC)-NL study. Diabetes care *33*, 43-48.

Smith, G.I., Yoshino, J., Kelly, S.C., Reeds, D.N., Okunade, A., Patterson, B.W., Klein, S., and Mittendorfer, B. (2016). High-Protein Intake during Weight Loss Therapy Eliminates the Weight-Loss-Induced Improvement in Insulin Action in Obese Postmenopausal Women. Cell reports *17*, 849-861.

Soberg, S., Sandholt, C.H., Jespersen, N.Z., Toft, U., Madsen, A.L., von Holstein-Rathlou, S., Grevengoed, T.J., Christensen, K.B., Bredie, W.L.P., Potthoff, M.J*., et al.* (2017). FGF21 Is a Sugar-Induced Hormone Associated with Sweet Intake and Preference in Humans. Cell metabolism *25*, 1045-1053.e1046.

Softic, S., Gupta, M.K., Wang, G.X., Fujisaka, S., O'Neill, B.T., Rao, T.N., Willoughby, J., Harbison, C., Fitzgerald, K., Ilkayeva, O*., et al.* (2017). Divergent effects of glucose and fructose on hepatic lipogenesis and insulin signaling. The Journal of clinical investigation *127*, 4059-4074.

Solinas, G., and Karin, M. (2010). JNK1 and IKKbeta: molecular links between obesity and metabolic dysfunction. FASEB journal : official publication of the Federation of American Societies for Experimental Biology *24*, 2596-2611.

Solon-Biet, S.M., Cogger, V.C., Pulpitel, T., Heblinski, M., Wahl, D., McMahon, A.C., Warren, A., Durrant-Whyte, J., Walters, K.A., Krycer, J.R*., et al.* (2016). Defining the Nutritional and Metabolic Context of FGF21 Using the Geometric Framework. Cell metabolism *24*, 555-565.

Solon-Biet, S.M., Mitchell, S.J., de Cabo, R., Raubenheimer, D., Le Couteur, D.G., and Simpson, S.J. (2015). Macronutrients and caloric intake in health and longevity. The Journal of endocrinology *226*, R17-28.

Sonoda, J., Chen, M.Z., and Baruch, A. (2017). FGF21-receptor agonists: an emerging therapeutic class for obesity-related diseases. Hormone molecular biology and clinical investigation *30*.

Staiger, H., Keuper, M., Berti, L., Hrabe de Angelis, M., and Haring, H.U. (2017). Fibroblast Growth Factor 21-Metabolic Role in Mice and Men. Endocr Rev *38*, 468-488.

Stamatikos, A.D., da Silva, R.P., Lewis, J.T., Douglas, D.N., Kneteman, N.M., Jacobs, R.L., and Paton, C.M. (2016). Tissue Specific Effects of Dietary Carbohydrates and Obesity on ChREBPalpha and ChREBPbeta Expression. Lipids *51*, 95-104.

Steenackers, N., Gesquiere, I., and Matthys, C. (2018). The relevance of dietary protein after bariatric surgery: what do we know? Current opinion in clinical nutrition and metabolic care *21*, 58-63.

Stefan, N., and Haring, H.U. (2013). The role of hepatokines in metabolism. Nature reviews Endocrinology *9*, 144-152.

Stelmanska, E., Sledzinski, T., Turyn, J., Presler, M., Korczynska, J., and Swierczynski, J. (2013). Chemerin gene expression is regulated by food restriction and food restriction-refeeding in rat adipose tissue but not in liver. Regulatory peptides *181*, 22-29.

Stephens, J.M. (2012). The fat controller: adipocyte development. PLoS biology *10*, e1001436.

Szczepaniak, L.S., Nurenberg, P., Leonard, D., Browning, J.D., Reingold, J.S., Grundy, S., Hobbs, H.H., and Dobbins, R.L. (2005). Magnetic resonance spectroscopy to measure hepatic triglyceride content: prevalence of hepatic steatosis in the general population. American journal of physiology Endocrinology and metabolism *288*, E462-468.

Talukdar, S., Owen, B.M., Song, P., Hernandez, G., Zhang, Y., Zhou, Y., Scott, W.T., Paratala, B., Turner, T., Smith, A.*, et al.* (2016). FGF21 Regulates Sweet and Alcohol Preference. Cell metabolism *23*, 344-349.

Tonjes, A., Scholz, M., Breitfeld, J., Marzi, C., Grallert, H., Gross, A., Ladenvall, C., Schleinitz, D., Krause, K., Kirsten, H.*, et al.* (2014). Genome wide meta-analysis highlights the role of genetic variation in RARRES2 in the regulation of circulating serum chemerin. PLoS genetics *10*, e1004854.

Ullah, R., Rauf, N., Nabi, G., Ullah, H., Shen, Y., Zhou, Y.D., and Fu, J. (2019). Role of Nutrition in the Pathogenesis and Prevention of Non-alcoholic Fatty Liver Disease: Recent Updates. International journal of biological sciences *15*, 265-276.

Van Nieuwenhove, Y., Dambrauskas, Z., Campillo-Soto, A., van Dielen, F., Wiezer, R., Janssen, I., Kramer, M., and Thorell, A. (2011). Preoperative very low-calorie diet and operative outcome after laparoscopic gastric bypass: a randomized multicenter study. Archives of surgery (Chicago, Ill : 1960) *146*, 1300-1305.

von Holstein-Rathlou, S., BonDurant, L.D., Peltekian, L., Naber, M.C., Yin, T.C., Claflin, K.E., Urizar, A.I., Madsen, A.N., Ratner, C., Holst, B.*, et al.* (2016). FGF21 Mediates Endocrine Control of Simple Sugar Intake and Sweet Taste Preference by the Liver. Cell metabolism *23*, 335-343.

von Holstein-Rathlou, S., and Gillum, M.P. (2019). Fibroblast growth factor 21: an endocrine inhibitor of sugar and alcohol appetite. The Journal of physiology.

Walker, V. (2014). Ammonia metabolism and hyperammonemic disorders. Advances in clinical chemistry *67*, 73-150.

Waluga, M., Kukla, M., Zorniak, M., Kajor, M., Liszka, L., Dyaczynski, M., Kowalski, G., Zadlo, D., Waluga, E., Olczyk, P.*, et al.* (2017). Fibroblast growth factor-21 and omentin-1 hepatic mRNA expression and serum levels in morbidly obese women with non-alcoholic fatty liver disease. Journal of physiology and pharmacology : an official journal of the Polish Physiological Society *68*, 363-374.

Wang, Y., Rimm, E.B., Stampfer, M.J., Willett, W.C., and Hu, F.B. (2005). Comparison of abdominal adiposity and overall obesity in predicting risk of type 2 diabetes among men. The American journal of clinical nutrition *81*, 555-563.

Wanninger, J., Bauer, S., Eisinger, K., Weiss, T.S., Walter, R., Hellerbrand, C., Schaffler, A., Higuchi, A., Walsh, K., and Buechler, C. (2012). Adiponectin upregulates hepatocyte CMKLR1 which is reduced in human fatty liver. Molecular and cellular endocrinology *349*, 248-254.

Wargent, E.T., Zaibi, M.S., O'Dowd, J.F., Cawthorne, M.A., Wang, S.J., Arch, J.R., and Stocker, C.J. (2015). Evidence from studies in rodents and in isolated adipocytes that agonists of the chemerin receptor CMKLR1 may be beneficial in the treatment of type 2 diabetes. PeerJ *3*, e753.

Way, S.W., and Popko, B. (2016). Harnessing the integrated stress response for the treatment of multiple sclerosis. The Lancet Neurology *15*, 434-443.

Weickert, M.O., Roden, M., Isken, F., Hoffmann, D., Nowotny, P., Osterhoff, M., Blaut, M., Alpert, C., Gogebakan, O., Bumke-Vogt, C.*, et al.* (2011). Effects of supplemented isoenergetic diets

differing in cereal fiber and protein content on insulin sensitivity in overweight humans. The American journal of clinical nutrition *94*, 459-471.

Weigert, J., Neumeier, M., Wanninger, J., Filarsky, M., Bauer, S., Wiest, R., Farkas, S., Scherer, M.N., Schaffler, A., Aslanidis, C.*, et al.* (2010). Systemic chemerin is related to inflammation rather than obesity in type 2 diabetes. Clinical endocrinology *72*, 342-348.

Weiss, A., Beloosesky, Y., Boaz, M., Yalov, A., Kornowski, R., and Grossman, E. (2008). Body mass index is inversely related to mortality in elderly subjects. Journal of general internal medicine *23*, 19-24.

Welch, W.J., and Brown, C.R. (1996). Influence of molecular and chemical chaperones on protein folding. Cell stress & chaperones *1*, 109-115.

Wittamer, V., Bondue, B., Guillabert, A., Vassart, G., Parmentier, M., and Communi, D. (2005). Neutrophil-mediated maturation of chemerin: a link between innate and adaptive immunity. Journal of immunology (Baltimore, Md : 1950) *175*, 487-493.

Wittamer, V., Franssen, J.D., Vulcano, M., Mirjolet, J.F., Le Poul, E., Migeotte, I., Brezillon, S., Tyldesley, R., Blanpain, C., Detheux, M.*, et al.* (2003). Specific recruitment of antigen-presenting cells by chemerin, a novel processed ligand from human inflammatory fluids. The Journal of experimental medicine *198*, 977-985.

Wolfs, M.G., Gruben, N., Rensen, S.S., Verdam, F.J., Greve, J.W., Driessen, A., Wijmenga, C., Buurman, W.A., Franke, L., Scheja, L.*, et al.* (2015). Determining the association between adipokine expression in multiple tissues and phenotypic features of non-alcoholic fatty liver disease in obesity. Nutrition & diabetes 5, e146.

World Health Organization (16.02.2018). Fact sheet: Obesity and overweight. URL: https://www.who.int/news-room/fact-sheets/detail/obesity-and-overweight (last visited: 26.07.2019)

World Health Organization (2016). Global Report on Diabetes. URL: https://apps.who.int/iris/bitstream/handle/10665/204871/9789241565257_eng.pdf;jsessionid=1D0E193AACADB5BBF85E787005714D73?sequence=1 (last visited: 26.07.2019)

Xu, H., Barnes, G.T., Yang, Q., Tan, G., Yang, D., Chou, C.J., Sole, J., Nichols, A., Ross, J.S., Tartaglia, L.A.*, et al.* (2003). Chronic inflammation in fat plays a crucial role in the development of obesity-related insulin resistance. The Journal of clinical investigation *112*, 1821-1830.

Yamawaki, H., Kameshima, S., Usui, T., Okada, M., and Hara, Y. (2012). A novel adipocytokine, chemerin exerts anti-inflammatory roles in human vascular endothelial cells. Biochemical and biophysical research communications *423*, 152-157.

Yan, H., Xia, M., Chang, X., Xu, Q., Bian, H., Zeng, M., Rao, S., Yao, X., Tu, Y., Jia, W.*, et al.* (2011). Circulating fibroblast growth factor 21 levels are closely associated with hepatic fat content: a cross-sectional study. PloS one *6*, e24895.

Yang, C., Jin, C., Li, X., Wang, F., McKeehan, W.L., and Luo, Y. (2012). Differential specificity of endocrine FGF19 and FGF21 to FGFR1 and FGFR4 in complex with KLB. PloS one *7*, e33870.

Yang, C., Lu, W., Lin, T., You, P., Ye, M., Huang, Y., Jiang, X., Wang, C., Wang, F., Lee, M.H.*, et al.* (2013). Activation of Liver FGF21 in hepatocarcinogenesis and during hepatic stress. BMC gastroenterology *13*, 67.

Ye, D.W., Rong, X.L., Xu, A.M., and Guo, J. (2017). Liver-adipose tissue crosstalk: A key player in the pathogenesis of glucolipid metabolic disease. Chinese journal of integrative medicine *23*, 410-414.

Ye, Z., Wang, S., Yang, Z., He, M., Zhang, S., Zhang, W., Wen, J., Li, Q., Huang, Y., Wang, X.*, et al.* (2014). Serum lipocalin-2, cathepsin S and chemerin levels and nonalcoholic fatty liver disease. Molecular biology reports *41*, 1317-1323.

Yilmaz, Y., Eren, F., Yonal, O., Kurt, R., Aktas, B., Celikel, C.A., Ozdogan, O., Imeryuz, N., Kalayci, C., and Avsar, E. (2010). Increased serum FGF21 levels in patients with nonalcoholic fatty liver disease. European journal of clinical investigation *40*, 887-892.

Younossi, Z., Anstee, Q.M., Marietti, M., Hardy, T., Henry, L., Eslam, M., George, J., and Bugianesi, E. (2018). Global burden of NAFLD and NASH: trends, predictions, risk factors and prevention. Nature reviews Gastroenterology & hepatology *15*, 11-20.

Zabel, B.A., Allen, S.J., Kulig, P., Allen, J.A., Cichy, J., Handel, T.M., and Butcher, E.C. (2005). Chemerin activation by serine proteases of the coagulation, fibrinolytic, and inflammatory cascades. The Journal of biological chemistry *280*, 34661-34666.

Zabel, B.A., Ohyama, T., Zuniga, L., Kim, J.Y., Johnston, B., Allen, S.J., Guido, D.G., Handel, T.M., and Butcher, E.C. (2006). Chemokine-like receptor 1 expression by macrophages in vivo: regulation by TGF-beta and TLR ligands. Experimental hematology *34*, 1106-1114.

Zhang, Y., Xie, Y., Berglund, E.D., Coate, K.C., He, T.T., Katafuchi, T., Xiao, G., Potthoff, M.J., Wei, W., Wan, Y.*, et al.* (2012). The starvation hormone, fibroblast growth factor-21, extends lifespan in mice. eLife *1*, e00065.

Zhen, E.Y., Jin, Z., Ackermann, B.L., Thomas, M.K., and Gutierrez, J.A. (2016). Circulating FGF21 proteolytic processing mediated by fibroblast activation protein. The Biochemical journal *473*, 605-614.

Zhuang, X., Sun, F., Li, L., Jiang, D., Li, X., Sun, A., Pan, Z., Lou, N., Zhang, L., and Lou, F. (2015). Therapeutic Effect of Metformin on Chemerin in Non-Obese Patients with Non-Alcoholic Fatty Liver Disease (NAFLD). Clinical laboratory *61*, 1409-1414.

Zoncu, R., Efeyan, A., and Sabatini, D.M. (2011). mTOR: from growth signal integration to cancer, diabetes and ageing. Nature reviews Molecular cell biology *12*, 21-35.

8 Appendix

Table A1 I Baseline characteristics of the LEMBAS study participants (cohort 1).

Parameter	LP	HP	P_{LPvsHP}
N	10	9	
Sex [f/m]	6 / 4	6 / 3	
Age [y]	47.2 ± 8.7	48.7 ± 9.1	0.188
BMI [kg/m²]	45.2 ± 1.2	44.5 ± 1.3	0.693
Glucose [mmol/l]	7.94 ± 1.04	6.39 ± 0.19	0.374
Insulin [mU/l]	32.8 ± 6.5	21.1 ± 3.2	0.187
HOMA-IR	11.7 ± 2.4	6.10 ± 1.06	0.263
HbA1c [%]	6.34 ± 0.62	5.60 ± 0.07	0.263
Urea [mmol/l]	5.26 ± 0.39	4.69 ± 0.47	0.110
TAG [mmol/l]	2.11 ± 0.22	1.48 ± 0.11	**0.021**
Cholesterol [mmol/l]	4.81 ± 0.35	4.87 ± 0.44	0.922
HDL [mmol/l]	0.981 ± 0.065	1.11 ± 0.10	0.302
LDL [mmol/l]	2.87 ± 0.30	3.09 ± 3.84	0.655
FFA [mmol/l]	0.599 ± 0.064	0.69 ± 0.06	0.333
IHL [%]	22.7 ± 3.53	12.3 ± 2.2	**0.032**
CRP [mg/l]	10.1 ± 1.8	10.9 ± 3.0	0.827
AST [U/l]	32.3 ± 6.6	24.4 ± 3.4	0.335
ALT [U/l]	44.3 ± 10.8	36.7 ± 8.3	0.597
γ-GT [U/l]	66.2 ± 24.1	34.6 ± 10.9	0.288

Morbidly obese subjects consumed a hypocaloric low-protein (LP, 10 EN%) or high-protein (HP, 30 EN%) diet 3 weeks prior to bariatric surgery. Parameters in blood were measured after overnight fast. IHL were determined by MRI$_{spec.}$ Data are mean ± SEM. Statistical differences in baseline parameters between the groups were tested by unpaired Student's t-test or Mann-Whitney-U test dependent on a normal or skewed distribution, respectively. Significant values ($P < 0.05$) are marked in bold.

Appendix

Table A2 I Correlation of FGF21 with anthropometric and routine clinical parameters in LEMBAS.

Correlation of FGF21 with	Baseline	Surgery[†]
Anthropometry		
Age	0.067	0.078
BMI	0.133	0.196
WHR	0.322	- 0.007
Absolute fat mass	- 0.176	- 0.108
Relative fat mass	- 0.269	- 0.235
Lipid metabolism		
TAG	0.089	**0.505****
Cholesterol	0.172	0.136
LDL-c	0.110	0.036
HDL-c	- 0.111	0.012
NEFA	- 0.049	**0.456****
IHL	0.509	**0.900*****
Insulin sensitivity		
Glucose	0.018	0.302
Insulin	0.160	- 0.078
HbA1c	0.317	**0.455***
HOMA-IR	0.251	0.026
Adipo-IR	0.183	0.119
Liver transaminases		
ALT	0.362	0.259
AST	**0.527***	0.273
γ-GT	0.412	0.106
Organokines		
Adiponectin	- 0.216	- 0.120
Leptin	0.133	0.182
Omentin	0.207	0.134
Chemerin	0.046	0.107

Data are Pearson or Spearman correlation coefficients dependent on a normal or skewed distribution, respectively. Asterisks indicate statistical significance as follows *$P < 0.05$, **$P < 0.01$, **$P < 0.001$. Significant values are marked in bold.
[†] Blood parameters at baseline as well as all anthropometric measurements, and indices based on these measurements, are representative for the two intervention groups, LP and HP group. Blood samples collected during surgery include the RP group.

Appendix

Table A3 ı Changes in anthropometric and routine clinical parameters in cohort 2, n = 92.

Parameter	LF6	HF1	HF6	*P*
Sex [f/m]	58/34			
Age [y]	31.5 ± 1.5			
BMI [kg/m²]	22.5 ± 0.3	22.5 ± 2.3	22.7 ± 0.3	**< 0.001**
Glucose [mmolLl]	5.22 ± 0.08	5.15 ± 0.06	5.22 ± 0.06	0.550
Insulin [mU/l]	4.71 ± 0.33	5.55 ± 0.38	5.11 ± 0.37	**0.006**
HOMA-IR	1.09 ± 0.08	1.29 ± 0.09	1.21 ± 0.09	**0.012**
HbA1c [%]	5.02 ± 0,04	5.06 ± 0.04	5.12 ± 0.04	**0.040**
Urea [mmol/l]	3.80 ± 0.11	4.31 ± 0.12	4.19 ± 0.10	**< 0.001**
TAG [mmol/l]	0.954 ± 0.044	0.894 ± 0.037	0.909 ± 0.039	0.449
Cholesterol [mmol/l]	4.29 ± 0.09	4.47 ± 0.09	4.70 ± 0.09	**< 0.001**
HDL [mmol/l]	1.27 ± 0.03	1.32 ± 0.04	1.41 ± 0.04	**< 0.001**
LDL [mmol/l]	2.59 ± 0.07	2.71 ± 0.08	2.86 ± 0.08	**< 0.001**
FFA [mmol/l]	0.607 ± 0.022	0.575 ± 0.021	0.499 ± 0.019	**< 0.001**
IHL [%]	2.15 ± 0.43	2.15 ± 0.43	2.33 ± 0.44	0.715
CRP [mg/l]	0.294 ± 0.047	0.462 ± 0.064	0.644 ± 0.095	**< 0.001**
AST [U/l]	20.3 ± 0.4	19.8 ± 0.4	20.5 ± 0.5	0.353
ALT [U/l]	18.2 ± 0.6	18.5 ± 0.6	18.0 ± 0.8	0.682
γ-GT [U/l]	13.8 ± 1.1	12. ± 0.9	14.4 ± 1.2	0.043

Healthy, lean subjects (n = 92) were standardized for 6 weeks on a healthy low-fat diet (LF: 30 EN% fat, 55 EN% carbohydrates, 15 EN% protein) after which they switched to a high-saturated-fat diet (HF: 45 EN% fat, 40 EN% carbohydrates, 15 EN% protein) for 6 weeks. Parameters in blood were measured after overnight fast. IHL were determined by MRI$_{spec.}$ Data are mean ± SEM. Statistical differences between CIDs were tested by ANOVA repeated measures. Significant values (*P* < 0.05) are marked in bold. LF6 indicates clinical investigation day (CID) after 6 weeks on the LF diet; HF1, CID after 1 week on the HF diet; HF6, CID after 6 weeks on the HF diet.

Appendix

Table A4 | Correlation of chemerin with expression of inflammatory markers in SAT (cohort 2).

Correlation of *RARRES2/CMKLR1* with	LF	HF1	HF6
RRRES2			
TNFα	0.321***	0.427***	0.557***
MCP1	0.443***	0.279**	0.343**
IL6	0.321**	0.270*	0.207
NLRP3	0.648***	0.535***	0.616***
NFκB	-0.527***	-0.632***	-0.458***
IL1β	-0.313**	-0.261*	0.145
CD14	0.490***	0.348**	0.445***
CD68	0.670***	0.640***	0.737***
EMR1	-0.443***	-0.227*	- 0.209
CMKLR			
TNFα	0.268*	0.500***	0.389***
MCP1	0.318**	0.261*	0.517***
IL6	0.093	0.133	0.231
NLRP3	0.526***	0.422***	0.458***
NFκB	- 0.047	- 0.063	-0.329**
IL1b	0.023	0.017	- 0.227
CD14	0.469***	0.519***	0.444***
CD68	0.557***	0.578***	0.609***
EMR1	0.054	0.200	- 0.297*

Gene expression of cytokines and macrophage markers were determined by qRT-PCR in SAT biopsies of cohort 2. Data are Pearson or Spearman correlation coefficients dependent on a normal or skewed distribution, respectively. Asterisks indicate statistical significance as follows *$P < 0.05$, **$P < 0.01$, **$P < 0.001$. Significant values are marked in bold. TNFα indicates, tumor necrosis factor alpha; MCP1, monocyte chemoattractant protein 1; IL, interleukin; NLRP3, NLR family pyrin domain containing 3; NFκB, nuclear factor kappa-light-chain-enhancer of activated B cells; CD, cluster of differentiation; EMR1, EGF module-containing mucin-like receptor.

Appendix

Table A5 I Changes in anthropometric and routine clinical parameters in cohort 2, HP subcohort, n = 24.

Parameter	LF6	HF1	HF6	HP6	*P*
Sex [f/m]	14/10				
Age [y]	39 ± 3				
BMI [kg/m²]	23.72 ± 0.44	23.70 ± 0.44	23.93 ± 0.46	23.94 ± 0.48	**0.011**
Glucose [mmolLl]	5.38 ± 0.15	5.24 ± 0.14	5.49 ± 0.15	5.75 ± 0.14	**0.003**
Insulin [mU/l]	4.54 ± 0.65	4.70 ± 0.56	5.88 ± 0.90	3.56 ± 0.33	**0.002**
HOMA-IR	1.16 ± 0.19	1.10 ± 0.14	1.45 ± 0.23	0.90 ± 0.08	**0.020**
HbA1c [%]	4.91 ± 0.11	4.94 ± 0.11	4.94 ± 0.09	4.94 ± 0.09	0.178
Urea [mmol/l]	4.00 ± 0.17	4.38 ± 0.20	4.15 ± 0.15	6.09 ± 0.18	**0.000**
TAG [mmol/l]	1.01 ± 0.09	0.87 ± 0.07	0.92 ± 0.09	0.73 ± 0.04	0.086
Cholesterol [mmol/l]	4.38 ± 0.19	4.41 ± 0.22	4.82 ± 0.21	4.38 ± 0.17	**0.001**
HDL [mmol/l]	1.18 ± 0.06	1.21 ± 0.07	1.36 ± 0.09	1.22 ± 0.067	**0.000**
LDL [mmol/l]	2.74 ± 0.16	2.71 ± 0.18	2.97 ± 0.19	2.73 ± 0.14	0.051
FFA [mmol/l]	0.570 ± 0.050	0.543 ± 0.038	0.462 ± 0.034	0.596 ± 0.029	0.087
IHL [%]	2.16 ± 0.59	2.52 ± 0.91	2.96 ± 0.68	NA	0.470
CRP [mg/l]	0.55 ± 0.16	0.54 ± 0.13	0.47 ± 0.13	0.28 ± 0.07	0.132
AST [U/l]	19.91 ± 0.73	19.33 ± 0.81	20.50 ± 0.90	20.79 ± 0.85	0.243
ALT [U/l]	17.80 ± 0.90	18.45 ± 1.27	17.63 ± 1.34	18.24 ± 0.94	0.900
γ-GT [U/l]	13.60 ± 2.28	11.10 ± 1.45	14.36 ± 1.87	15.06 ± 1.57	0.068

At the end on the high-saturated-fat intervention, 24 subjects of cohort 2 agreed to continue on a 6-week high-protein diet (HP: 30 EN% fat, 40 EN% carbohydrates, 30 EN% protein) diet. Changes in anthropometric and routine clinical parameters of this subcohort (n = 24) are shown. Parameters in blood were measured after overnight fast. IHL were determined by MRI$_{spec.}$ Data are mean ± SEM. Statistical significance between CIDs were tested by ANOVA repeated measures. Significant values (*P* < 0.05) are marked in bold. NA, indicates not assessed.

Appendix

Table A6 | Changes in anthropometric and routine clinical parameters in cohort 3, n = 21.

Parameter	Baseline			10 EN%			30 EN% *versus* 15 EN%		
	HP	NP	P_{NPvsHP}	HP	NP	P_{NPvsHP}	HP	NP	P_{NPvsHP}
N	11	10							
Sex [f/m]	8/3	7/3							
Age [y]	62.0 ± 1.5	61.3 ± 2.7	0.820	NA	NA	NA	NA	NA	NA
BMI [kg/m²]	25.7 ± 1.3	25.5 ± 1.3	0.906	NA	NA	NA	NA	NA	NA
Glucose [mmol/l]	5.24 ± 0.09	5.71 ± 0.22	0.060	5.71 ± 0.22	5.24 ± 0.09	0.137	5.71 ± 0.22	5.24 ± 0.09	0.235
HbA1c [%]	5.52 ± 0.12	5.56 ± 0.05	0.754	NA	NA	NA	NA	NA	NA
Urea [mmol/l]	4.38 ± 0.26	5.27 ± 0.32	**0.040**	3.13 ± 0.16	3.67 ± 0.17	0.099	6.56 ± 0.38	4.79 ± 0.32	**0.005**
Creatinine [µmol/l]	77.1 ± 3.4	76.8 ± 2.7	0.945	76.95 ± 3.20	78.84 ± 2.51	0.863	74.15 ± 3.19	77.90 ± 3.24	0.512
Uric acid [µmol/l]	297.6 ± 24.9	302.4 ± 21.5	0.887	289.0 ± 24.3	298.9 ± 23.9	0.705	276.09 ± 22.8	309.4 ± 26.9	0.314
TAG [mmol/l]	1.02 ± 0.06	1.35 ± 0.19	0.106	0.82 ± 0.05	0.94 ± 0.08	0.282	1.04 ± 0.06	1.0 ± 0.10	0.809
Cholesterol [mmol/l]	5.97 ± 0.30	6.09 ± 0.28	0.691	5.72 ± 0.30	5.98 ± 0.33	0.605	5.92 ± 0.33	5.91 ± 0.36	1.000
HDL [mmol/l]	1.63 ± 0.10	1.68 ± 0.13	0.782	1.67 ± 0.10	1.67 ± 0.12	1.000	1.63 ± 0.11	1.62 ± 0.11	0.918
LDL [mmol/l]	3.88 ± 0.25	3.80 ± 0.26	0.834	3.68 ± 0.22	3.87 ± 0.31	0.809	3.81 ± 0.25	3.84 ± 0.33	0.973
FFA [mmol/l]	0.478 ± 0.040	0.457 ± 0.034	0.536	0.541 ± 0.056	0.474 ± 0.059	0.334	0.578 ± 0.099	0.514 ± 0.079	0.359
AST [U/l]	28.0 ± 9.3	21.4 ± 1.9	0.479	21.04 ± 1.73	25.67 ± 3.13	0.197	20.46 ± 1.82	23.68 ± 2.00	0.223
ALT [U/l]	23.0 ± 3.5	21.2 ± 3.8	0.349	21.81 ± 2.36	23.39 ± 4.72	0.426	20.02 ± 1.90	21.80 ± 3.62	0.705
γ-GT [U/l]	21.8 ± 3.5	29.4 ± 4.5	0.195	22.15 ± 4.07	28.28 ± 3.74	0.152	20.18 ± 3.67	27.04 ± 3.65	0.114
FGF21 [pg/ml]	249.4 ± 48.6	281.9 ± 22.8	0.557	294.3 ± 65.6	295.3 ± 32.0	0.705	111.9 ± 20.1	229.9 ± 30.0	**0.004**

Healthy, elderly subjects (n = 21) first consumed a low-protein diet for 3 days (10 EN% protein, 45 EN% carbohydrates, 45 EN% fat), followed by 3 days of a protein-enriched diet (HP: 30 EN% protein, 45 EN% carbohydrates, 25 EN% fat, n = 11) or a diet reflecting habitual protein intake (NP: 15 EN% protein, 45 EN% carbohydrates, 40 EN% fat, n = 10). Routine blood parameters were measured at baseline and at day 3 after each diet. Data are mean ± SEM. Significant values are marked in bold (*P* < 0.05). NA indicates not assessed.

Appendix

Table A7 | Components of NAFLD Activity Score (NAS) and Fibrosis Staging.

Item	Extent	Score
NAS components		
Steatosis[†]	< 5%	0
	5 - 33%	1
	> 33 - 66%	2
	< 66%	3
Lobular Inflammation[††]	No foci	0
	< 2 foci per 20x field	1
	2 - 4 foci per 20x field	2
	> 4 foci per 20x field	3
Hepatocyte Ballooning	None	0
	Few balloon cells[#]	1
	Many cells/prominent ballooning	2
Fibrosis stage (evaluated separately from NAS)		
Fibrosis	None	0
	Perisinusoidal or periportal	1
	Mild, zone 3, perisinusoidal	1A
	Moderate, zone 3, perisinusoidal	1B
	Portal/periportal	1C
	Perisinusoidal and portal/periportal	2
	Bridging fibrosis	3
	Cirrhosis	4

Components of NAS score according to (Kleiner et al., 2005). Total NAS score represents the unweighted sum of scores for steatosis, lobular inflammation, and ballooning, and ranges from 0-8. Fibrosis stage is evaluated separately from NAS.
[†] Low- to medium-power evaluation of parenchymal involvement by steatosis.
[††] Overall assessment of all inflammatory foci.
[#] Few indicates rare but definite ballooned hepatocytes and cases that are diagnostically borderline.

Appendix

Table A8 | Components of Steatosis, Activity, and Fibrosis (SAF) Score.

Item	Extent	Score
SAF components		
Steatosis[†]	< 5%	0
	5 - 33%	1
	> 33 - 66%	2
	< 66%	3
Activity[††]		
Hepatocellular ballooning	Normal hepatocytes	0
	Presence of clusters of hepatocytes with a rounded shape and pale cytoplasm	1
	Same as grade 1, but with at least one enlarged ballooned hepatocyte (at least 2-fold size that of normal cells)	2
Lobular inflammation[#]	None	0
	≤ 2 foci per 20X field	1
	>2 foci per 20X field	2
Fibrosis stage		
Fibrosis	None	0
	Perisinusoidal or portal/periportal	1
	Perisinusoidal and portal/periportal	1A
	Bridging fibrosis	1B
	Cirrhosis	1C

Components of SAF score according to (Bedossa et al., 2012). Cases with steatosis ≥ 1 were considered NAFLD. Severity of disease was categorized as NASH if activity and fibrosis scores ≥ 1.
[†] Quantities of large or medium-sized lipid droplets, but not foamy microvesicules.
[††] 0 = no activity, 1 = mild activity, 2 = moderate activity, 3 = severe activity.
[#] Foci of two or more inflammatory cells within the lobule.

9 Curriculum Vitae

Die Seite 129 (Lebenslauf) enthält persönliche Daten und ist daher nicht Bestandteil dieser Veröffentlichung.

Publikationen

Seebeck, N., Markova, M., Gantert, T., Hornemann, S., Haß, U., Schüler, R., Osterhoff, M. A., Xu, C., Frahnow, T., Coleman, V., Heidenreich, S., Pivovarova-Ramich, O., Schupp, M., Rosenthal, A., Lange, V., Rose, A. J., Ost, M., Klaus, S., Harger, A., Stemmer, K., Pfeiffer, A. F. H. High-protein diet downregulates circulating FGF21 and represses its hepatic expression in mice and humans through nitrogen metabolites. Manuskript eingereicht bei *Nature Communications*, 2. Revision.

Xu, C., Markova, M., **Seebeck, N**., Loft, A., Hornemann, S., Gantert, T., Kabisch, S., Herz, K., Loske, J., Ost, M., Coleman, V., Klauschen, F., Rosenthal, A., Lange, V., Machann J., Klaus, S., Herzig, S., Pivovarova-Ramich, O., Pfeiffer, A. F. H. Effects of high- and low-protein diets on hepatic fat content, autophagy, mitochondrial function and fat metabolism in humans. Manuskript eingereicht bei *Metabolism*, 2. Revision.

Horbelt, T., Hörbelt T., Tacke C., Markova M., Herzfeld de Wiza D., Van de Velde F., Bekaert M, Van Nieuwenhove Y., Hornemann S., Rödiger M., **Seebeck N**., Friedl E., Jonas W., Thoresen G., Kuss O., Rosenthal A., Lange V., Pfeiffer A. F. H., Schürmann A., Lapauw B., Rudovich N., Pivovarova O., Ouwens D. (2018). The novel adipokine WISP1 associates with insulin resistance and impairs insulin action in human myotubes and mouse hepatocytes. *Diabetologia*.

Schüler, R., **Seebeck, N.**, Osterhoff M. A., Witte, V., Flöel, A., Busahn, A., Jais, A., Brüning, J. C., Kabisch, S., Pivovarova O., Hornemann S., Kruse M., Pfeiffer, A. F. H. (2018). VEGF and GLUT1 are highly heritable, inversely correlated and affected by dietary fat intake: consequences for cognitive function in humans. *Molecular Metabolism*, 11, 129-136.

Küffel, N.*, Ziolkowski J., Haslberger A. G. (2013). Microbiota and diseases of the nervous system. *Journal für Ernährungsmedizin*, 15(3), 18-20.

Küffel, N.*, Meyer, A. L., Haslberger, A. G. (2013). Fötale Programmierung: Epigenetische Aspekte der frühkindlichen Ernährung. Österreichische Gesellschaft für Ernährung, *Ernährung aktuell*, 3, 1-4.

Konferenzbeiträge

Haß, U., **Seebeck, N**., Markova, M., Hornemann, S., Pivovarova-Ramich, O., Schupp, M., Heidenreich, S., Pfeiffer, A. F. H. Das metabolische Hepatokin Fibroblast Growth Factor-21 (FGF21) wird durch hohe Proteinaufnahme durch eine Harnstoffsynthese-assoziierte Regulation in Leberzellen akut und chronisch heruntergereguliert (2019). Vortrag *DDG-Tagung Nachwuchssymposium*, präsentiert von Ulrike Haß.

Schüler, R., **Küffel, N**.*, Osterhoff M. A., Witte, V., Flöel, A., Busahn, Kabisch, S., Pivovarova O., Hornemann S., Kruse M., Pfeiffer, A. F. H. (2017). GLUT1 and VEGF are highly heritable, regulated by fat intake and affect memory performance. Posterbeitrag *EASD Konferenz*, Portugal, präsentiert von Rita Schüler.

Küffel, N.*, Ernährungsstrategien für Gesundheit im Alter – Die NutriAct Interventionsstudie (2016). Vortrag *NutriAct Jahressymposium*, Potsdam-Rehbrücke.

Küffel, N.*, Schüler R., Osterhoff M. A., Frahnow T., Hornemann S., Seltmann A. C., Kruse M., Pivovarova O., Pfeiffer, A. F. H. (2016). Chemerin concentrations are heritable and increase in response to a high-fat diet in healthy, lean subjects. Posterbeitrag *EASD Konferenz*, München.

*unter Geburtsnamen

10 Danksagung

An dieser Stelle möchte ich mich herzlichst bei Herrn Prof. Dr. Andreas F. H. Pfeiffer bedanken, dass er mich in seine Arbeitsgruppe aufgenommen und mir ermöglicht hat, an dieser Studie zu arbeiten. Vielen Dank für das Vertrauen, die stete Unterstützung, die vielen Anregungen und Ideen und nicht zuletzt die absolute Begeisterung und ansteckende Freude für die Forschung.

Weiterhin gilt mein herzlicher Dank Frau Prof. Dr. Susanne Klaus für die Übernahme der Erstbetreuung, den wissenschaftlichen Austausch sowie die stets angenehme Zusammenarbeit am FGF21 Projekt.

Mein besonderer Dank gilt Frau PD Dr. Olga Ramich, die mich während des gesamten Arbeitsprozesses sehr unterstützt hat. Insbesondere schätze ich ihr exzellentes wissenschaftliches Verständnis, ihre positive Art sowie ihre besondere Fähigkeit Lösungen, statt Probleme zu sehen.

Ich möchte mich zudem bei allen Mitarbeitern der Abteilung Klinische Ernährung bedanken, ohne die diese Arbeit nicht möglich gewesen wäre. Das Gelingen einer humanen Studie ist nie eine Einzelleistung, sondern auf die abgestimmte Zusammenarbeit vieler Personen angewiesen. Insbesondere bedanke ich mich bei Mariya Markova, Chenchen Xu, Kathleen Herz, Thomas Gantert, Ulrike Haß, Elisabeth Friedl, der Studienärztin Silke Hornemann sowie den Studienschwestern und Technischen Assistenten für die Unterstützung der LEMBAS Studie. Weiterhin gilt mein Dank den Studienteilnehmern.

Meiner Familie danke ich sehr für ihr spürbares Vertrauen und den uneingeschränkten Rückhalt. Ganz besonderer Dank gilt meinem Ehemann, Andreas, der sich geduldig meine Ausführungen über die humane Physiologie angehört und mich bei Tiefpunkten neu motiviert hat. Mit ihm konnte ich wissenschaftliche Problemstellungen diskutieren, wobei er bemüht war (häufig mit Beispielen aus dem Rechnungswesen) mir neue Lösungswege aufzuzeigen. Nicht zuletzt danke ich meiner kleinen Tochter, Liv, die mich täglich neu mit ihrem Lachen verzaubert und mir letztlich ermöglicht hat, die Dissertation (während sie friedlich schlief) fertig zu stellen.

11 Erklärung

Hiermit erkläre ich, Nicole Seebeck, dass ich die vorliegende Arbeit selbstständig verfasst und keine anderen als die angegebenen Quellen und Hilfsmittel benutzt habe. Die Arbeit wurde bisher an keiner anderen Hochschule eingereicht.

_____

Nicole Seebeck   Potsdam, Oktober 2019